CNIC-01430
CNDC-0025
INDC(CPR)-049/L

COMMUNICATION OF NUCLEAR DATA PROGRESS

No.22 (1999)

China Nuclear Data Center

China Nuclear Information Centre

Atomic Energy Press

Beijing, December, 1999

EDITORIAL NOTE

This is the 22th issue of *Communication of Nuclear Data Progress* (CNDP), in which the achievements in nuclear data field for last year in China are carried. It includes the reaction mechanism and energy balance of light nuclei, the calculations of n+^{90,91,92,94,96,Nat}Zr, and γ+^{9}Be reactions; the evaluations of complete data for n+^{233}U, ^{239}Pu, ^{65}Cu, ^{90,91,92,94,96,Nat}Zr ^{69,71}Ga, γ+Al, Cr and the cross sections of ^{89,88}Y (n, 2n) ^{88,87}Y reactions; the evaluation of reference fission yield data and prompt γ-ray induced by thermal neutron capture; wavelength calculation of high stripped ions; and benchmark testing of CEND-2.1 for heavy water reactor.

The editors hope that our readers and colleagues will not spare their comments in order to improve this publication.

Please write to Profs. Liu Tingjin and Zhuang Youxiang
Mailing Address: China Nuclear Data Center
China Institute of Atomic Energy
P.O.Box 275 (41), Beijing 102413
People's Republic of China
Telephone: 86-10-69357729 or 69357830
Telex: 222373 IAE CN
Facsimile: 86-10-6935 7008
E-mail: tjliu @ mipsa.ciae.ac.cn or yxzhuang @ mipsa.ciae.ac.cn

EDITORIAL BOARD

CONTENTS

I THEORETICAL CALCULATION

Reaction Mechanism of Light Nuclei Below 20 MeV

Zhang Jingshang
(China Nuclear Data Center, CIAE)

Introduction

The light nuclei are the elements in 1p shell. At the incident neutron energies below 20 MeV, the reaction mechanism could be classified as follows

(1) A(n,b)B, one particle emission, like ^{6}Li(n,t)α.

(2) A(n,ab)B, Sequential two particle emission

A(n,2n)B, A(n,na)B, A(n,np)B, ···

(3) The two cluster separation, when the residual nuclei are

^{8}Be→+α, ^{5}He→n+α, and ^{5}Li→p+α.

A(n,a)B(1+2), like ^{6}Li(n,d) ^{5}He, ^{7}Li(n,t) ^{5}He, ^{10}B(n,t) ^{8}Be, ···

A(n,ab)B(1+2), like ^{6}Li(n,np) ^{5}He, ^{6}Li(n,2n) ^{5}Li, and ^{10}B(n,nd) ^{8}Be, ···

A(n,abc)B(1+2), like ^{7}Li(n,nnp) ^{5}He, ···

(4) Three body break-up process, when the residual nuclei are

^{10}Be*→n+n+^{8}Be, ^{6}He*→n+n+α.

Direct three body breakup n+^{9}Be→10Be*→n+n+^{8}Be*

A(n,a)B(1+2+3) like ^{9}Be(n,α) ^{6}He*, ^{6}Li(n,p) ^{6}He*, ···

A(n,ab)B(1+2+3) like ^{7}Li(n,np) ^{6}He*, ···

The Legendre coefficients of the double differential cross sections of outgoing particles in each type reaction mechanism are needed to be set up for the model calculating. The formulation will be published one after another in succession.

1 Double Differential Cross Section of Secondary Particle Emission from Level to Level

The physical quantities used in this paper are defined as following:

E^*: excitation energy;

E_n: incident neutron energy in L.S;

M_c, M_t: mass of compound nucleus and target;

$\vec{V}_c$,: velocity of compound nucleus in lab. system;

m_1, m_2: mass of the first and the second emitted particle, respectively;

ε_1, ε_2: energy of the first and the second emitted particle, respectively;

M_1, M_2: mass of residual nucleus after the first and the second emitted particle, respectively;

E_1, E_2: energy of residual nucleus after the first and the second emitted particle, respectively;

$\vec{v}_1, \vec{v}_2$: velocity of the first and the second emitted particle, respectively;

$\vec{V}_1, \vec{V}_2$: velocity of residual nucleus after the first and the second emitted particle, respectively;

B_1, B_2: binding energy of the first and the second emitted particle in its compound nucleus, respectively;

E_{k_1}, E_{k_2} : level energy with the level order number k_1, k_2 reached by the first and the second emitted particle, respectively;

$f_l^{m_1}$ (c), $f_l^{M_1}$ (c): Legendre expansion coefficient of the first emitted particle and its residual nucleus, respectively in C.M.S.;

$f_l^{m_2}$, $f_l^{M_2}$: Legendre expansion coefficient of the second emitted particle and its residual nucleus, respectively;

with

$$f_l^{M_1} = (-1) f_l^{m_1} \qquad (1)$$

Three motion systems are used in the model calculations, in which the physical quantity indicated by the superscript l, c, and r for laboratory, center of mass, and recoil residual nucleus, respectively.

The Legendre expansion coefficients of the first emitted particle and its residual

nucleus $f_l^{M_1}$ (c) and $f_l^{M_1}$ (c) can be obtained by the unified model. For low incident neutron energies (< 20 MeV) the isotropic distribution of the second particle emissions is used in this model. In the emission process from discrete level to discrete level the emitted energies of the first and second particles (from k_1 level $\varepsilon_1^c, \varepsilon_2^r$ to k_2 level) are given by

$$\varepsilon_1^c = \frac{M_1}{M_C}(E^* - B_1 - E_{k_1}) \tag{2}$$

$$\varepsilon_2^r = \frac{M_2}{M_1}(E_{k_1} - B_2 - E_{k_2}) \tag{3}$$

The formula of double differential cross section of the recoil residual nucleus after the first particle emission in C.M.S is given by

$$\frac{d\sigma}{d\cos\theta_{M_1}^c} = \sum_l \frac{2l+1}{2} f_l^{M_1}(c) P_l(\cos\theta_{M_1}^c) \tag{4}$$

The velocity relation reads

$$\vec{v}_2^c = \vec{V}_1^c + \vec{v}_2^r \tag{5}$$

Therefore the maximum and the minimum energies of the emitted second particle in C.M.S. are obtained by

$$\varepsilon_{2,\min}^c = \frac{1}{2} m_2 \left| V_1^c - v_2^r \right|^2 = \varepsilon_2^r (1-\gamma)^2 \tag{6}$$

$$\varepsilon_{2,\max}^c = \frac{1}{2} m_2 \left| V_1^c + v_2^r \right|^2 = \varepsilon_2^r (1+\gamma)^2 \tag{7}$$

where γ is defined by

$$\gamma = \frac{V_1^c}{v_2^r} = \sqrt{\frac{E_1^c m_2}{\varepsilon_2^r M_1}} \tag{8}$$

The spectrum of the second emitted particle is a ring-type in C.M.S. Based on the momentum conservation the relation of v_2^c, v_2^r and V_1^c can be obtained by

$$(v_2^c)^2 = (v_2^r)^2 + (V_1^c)^2 + 2 v_2^r V_1^c \cos\Theta$$

where

$$\cos\Theta = \cos\theta_2^{\mathrm{r}}\cos\theta_{M_1}^{\mathrm{c}} + \sin\theta_2^{\mathrm{r}}\sin\theta_{M_1}^{\mathrm{c}}\cos(\phi_2^{\mathrm{r}} - \phi_{m_1}^{\mathrm{c}}) \tag{9}$$

We obtain the relations

$$\cos\theta_2^{\mathrm{c}} = \frac{\cos\theta_2^{\mathrm{r}} + \gamma\cos\theta_{M_1}^{\mathrm{c}}}{\sqrt{1+2\gamma\cos\Theta+\gamma^2}} \tag{10}$$

and

$$\varepsilon_2^{\mathrm{c}} = \varepsilon_2^{\mathrm{r}}(1+2\gamma\cos\Theta+\gamma^2) \tag{11}$$

Since Ω_2^{r} can be determined by $\Omega_{M_1}^{\mathrm{c}}$ and, Ω_2^{c} we have

$$\cos\Theta = \sqrt{\frac{\varepsilon_2^{\mathrm{c}}}{\varepsilon_2^{\mathrm{r}}}}[\cos\theta_2^{\mathrm{c}}\cos\theta_{M_1}^{\mathrm{c}} + \sin\theta_2^{\mathrm{c}}\sin\theta_{M_1}^{\mathrm{c}}\cos(\phi_{m_1}^{\mathrm{c}} - \phi_2^{\mathrm{c}})] - \gamma \tag{12}$$

From the basic relation

$$\frac{\mathrm{d}^2\sigma}{\mathrm{d}\varepsilon_2^{\mathrm{c}}\mathrm{d}\,\Omega_{m_2}^{\mathrm{c}}} = \sqrt{\frac{\varepsilon_2^{\mathrm{c}}}{\varepsilon_2^{\mathrm{r}}}}\frac{\mathrm{d}^2\sigma}{\mathrm{d}\varepsilon_2^{\mathrm{r}}\mathrm{d}\,\Omega_{m_2}^{\mathrm{r}}} \tag{13}$$

averaging by all of the recoil angular distribution the double differential cross section of the second emitted particle is obtained by

$$\frac{\mathrm{d}^2\sigma}{\mathrm{d}\varepsilon_2^{\mathrm{c}}\mathrm{d}\,\Omega_{m_2}^{\mathrm{c}}} = \sqrt{\frac{\varepsilon_2^{\mathrm{c}}}{\varepsilon_2^{\mathrm{r}}}}\int\mathrm{d}\,\Omega_{M_1}^{\mathrm{c}}\frac{\mathrm{d}\sigma}{\sigma\mathrm{d}\,\Omega_{M_1}^{\mathrm{c}}}\frac{\mathrm{d}^2\sigma}{\mathrm{d}\varepsilon_2^{\mathrm{r}}\mathrm{d}\,\Omega_{m_2}^{\mathrm{r}}} \tag{14}$$

In the case of discrete level emissions $\varepsilon_2^{\mathrm{r}}$=const, the Eq.(14) can be reduced to

$$\frac{\mathrm{d}^2\sigma}{\mathrm{d}\varepsilon_2^{\mathrm{c}}\mathrm{d}\,\Omega_{m_2}^{\mathrm{c}}} = \frac{\mathrm{d}\sigma}{\mathrm{d}\,\Omega_{m_2}^{\mathrm{r}}}\delta(\varepsilon_2^{\mathrm{c}} - \varepsilon_2^{\mathrm{r}}(1+2\gamma\cos\Theta+\gamma^2)) \tag{15}$$

The isotropic distribution in the residual nucleus system is used

$$\frac{\mathrm{d}\sigma}{\mathrm{d}\,\Omega_{m_2}^{\mathrm{r}}} = \frac{\sigma}{4\pi} \tag{16}$$

Substituting eqs. 15 and 16 in Eq.14, we have

$$\frac{\mathrm{d}^2\sigma}{\mathrm{d}\varepsilon_2^{\mathrm{c}}\mathrm{d}\,\Omega_{m_2}^{\mathrm{c}}}=\frac{1}{4\pi}\sqrt{\frac{\varepsilon_2^{\mathrm{c}}}{\varepsilon_2^{\mathrm{r}}}}\int\mathrm{d}\,\Omega_{M_1}^{\mathrm{c}}\delta(\varepsilon_2^{\mathrm{c}}-\varepsilon_2^{\mathrm{r}}(1+2\gamma\cos\Theta+\gamma^2)) \tag{17}$$

The δ function gives the integration limits by the energy relation.

Using

$$\int F(x)\delta(g(x))\mathrm{d}x=\sum_i\frac{F(x_{0_i})}{\left|\frac{\mathrm{d}g(x)}{\mathrm{d}x}\right|_{x=x_{0_i}}} \tag{18}$$

where $g(x_{0_i})$ for i=1,2,...

Carrying out the integration over $\phi_{M_1}^{\mathrm{c}}$ and

$$\left|\frac{\mathrm{d}(\varepsilon_2^{\mathrm{c}}-\varepsilon_2^{\mathrm{r}}(1+2\gamma\cos\Theta+\gamma^2))}{\mathrm{d}\phi_{m_1}^{\mathrm{c}}}\right|=\left|2\gamma\varepsilon_2^{\mathrm{r}}\frac{\mathrm{d}\cos\Theta}{\mathrm{d}\phi_{m_1}^{\mathrm{c}}}\right|$$

$$=\left|\sqrt{\frac{\varepsilon_2^{\mathrm{c}}}{\varepsilon_2^{\mathrm{r}}}}2\gamma\varepsilon_2^{\mathrm{r}}\sin\theta_2^{\mathrm{c}}\sin\theta_{M_1}^{\mathrm{c}}\sin(\phi_{m_1}^{\mathrm{c}}-\phi_2^{\mathrm{c}})\right|$$

$$=\left|\pm\sqrt{\frac{\varepsilon_2^{\mathrm{c}}}{\varepsilon_2^{\mathrm{r}}}}2\gamma\varepsilon_2^{\mathrm{r}}\sqrt{\sin^2\theta_{M_1}^{\mathrm{c}}\sin^2\theta_2^{\mathrm{c}}-(\eta-\cos\theta_2^{\mathrm{c}}\cos\theta_{M_1}^{\mathrm{c}})^2}\right| \tag{19}$$

where

$$\eta=\sqrt{\frac{\varepsilon_2^{\mathrm{r}}}{\varepsilon_2^{\mathrm{c}}}}\frac{\frac{\varepsilon_2^{\mathrm{c}}}{\varepsilon_2^{\mathrm{r}}}-1+\gamma^2}{2\gamma} \tag{20}$$

denoting

$$x=\cos\theta_{M_1}^{\mathrm{c}}$$

$$c=1-\cos^2\theta_2^{\mathrm{c}}-\eta^2$$

$$\left|\frac{\mathrm{d}(\varepsilon_2^{\mathrm{c}}-\varepsilon_2^{\mathrm{r}}(1+2\gamma\cos\Theta+\gamma^2))}{\mathrm{d}\phi_{M_1}^{\mathrm{c}}}\right|=\left|\pm\sqrt{\frac{\varepsilon_2^{\mathrm{c}}}{\varepsilon_2^{\mathrm{r}}}}2\gamma\varepsilon_2^{\mathrm{r}}\sqrt{c+2\eta\cos\theta_2^{\mathrm{c}}x-x^2}\right| \tag{21}$$

there are two zero points in the integrated function ($\sin\phi^{c}_{M_1}$ and $\sin(\pi-\phi^{c}_{M_1})$), so that the factor 2 must be put in the result.

Thus, the double differential cross section of the second emitted particle in C.M.S is given by

$$\frac{d^2\sigma}{d\varepsilon_2^c d\,\Omega_{m_2}^c}=\frac{1}{8\pi^2\gamma\varepsilon_2^r}\int_{x_1}^{x_2}dx\frac{d\sigma}{dx}\frac{1}{\sqrt{c+2\eta\cos\theta_2^c x-x^2}} \tag{22}$$

When $x^2-2\eta\ \cos\theta_2^c x-c\le 0$ is held, then the integration limits are given by

$$x_1=\eta\cos\theta_2^c-\sqrt{(1-\eta^2)\sin^2\theta_2^c}$$

$$x_2=\eta\cos\theta_2^c+\sqrt{(1-\eta^2)\sin^2\theta_2^c}$$

One can check that $\eta\le 1$ is held if $x_1\le x\le x_2$, which means

$$\left(\sqrt{\frac{\varepsilon_2^c}{\varepsilon_2^r}}-\gamma\right)^2\le 1$$

When the variable x is substituted again by

$$x=y+\eta\cos\theta_2^c$$

and

$$y=\sqrt{(1-\eta^2)\sin^2\theta_2^c}\cos t$$

then the integration becomes

$$\int_{x_1}^{x_2}dx\frac{d\sigma}{dx}\frac{1}{\sqrt{c+2\eta\cos\theta_2^c x-x^2}}$$

$$=\sum_l\frac{2l+1}{2}f_l^{M_1}(c)\int_0^{\pi}dt\mathrm{P}_l\left(\sqrt{(1-\eta^2)\sin^2\theta_2^c}\cos t+\eta\cos\theta_2^c\right) \tag{23}$$

The integration can be carried out analytically by

$$\int_0^{\pi}dt\mathrm{P}_l\left(\sqrt{(1-\eta^2)\sin^2\theta_2^c}\cos t+\eta\cos\theta_2^c\right)=\pi\mathrm{P}_l(\eta)\mathrm{P}_l(\cos\theta_2^c) \tag{24}$$

Proof let $\eta=\cos\theta'$, $\cos\theta=\cos\theta_2^c$ and $t=\phi-\phi'$

$$\cos\Theta = \cos\theta\cos\theta' + \sin\theta\sin\theta'\cos(\phi-\phi')$$

using addition formula of Legendre polynomial

$$\mathrm{P}_l(\cos\Theta) = \mathrm{P}_l(\cos\theta)\mathrm{P}_l(\cos\theta') + 2\sum_{m=1}^{l}\frac{(l-m)!}{(l+m)!}\mathrm{P}_l^m(\cos\theta)\mathrm{P}_l^m(\cos\theta')\cos m(\phi-\phi') \tag{25}$$

then

$$\int_0^{\pi}\mathrm{P}_l(\cos\Theta)\mathrm{d}t = \pi\mathrm{P}_l(\eta)\mathrm{P}_l(\cos\theta_2^{\mathrm{c}}) \tag{26}$$

A very interesting result is obtained, the Legendre expansion coefficient is still a Legendre polynomial. Thus Legendre expansion of the second emitted particle in C.M.S can be given by

$$\frac{\mathrm{d}^2\sigma}{\mathrm{d}\varepsilon_2^{\mathrm{c}}\mathrm{d}\,\Omega_{m_2}^{\mathrm{c}}} = \frac{\sigma}{4\pi}\sum_l(2l+1)f_l^{m_2}(\varepsilon_2^{\mathrm{c}})\mathrm{P}_l(\cos\theta_{m_2}^{\mathrm{c}}) \tag{27}$$

and

$$f_l^{m_2}(\varepsilon_2^{\mathrm{c}}) = \frac{(-1)^l}{4\gamma\varepsilon_2^{\mathrm{r}}}f_l^{m_1}\mathrm{P}_l(\eta) \tag{28}$$

It is easy to check that the energy spectrum is normalized

$$\int_{\varepsilon_{2,\min}^{\mathrm{c}}}^{\varepsilon_{2,\max}^{\mathrm{c}}}\mathrm{d}\varepsilon_2^{\mathrm{c}}f_0^{m_2}(\varepsilon_2^{\mathrm{c}}) = \int_{\varepsilon_{2,\min}^{\mathrm{c}}}^{\varepsilon_{2,\max}^{\mathrm{c}}}\mathrm{d}\varepsilon_2^{\mathrm{c}}\frac{1}{4\gamma\varepsilon_2^{\mathrm{r}}} = 1 \tag{29}$$

This formula of double differential cross section is used for the second neutron in ^{9}Be(n,2n) ^{8}Be channel and the α particle in ^{9}Be(n,nα) ^{5}He channel.

With same procedure for the recoil residual nucleus of the second emitted particle, the double differential cross section is obtained by

$$\frac{\mathrm{d}^2\sigma}{\mathrm{d}E_2^{\mathrm{c}}\mathrm{d}\,\Omega_{M_2}^{\mathrm{c}}} = \frac{\sigma}{4\pi}\sum_l(2l+1)f_l^{M_2}(E_2^{\mathrm{c}})\mathrm{P}_l(\cos\theta_{M_2}^{\mathrm{c}}) \tag{30}$$

where

$$f_l^{M_2}(E_2^{\mathrm{c}}) = \frac{(-1)^l}{4\gamma E_2^{\mathrm{r}}}f_l^{m_1}\mathrm{P}_l(\eta_R) \tag{31}$$

$$\gamma_R = \sqrt{\frac{E_1^{\mathrm{c}}M_2}{E_2^{\mathrm{r}}M_1}} = \frac{M_2}{m_2}\gamma \tag{32}$$

$$E_2^{\mathrm{r}} = \frac{m_2}{M_2}\varepsilon_2^{\mathrm{r}} \tag{33}$$

$$\eta_R = \sqrt{\frac{E_2^{\mathrm{r}}}{E_2^{\mathrm{c}}}\frac{\frac{E_2^{\mathrm{c}}}{E_2^{\mathrm{r}}} - 1 + \gamma_R^2}{2\gamma_R}} \tag{34}$$

The energy range of M_2 in C.M.S. is

$$E_{2,\min}^{\mathrm{c}} \le E_2^{\mathrm{c}} \le E_{2,\max}^{\mathrm{c}} \tag{35}$$

where

$$E_{2,\min}^{\mathrm{c}} = E_2^{\mathrm{r}}(1-\gamma_R)^2 \tag{36}$$

$$E_{2,\max}^{\mathrm{c}} = E_2^{\mathrm{r}}(1+\gamma_R)^2 \tag{37}$$

This formula of double differential cross section is used for the residual nucleus ^{8}Be in ^{9}Be(n,2n) ^{8}Be channel and the residual nucleus ^{5}He in ^{9}Be(n,nα) ^{5}He channel.

As the analytical expressions of all kinds of double differential cross sections can be given, the energies carried by each type of outgoing particle can also be obtained in analytical form. Since the recoil effect is taken into account in a strict way, the energy carried by each type of outgoing particle for normalized spectrum are shown as follows. In the C.M.S the energies carried by the first emitted particle and its residual nucleus are given by

$$E^{\mathrm{c}}(m_1) = \frac{M_1}{M_{\mathrm{C}}}(E^* - B_1 - E_{k_1}) \tag{38}$$

and

$$E^{\mathrm{c}}(M_1) = \frac{m_1}{M_{\mathrm{C}}}(E^* - B_1 - E_{k_1}) \tag{39}$$

In the laboratory system they become the following form:

$$E^{\mathrm{L}}(m_1) = \frac{m_n m_1}{M_{\mathrm{C}}^2}E_{\mathrm{n}} + E^{\mathrm{c}}(m_1) + \frac{2}{M_{\mathrm{C}}}\sqrt{m_{\mathrm{n}}M_1E_{\mathrm{n}}E^{\mathrm{c}}(M_1)}f_1^{m_1}(\mathrm{c}) \tag{40}$$

and

$$E^{\mathrm{L}}(M_1)=\frac{m_{\mathrm{n}}M_1}{M_{\mathrm{C}}^2}E_{\mathrm{n}}+E^{\mathrm{c}}(M_1)-\frac{2}{M_{\mathrm{C}}}\sqrt{m_{\mathrm{n}}M_1E_{\mathrm{n}}E^{\mathrm{c}}(M_1)}f_1^{m_1}(\mathrm{c}) \tag{41}$$

If a reaction channel is ended by gamma decay, then E_{k_1} is the gamma decay energy. Therefore, the total released energy reads

$$E_{\mathrm{total}}^{\mathrm{L}}=E^{\mathrm{L}}(m_1)+E^{\mathrm{L}}(M_1)+E_{k_1}=E_{\mathrm{n}}+B_{\mathrm{n}}-B_1 \tag{42}$$

and the energy balance is held. When the secondary particle can be emitted from level E_{k_1}, in terms of the formulation of the above, the energies carried by the second emitted particle m_2 and its residual nucleus M_2 in C.M.S are obtained by

$$E^{\mathrm{c}}(m_2)=\frac{M_2}{M_1}(E_{k_1}-B_2-E_{k_2})+2\frac{m_2}{M_1}E^{\mathrm{c}}(M_1) \tag{43}$$

and

$$E^{\mathrm{c}}(M_2)=\frac{m_2}{M_1}(E_{k_1}-B_2-E_{k_2})+2\frac{M_2}{M_1}E^{\mathrm{c}}(M_1) \tag{44}$$

The energies carried by m_2, M_2 in the laboratory system are given by

$$E^{\mathrm{L}}(m_2)=\frac{m_{\mathrm{n}}m_2}{M_{\mathrm{C}}^2}E_{\mathrm{n}}+E^{\mathrm{c}}(m_2)-2\frac{m_2}{M_{\mathrm{C}}}\sqrt{\frac{m_{\mathrm{n}}E_{\mathrm{n}}}{M_1}}\sqrt{E^{\mathrm{c}}(M_1)}f_1^{m_1}(\mathrm{c}) \tag{45}$$

and

$$E^{\mathrm{L}}(M_2)=\frac{m_{\mathrm{n}}M_2}{M_{\mathrm{C}}^2}E_{\mathrm{n}}+E^{\mathrm{c}}(M_2)-2\frac{M_2}{M_{\mathrm{C}}}\sqrt{\frac{m_{\mathrm{n}}E_{\mathrm{n}}}{M_1}}\sqrt{E^{\mathrm{c}}(M_1)}f_1^{m_1}(\mathrm{c}) \tag{46}$$

If the reaction is ended by gamma decay, then the E_{k_2} level carries out gamma decay. Therefore, the total released energy read as follows:

$$E_{\mathrm{total}}^{\mathrm{L}}=E^{\mathrm{L}}(m_1)+E^{\mathrm{L}}(m_2)+E^{\mathrm{L}}(M_2)+E_{k_2}=E_{\mathrm{n}}+B_{\mathrm{n}}-B_1-B_2 \tag{47}$$

The energy balance is still held. If the residual nuclei proceed via two-body separation at the state of the E_{k_2} level, the energies carried by two clusters in the C.M.S can also be obtained Analytically[1].

The energy balance of other reaction mechanism can also be given by one after another in succession.

Reference

[1] J.S.Zhang, Y.L.Hah and L.G.Cao Nucl. Sci. & Eng. 133 p.218 1999

CN0101625

Theoretical Calculations of Neutron Induced Reaction on $^{90,91,92,94,96}Zr$ and ^{Nat}Zr in the Energy Region from 0.01 MeV to 20 MeV

Liu Jianfeng Zhang Wei
(Department of Physics, Zhengzhou University, Zhengzhou)

Zhang Jingshang Liu Tingjin
(China Nuclear Data Center, CIAE, Beijing)

Abstract

Using program NUNF, all reaction cross sections, angular distributions of the elastic and discrete level inelastic scattering, double differential cross sections of the secondary particles and γ production data for n+^{90}Zr, ^{91}Zr, ^{92}Zr, ^{94}Zr, ^{96}Zr and ^{Nat}Zr in the nutron incident energy region from 0.01 MeV to 20 MeV were calculated. The calculated results were compared with the experimental data and the better coincidences were obtained. The calculated results are given in ENDF/B-6 format for both the natural element and its isotopes.

Introduction

The natural element Zr and its isotopes are important construction materials and the complete neutron nuclear reaction data are very important both for the basic science research and for the nuclear engineering as well as other science and technical domains.

The natural Zr has stable isotopes: ^{90}Zr, ^{91}Zr, ^{92}Zr, ^{94}Zr and ^{96}Zr, the abundance of them are 51.46%, 11.23%, 17.11%, 17.40% and 2.8% respectively. There are some experimental data both for the natural element and for its isotopes. They are mainly the total cross sections for ^{Nat}Zr, ^{90}Zr, ^{91}Zr, ^{92}Zr and ^{94}Zr, the nonelastic cross sections for ^{Nat}Zr, the (n,2n) cross sections for ^{Nat}Zr, ^{90}Zr and ^{96}Zr, the (n,p) crss sections for ^{90}Zr, ^{91}Zr, ^{92}Zr and ^{94}Zr, the (n,α) cross sections for ^{92}Zr, ^{94}Zr and ^{96}Zr, the (n, γ) cross sections for ^{Nat}Zr, ^{90}Zr and ^{91}Zr, the angular distributions of the elastic and

discrete level inelastic scattering, for ^{Nat}Zr ^{90}Zr, ^{91}Zr, ^{92}Zr and ^{94}Zr, and some cross sections of the elastic and discrete inelastic scattering as well as some double differential cross sections. The experimental data are all taken from EXFOR. As the experimental data are insufficient to practical application, the theoretical calculations of the complete nuclear reaction data are indispensable.

The trial calculations of the complete data for the natural Zr and its isotopes have once been done in terms of the program NDCP[1]. The calculated results show that when the compound statistical processes are considered alone, the emission probabilities of the higher energy charged particles will be reduced, when the incident energy is much higher, the cross sections of the charged particle emissions will be much less than the experimental values. The program NUNF[2] included the direct reactions, the pre-equilibrium processes and the compound statistical processes, and the ENDF-B6 format output, and in this code the energy balance is considered carefully. It will be seen that the calculated results coincide well with the experimental data.

As the complete reaction data both for the natural Zr and for its isotopes are required to give in ENDF/B-6 format respectively, the consistence between the data of the isotopes with that of the natural element should be considered. In the calculations of the natural element, the same optical potential parameters are used for all isotopes, but in the calculations of the isotopes, each isotope has its own optical potential parameters, therefore the consistence between the natural element and the isotopes is not easily to be obtained generally. In this work, some attentions in the adjustments of the parameters have been given to improve the consistence.

1 Parameters and Calculation Results

Using the program NUNF, the complete neutron reaction data for ^{90}Zr, ^{91}Zr, ^{92}Zr, ^{94}Zr, ^{96}Zr as well as ^{Nat}Zr have been calculated. The parameters of the discrete levels used in the calculations were taken from Nuclear Data Sheets. The cross sections and the angular distribution data of the direct inelastic scattering for the 5 isotopes calculated by Han Yinlu were adopted. The optical potential parameters, the level density parameters and the giant dipole resonance parameters have been adjusted in

the calculations. Their original values were taken from references [3],[4] and [6].

The neutron optical potential parameters used in the calculations for the direct inelastic scattering were adjusted slightly in the calculations of the total cross sections and the elastic scattering angular distributions for both the natural element and its 5 isotopes in order to obtain one group of the neutron optical potential parameters which are available for both the natural element and its isotopes. This ensures the consistence for the total and nonelastic cross sections between the natural element and its isotopes. The level density parameters of the residual nuclei and the exiton model parameters were adjusted first to obtain the better coincidence of the calculated neutron data with the experimental values. Then adjusting the optical potential of the charged particles and the level density parameters of the corresponding residual nucleus to obtain the better coincidences of the calculated results with the experiments. Finally the level density parameters and the giant dipole resonance parameters of the compound nucleus were adjusted to obtain the better coincidences of calculated results of the (n, γ) reaction data with the experimental values. The calculated results of the γ production data of the residual nucleus can be improved by adjusting its giant dipole resonance parameters. For the calculations of the natural element, the optical potential of ^{90}Zr is adopted. The level density parameters were adjusted again to improve the coincidences of the calculated results with the experimental data.

The final optical potential parameters of the neutron channel used for both the natural element and its 5 isotopes are:

V_0=54.896 V_1=-0.3867 V_2=0.00612 V_3=-24.0 V_4=0.0

U_0=-5.202 U_1=0.2234 U_2=-0.00057

W_0=9.5198 W_1=-0.1883 W_2=-12.0

V_{so}=5.518

r_r=1.1766 r_v=1.4691 r_s=1.2417 r_{so}=1.2423 r_c=1.25

a_r=0.7861 a_v=0.4001 a_s=0.4700 a_{so}=0.6525

The final optical potential parameters of α and p channels adopted for the 5 isotopes are listed in Table 1.

Table 1 The optical potential parameters for α and p

		V_R	r_R	a_R	W_V	W_S	r_I	a_I	V_{so}	r_{so}	a_{so}	r_c
^{90}Zr	P	-47.52+0.32E	1.17	0.75	2.7-0.22E	-10.62+0.25E	1.32	0.51	6.2	1.01	0.75	1.25
	α	-110.0+0.25E	1.15	0.75	-5.25+0.16E		1.40	0.84				1.30
^{91}Zr	P	-44.82+0.32E	0.971	0.615	2.7-0.22E	-8.26+0.175E	1.32	0.51	6.2	1.01	0.75	1.25
	α	-126.0+0.25E	1.15	0.75	-6.25+0.16E		1.19	0.84				1.30
^{92}Zr	P	-54.0+0.32E	1.17	0.75	2.7-0.22E	-11.8+0.25E	1.32	0.51	6.2	1.01	0.75	1.25
	α	-110.0+0.25E	1.15	0.75	-5.25+0.16E		1.40	0.84				1.25
^{94}Zr	P	-54.0+0.32E	1.17	0.75	2.7-0.22E	-11.8+0.25E	1.32	0.51	6.2			1.25
	α	-102.0+0.25E	1.15	0.75	-5.25+0.16E		1.40	0.84				1.25
^{96}Zr	P	-54.0+0.32E	1.17	0.75	2.7-0.22E	-11.8+0.25E	1.32	0.51	6.2	1.01	0.75	1.25
	α	-180.0+0.25E	1.20	0.75	-41.7+0.33E		1.40	0.84				1.25

Fig. 1 and Fig. 2 show the comparisons of the calculated results of the total cross sections with the experimental data for ^{90}Zr and ^{Nat}Zr respectively. Fig. 3 shows the comparisons of the calculated results of the nonelastic cross sections with the experiments for ^{Nat}Zr. Fig. 4 through Fig. 6 give the calculated results of the (n,2n) reation cross sections and their comparisons with the experimental results for ^{90}Zr, ^{96}Zr and ^{Nat}Zr respectively. Fig. 7 is the calculated results of the elastic scattering cross sections and their comparisons with the experiments for ^{Nat}Zr. Fig. 8 through Fig. 10 give the calculated results of the (n,p) cross sections and the comparisons with the experimental values for ^{90}Zr, ^{91}Zr and ^{92}Zr respectively. The calculated results of the (n,α) cross sections and the comparisons with the experiments for ^{92}Zr and ^{94}Zr are shown in Fig. 11 and Fig. 12 respectively. Fig. 13 and Fig. 14 are the calculated results of the (n,γ) cross sections and the comparisons with the experimental data for ^{90}Zr and ^{Nat}Zr respectively. Fig. 15 to Fig. 18 show the calculated results of the angular distributions of the elastic scattering and their comparisons with the experimental values at the neutron incident energy 5.9 MeV for ^{90}Zr as well as 14 MeV for ^{Nat}Zr. Fig. 19 through Fig. 22 show the calculated results of the cross sections and the angular distributions at the neutron incident energy 8 MeV of the discrete level inelastic scatterings to the first and the fourth levels for ^{94}Zr respectively. In Fig. 23and Fig. 24 are shown the double differential cross sections of all emission neutrons at E_n=14.1 and 18 MeV. From the figures mentioned above one can see that the calculated results are all well agreed with the experimental data.

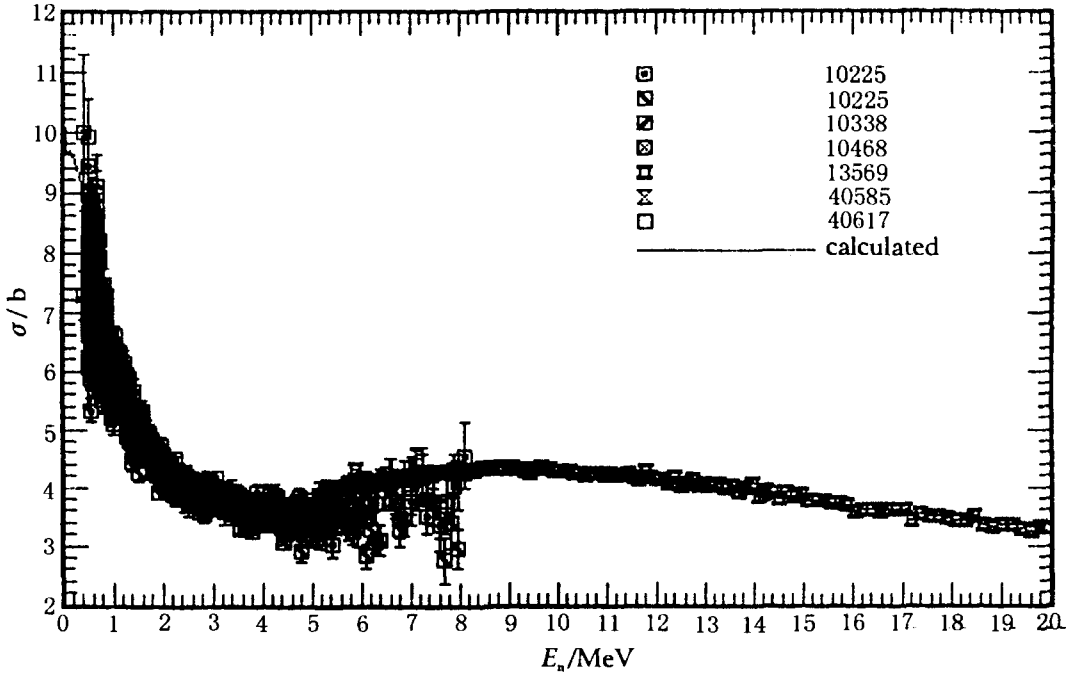

Fig. 1 ^{90}Zr total cross section

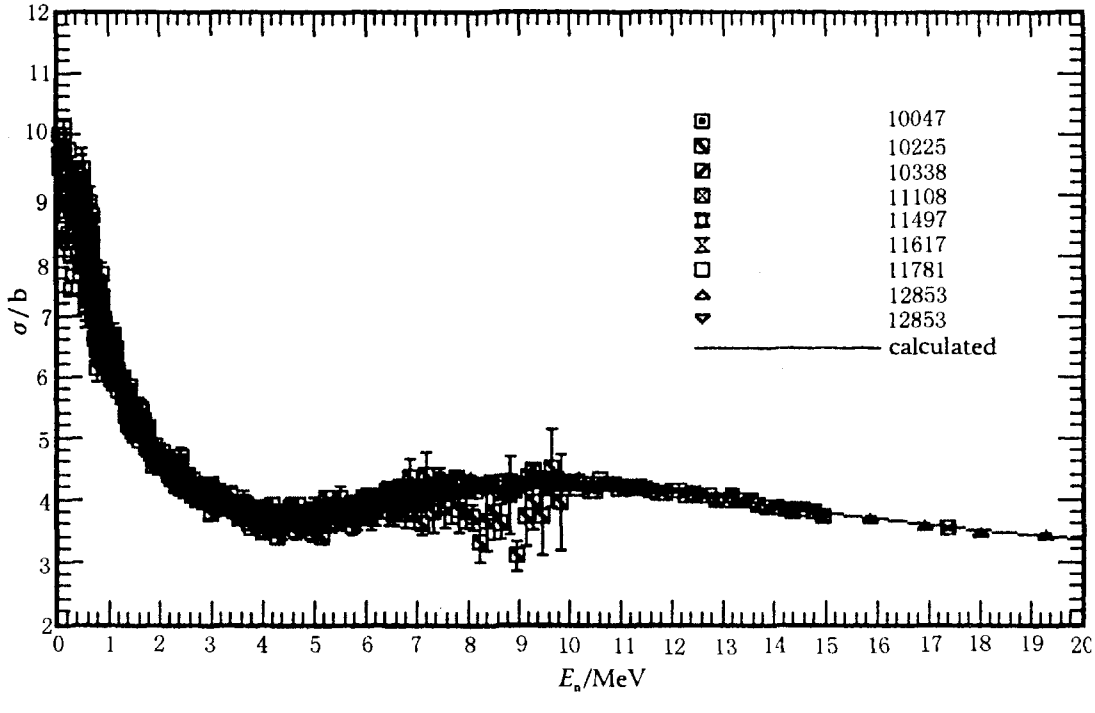

Fig. 2 ^{Nat}Zr total cross section

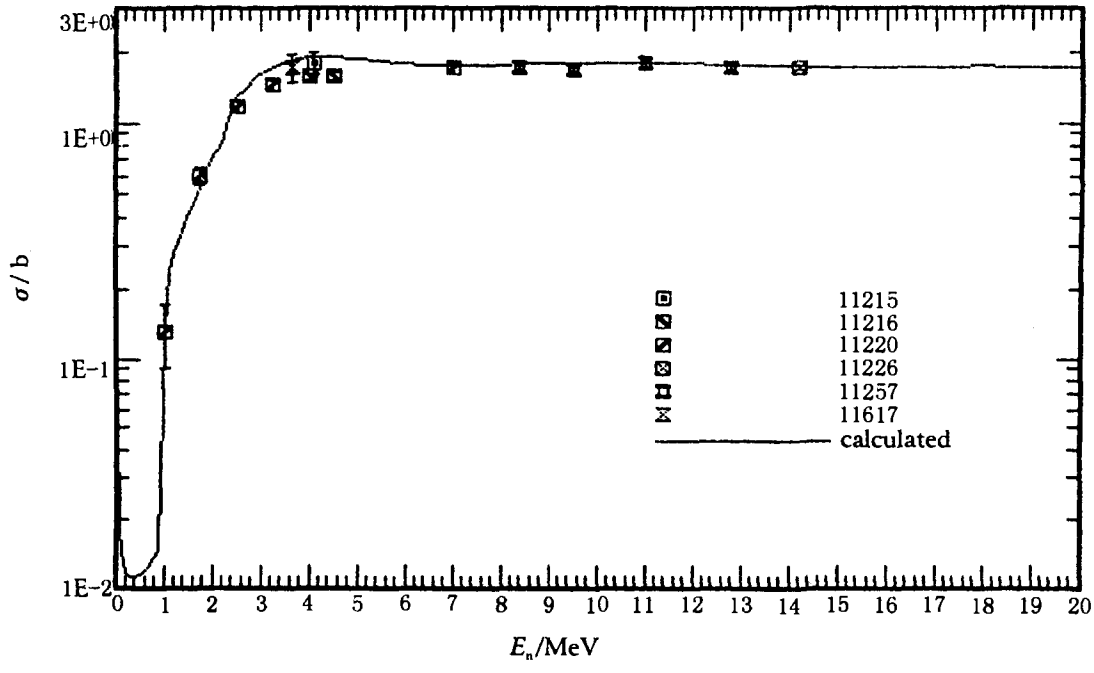

Fig. 3 ^{Nat}Zr (n,non) cross section

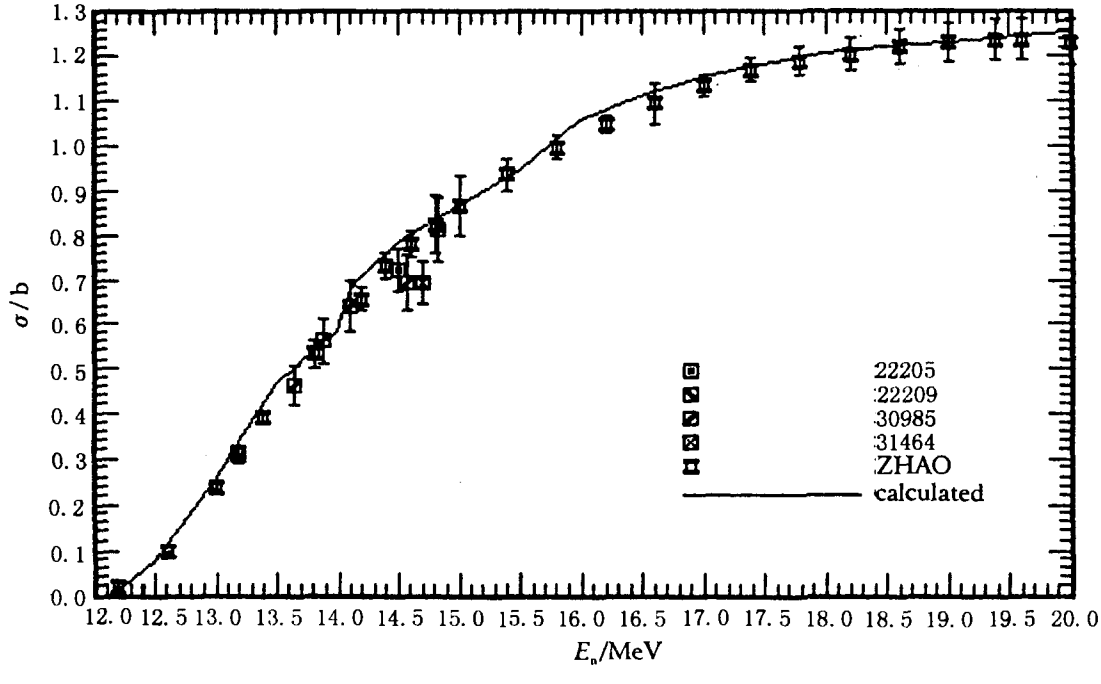

Fig. 4 ^{90}Zr (n,2n) cross section

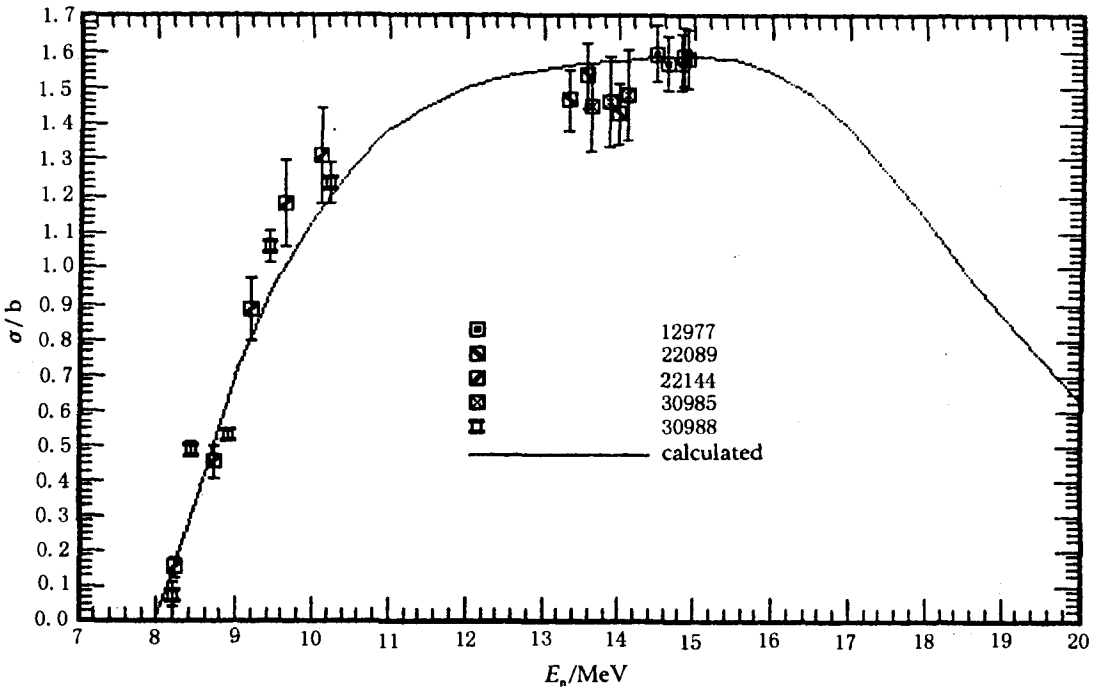

Fig. 5 ^{96}Zr (n,2n) cross section

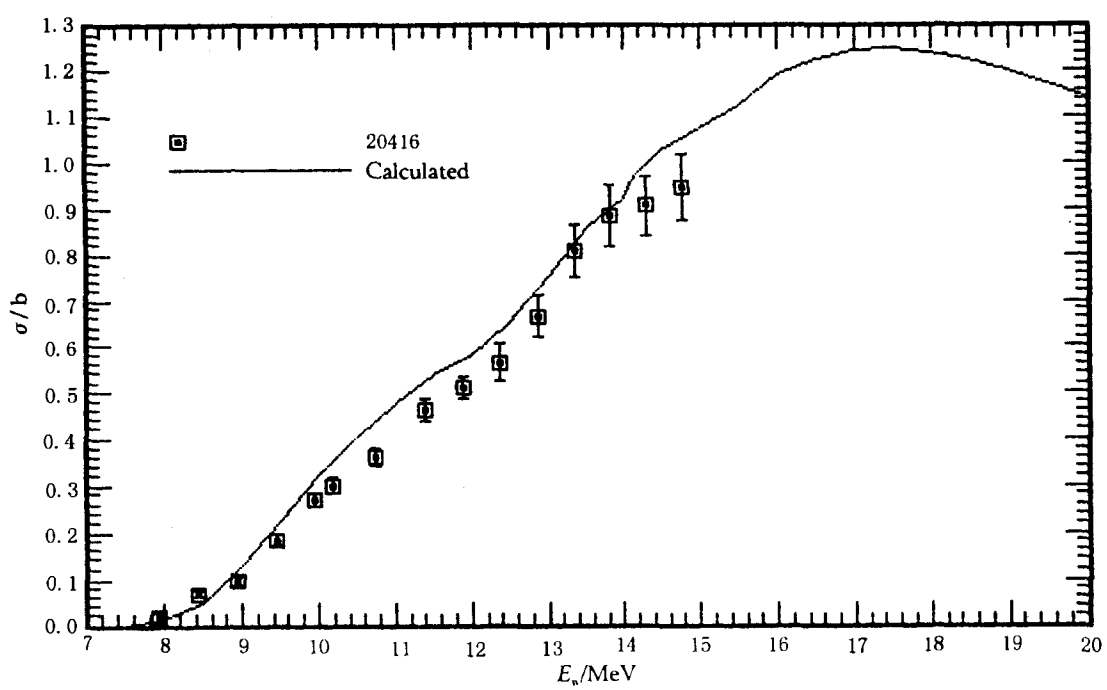

Fig. 6 ^{Nat}Zr (n,2n) cross section

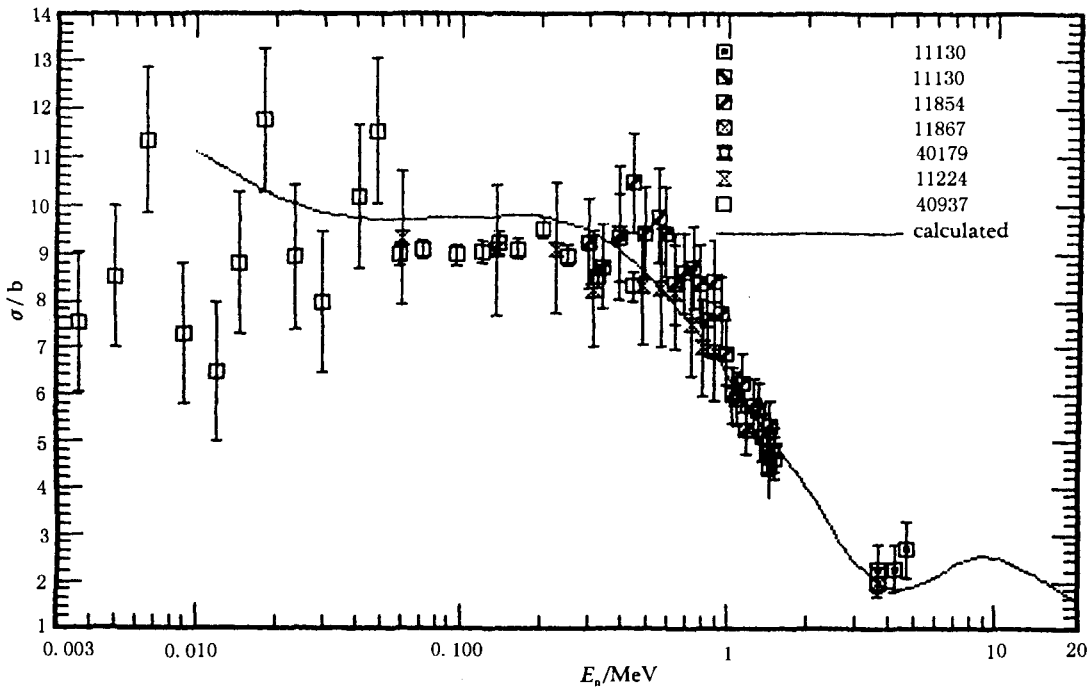

Fig. 7 ^{Nat}Zr (n,eL) cross section

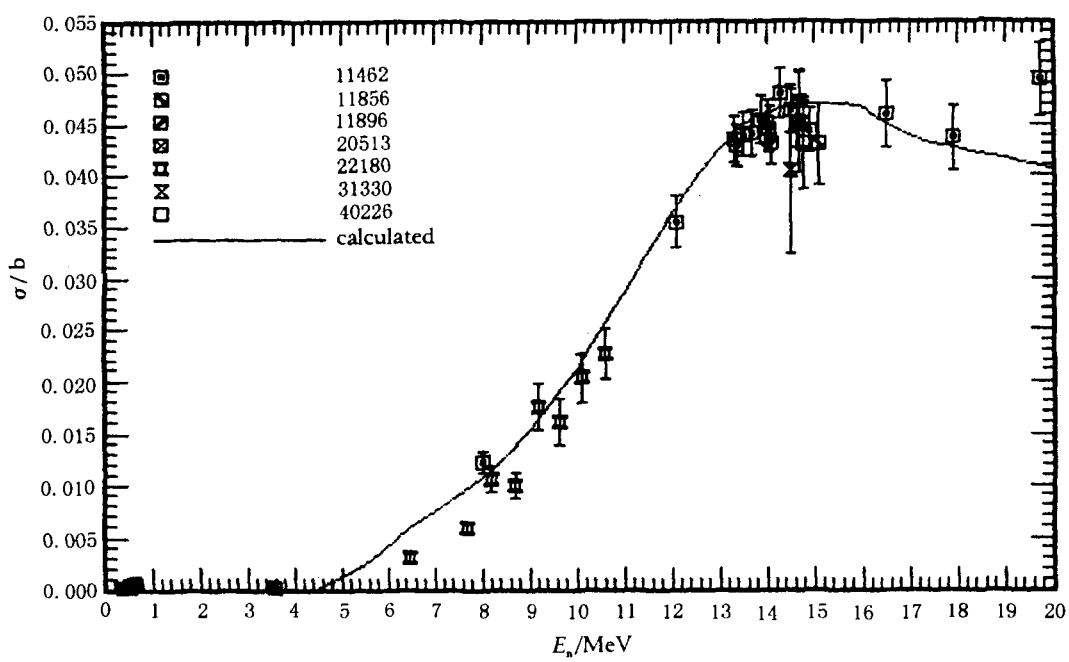

Fig. 8 ^{90}Zr (n,P) cross section

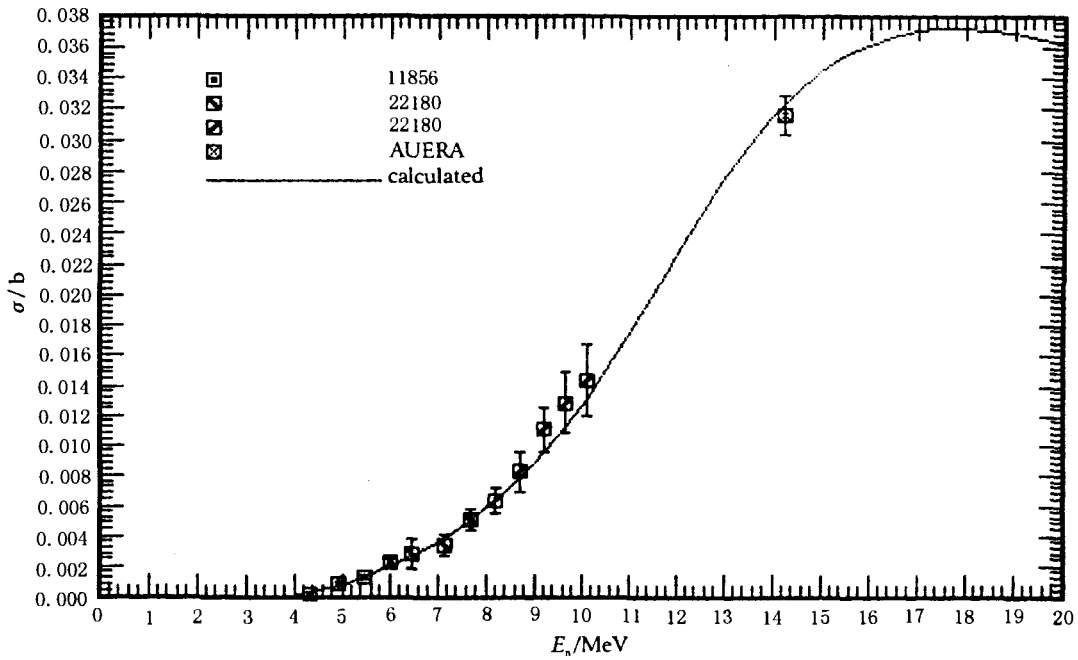

Fig. 9 ^{91}Zr (n,P) cross section

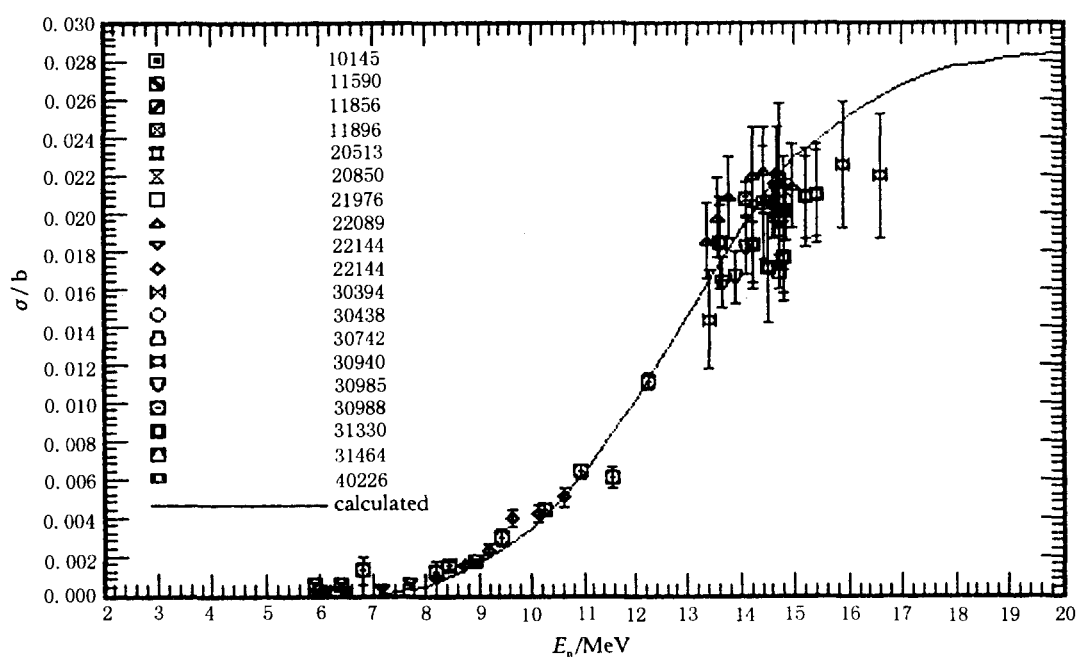

Fig. 10 ^{92}Zr (n,P) cross section

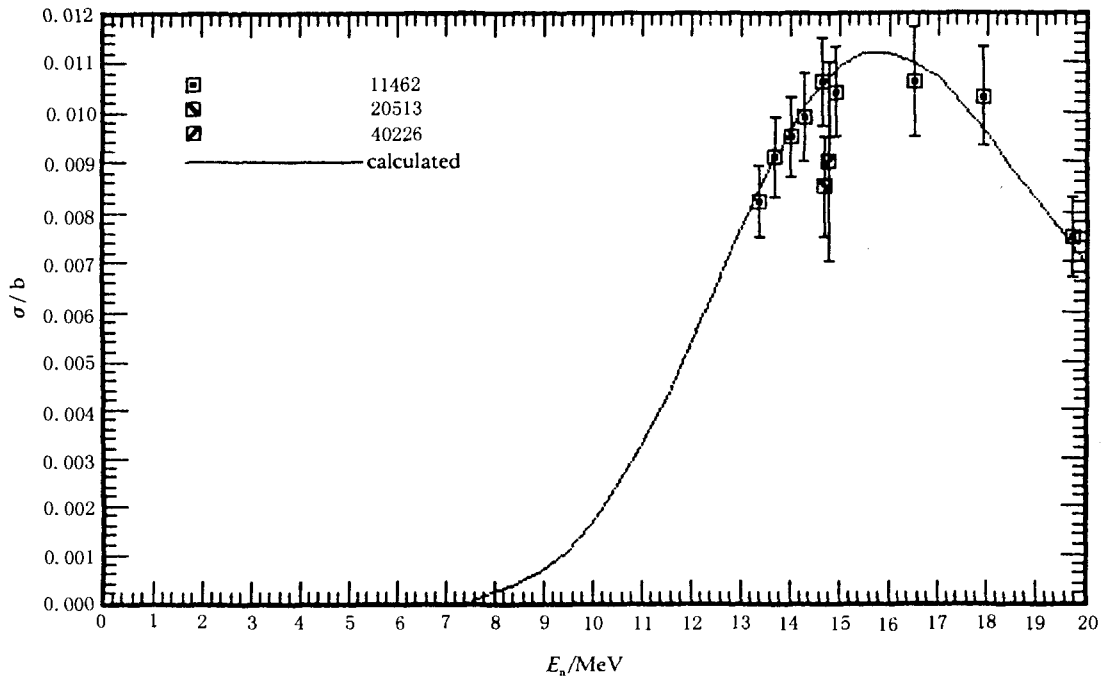

Fig. 11 ^{92}Zr (n,α) cross section

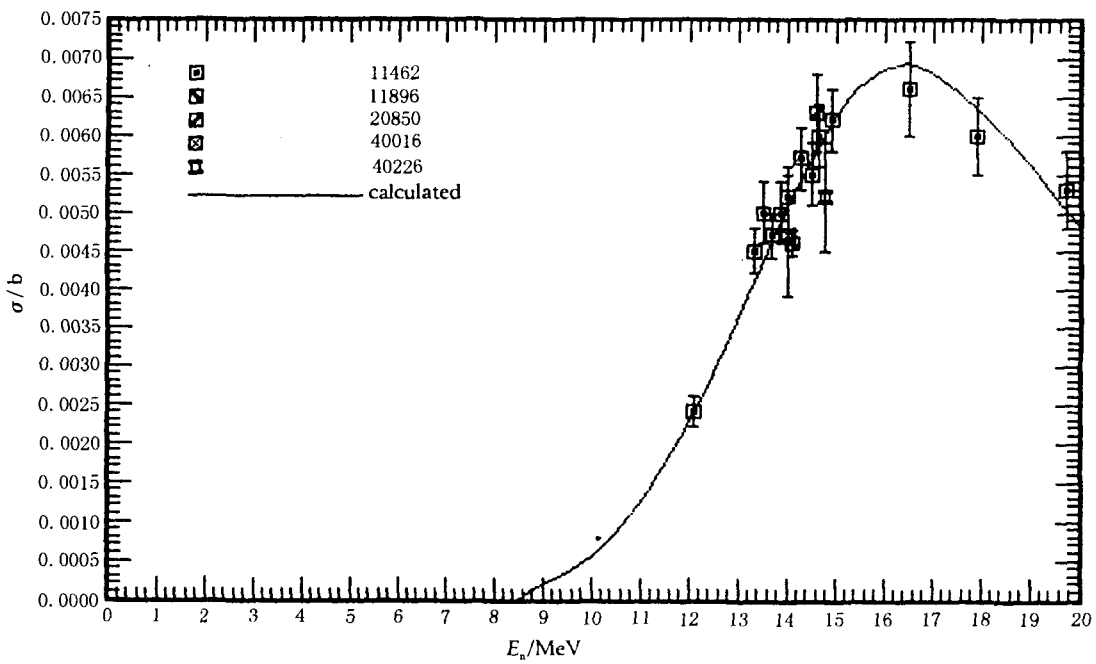

Fig. 12 ^{94}Zr (n, α) cross section

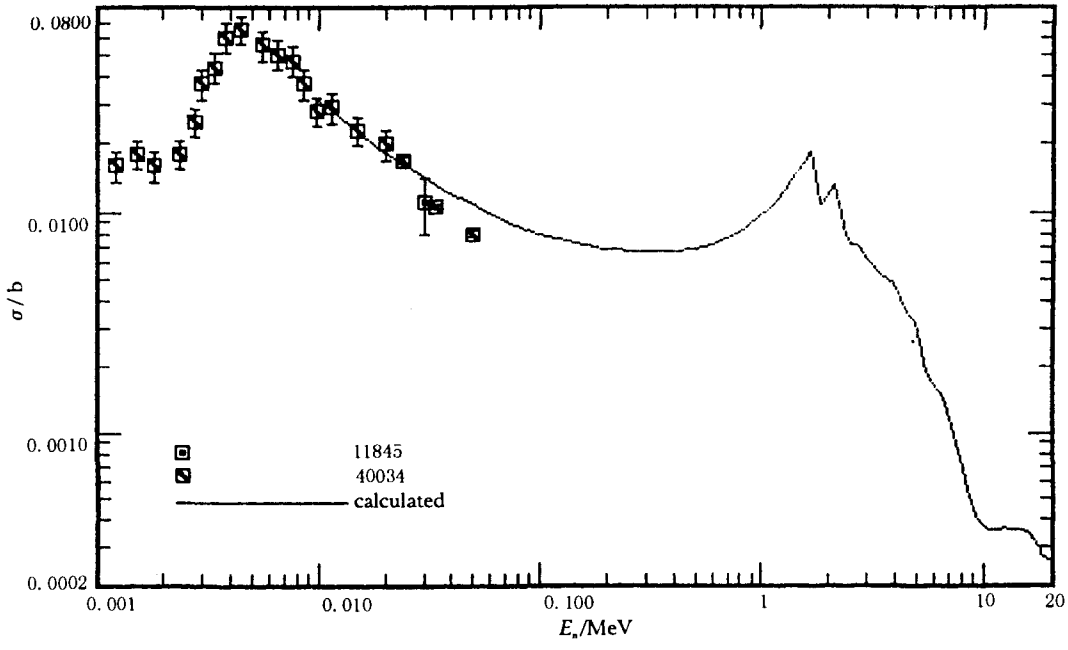

Fig. 13 ^{90}Zr (n,γ) cross section

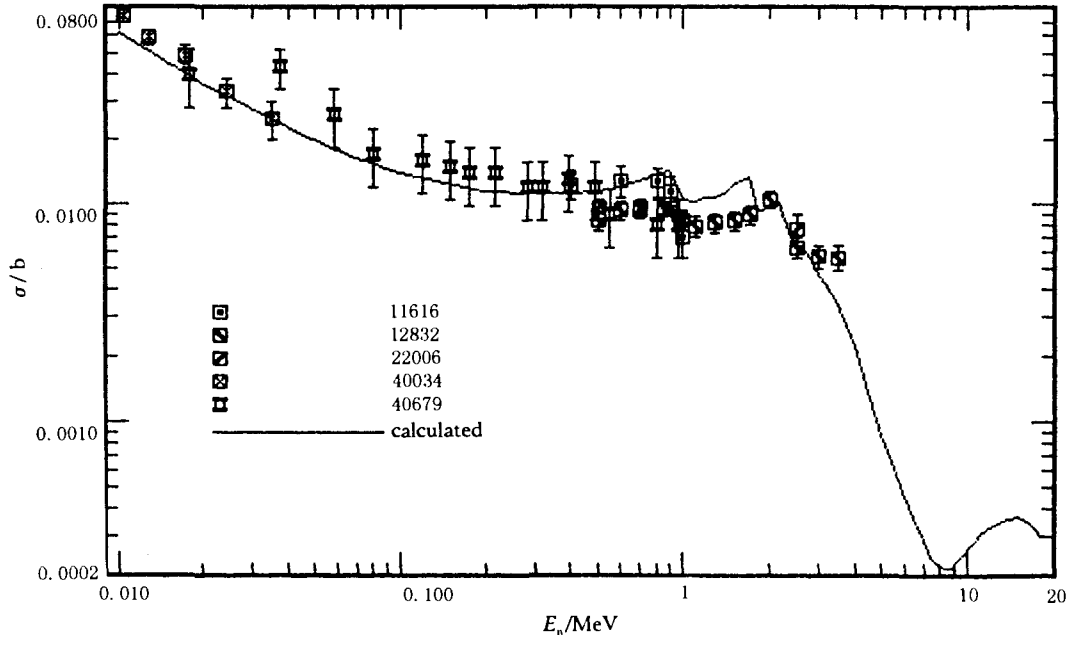

Fig. 14 ^{Nat}Zr (n,γ) cross section

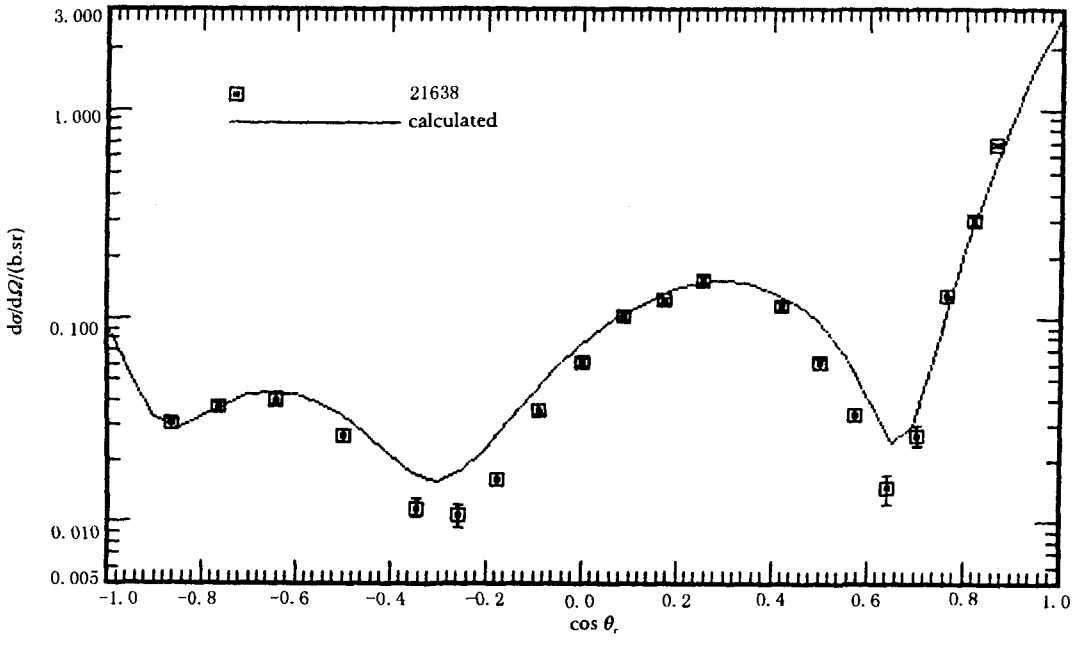

Fig. 15 ^{90}Zr (n,eL) augular distribution at 5.9 MeV

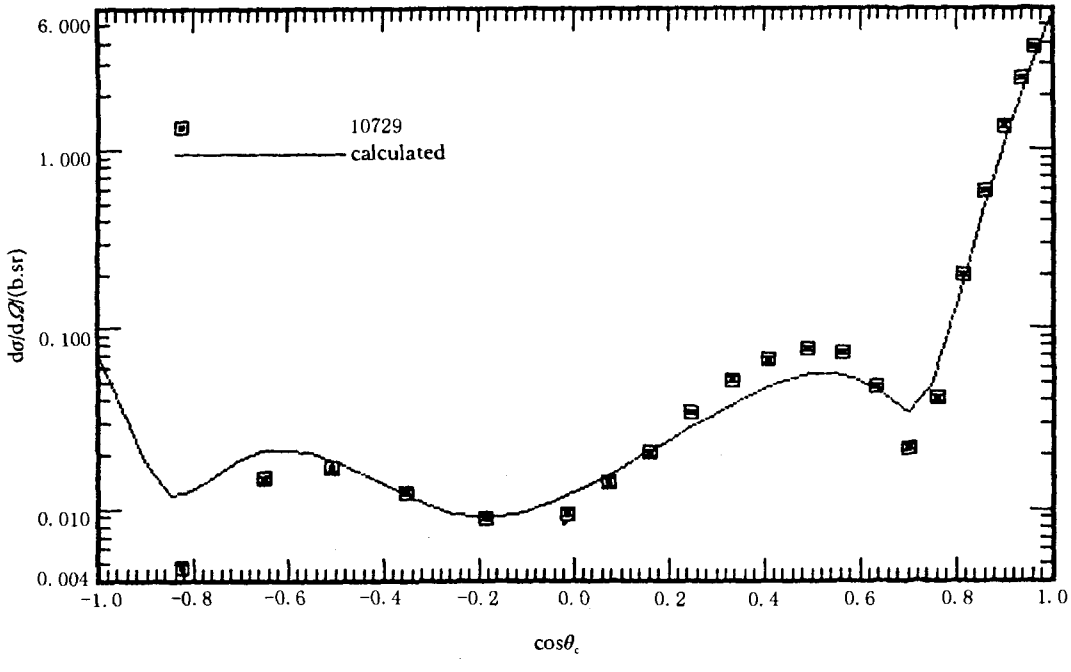

Fig. 16 ^{90}Zr (n,eL) augular distribution at 11 MeV

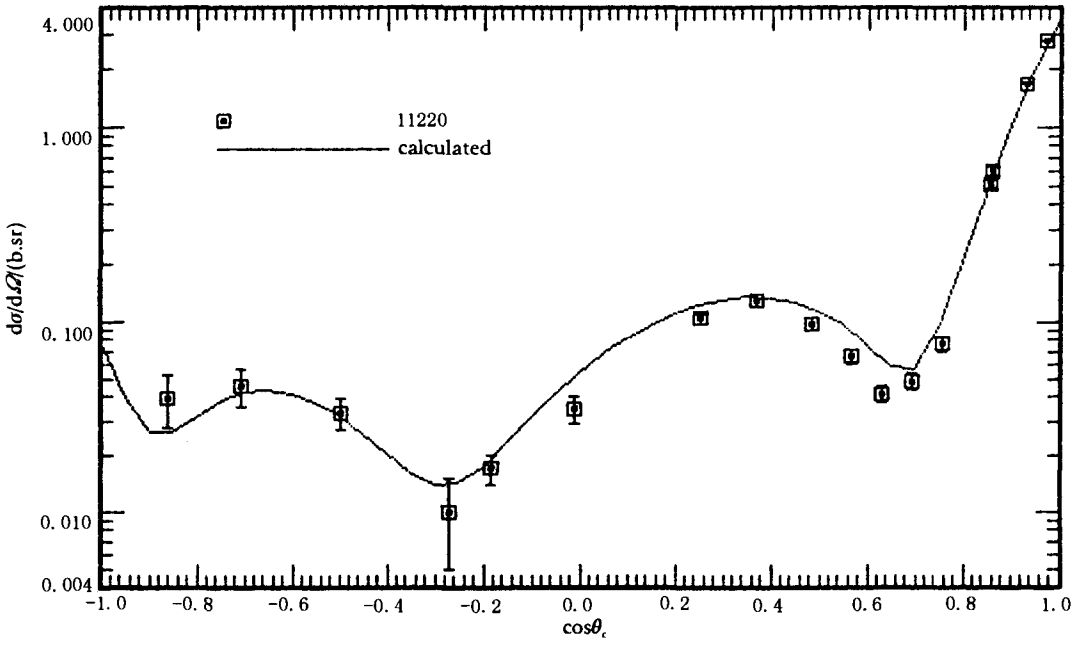

Fig. 17 ^{Nat}Zr (n,eL) augular distribution at 7 MeV

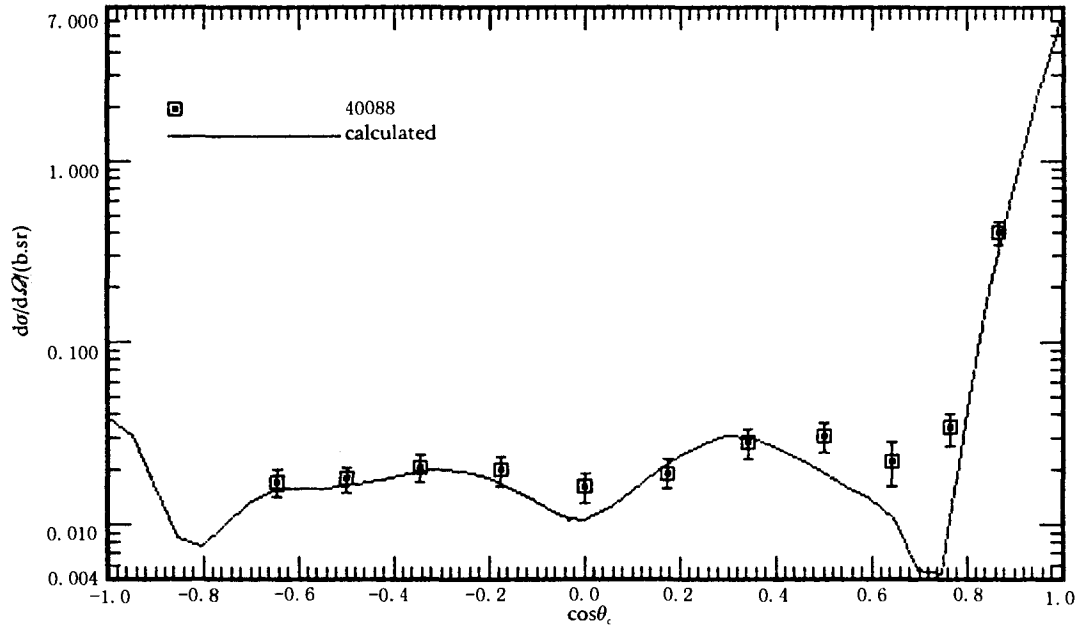

Fig. 18 ^{Nat}Zr (n,eL) augular distribution at 14 MeV

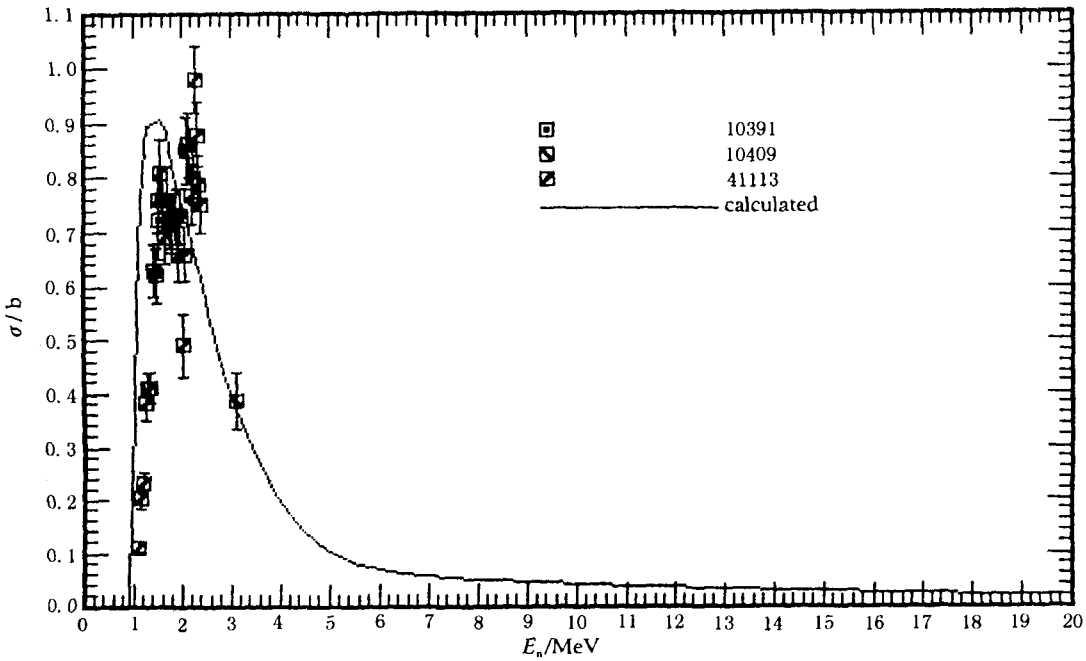

Fig. 19 ^{94}Zr (n,inL) to the first level cross section

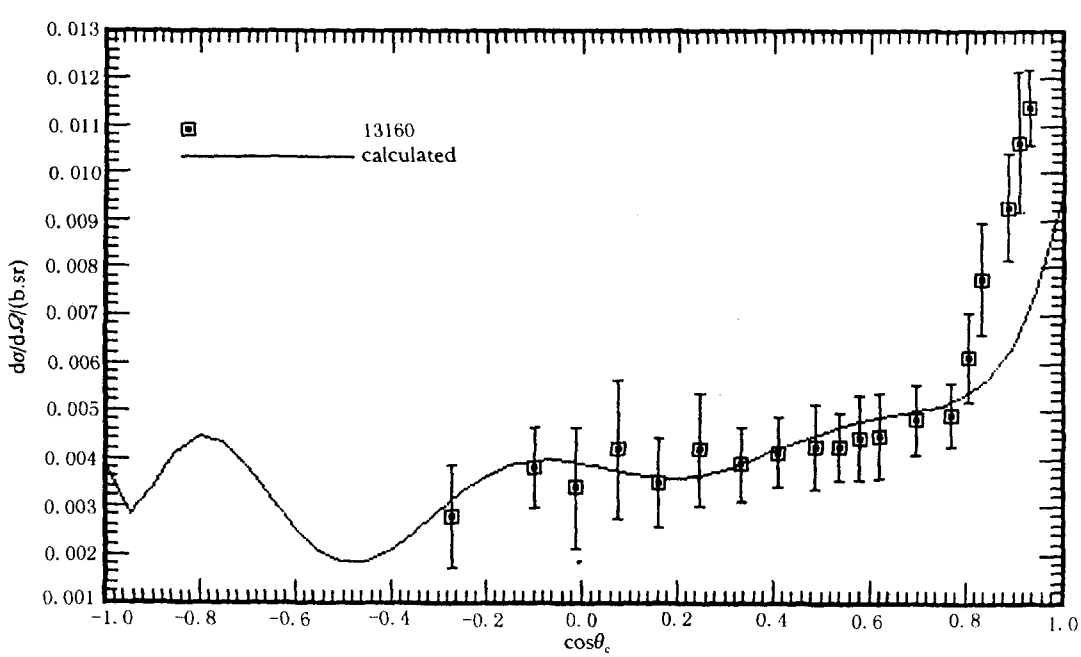

Fig. 20 ^{94}Zr (n,inL) augular distribution to the first level at 8 MeV

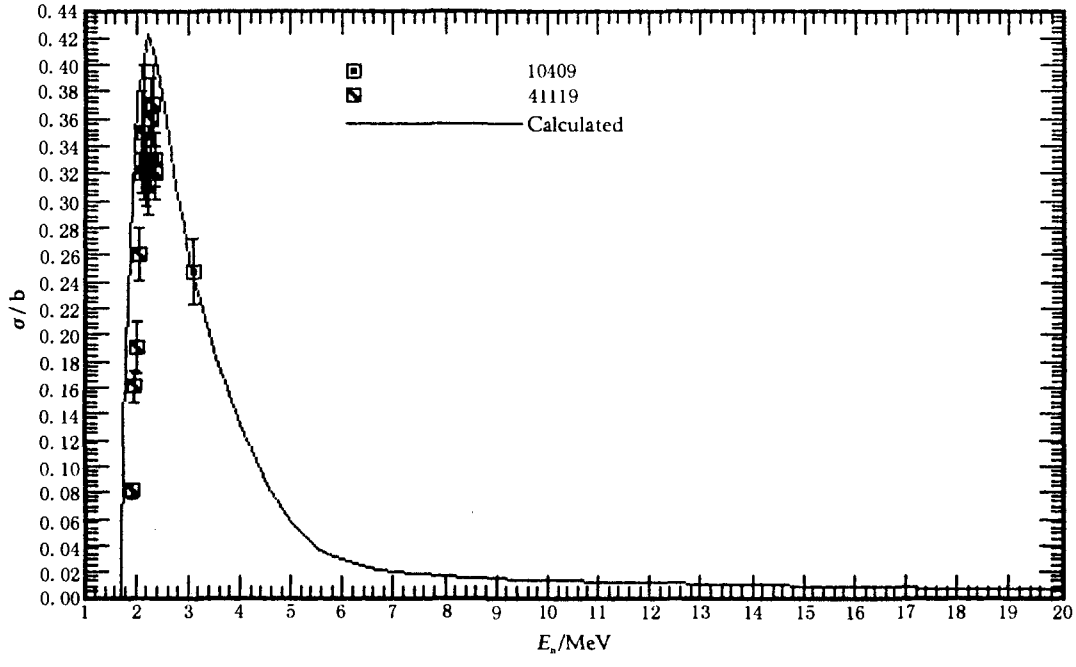

Fig. 21 ^{94}Zr (inL) cross section to the fourth level

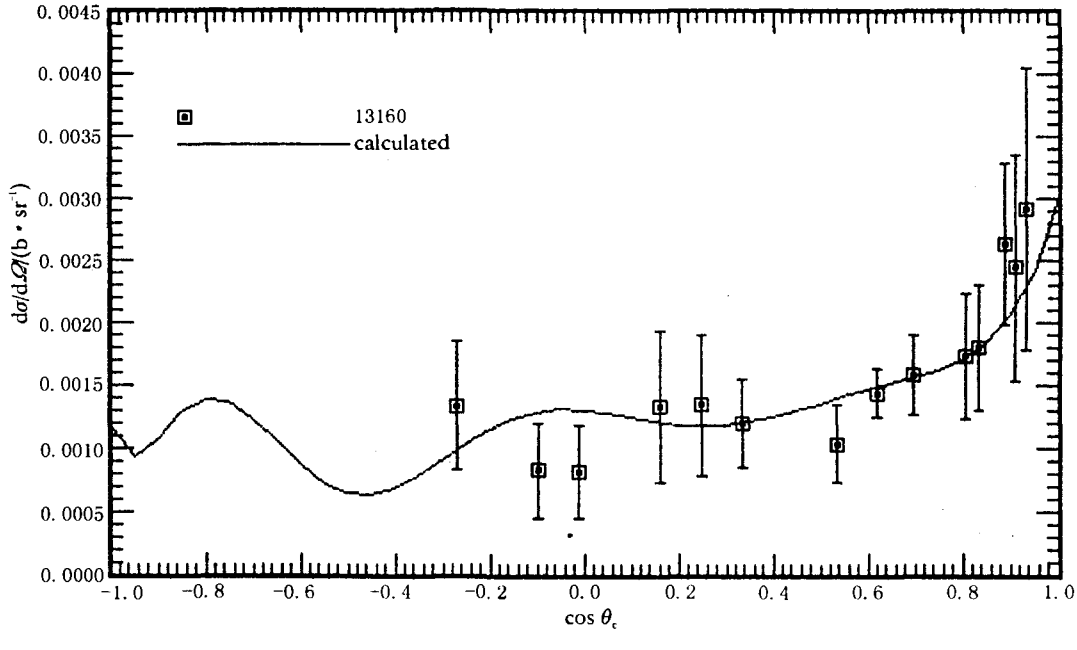

Fig. 22 ^{94}Zr (inL) augular distribution to the fourth level at 8 MeV

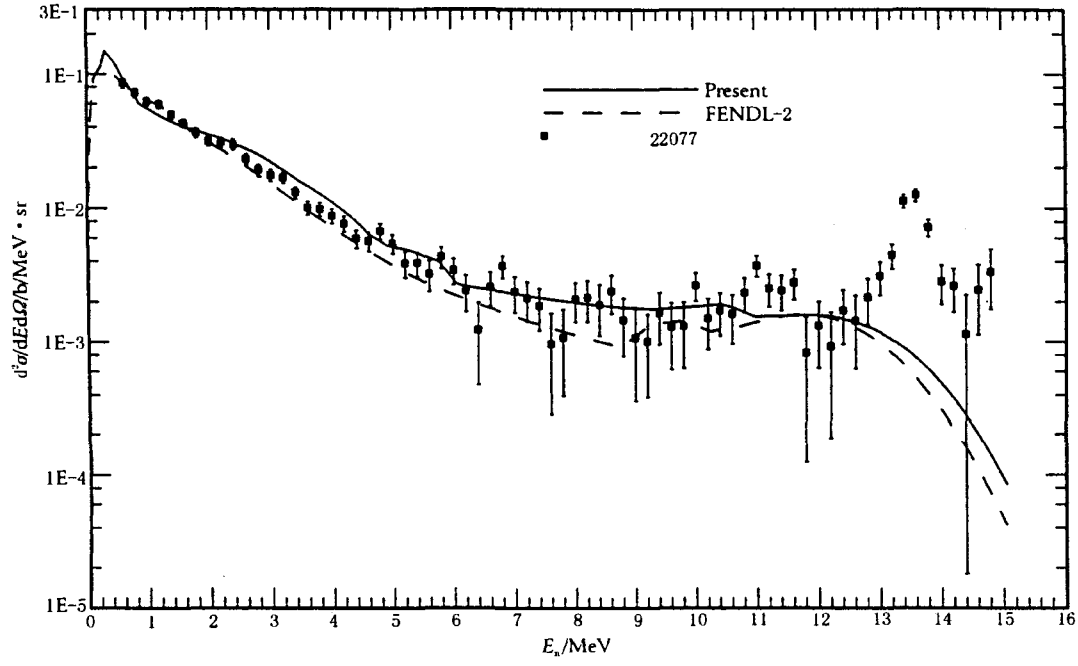

Fig. 23 Total double differ. CS of natural Zr at E_n=14.1 MeV, θ=150°

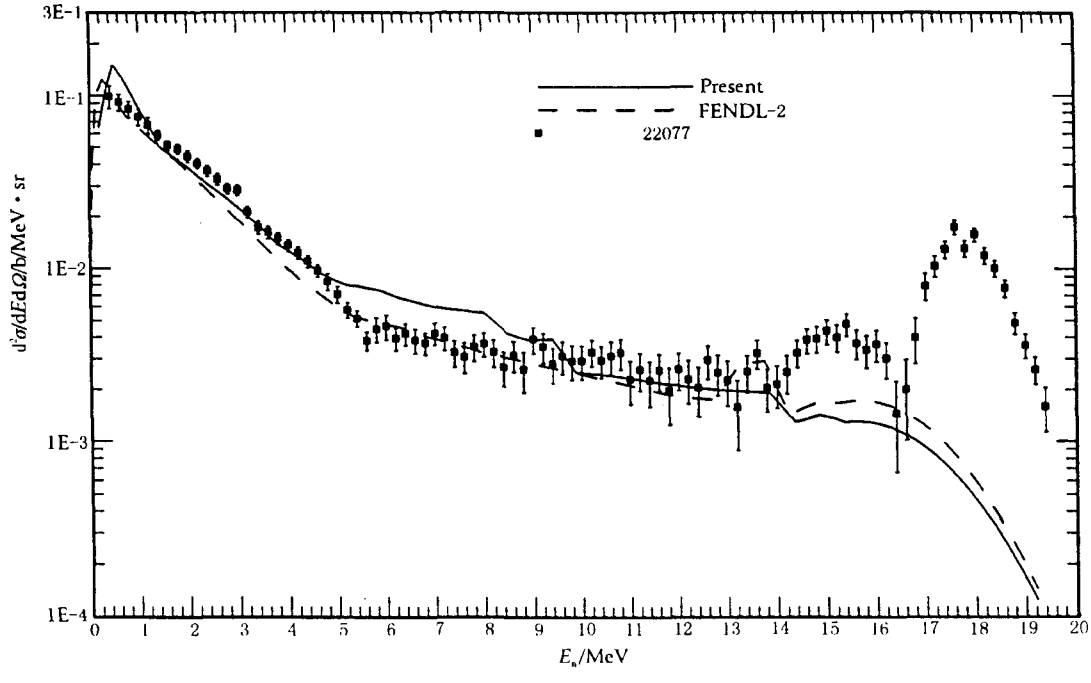

Fig. 24 Total double differ. CS of natural Zr at E_n=18 MeV, θ=60°

2 Summary

Using the program NUNF, the complete neutron reaction data for ^{90}Zr, ^{91}Zr, ^{92}Zr, ^{94}Zr, ^{96}Zr and ^{Nat}Zr were calculated and the calculated results were compared with the experimental data. The results show that.

1) As the pre-equilibrium processes are considered carefully in NUNF, the calculated results of the charged particle reaction cross sections, especially (n, α) and (n,p) cross sections, agree well with the experimental values.

2) Because the theoretical calculation results are all in agreement with the experimental values, the theoretical calculation results are reliable.

The authors would like to thank Han Yinlu for offering the useful data of the discrete inelatic scattering.

References

[1] Liu Jianfeng et al.,Commu. of Nucl. Data Progress, 10, 28(1993).

[2] Zhang Jinshang, Commu. of Nucl. Data Progress, 7, 14(1992).

[3] C.M. Perey et al., Atomic Data and Nuclear Data Tables, 17, 1(1976).

[4] A.Gilbert et al., Can. J. Phys., 43, 1446(1965).

[5] J. L. Cook et al., Aust. J. Phys., 20, 477(1967).

[6] S. S. Dietrich et al., Atomic Data and Nuclear Data Tables, 38, 199(1988).

Energy Balance on Light Nuclear Reactions

Zhang Jingshang

(China Nuclear Data Center, CIAE)

Introduction

A new model has been developed for calculating all kinds of reaction cross sections and double differential cross sections for neutron induced reactions on light nuclei[1]. In this model the recoil effect is taken into account exactly to keep the energy balance both in C.M.S. and L.S.

Because the Legendre expansion can be employed in C.M.S. for the file-6 outputting it will reduce the size of file-6 obviously. Since the emission of the first particle has definite energy, the secondary particle emissions have ring-type spectra in C.M.S. So the histogram form is the suitable format to record the file-6.

Based on the Heisenberg's uncertainty relation

$$\Delta E \Delta t \sim \frac{\hbar}{2} \tag{1}$$

the levels of light nuclei have their widths $\Gamma = \Delta E$, in other words the level have life time $\tau = \Delta t$. It means

$$\Gamma = \frac{\hbar}{2\tau} \tag{2}$$

The energy conservation is the eternal truth. On the other hand, beside energy resolution all of measurements have energy uncertainty due to the level's life time. Therefore the fitting procedure must involve the level broadening and energy resolution, but which is not needed in file-6 outputting.

The life time of levels means that the level has definite energy and does not have energy distribution, otherwise the reaction threshold would be undefined. Thus, there is not any contradiction between the Heisenberg's uncertainty relation and energy conservation.

1 Energy balance both in C.M.S. and L.S.

The physical quantities used in this section are defined as following:

E^*: excitation energy;

E_L: incident neutron energy;

M_C, M_T: mass of compound nucleus and target;

m_1, m_2: mass of the first and the second emitted particle, respectively;

ε_1, ε_2: energy of the first and the second emitted particle, respectively;

M_1, M_2: mass of residual nucleus after the first and the second emitted particles, respectively;

E_1, E_2: energy of residual nucleus after the first and the second emitted particles, respectively;

B_1, B_2: binding energy of the first and the second emitted particles in its compound nucleus, respectively;

E_{k_1}, E_{k_2} : level energy with the level order number k_1,k_2 reached by the first and the second emitted particles, respectively;

$f_l^{m_1}$ (c), $f_l^{M_1}$ (c): Legendre expansion coefficient of the first emitted particle and its residual nucleus, respectively in C.M.S.;

$f_l^{m_2}$, $f_l^{M_2}$: Legendre expansion coefficient of the second emitted particle and its residual nucleus, respectively;

with

$$f_l^{M_1} = (-1)^l \, f_l^{m_1} \tag{3}$$

Three motion systems are used in the model calculations, the physical quantities are specified by l, c and r for laboratory system (L.S.), center of mass system (C.M.S.) and recoil residual nucleus system (R.N.S.), respectively. The R.N.S. is a moving system accompanied with the recoil residual nucleus.

The normalized double differential cross section of outgoing in C.M.S is expressed by

$$\frac{\mathrm{d}^2\sigma}{\mathrm{d}\varepsilon_\mathrm{c}\,\mathrm{d}\,\Omega_\mathrm{c}} = \frac{1}{4\pi}\sum_l (2l+1) f_l^\mathrm{c}(\varepsilon_\mathrm{c})\mathrm{P}_l(\cos\theta_\mathrm{c})$$

In C.M.S the energy released by outgoing particles reads

$$E^\mathrm{c}_\mathrm{releas} = \sum_i E_i^\mathrm{c} = \frac{M_\mathrm{T}}{M_\mathrm{C}} E_\mathrm{L} + Q, \qquad E_i^\mathrm{c} = \int f_0^i(\varepsilon_\mathrm{c})\,\varepsilon_\mathrm{c}\mathrm{d}\,\varepsilon_\mathrm{c}$$

In C.M.S. the explicit expressions are given as follows:

The energy carried by the first emitted particle is

$$\varepsilon_1^\mathrm{c} = \frac{M_1}{M_\mathrm{C}}(E^* - B_1 - E_{k_1}) \tag{4}$$

The energy carried by its residual nucleus is

$$E_1^\mathrm{c} = \frac{m_1}{M_\mathrm{C}}(E^* - B_1 - E_{k_1}) \tag{5}$$

The energy carried by the second emitted particle is

$$\varepsilon_2^{\mathrm{c}} = \int_{\varepsilon_{2,\min}^{\mathrm{c}}}^{\varepsilon_{2,\max}^{\mathrm{c}}} f_0(\varepsilon_2^{\mathrm{c}})\varepsilon_2^{\mathrm{c}}\mathrm{d}\varepsilon_2^{\mathrm{c}} = \frac{M_2}{M_1}(E_{k_1} - B_2 - E_{k_2}) + \frac{m_2}{M_1}E_1^{\mathrm{c}} \tag{6}$$

The energy carried by its residual nucleus is

$$E_2^{\mathrm{c}} = \int_{\varepsilon_{2,\min}^{\mathrm{c}}}^{\varepsilon_{2,\max}^{\mathrm{c}}} f_0(\varepsilon_2^{\mathrm{c}})\varepsilon_2^{\mathrm{c}}\mathrm{d}\varepsilon_2^{\mathrm{c}} = \frac{M_2}{M_1}(E_{k_1} - B_2 - E_{k_2}) + \frac{M_2}{M_1}E_1^{\mathrm{c}} \tag{7}$$

Thus, the energy released by the first particle emission, the second particle emission and its residual nucleus with the final state at E_{k_2} is obtained by

$$\varepsilon_1^{\mathrm{c}} + \varepsilon_2^{\mathrm{c}} + E_2^{\mathrm{c}} = E^* - B_1 - B_2 - E_{k_2} \tag{8}$$

The residual nucleus at the excited state E_{k2} can emit the third particle or proceed three body break-up process or gamma decay. The explicit expressions can be found in the reference in detail. Therefore the energy balance is satisfied.

From the relation between C.M.S. and L.S. the velocity reads

$$\vec{V}_l = \vec{V}_0 + \vec{V}_{\mathrm{c}}$$

where $V_0 = \frac{\sqrt{2m_{\mathrm{n}}E_{\mathrm{L}}}}{M_{\mathrm{C}}}$ stands for the motion velocity of center of mass. Therefore the energy relation has the form

$$\varepsilon_{\mathrm{l}}^{\mathrm{i}} = \varepsilon_{\mathrm{c}}^{\mathrm{i}} + \frac{m_{\mathrm{n}}m_{\mathrm{i}}}{M_{\mathrm{C}}^2}E_{\mathrm{L}} + 2\frac{\sqrt{m_{\mathrm{n}}m_{\mathrm{i}}}}{M_{\mathrm{C}}}\sqrt{E_{\mathrm{L}}\varepsilon_{\mathrm{c}}^{\mathrm{i}}}\cos\theta_{\mathrm{c}}$$

In L.S. the energy released by outgoing particles reads

$$E_{\mathrm{releas}}^{\mathrm{l}} = \sum_i E_{\mathrm{i}}^{\mathrm{l}} = E_{\mathrm{L}} + Q$$

where

$$E_{\mathrm{i}}^{\mathrm{l}} = E_{\mathrm{i}}^{\mathrm{c}} + \frac{m_{\mathrm{n}}m_{\mathrm{i}}}{M_{\mathrm{C}}^2} + 2\frac{\sqrt{m_{\mathrm{n}}m_{\mathrm{i}}}}{M_{\mathrm{C}}}\sqrt{E_{\mathrm{L}}}\int f_{\mathrm{l}}^{\mathrm{i}}(\varepsilon_{\mathrm{c}})\sqrt{\varepsilon_{\mathrm{c}}}\mathrm{d}\varepsilon_{\mathrm{c}}$$

Since $\sum_i m_{\mathrm{i}} = M_{\mathrm{C}}$, the Legendre coefficients for l=1 satisfy the relation

$$\sum_i \sqrt{m_i} \int f_1^i(\varepsilon_c)\sqrt{\varepsilon_c}\,d\varepsilon_c = 0 \tag{9}$$

Taking n+^{9}Be as an example, there are five approaches to the (n,2n) reaction channel. The direct three body break-up process and the ^{5}He+^{5}He process are in isotropic distribution. So all of f_1=0, which is satisfied the above relation. The other two reaction channels, like n+n+^{8}Be, n+α +^{5}He approaches, have forward angular distribution for the first particle emission, while the sequential two-body reactions have backward angular distribution.

Denoting

$$J = \int f_1(\varepsilon_c)\sqrt{\varepsilon_c}\,d\varepsilon_c$$

thus,

$$J_{m_1} = f_1^{m_1}\sqrt{\frac{M_1}{M_C}(E^* - B_1 - E_{k_1})} \tag{10}$$

For the second emitted particle

$$J_{m_2} = \int_{\varepsilon_2^r(1-\gamma)^2}^{\varepsilon_2^r(1+\gamma)^2} f_1^{m_2}(\varepsilon_2^c)\sqrt{\varepsilon_2^c}\,d\varepsilon_2^c = -\frac{1}{4\gamma\varepsilon_2^r}\int f_1^{m_1} P_1(\eta)\sqrt{\varepsilon_2^c}\,d\varepsilon_2^c$$

where

$$\gamma = \sqrt{\frac{E_1^c m_2}{\varepsilon_2^r M_1}}, \qquad \varepsilon_2^r = \frac{M_2}{M_1}(E^* - B_1 - E_{k_1}), \qquad \eta = \sqrt{\frac{\varepsilon_2^r}{\varepsilon_2^c}}\left(\frac{\frac{\varepsilon_2^c}{\varepsilon_2^r} - 1 + \gamma^2}{2\gamma}\right)$$

one gets

$$J_{m_2} = -f_1^{m_1}\sqrt{\frac{m_2 m_1}{M_1 M_C}(E^* - B_1 - E_{k_1})} \tag{11}$$

The last two outgoing particles are from the separation of ^{8}Be or ^{5}He, the masses are denoted by m_3 and M_3, respectively.

$$J_{m_3} = \int_{\varepsilon_{min}^c}^{\varepsilon_{max}^c} f_1^{m_3}(\varepsilon^c)\sqrt{\varepsilon^c}\,d\varepsilon^c$$

where

$$f_1^{m_3}(\varepsilon^{\mathrm{c}}) = \int \frac{1}{4\gamma_{m_3}\varepsilon_3^{\mathrm{r}}} f_1^{M_2}(E_2^{\mathrm{c}})\eta_{m_3}\mathrm{d}E_2^{\mathrm{c}}$$

and

$$\eta_{m_3} = \sqrt{\frac{\varepsilon_3^{\mathrm{r}}}{\varepsilon^{\mathrm{c}}}\frac{\frac{\varepsilon^{\mathrm{c}}}{\varepsilon_3^{\mathrm{r}}} - 1 + \gamma_{m_3}^2}{2\gamma_3}} \qquad \gamma_{m_3} = \sqrt{\frac{E_2^{\mathrm{c}} m_3}{\varepsilon_3^{\mathrm{r}} M_2}}, \qquad \varepsilon_3^{\mathrm{r}} = \frac{M_3}{M_2}(E_{k_2} + Q)$$

and

$$f_1^{M_2}(E_2^{\mathrm{c}}) = -\frac{1}{4\gamma_R E_2^{\mathrm{r}}} f_1^{m_1} \mathrm{P}_1(\eta_R)$$

with

$$\eta_R = \sqrt{\frac{E_1^{\mathrm{c}}}{E_2^{\mathrm{c}}}\frac{\frac{E_2^{\mathrm{c}}}{E_2^{\mathrm{r}}} - 1 + \gamma_R^2}{2\gamma_R}}, \qquad E_2^{\mathrm{r}} = \frac{m_2}{M_1}(E_{k_1} - B_2 - E_{k_2}), \qquad \gamma_R = \sqrt{\frac{E_1^{\mathrm{c}} M_2}{E_2^{\mathrm{r}} M_1}}$$

$$\varepsilon_{M_2\,\min}^{\mathrm{c}} = E_2^{\mathrm{r}}(1-\gamma_R)^2, \qquad \varepsilon_{M_2\,\max}^{\mathrm{c}} = E_2^{\mathrm{r}}(1+\gamma_{\mathrm{R}})^2$$

So we have

$$f_1^{M_2}(E_2^{\mathrm{c}}) = -\frac{f_1^{m_1}}{8\gamma_R^2\sqrt{E_2^{\mathrm{r}}E_2^{\mathrm{c}}}}\left(\frac{E_2^{\mathrm{c}}}{E_2^{\mathrm{r}}} - 1 + \gamma_R^2\right)$$

Exchanging integration order J_{m_3} becomes

$$J_{m_3} = -\int_{\varepsilon_{M_2\,\min}^{\mathrm{c}}}^{\varepsilon_{M_2\,\max}^{\mathrm{c}}} \mathrm{d}E_2^{\mathrm{c}} \int_{\varepsilon_{\mathrm{c,min}}}^{\varepsilon_{\mathrm{c,max}}} \mathrm{d}\varepsilon_{\mathrm{c}} \frac{\frac{\varepsilon_{\mathrm{c}}}{\varepsilon_3^{\mathrm{r}}} - 1 + \gamma_{m_3}^2}{8\gamma_{m_3}^{\mathrm{r}}\sqrt{\varepsilon_3^{\mathrm{r}}}} \frac{f_1^{m_1}}{8\gamma_R^2\sqrt{E_2^{\mathrm{r}}E_2^{\mathrm{c}}}}\left(\frac{E_2^{\mathrm{c}}}{E_2^{\mathrm{r}}} - 1 + \gamma_R^2\right)$$

for a given value of E_2^{c}

with $\quad \varepsilon_{\mathrm{c,min}} = \left(\sqrt{\frac{m_3}{M_2}E_2^{\mathrm{c}}} - \sqrt{\varepsilon_3^{\mathrm{r}}}\right)^2 \qquad \varepsilon_{\mathrm{c,max}} = \left(\sqrt{\frac{m_3}{M_2}E_2^{\mathrm{c}}} + \sqrt{\varepsilon_3^{\mathrm{r}}}\right)^2$

Carrying out the integration over ε_{c}

$$J_{m_3} = \sqrt{\frac{m_3}{M_2}}\frac{f_1^{m_1}}{8\gamma_R^2\sqrt{E_2^{\mathrm{r}}}}\int_{\varepsilon_{M_2\,\min}^{\mathrm{c}}}^{\varepsilon_{M_2\,\max}^{\mathrm{c}}}\left(\frac{E_2^{\mathrm{c}}}{E_2^{\mathrm{r}}} - 1 + \gamma_R^2\right)\mathrm{d}E_2^{\mathrm{c}}$$

and carrying out the integration over E_2^{c}, it is obtained as

$$J_{m_3} = -f_1^{m_1}\sqrt{\frac{m_1 m_3}{M_1 M_C}(E^* - B_1 - E_{k_1})} \tag{12}$$

With the same procedure for M_3 we have

$$J_{M_3} = -f_1^{m_1}\sqrt{\frac{m_1 M_3}{M_1 M_C}(E^* - B_1 - E_{k_1})} \tag{13}$$

To check the energy conservation in L.S. the condition of eq. 9 becomes into the following form

$$\sqrt{m_1}J_{m_1} + \sqrt{m_2}J_{m_2} + \sqrt{m_3}J_{m_3} + \sqrt{M_3}J_{M_3}$$

$$= f_1^{m_1}\sqrt{\frac{m_1}{M_C M_1}(E^* - B_1 - E_{k_1})}[M_1 - m_2 - m_3 - M_3] = 0 \tag{14}$$

Since $M_1 - m_2 - m_3 - M_3$ the energy conservation in L.S. is still held.

In the ^{9}Be (n,α) ^{6}He* channel, ^{6}He proceeds the three body kreak-up process of ^{6}He* →n+n+α. The masses of the three body are denoted by m_a, m_b and m_c, respectively. For the first particle of the three body break-up process of ^{6}He*.

$$J_a = \int_{\varepsilon^c_{a\min}}^{\varepsilon^c_{a\max}} F_1^{(a)}(\varepsilon_c)\sqrt{\varepsilon_c}\,d\varepsilon_c$$

where

$$F_1^{(a)}(\varepsilon_c) = -\frac{f_1^{m_a}}{4\beta}\int_{\varepsilon^c_{a.\min}}^{\varepsilon^c_{a.\max}} \frac{S(\varepsilon_a)}{\sqrt{\varepsilon_a}} P_1\left(\frac{\varepsilon_c + \beta^2 - \varepsilon_a}{2\beta\sqrt{\varepsilon_c}}\right)d\varepsilon_a$$

$$\beta = \sqrt{\frac{m_a}{M_1}E_1^c}$$

Carrying out the integration with exchanging integration order and using the condition

$$\int_0^{\varepsilon^c_{1\max}} S(\varepsilon_a^c)\,d\varepsilon_a^c = 1$$

we have

$$J_a = -\frac{f_1^{m_a}}{8\beta^2}\int_0^{\varepsilon_{a,\max}^c} \mathrm{d}\varepsilon_a^c \frac{S(\varepsilon_a^c)}{\sqrt{\varepsilon_a^c}} \int_{(\sqrt{\varepsilon_a^c}+\beta)^2}^{(\sqrt{\varepsilon_a^c}+\beta)^2} (\varepsilon_c + \beta^2 - \varepsilon_a^c)\mathrm{d}\varepsilon_c = -f_1^{m_a}\sqrt{\frac{m_a}{M_1}E_1^c}$$

With the same procedure one can get J_b and J_c. The summation of the three body reads

$$J_a+J_b+J_c=-(m_a+m_b+m_c)\, f_1^{m_1}\ R \tag{15}$$

where

$$R = \sqrt{\frac{m_1}{M_1 M_C}(E^* - B_1 - E_{k_1})}$$

Adding the first emitted particle, we still obtain the identical result

$$J_{m_l}+ J_a+J_b+J_c =(M_l- m_a+m_b+m_c)\, f_1^{m_1}\ R=0 \tag{16}$$

Since $M_l= m_a+m_b+m_c$ the energy conservation in L.S. is still held for three body break-up process.

From the results one can see that the Legendre coefficients of l=1 of the emitted particles are always negative except the first one.

2 Conclusion and Remarks

The energy balance must be satisfied in the ENDF-B6 format to meet the needs in nuclear engineering applications.

- Because the new model can reproduce the experimental data satisfactorily, meanwhile the new model provides the way to output the file 6 for the light nuclei by Legendre coefficients in C.M.S. At first the fitting procedure is carried out, then the theoretical model can distinguish the double differential cross sections of the outgoing particles from different reaction channels to record the double differential cross section in its reaction channel.
- In the ENDF-B6 format the Legendre polynomial expansion can be used, in this way the size of the file 6 is reduced obviously, roughly the size in the form of the Legendre polynomial expansion is one order of magnitude smaller than the energy-angular tabular form.
- To obtain the energy-angular spectrum in laboratory system at a given angle θ_L, the formula are given as follows.

For the Legendre polynomial expansion at the incident neutron energy E_n with the energy region from $\varepsilon_{c(min)}=0$ to $\varepsilon_{c(max)}$, the maximum and the minimum outgoing energy at θ_L in L.S can be obtained as

$$\varepsilon_{L(min)}=0$$

and

$$\varepsilon_{L(max)}=(\beta\cos\theta_l+\sqrt{\varepsilon_{c(max)}-\beta^2\sin^2\theta_l})^2$$

where

$$\beta=\sqrt{\frac{m_n m_b}{M_c}}\sqrt{E_n}$$

Therefore in the energy region $\varepsilon_{L(min)}\leq\varepsilon_L\leq\varepsilon_{L(max)}$ the spectrum can be obtained as

$$\frac{d^2\sigma}{d\varepsilon_L d\Omega_L}=\frac{\sigma}{4\pi}\sqrt{\frac{\varepsilon_L}{\varepsilon_c}}\sum_l(2l+1)f_l(\varepsilon_c)P_l(\cos\theta_c)$$

The relation between ε_c, $\cos\theta_c$ and ε_L, $\cos\theta_L$ are

$$\varepsilon_c=\varepsilon_L+\beta^2-2\beta\sqrt{\varepsilon_L}\cos\theta_L$$

and

$$\cos\theta_c=\frac{\sqrt{\varepsilon_L}\cos\theta_L-\beta}{\sqrt{\varepsilon_L+\beta^2-2\beta\sqrt{\varepsilon_L}\cos\theta_L}}$$

The formulation of the new model gives the energy conservation exactly both in C.M.S. and L.S., and the ENDF-B6 outputting is reliable.

Reference

[1] J. S. Zhang et al., Nucl. Sci. Engin.133, 218 (1999)

$\gamma+{}^{9}$Be Reaction Below 30 MeV

Zhang Jingshang, Yu Baosheng, Han Yinlu
(China Nuclear Data Center. CIAE)

1 Reaction Mechanism of $\gamma+{}^{9}$Be Reaction

At low energies below 30 MeV, the Giant-Dipole Resonance (GDR) is the dominant excitation mechanism, in this energy region a simple approximation of isotropy is used to the angular distributions for outgoing particles. Semiclassical pre-equilibrium exciton model has been proved to be powerful tool for predicting particle emission spectra. Because of a strong recoil effect in light nucleus reactions, like ^{9}Be, the energy balance is strictly taken into account. The pre-equilibrium exciton model is implemented using a master equation approach, and generalized to include angular momentum and parity conservation, which allows a unified treatment of pre-equilibrium and equilibrium emission. The pick-up mechanism for cluster emissions are also included.

In view of $\gamma+{}^{9}$Be reactions for $E_{\gamma}\leq 30$ MeV the reaction channels are listed as the follows

$$\gamma+{}^{9}\mathrm{Be}=\begin{cases}\gamma+{}^{9}\mathrm{Be} & Q=0.0\ \mathrm{MeV}\\ n'+{}^{8}\mathrm{Be} & Q=-1.665\ \mathrm{MeV}\\ P+{}^{8}\mathrm{Li} & Q=-16.886\ \mathrm{MeV}\\ \alpha+{}^{5}\mathrm{He} & Q=-2.467\ \mathrm{MeV}\\ {}^{3}\mathrm{He}+{}^{6}\mathrm{He} & Q=-21.175\ \mathrm{MeV}\\ d+{}^{7}\mathrm{Li} & Q=-16.695\ \mathrm{MeV}\\ t+{}^{6}\mathrm{Li} & Q=-17.688\ \mathrm{MeV}\\ 2n+{}^{7}\mathrm{Be} & Q=-20.563\ \mathrm{MeV}\\ n,p+{}^{7}\mathrm{Li} & Q=-18.919\ \mathrm{MeV}\\ n,\alpha+\alpha & Q=-1.523\ \mathrm{MeV}\\ p,n+{}^{7}\mathrm{Li} & Q=-18{,}919\ \mathrm{MeV}\end{cases}$$

The (γ, ^{3}He) reaction is caused by emitting a ^{3}He to the ground state of ^{6}He,

while the levels of ^{6}He, will decay into $n+n+\alpha$ by three body break-up process. Reaction mechanism in the $\gamma+{}^9$Be system leading to decay into one neutron and two α particles may proceed via a number of different reaction channels, as two body break-up process or three body break-up process, the different approach strongly differs each other in their respective neutron and α particle energy spectra. The reaction channels to ^{9}Be(γ,n) 2α channel involved in the calculation are as follows:

(a) $\gamma+{}^9\mathrm{Be}\rightarrow n+{}^8\mathrm{Be}^*$ ($\alpha+\alpha$)

(b) $\gamma+{}^9\mathrm{Be}\rightarrow \alpha+{}^5\mathrm{He}^*$ ($n+\alpha$)

(c) $\gamma+{}^9\mathrm{Be}\rightarrow n, \alpha$

The discrete level scheme of every reaction channels at $E_\gamma \leq 30$ MeV are taken from the "Table of Isotopes", 1996[1]

The reaction situation from the compound nucleus ^{9}Be* to the discrete levels of the residual nuclei up to E_γ=30 MeV is presented in table 1. E_{th} refers to the threshold energy needed to open the k_2 level of the residual nucleus via k_1 level.

From Table 1 one can see that all of the excited levels of ^{9}Be can emit the secondary particles, therefore the (γ,$n\gamma$) reaction channel is always small enough to be omitted.

Following the first proton emission the residual nucleus is ^{8}Li. The ground state of ^{8}Li becomes into ^{8}Be through β^- decay, while the excited states of ^{8}Li can emit neutron and becomes into ^{7}Li. The ^{3}He emission results the residual nucleus ^{6}He, the ground state of which becomes to ^{6}Li through β^- decay, while the excited state of ^{6}He undergoes the three-body breakup process to $n+n+\alpha$. The residual nucleus of (γ,2n) reaction channel is ^{7}Be, which becomes ^{7}Li through EC with $T_{1/2}$=53.29 d. The residual nucleus ^{5}He of the (γ,α) reaction channel is separated spontaneously into $n+\alpha$.

2 Reaction Mechanism from Levels to Levels

The formulation of the double differential cross sections from discrete levels to discrete levels of sequential two-body reactions, three-body breakup process and the double differential cross sections of cluster separation can be found in the Refs 2 and 3.

The residual nuclei ^{8}Be and ^{5}He are unstable and separated into two clusters

spontaneously. For instance $^{8}Be \rightarrow \alpha+\alpha$, with Q=0.092MeV, $^{5}He \rightarrow \gamma+\alpha$, with Q=0.894 MeV, respectively.

Table 1. The reaction situation of the (γ,2n), (γ,np) (γ,nα) and (γ,pn) reactions up to E_γ=30 MeV.

	E_{th}/ MeV	k_1	k_2			E_{th}/ MeV	k_1	k_2
(γ,2n)	20.58	7	gs		(γ,2n)	20.74	8	gs
(γ,2n)	20.91	9	gs		(γ,2n)	21.07	10	gs
(γ,2n)	21.53	11	gs		(γ,2n)	21.77	12	gs
(γ,2n)	21.87	13	gs		(γ,2n)	22.57	14	gs
(γ,2n)	23.37	15	gs		(γ,2n)	23.67	16	gs
(γ,2n)	23.72	17	gs					
(γ,np)	19.31	5	gs		(γ,np)	19.82	6	gs - 1
(γ,np)	20.58	7	gs - 1		(γ,np)	20.74	8	gs - 1
(γ,np)	20.91	9	gs - 1		(γ,np)	21.07	10	gs - 1
(γ,np)	21.53	11	gs - 1		(γ,np)	21.77	12	gs - 1
(γ,np)	21.87	13	gs - 1		(γ,np)	22.57	14	gs - 1
(γ,np)	23.37	15	gs - 1		(γ,np)	23.67	16	gs - 2
(γ,np)	23.72	17	gs - 2					
(γ,nα)	4.705	1	gs		(γ,nα)	13.07	2	gs
(γ,nα)	13.07	3	gs		(γ,nα)	18.29	4	gs
(γ,nα)	19.31	5	gs		(γ,nα)	19.82	6	gs
(γ,nα)	20.58	7	gs		(γ,nα)	20.74	8	gs
(γ,nα)	20.91	9	gs		(γ,nα)	21.07	10	gs
(γ,nα)	21.53	11	gs		(γ,nα)	21.77	12	gs
(γ,nα)	21.87	13	gs		(γ,nα)	22.57	14	gs
(γ,nα)	23.37	15	gs		(γ,nα)	23.67	16	gs
(γ,nα)	23.72	17	gs					
(γ,pn)	19.16	2	gs		(γ,pn)	20.12	3	gs - 1
(γ,pn)	22.31	4	gs - 1		(γ,pn)	23.01	5	gs - 1
(γ,pn)	23.45	6	gs - 1		(γ,pn)	24.91	7	gs - 1

3 Results and Summary

The GLUNF code is developed for calculating the inter-related data below 30 MeV. The physical quantities calculated numerically by GLUNF code contain:

(1) photoabsorption cross sections;

(2) all kinds of reaction cross sections with different reaction mechanism and spectra of particles, like neutron, proton, α particle, triton and deuteron;.

(3) the total spectrum of the emitted neutron;

(4) outputting the data in ENDF/B-6 format.

The model has been used for calculating the cross sections of $\gamma+^{9}Be$ reactions. The plotting of the (γ, abs), (γ, 2n) and (γ, n+np+2n) evaluated cross sections are shown through Fig.1 to Fig.4, the experimental data are taken from Refs. 4 to 9. All of the comparisons between the experimental data and the calculated results are in good fitting. The plotting of every reaction channels is shown in Fig.5.

Lack of the experimental data on energy spectrum, so this kind of plotting is not given.

In this model the sequential emissions, two-body separation reactions and three-body breakup process are included, from which the different respective energy-spctra are obtained as the components of the total spectrum of outgoing particles. The E_1, M_1 and E_2 mechanism are taken into account for γ emission in pre-equilibrium and equilibrium processes. For light nucleus the direct emissions are not included, due to very small contribution at low energies.

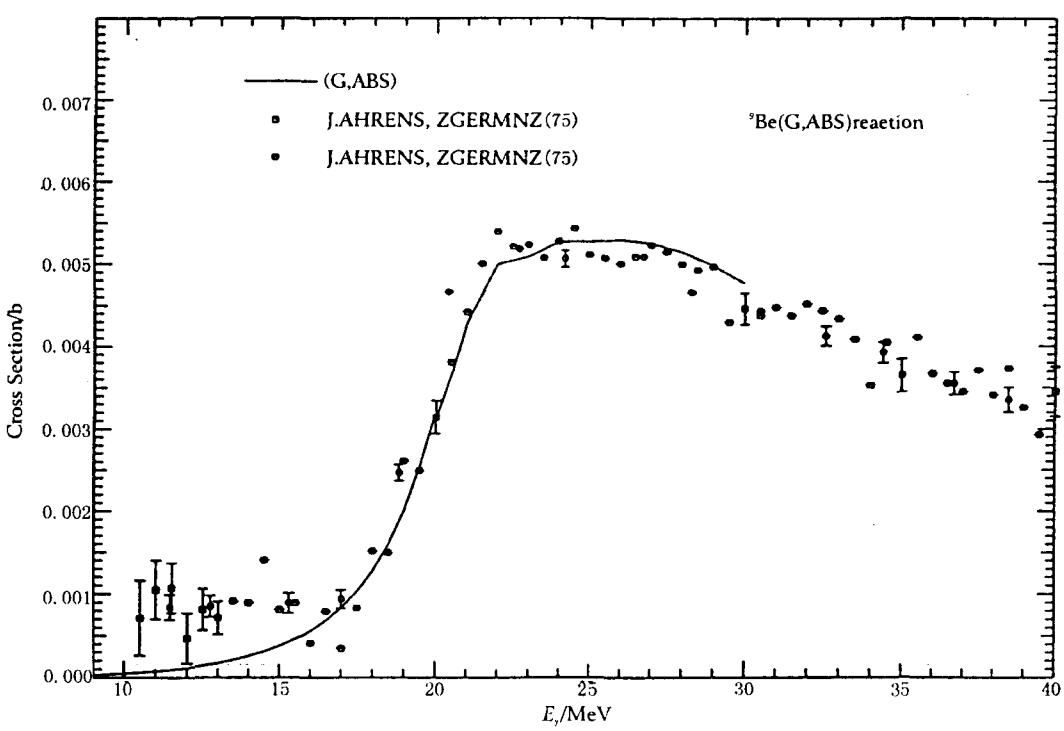

Fig. 1 Comparison of evaluated and measured data on ^{9}Be

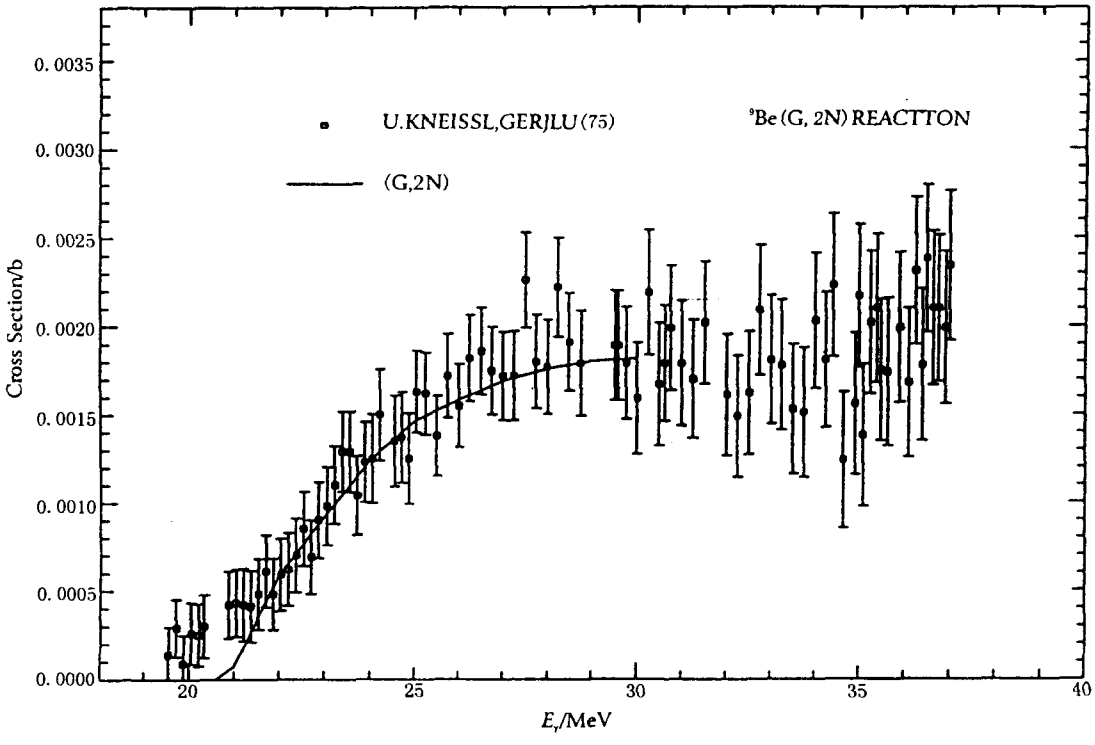

Fig. 2 Comparison of evaluated and measured data on ^{9}Be

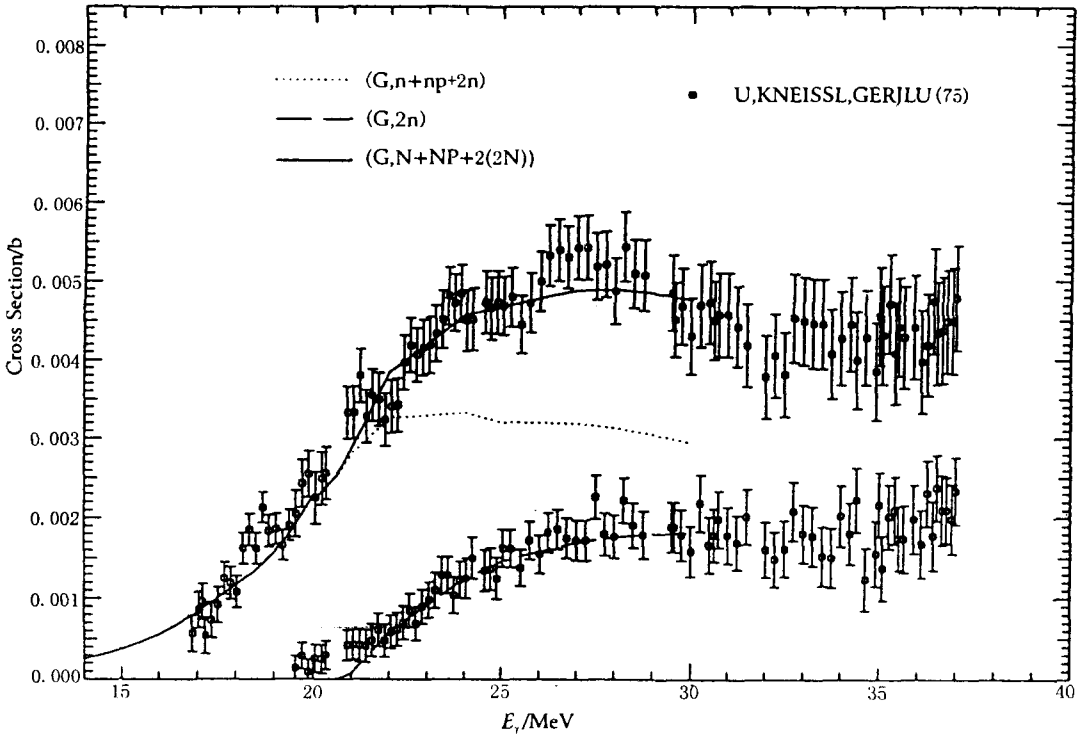

Fig. 3 Comparison of evaluated and measured data on ^{9}Be

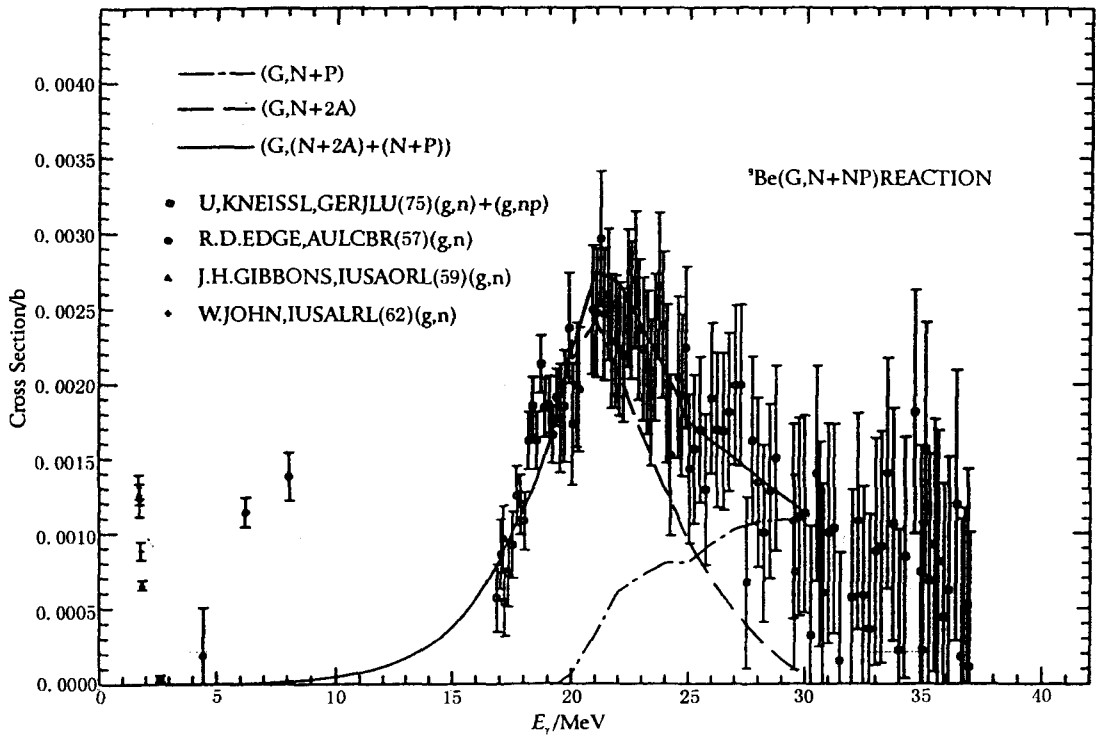

Fig. 4 Comparison of evaluated and measured data on ^{9}Be

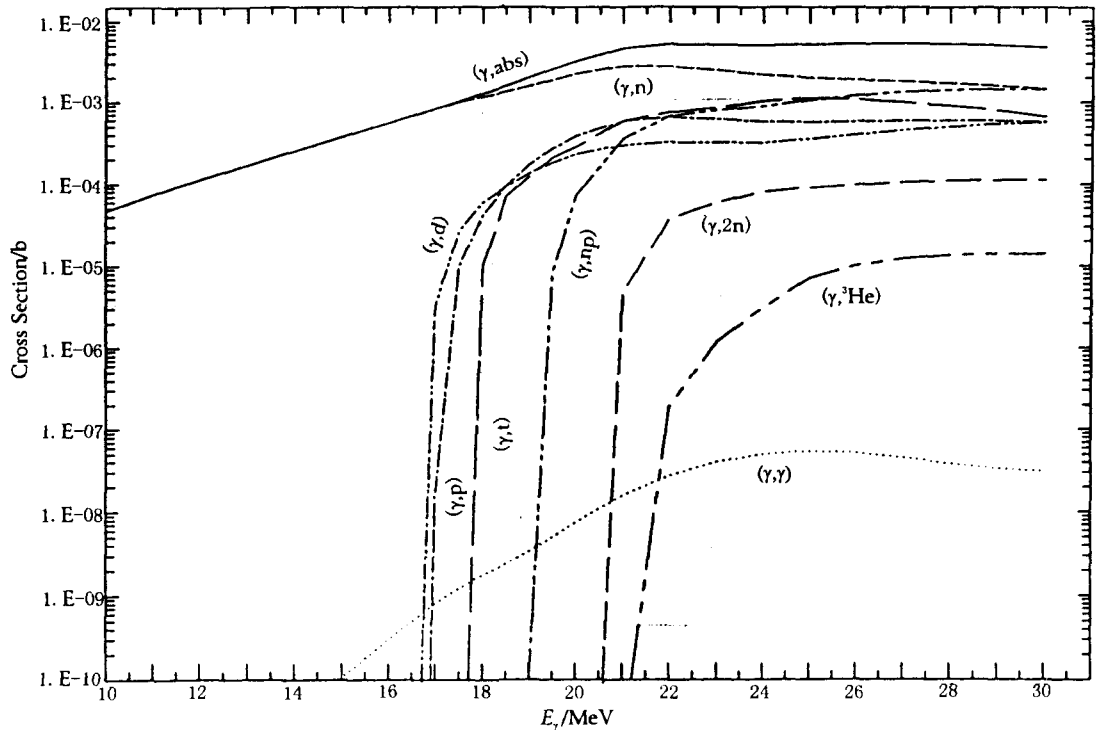

Fig. 5 Evaluated photonuclear data on ^{9}Be

The equilibrium mechanism and pre-equilibrium mechanism are involved in the model calculations. The pre-equilibrium mechanism plays important role in $\gamma+^{9}Be$ reactions.

The new model for photonuclear light nucleus reactions has been proposed. The initial nuclear excitation can be understood in terms of particle-hole excitations (1p1h) for GDR. The key point in this model is the description of the particle emissions between discrete levels in both equilibrium state and pre-equilibrium state. The pre-equilibrium emission mechanism dominates the reaction processes.

Reference

[1] R. B. FIRESTONE and V.S.SHIRLEY, Table of Isotopes 8_{th} ed., John Wiley and Sons (1996).

[2] J.S. ZHANG, Y.L. HAN and L.G.CAO "Model calculation of $n+^{12}C$ Reactions from 4.8 to 20 MeV" Nucl. Sci. Eng. 133, 218(1999).

[3] J.S. ZHANG et al., "Model calculation of $n+^{12}C$ Reactions from 4.8 to 20 MeV" (to be published).

[4] R.D.Edge et al., Nncl.Phys. 2,248 (1957).

[5] J.H.Hibbons et al., Phys.Rew 114,1319 (1959).

[6] W.John et al., Phys.Rew 127,231 (1962).

[7] M.Fujishiro et al., J.CJP, 60,1672 (1982). EXFOR M0438002

[8] U. Kneissl et al Nucl.Phys. A, 247,91 (1975).

[9] J.Ahrens et al Nucl.Phys. A, 251,479 (1975).

II DATA EVALUATION

Evaluation of Complete Neutron Data of n + ^{239}Pu from 10^{-5} eV to 20 MeV

Yu Baosheng Wang Shunuan
(China Nuclear data Center, CIAE)

Abstract

A complete set neutron nuclear cross sections, angular distributions, double differential cross section, and gamma production data as well as the charged particle emission cross sections of n +^{239}Pu from 10^{-5} eV to 20 MeV were recommended based on evaluated experimental data and calculated theoretically results in ENDF/B-6 format.

Introduction

The complete neutron data of ^{239}Pu play an important role for the fuel cycles of all thermal and fast reactor systems. A complete set of neutron nuclear data of ^{239}Pu was recommended from 10^{-5} eV to 20 MeV for CENDL-3. The recommended data were performed based on evaluated experimental data and adjusted theoretical calculated results, except the resonance parameters which were taken from ENDF/B-6. In this work, the direct inelastic scattering cross sections for first 7 levels were calculated with the coupled channel method using ECIS-95 and the charged particle emission cross sections were given. The comparison of our evaluated data with other recommendations from ENDF/B-6 and JENDL-3 has been performed.

1 Thermal Cross Sections and Resonance Parameters

Present resolved resonance parameters which were obtained with SAMMY

code to fit the high-resolution experimental data were performed at ORNL (Oak Ridge National Laboratory, USA) by H. Derrienand, G. De Saussure and at JAERI by H. Derrien and T. Nakagawa. The resolved resonance parameters are same in the energy region from 1.0^{-5} eV to 2.5 keV from ENDF/B-6 and JENDL-3.2. The resonance parameters from ENDF/B-6 were adopted in this work.

The total neutron number per fission is the sum of prompt and delayed neutron number. The delayed yields and spectra were evaluated by T.R. England[1]. The evaluated data for prompt fission neutron relied heavily on the measurement with respect to ^{235}U and ^{252}Cf, in this case the standard, recommended by CSEWG were used.

2 Smooth Cross Sections

2.1 Total Cross Section

Above unresolved resonancesz energy range (0.03~20 MeV), there are lot of experimental data. These data are mainly measured at 8 laboratories [2~9], the early measured data by D.G Foster[2] are higher than other ones systematically. Due to the inelastic and multiple scattering in sample were neglected, the data measured by J. Cabe[6] also higher 5% than other ones around 4 MeV.

Other measured data are consistent with each other, particularly the measured data by R.B. Schwartz[7] from 0.48 to 17.0 MeV using white neutron source and isotopic composition sample of ^{239}Pu at National Bureau of Standards of USA in 1974 and the data of K.A. Nadolny[5] from 0.5 to 31 MeV with 250 meter flight path at Linac in 1973. These two measured data are more important and in good agreement with each other within errors. The measured data carried out by W.P. Poenitz[8,9] in energy region of 16 to 20 MeV are consistent with what from Refs. [4,7]. The measured data below 1.5 MeV were given by A.B. Smith[4] .

For elastic scattering angular distributions, there are enough measured data from 0.5 MeV to 14.1 MeV, which were carried out at 6 laboratories [10~15]. In order to get the optimal optical potential parameter, below the threshold energy of (n,2n) reaction, the experimental data $\sigma_{n,\gamma}+\sigma_{n,n}+\sigma_{n,f}$ used as experimental σ_{non} for automatically searching the optimal optical potential parameters. The theoretical calculation was performed based on the evaluated experimental data as mentioned above.

2.2 Fission Cross Section

A lot of the experimental data of fission cross sections are available. However, most of the neutron-induced the later measured data are 10%~31% lower than early once[16] with energy increasing from 2.0 to 18 MeV, and in some energy region, experimental data are lacking. In order to resolve discrepancies of ratios measured and fill in the gaps, some accurate measurements were performed.

The improvements of measurement technology were conducted using ionization fission chamber at the time-of-flight spectrometer at Linac in 1978. The new procedure is called "threshold cross section method" those advantage is that it does not require knowledge of the relative masses in the high-purity fission chambers and the detector efficiency. Furthermore, the procedure is suitable to the white neutron source.

Therefore, some accurate fission cross sections were obtained in widely energy region using white neutron source. The fission cross sections were measured by J.W. Meadows [17] in energy region 0.146 MeV~9.9 MeV and by K. Kari[18] in energy region 0.99 MeV~21 MeV in 1978. Their data are consistent with each other within errors. The uncertainties were improved, either eliminated or significantly reduced.

There are 8 measarements around 14.7 MeV, in their differences are more than 10 %. It is found that, in geneval, the measured data with neutral abundance sample are higher, and the measured values using associated particle method with the isotopically pure sample and carefully subtraction the fission-fragments correlated background are lower. The evaluated value at 14.7 MeV was obtained by the weighted averaging the measured data. the value is 23.31 ± 0.015 b.

J.W. Meadows[9] and L.W. Weaston[20] measured the data in energy region from 9.7 eV to 0.2 MeV and from 0.1 keV to 20 keV, respectively. The measured data were very important for low energy region evaluation.

The evaluation was based on all collected experimental data and including evaluated data[21]. Combining the simultaneous evaluated results with the analysis of the experimental data, the evaluated data was given and was shown in Fig.1

2.3 Radiation Capture Cross Section

For the $^{239}Pu(n,\gamma)^{240}Pu$ reaction, there are some experimental data[22~24] in energy region from 0.002 eV to 1.0 MeV.

The data were measured by J.C. Hopkins[22] in 0.03~1.0 MeV, using the capture to fission cross section ratios method (α value) in 1962, in order to get the $\sigma_{n,\gamma}$, the alpha value were multiplied by the fission cross section. The data were also measured by M.G. Schomberg[23] from energy region from 100 eV to 30 keV in 1970 and by V.N. Kononov[24] in 10.0keV to 80.0 keV in 1975 by using same method, respectively. The data are in very good agreement with each other within errors.

Based on the theoretical calculated and experimental data, the evaluated data were obtained and show in Fig. 2, the evaluated data could reproduce the experimental data very well.

2.4 (n,2n), (n,3n) and (n,4n) Cross Sections

There are no experimental data for (n, 3n) and (n, 4n) reactions. Only for (n,2n) reaction there exist a few measured data. The data measured by J. Frehaut[25] were evaluated and adopted in this work. It was shown in Fig. 3.

3 Theoretical Calculation and Parameter Adjusting Parameters

3.1 Nonelastic Scattering Cross Section

Based on the available total cross sections of ^{239}Pu, nonelastic scattering cross sections evaluated by us from (n, γ), (n, n'), (n, f) ,(n,2n) etc. for ^{239}Pu in energy region 0.001~14 MeV (see Fig. 4) as well as 15 experimental data of elastic angular distributions, a set of neutron optical potential parameters was obtained in the energy region 0.001~20 MeV by using automatically searching code APFO96 [26], and AUTOFTO[27], for the detail, see the ref. [32].

$$V = 50.593750-0.38913181E-0.01268969E^2 - 24(N-Z)/A$$

$$W_S = \max\{0.0, 4.00000- 0.11215307E - 12.0(N-Z)/A\}$$

$$W_V = \max\{0.0, -1.65087783+ 0.08693016E\}$$

$$W_{so} = 6.2$$

$r_{so} = r_r = 1.30871$ $\quad r_s = 1.27787423$ $\quad r_v = 1.17236149$

$a_{so} = a_r = 0.59236091$ $\quad a_s = 0.80000001$ $\quad a_v = 0.3600001$

Using this set of neutron optical potential parameters and adjusted level density and giant dipole resonance parameters as well as fission parameters, a set of complete neutron data were calculated with FUNF code[33] by Wang [32].

3.2 Inelastic Scattering Cross Section

The inelastic scattering cross sections were calculated. The theoretical calculated total inelastic scattering cross sections were adjusted based on the experimental data[11,34].

Coupled channel optical model calculations with the ECIS–95 code[35] were used to provide the direct component to the first 7 members of the ground state rotational band and inelastic angular distributions to the rotational levels.

Other levels belonging to compound nuclear reactions were calculated using FUNF[33] code with the width fluctuations theory.

The direct inelastic scattering data were used as the input data of FUNF. The discrete levels were taken from China Nuclear Parameter Library, they are as follows:

NO.	Energy(keV)	Spin-Parity		NO.	Energy(keV)	Spin-Parity	
G.S.	0.0	1/2	+	14	469.80	3/2	-
1	7.90	3/2	+	15	487.00	11/2	-
2	57.30	5/2	+	16	492.10	3/2	-
3	75.70	7/2	+	17	505.50	5/2	-
4	163.80	9/2	+	18	511.80	7/2	+
5	192.80	11/2	+	19	519.20	17/2	+
6	285.50	5/2	+	20	538.00	13/2	-
7	318.10	13/2	+	21	556.10	7/2	-
8	330.10	7/2	+	22	565.00	9/2	+
9	358.10	15/2	+	23	570.10	19/2	+
10	387.40	9/2	+	24	583.00	9/2	-
11	391.40	7/2	-	25	620.00	15/2	-
12	434.00	9/2	-	26	634.00	11/2	+
13	462.00	11/2	+	27	659.00	11/2	-

Continuum levels were assumed above 659.00 keV.

The calculated inelastic scattering cross section are shown in Figs. 5~8

4 Comprehensive Recommendation

4.1 Reaction Cross Sections

The recommended cross sections for (n, n'), (n, 2n), (n, 3n), (n, γ), (n, f) etc.

were given based on the measured and theoretically calculated data. The cross section of (n,p) reaction was only measured at 14.5 MeV by R.F.Coleman[36]. The calculated data could reproduce the experimental data very well as (Fig.9) showing.

All the recommended cross sections for n+ ^{239}Pu reactions are shown in Fig. 10.

4.2 Doublc Differeastial Cross Section

The Doublc Differeastial Cross Section for (n,2n), (n,3n), (n,f) and (n,n'$_{continuum}$) reactions were calculated with code FUNF.

4.3 Photon-Production Data

All photon-production data were calculated with code FUNF, including. MF=12 and 14 for MT=51-77 and 102, and MF=15 for MT=102.

5 Summary

Based on available experimeatal and theoretilal calculation, the complete data of ^{239}Pu were evaluated.. The recommended data, including the total, nonelastic cross sections charged particle emission cross sections and elastic scattering angular distribution could, reproduce the experimental data very well.

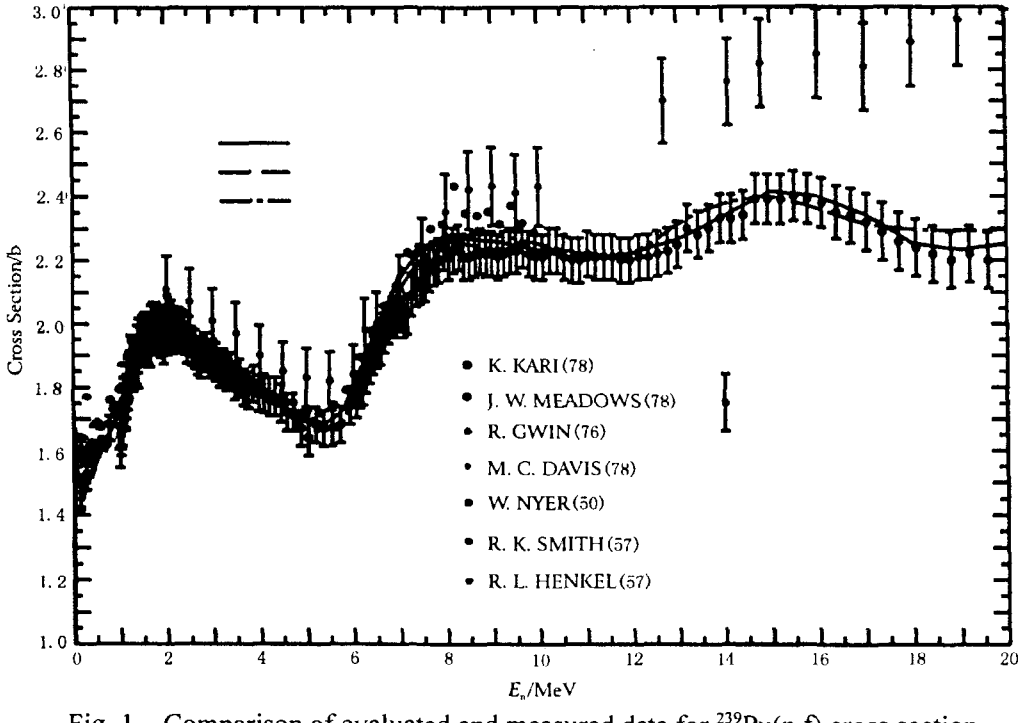

Fig. 1 Comparison of evaluated and measured data for ^{239}Pu(n,f) cross section

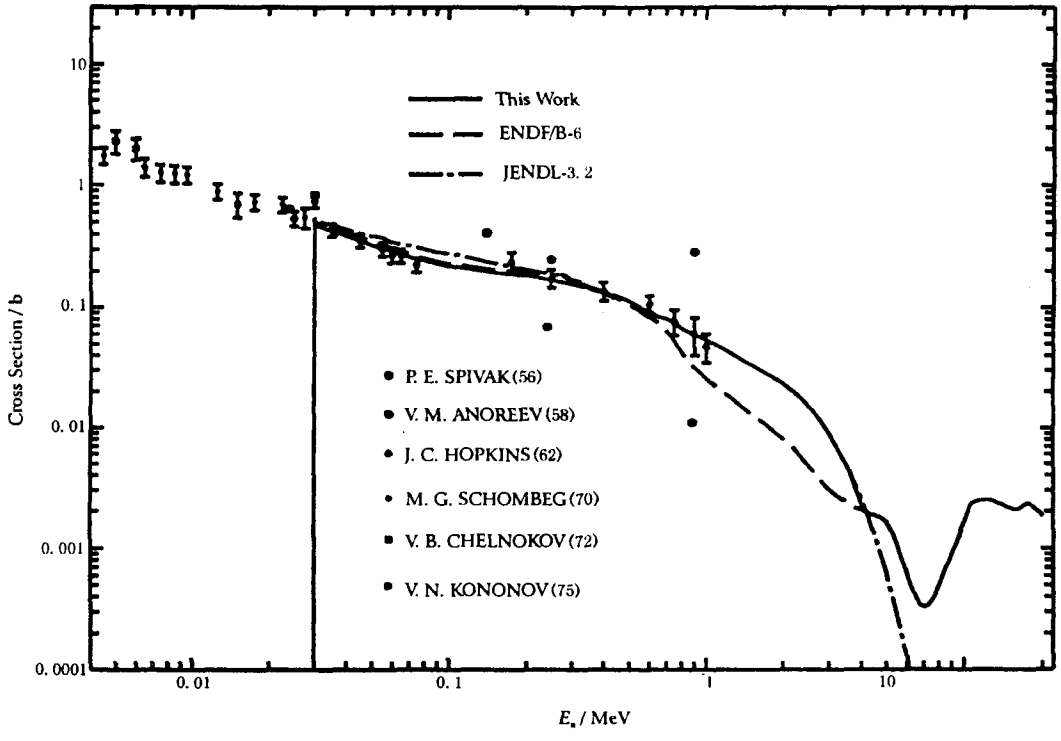

Fig. 2 Comparison of evaluated and measured data for $^{239}Pu(n,\gamma)$ cross section

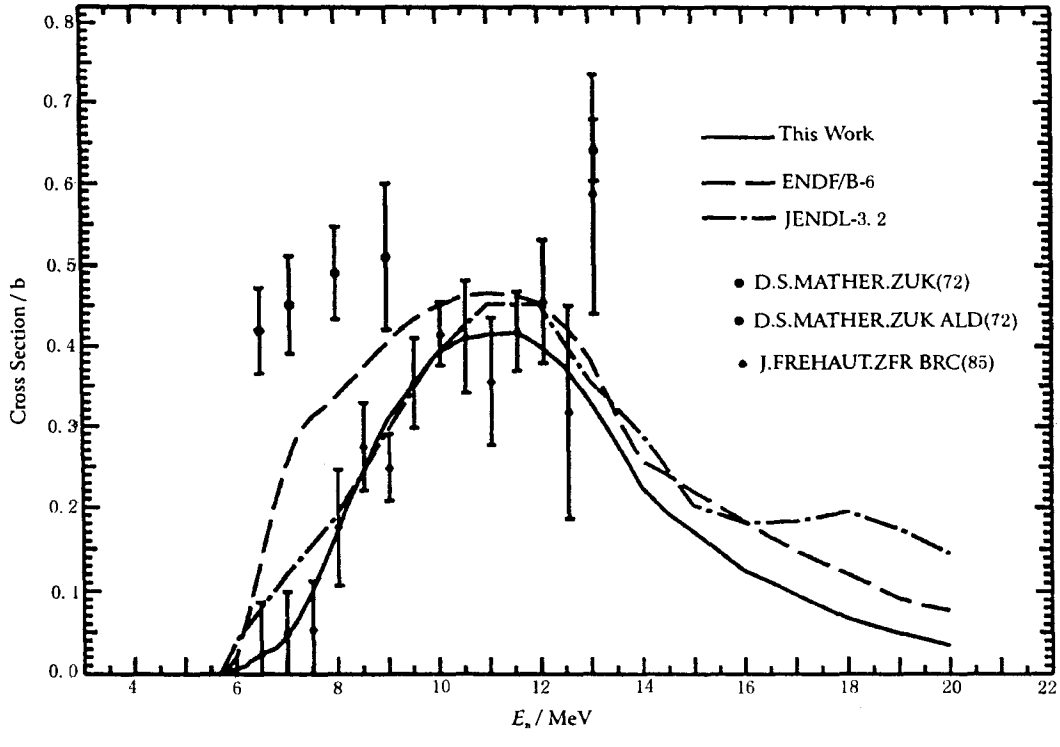

Fig. 3 Comparison of evaluated and measured data for $^{239}Pu(n,2n)$ cross section

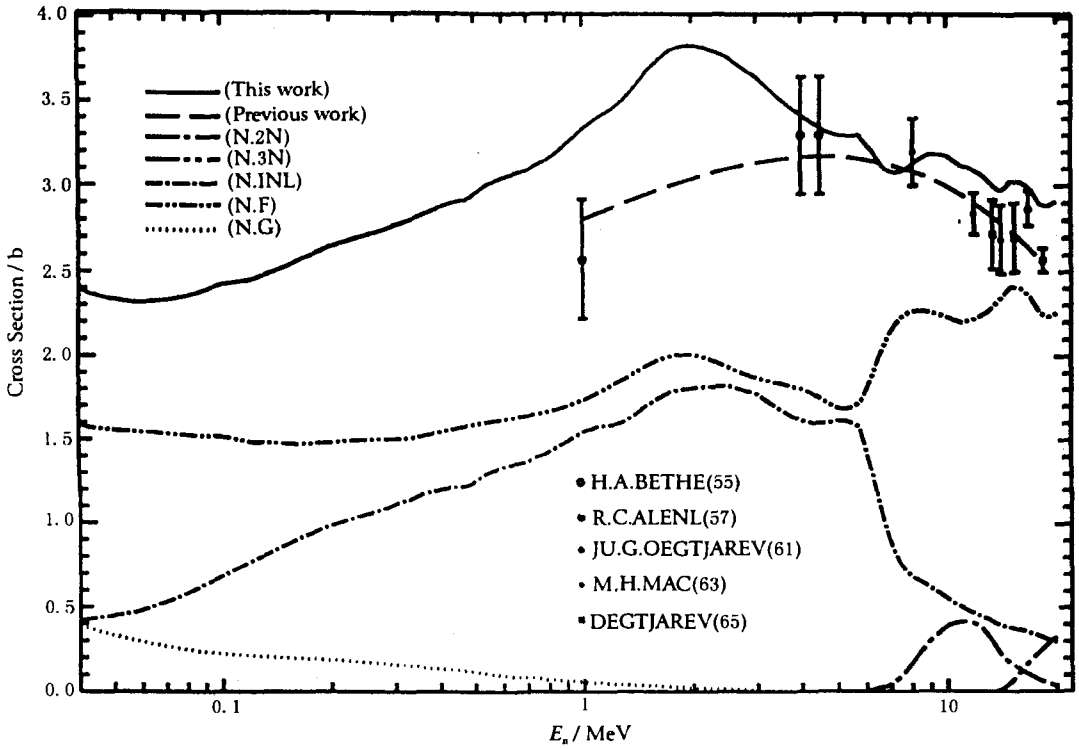

Fig. 4 Comparison of evaluated and measured data for ^{239}Pu non elastic cross section

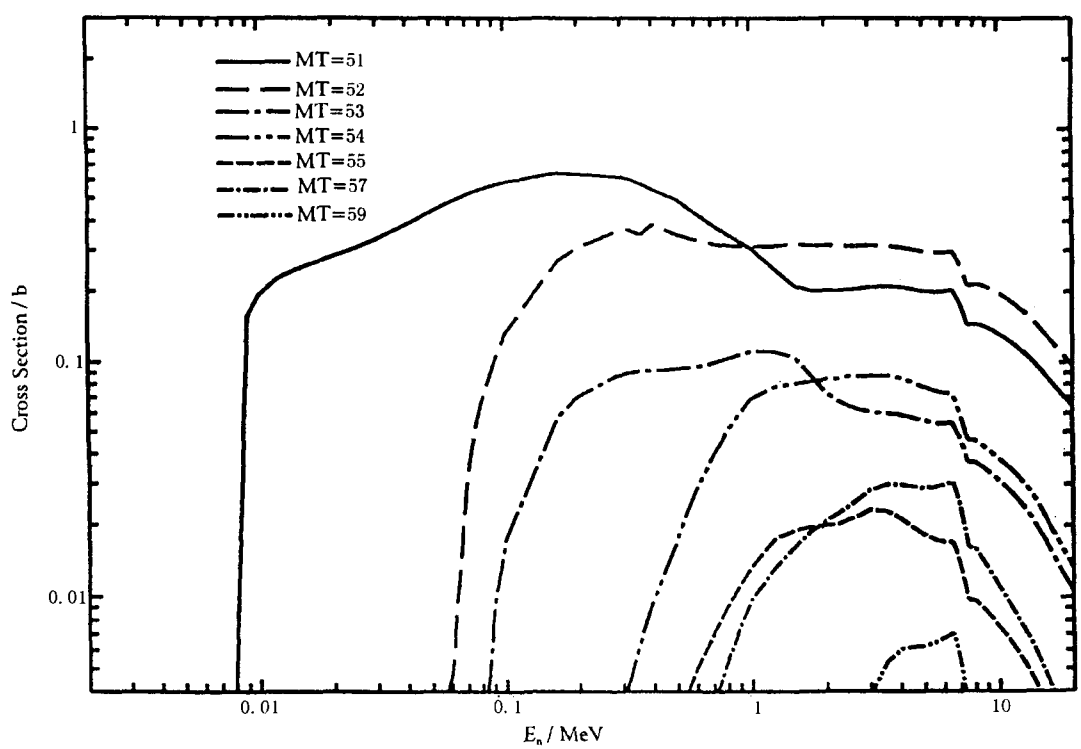

Fig. 5 The cross sections of inelastic scattering to discrete levels

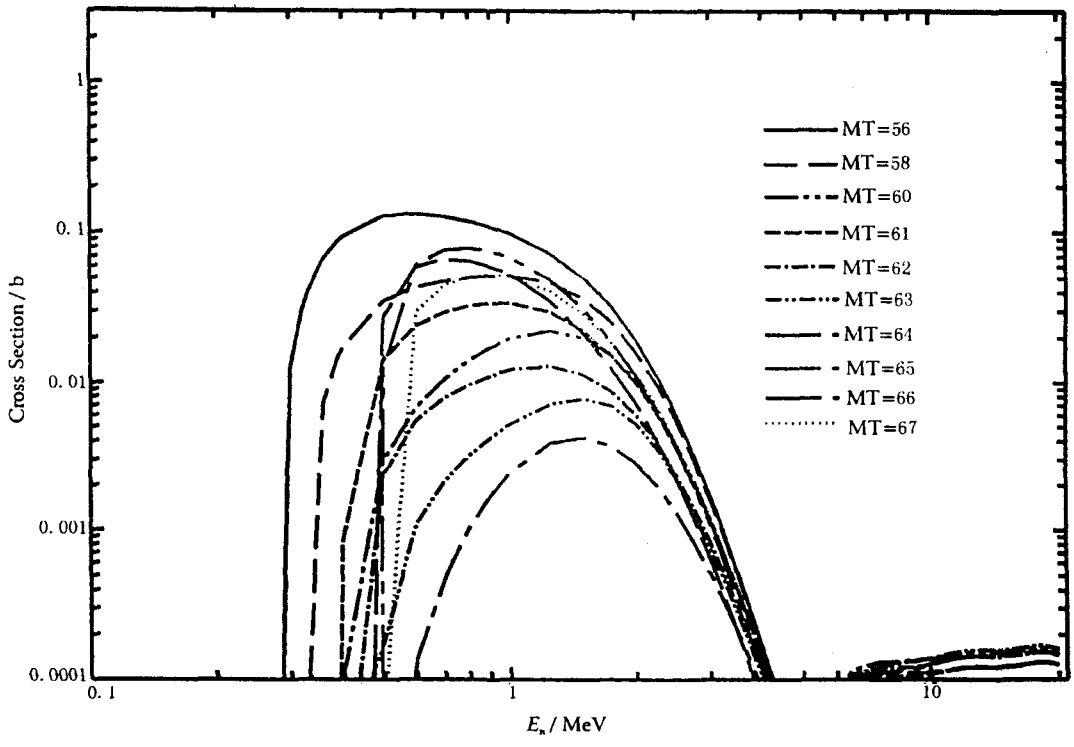

Fig. 6 The cross sections of inelastic scattering to discrete levels

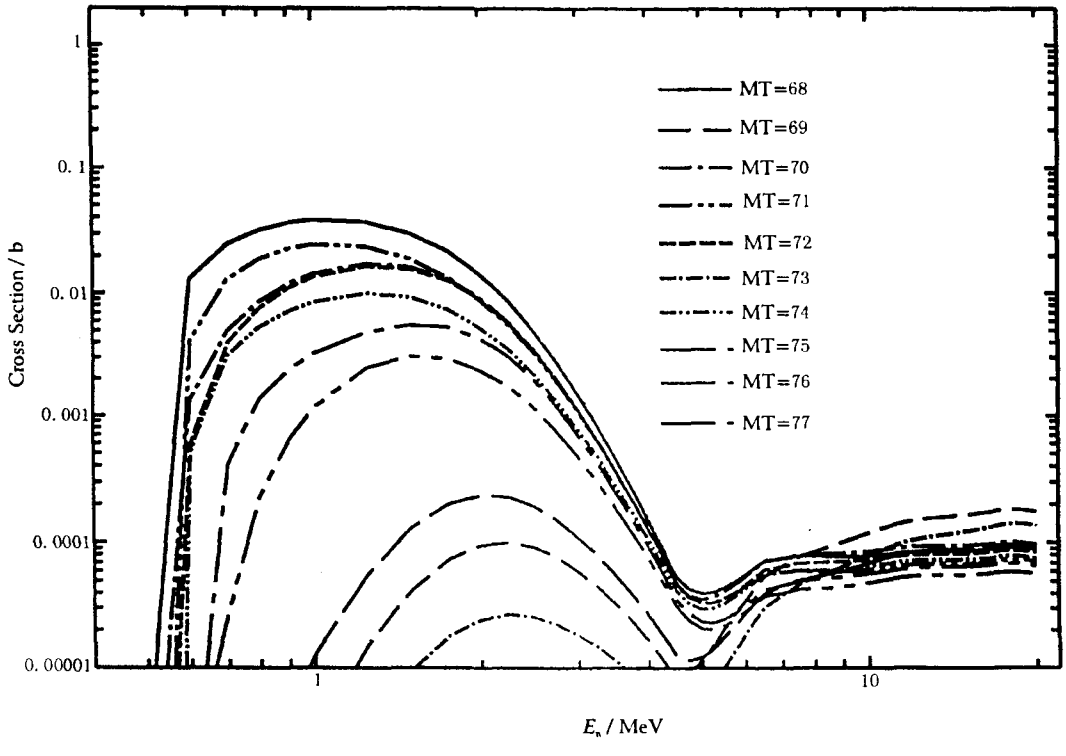

Fig. 7 The cross sections of inelastic scattering to discrete levels

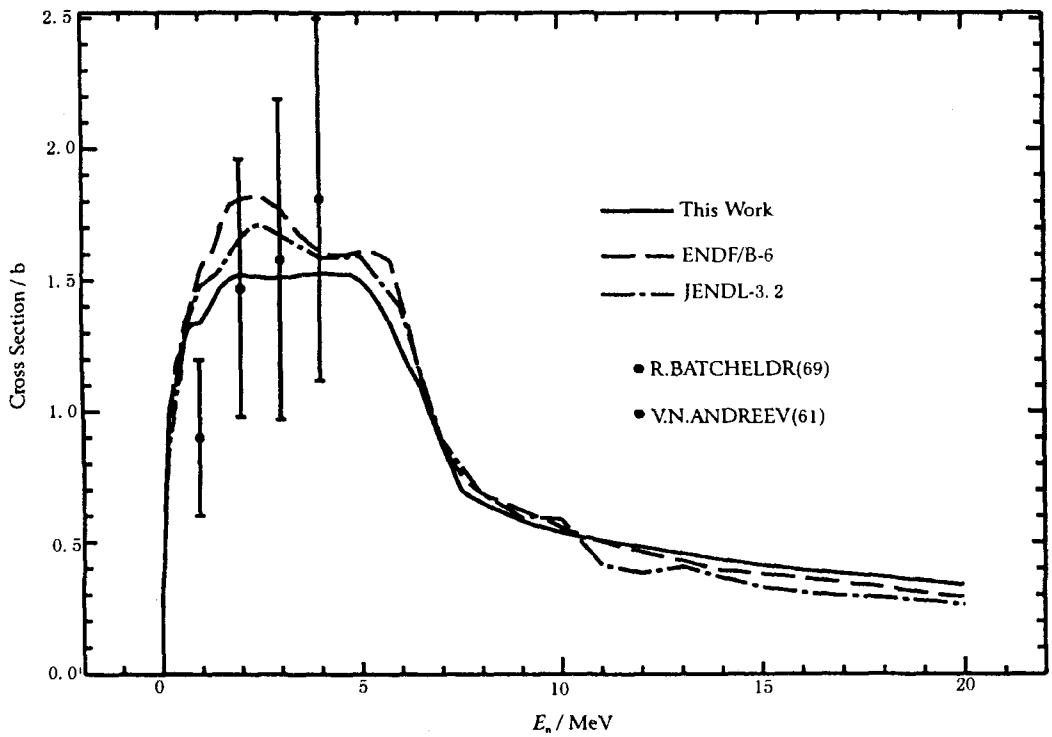

Fig. 8 Comparison of evaluated and measured data for ^{239}Pu(n,inl) cross section

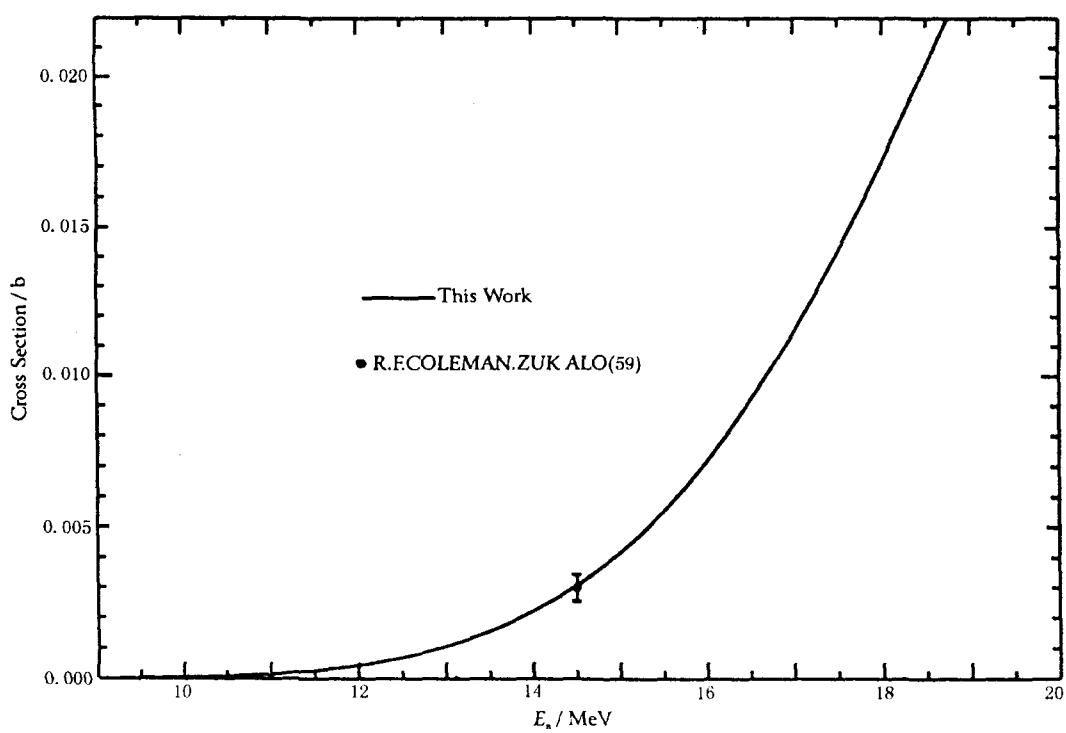

Fig. 9 Comparison of evaluated data for ^{239}Pu(n,p) cross section

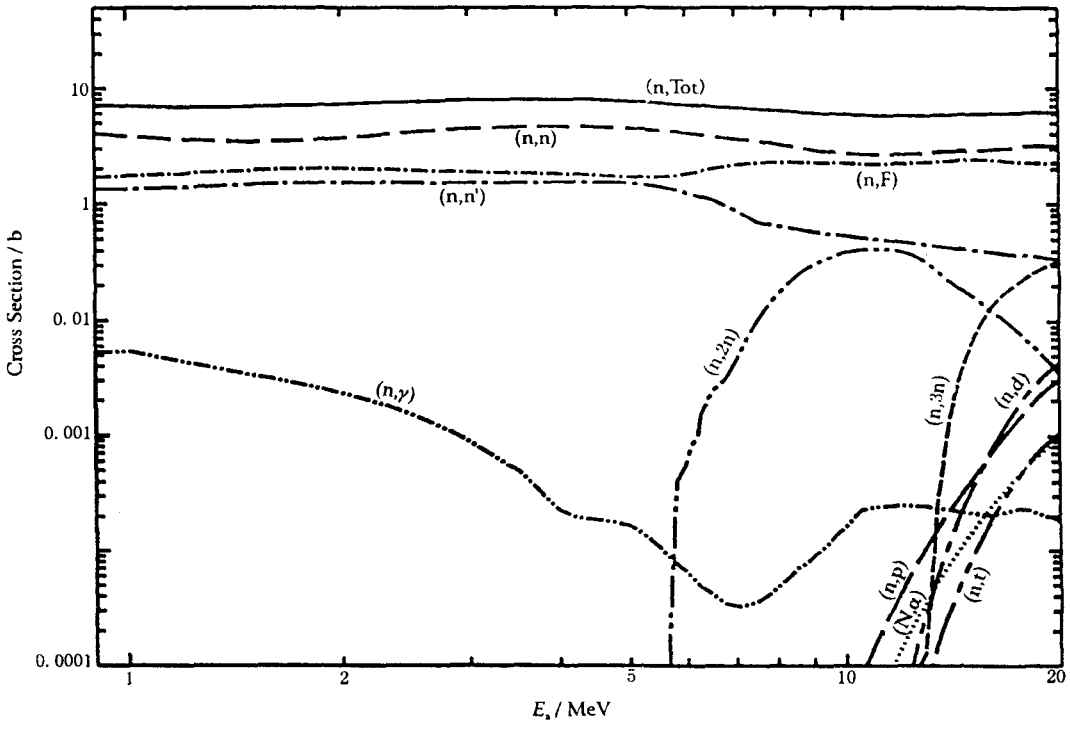

Fig. 10 Evaluated cross sections for ^{239}Pu

Acknowledgments

The authors are indebted to CNNC (China National Nuclear Corporation) and CIAE for their supports, and thank Drs. Liu Tingjing, Liang Qichang for the interesting and useful discussions and for making this collaboration possible.

References

[1] T.R.England et al,LA-11151-MS(1988),LA-11534-T(1989)

[2] D.G.Foster et al., Phys.Rev.,C3,576(1971)

[3] J.M.Peterson et al., Phy.Rev.,120,521(1960)

[4] A.B.Smith et al., J.Nuc.En.,27,317(1973).

[5] K.A.Nadolny et al., USNDC-9 (1973)p.170

[6] J.Cabe et al., CEA-R-4524 (1973).

[7] R.B.Schwartz et al., Nuc.Sci.Eng.,54,322(1974).

[8] W.P.Poenitz et al., Nuc.Sci.Eng.,78, 333(1981).

[9] W.P.Poenitz et al., ANL-NDM-80, 1983.

[10] R.C.Allen et al., Phys. ReV., 104,731(1956)

[11] R.Batchelor et al., AWRE-O-55/69(1969)

[12] M.Copploa et al., Z. Physik., 232,286(1970)

[13] G. Haouat et al., Nucl. Sci. Eng., 81,491(1982) (1985)

[14] G.V.Anikin et al., AE,60,51(1986)

[15] L.F.Hansen et al., Phy.Rev/c,34,2075(1986)

[16] R.K.Smith et al., BAP,2,196(1957)

[17] J.Meadows et al., Nucl. Sci. Eng.,68,360(1978)

[18] K.kari et al., Conf. on Nuclear data for sci. and tech., Juelich, Germany,13-17 (1991) p-510

[19] J.W.Meadows et al., Annual of Nuclear Energy,15,421(1988)

[20] L.W.Weaston et al., Nucl. Sci. and Eng.,111,415(1991)

[21] Liu Tingjin et al., CNDP,4,49(1990)

[22] J.C.Hopkins et al., Nucl. Sci. and Eng., 12,169(1962)

[23] H.G.Schomberg et al., 70 Helsink,1,315

[24] V.N.Kononov et al., AE,38,81(1975)

[25] J.Frehaut et a., NEANDC(E) 238/L (1986).

[26] Shen Qingbiao, APFO96 Code, CNDC Report(1996)

[27] Liu Tong, AUTOFOT System, CNDC Report(1996)

[28] H.A.bethe et al., LA-1939(1955)

[29] R.C.Allen et al., Nucl. Sci. and Eng.,2,787(1957)

[30] Ju.G.degtjarev et al., AE,19,456(1965)

[31] M.H.Mac Gregor et al., Phys. Rev., 130,1471(1963)

[32] Wang Shunuan, CNDP,20,57(1998)

[33] Zhang Jingshang et al., FUNF Code, CNDC report(1996)

[34] A.N.Andreev et al., SPN,211(1961)

[35] Wang Shunuan, CNDP,21,28(1999)

[36] R.F.Coleman et al., PPS,73,215(1959)

The Evaluation for ^{85}As etc. 25 Reference Product Yields from ^{235}U Fission

Liu Tingjin Liang Qichang
(China Nuclear Data Certor,CIAE)

Introduction

The fission yield, used as standards in the fission yield data measurement and evaluation and as monitor in the nuclear industry for decay heat estimation, burn-up credit study etc., are refered to the reference yield. Among them, the data of ^{235}U fission, especially at thermal energy, are most important ones. The data for 15 product nuclides from ^{235}U fission were evaluated in this work.

1 Data Collection and Evaluation

The all data up to now were retrieved from EXFOR master data library and the EXFOR file by using EXFOR manage system and supplementary retrieval programs for fission yield data[1]. The data were also collected from the publications concerned. Altogether 44 entries(subentries) or papers were collected, they are listed in table 1.

The data were decided to be adopted or abandoned according to the measured date, method, facility, detector, monitor, data error and discrepancy situation with others. In general, the following data were abandoned:

a. The quantity measured is not required;

b. Large discrepancy with others and measured method is not reliable or no information in detail;

c. Some thing is wrong in the measurements or data processing.

d. The data, relatively measured and the standards are not given, were not used as much as possible, except they have to be used, for example in the case that there

are no other data or very few data, for them could not be corrected.

As a result, 9 entries (subentries) of them were completely or partially abandoned (they are marked 'A' in table 1), and others were taken (marked by 'T' in Table 1).

The errors given in the EXFOR data table are very different and complicated. They must be corrected or assigned to give 'total' error for all entries. The errors were estimated for different measurement methods, they are listed in Table 3. In general case, if the errors were given by authors in these region, they were not changed, if not they were corrected or assigned. The error could be changed in the region for same method and period, depending on the value of the yield, measured energy point, date and library. If there were no error given, the error were assigned according to the case, generally upper limit. It should be pointed that this is just 'general' case, in the special case the error could be out of the given region.

The data were corrected for standard yield data, gamma intensity, and fission cross section. The procedures and the new standards taken are the same as ref. [2,3].

2 Data Processing

The EXFOR entries were processed by using fission yield data evaluation system FYDES[1], including EXFOR data retrieval, data table standardization, corrections for fission yield standard, gamma intensity and fission cross section, weighted average and simultaneous evaluation.

3 Result and Recommendation

The results are shown in Table 4. 25 yield data of 15 product nuclides were evaluated (others are no experimental data).

It can be seen that the errors are about 2% for about one third of the data, which were measured by means of mass spectrometer method, and about 5% for another one third of data, which were measured by means of gamma spectrometer or radio-chemistry methods. The errors are larger for remain one third of data, which comes

from the discrepancy between the measured data or few poor measurements.

The evaluated data were compared with ENDF/B-6, shown in Table 5. It can be seen that the data are in good agreement among the present and ENDF/B-6 for ^{89}Br (T), ^{92}Sr (T), ^{97}Mo (T,F), ^{13}Sb (T), ^{135}I (T,H), ^{136}Cs (T), ^{147}Sm (F), but large different for ^{85}As (T), ^{90}Br (T), ^{91}Br (T), ^{115m}Cd (T,F,H), ^{115}Cd (T), especially for ^{115m}Cd (H).

The data of ^{85}As (T), ^{91}Br (T), ^{115m} Cd (F) and ^{115m}Cd (H) are not recommended (marked by 'N' in Table 4), for there are only one or two sets of measured data for them and there is largely discrepancy with ENDF/B-6. The data of ^{92}Sr (T) and ^{147}Sm (F) are recommended but only can be taken as reference (marked by '(R)' in table 4), for there is also only one set of measured data, although they are in agreement with ENDF/B-6. Others are reliable and recommended (marked by 'R' in table 4), for there are more measured data for them.

4 Conclusion and Discussion

The 25 cumulative fission yield for 15 product nuclides, which can be used as reference yield, were evaluated based on available experimental data up to now and processed by using fission yield data evaluation program system FYDES. Based on the situation of measured data and comparison with ENDF/B-6, 19 of them are recommended as reference data to use (Table 4).

It is a general impression that the available experimental data are not so much for these yield data, so it should be updated in case of the new experimental data are available.

There are 8 set of measured data for the yield of ^{115}Cd at thermal energy, it should be reliable, but the difference is 34.2% between it and ENDF/B-6 and 43.7% between it and JENDL-3. The attention must be paid to this situation.

The author wish to acknowledge IAEA for their supporting this work.

Table 1 The EXFOR as well as other experimental data and their processing

EXFOR No.	auther	laboratory	referenec	date	energy	method	Quantity (/standard)	processed	comments
12926019	R.W.WA-LDO	1USALRL	PR/C,23,1113	8103	1.0+06	REAC(1.0)	FY(AB)		T(no detail)
13065005	H.FARR-AR	1CANM-CM	CJP,40,1017	62	1.5–02	MA, REAC(mxw)	Ro(/^{100}Mo)	Ref. Ro, others:Y=Ro*^{100}Mo(eval.)	T
13091002	H.G.HIC-KS	1USALRL	PR,128,700	6210	1.4+07	RC,CCW(14.0)	Rv(/^{99}Mo,mxw)	Ro=Rv*^{99}Mo (h/mxw) (eval.)	T
13207004	P.L.REE-DER	1USABNW	75WASH,1, 401	7503	2.5–02	MA, REAC(mxw)	Ro(/^{88}Br)	Ro, simul eval.	T,A(^{90}Br,ΔY large,disc)
13255004	G.P.FORD	1USALAS	LA-6129	7602	1.5+07	RC,CCW(14.7)	Rv(/^{99}Mo,mxw)	Ro=Rv*^{99}Mo (h/mxw) (eval.)	T
13268005	L.H.GEV-AERT	1CANTOR	CJC,48,641	70	2.5–02	RC(GEMUC), CCW(mxw)	FY(/^{99}Mo)	DD	T
13270003	F.L.LIS-MAN	1USMATR	NSE,42,191	70	2.5–02	MA, REAC(mxw)	FY(?)	^{100}Mo, eΔY 0.5%→1.5% ^{152}Sm, eΔY 3%→10%(disc)	T,A(^{131}Xe,some error)
13270016	F.L.LIS-MAN	1USMATR	NSE,42,191	70	5.0+05	MA, REAC(0.5)	FY(/^{148}Nd,1.75±0.03)	Ref. Ro=Y/1.75, others: Y=Ro*^{148}Nd(eval.), ΔY→2%	T
13270017	F.L.LIS-MAN	1USMATR	NSE,42,191	70	5.0+05	MA, REAC(0.5)	FY(AB→100%)		T
13286002	T.P.MCL-AUGHL	1USMUSA	MC-LAUGHLIN	7109	2.5–02	RC(γ,GeLi), REAC(mxw)	FY(AB)	DD(used part)	T
13352003	M.G.ING-HRAM	1USAANL	PR,79,271	5007	2.5–02	MA, REAC(mxw)	FY(/^{149}Sm,1.10)	Ref. Ro=Y/1.10, ΔR→1.5%, others: CY:1.10→1.01(eval.), ΔY→3%	T
13368004	A.C.WA-HL	1USALAS	PR,85,570	5202	1.4+07	RC(β),CCW (14.0)	FY(?)	ΔY→10%	T
13384005	E.A.ME-LALKA	1CANM-CM	CJC,33,830	55	2.5–02	MA, REAC (NRX,mxw)	FY(/^{149}Sm)	ΔY→2%	T

Table 1 continue

EXFOR No.	auther	laboratory	referenec	date	energy	method	Quantity (/standard)	processed	comments
13386006	J.A.PET-RUSKA	1CANM-CM	CJP,33,693	55	2.5–02	MA, REAC (NRX,mxw)	FY(/^{149}Sm,1.13)	Ref. Ro=Y/1.13, ΔRo→1.5%	T
13388002	A.C.WA-HL	1USALAS	PR,99,730	5508	2.5–02	RC(β),CCW (14.0)	Ro(/FYmxw)		T,A (^{131m}Te,ΔR too large)
13395002	B.FINKLE	1USAUSA	RCS,3,1368	51	2.5–02	RC, REAC(mxw)	FY(/^{140}Ba,6.1)	CY:6.1→6.206(eval.), ΔY→15%	T,A(^{133,135}I,^{106}Ru,disc)
13395003	B.FINKLE	1USAUSA	RCS,3,1368	51	2.5–02	RC, REAC(mxw)	FY(/^{140}Ba,6.1)	Ref. Ro=Y/6.1, others: CY:6.1→6.206(eval.), ΔY→15%	T
13396002	D.W.ENG-ELKEME	1USAUSA	RCS,3,1372	51	2.5–02	RC, REAC(mxw)	FY(/^{140}Ba,6.1)	CY:6.1→6.206(eval.), ΔY→15%	T
13410002	R.P.MET-CALF	1USAUSA	RCS,2,891	51	2.5–02	RC, REAC(mxw)	FY(/^{140}Ba,6.1)	CY:6.1→6.206(eval.), ΔY→15%	T
13411002	R.P.MET-CALF	1USAUSA	RCS,2,898	51	2.5–02	RC, REAC(mxw)	FY(/^{140}Ba,6.1)	CY:6.1→6.206(eval.), ΔY→15%	T
13425002	D.W.ENG-ELKEME	1USAANL	ANL-4927	5211	2.5–02	RC(GEMUC,IOCH), REAC(mxw)	FY(/^{140}Ba,6.4)	CY:6.4→6.206(eval.), ΔY→20%	T
13428002	L.E.GLE-NDENIN	1USAANL	CLENDEN-IN	55	2.5–02	MA, REAC(mxw)	FY(?)	ΔY→2%	T
13436002	R.NASU-HOGLU	1USAANL	PR,108,1522	5712	2.5–02	RC, REAC (CP-5,mxw)	FY(/^{89}Sr,4.8)	Ro=^{115}Cd/^{127}Sb, ΔR→6%	A(disc)
13440003	W.J.MAE-CK	1USAINL	ENICO-1028	8002	7.0+05	MA, REAC (EBR-2,0.7)	CHN, FY(100% of light and heavy peaks)	Take CUM=CHN, eΔY<1%→1%	T
13443002	G.P.FORD	1USALAS	LA-6129	7602	1.2+06	RC,VDG(1.2)	Rv(/^{99}Mo,mxw)	eΔRv 1.9%→3%, Ro=Rv* ^{99}Mo(1.2/mxw) (eval)	T
13444003	G.P.FORD	1USALAS	LA-6129	7602	1.5+07	RC,CCW(14.7)	Rv(/^{99}Mo,mxw)	Ro=Rv* ^{99}Mo(H/mxw) (eval)	T
13445002	G.P.FORD	1USALAS	LA-6129	7602	5.0+05	RC, REAC(0.5)	Rv(/^{99}Mo,mxw)	Ro=Rv* ^{99}Mo(F/mxw) (eval) ΔR→6%	T
13446002	G.P.FORD	1USALAS	LA-6129	7602	1.0+06	RC, REAC(1.0)	Rv(/^{99}Mo,mxw)	Ro=Rv* ^{99}Mo(F/mxw) (eval) ΔR→5%	A(disc,two time)
13461002	A.C.PAP-PAS	1USAMIT	MIT-REP-63	53	2.5–02	RC(GEMUC), CYCLO(mxw)	FY(/^{140}Ba,6.17)	CY:6.17→6.206(eval.), ΔY→15%	T,A(^{127,131}Sb,^{133m}Te)

Table 1 continue

EXFOR No.	auther	laboratory	referenec	date	energy	method	Quantity (/standard)	processed	comments
13487002	A.P.BAE-RG	1CANCRC	CJC,38,2147	6011	2.5–02	RC(β), REAC (NRX ,mxw)	Ro(/CHN)	Y=Ro* CHN(B6), ΔY→20%	T,(^{136}Cs),A(others)
20521003	J.V.KRA-TZ	2GERMNZ	JIN,35,1407	7305	2.5–02	RC(PROPC,NaI,GeLi), REAC(mxw)	FY(/^{92}Sr)	ΔY take 0.02 for all (^{85,87}As)	T
20878004	H.O.DEN-SCHLAG	2GERMNZ	DENSCHL-AG	7706	2.5–02	RC(GeLi, PROPC), REAC(mxw)	Ro(/CHN)	Y=Ro* CHN(B6), ΔY→5%	T(A=135,144)
21550006	R.BRISS-OT	2FR GRE	NP/A,255, 461	7512	2.5–02	MA(on-line), REAC(mxw)	FY(/CHN)	^{137}I, eΔY 2.9%→6%(disc)	T
21590002	J.BLAC-HOT	2FR GRE	JIN,36,495	74	2.5–02	RC(GeLi), REAC(mxw)	FY(/^{140}Ba,6.34)	Ref. Ro=Y/6.34, other: CY: 6.17→6.206(eval.) CD(used part), ^{135}I, eΔY→10%	T
21708002	J.LAUR-EC	2FR BRC	CEA-R-5147	8112	1.5+07	RC(GeLi), CCW(W14.7)	FY(AB)	eΔY<3.8%→3.8%, ^{103}Ru, eΔY→10%	T
21743003	G.MARIO-LOPOUL	2FR GRE	NP/A,361,1, 21	8105	2.5–02	γ(GeLi), REAC (HFR,mxw)	FY(/^{144}La, ^{145}Ce)	CD(all)	T
22161002	G.RUDS-TAM	2SWDSWR	AA,0,0	9101	2.5–02	OLMA(GeLi), REAC(mxw)	FY(AB?),Data2	CD(used part), ^{135}I, eΔY→10%	T,A(^{85}Br,^{90,90m}Rb, ^{135}Sb,^{133,135}Te,^{143,147}Cs,disc)
30575002	A.RAMAS-WAMI	3INDTRM	JIN,42,(9),12	8009	2.5–02	γ(GeLi,TRD), REAC(mxw)	FY(AB)	CD(all), ^{88}Kr, ^{135}I, eΔY→15%	T
40257003	A.A.BYA-LKO	4CCPMIF	INIS-SU-38	78	1.3+06	RC, REAC (BR-1,1.3)	FY(/^{140}Ba,5.85)	CY: 5.85→6.206(eval.)	T
40554004	A.N.GU-DKOV	4CCPMIF	77KIEV,3, 192	7704	1.3+06	γ(GeLi), REAC(BR-1,1.3)	FY(AB?)	eΔY<4%→4%	T,A(^{127}Sb,^{131}Te,disc)
*32600000	QI LINKUN	3CPRAEP	88MITO,967	8805	1.95+06	γ(GeLi), RC,REAC(1.95)	FY(AB)		T
	E.K.BON-YUSHKIN	1USA ARE	AEC-TR-4682	60	1.95+06		FY		T(quoted by Qi)
	K.A.PET-RZHAK	1USA ARE	AEC-TR-4692	60	1.95+06		FY		T(quoted by Qi)
	A.FERRI-EU	2UK HAR	AERE-R8753	77	1.95+06		FY		T(quoted by Qi)

*, Not in EXFOR Library, only coded in this paper

notes:

1) The meaning of abbreviation and symbols in the table:

VDG	Van de Graaff accderator	RC	Radio chemistry method
CYCLO	Cyclotron accelerator	γ	γ spectrometer method
REAC	Reactor	MA	Mass spectrometer method
CCW	Cock croft-Walton accelerator	OLMA	On-line mass spectrometer method
FNG	Fast neutron generator	TOF	Time-of-Flight method
GeLi	GeLi Detector	CHN	Chain yield
GEMUC	Geiger-Muller countor	CUM	Cumulative yield
PROPC	Proportional counter	IND	Independent yield
IOCH	Ionization chamber	Y	Absolute yield
FISCH	Fission chamber	REL	Relative yield
TRD	Trace detector	Ref	Standard
FY(/x)	Measured yield relatively to x	mxw	Thermal energy
AB(x)	Absolutely measured yield with method x	$\Delta Y \rightarrow x\%$	Design error x% to Y
Ro(/x)	Ratio relative to x	$e\Delta Y(x_0\%) \rightarrow x\%$	Elarge error of Y (from x_0%) to x%
Rv(/x,mxw)	R value relative to x at energy point measured and thermal energy point	CD	Corrected to decay data
		CY	Corrected to standard yield
T	Taken	$C\sigma_f$	Corrected to fission cross section
A(x)	Abandoned for reason x	Calcu	Calculated
eval.	evaluated	Disc	Discrepant

2) The energy is in "MeV" , except there is special indication , but is in "eV" in column "energy".

Table 2 EXFOR index each product nuclides

Z	A	EXFOR entry number
33	85	20521003 22161002
35	88	13207004 21550006 21743003 22161002
	89	13207004 21550006 22161002
	90	13207004 21550006 22161002
	91	22161002
38	92	13286002 30575002 40554004
42	97	13065005 13270003 13270016 13428002 13440003
48	115	13091002 13255004 13268005 13368004 13395002 13396002 13410002 13411002 13425002
		13436002 13443002 13444003 13445002 13446002
	115m	13255004 13368004 32600000
51	135	20878004 22161002
53	135	13286002 13388002 13395003 13461002 21590002 22161002 30575002 32600000 40257003
		40554004
	137	12926019 21550006 22161002
55	136	13091002 13487002 21708002
62	147	13270003 13440003 13384005 13386006
	152	13352003 13270003 13270017 13440003 13384005 13386006

Table 3 The error(%) of measured fission yield data with different methods

Methods		Fission Yield		Ratio
		Before 1965	After 1965	
RC	GeLi	7~15	4~8	3~5
	NaI	8~15	6~8	3~4
	Geiger	15~25		5~6
γ Spectrum		6~10	3~6	2~3
MA		2~3	1~2	1~2

Note:

1) The error depends on fission yield value, energy point, year and laboratory measured, it can be changed in the corresponding region.
2) If the error is not given, in general case, the upper limit is taken for that.
3) The region listed in the table is just for general case, the error may be outside of the region in special case.

Table 4. The some evaluated reference and monitor fission yield of ^{235}U

nuclide	energy	yield Y	error of Y	points	processed	recommondation
33-As-85	T	3.4494E-01	1.8974E-02	1(1)	A	N
35-Br-88	T	1.6358E+00	8.0621E-02	3	A S	R
35-Br-89	T	1.0988E+00	5.5885E-02	2+1	A S	R
35-Br-90	T	4.2893E-01	7.6576E-02	3	A	R
35-Br-91	T	3.4000E-01	9.0000E-02	1		N
38-Sr-92	T	6.0000E+00	1.7000E-01	1		(R)
42-Mo-97	T	5.9674E+00	8.7080E-02	2+1	A S	R
	F	5.8971E+00	5.3304E-02	1+1	S	R
48-Cd-115M	T	8.2810E-04	6.4324E-05	2+(1)	A S	R
	F	1.9000E-02	4.0000E-03	1		N
	H	7.1261E-02	5.4627E-03	1+1	S	N
48-Cd-115	T	1.7587E-02	7.5623E-04	3+(5)	A S	R
	F	3.7075E-02	4.4833E-03	+2	S	R
	H	6.7990E-01	3.2034E-02	1+3	S	R
51-Sb-135	T	1.5040E-01	7.5200E-03	1		R
53-I-135	T	6.2543E+00	2.9860E-01	5	A	R
	F	6.7447E+00	1.7049E-01	3	A	R
	H	4.3150E+00	2.4200E-01	+1		R
53-I-137	T	2.7757E+00	2.8616E-01	4	A	R
	F	3.0000E+00	6.0000E-01	1		R
55-Cs-136	T	5.4965E-03	3.6828E-04	1+(1)	A	R
62-Sm-147	T	2.1184E+00	2.2587E-02	2+1	A S	R
	F	2.1650E+00	2.2000E-02	1		(R)
62-Sm-152	T	2.5316E-01	4.4089E-03	2+1	A S	R
	F	2.9522E-01	6.6607E-03	2	A	R

The meaning of the symbols in the table :

In column of "points"

Number the set number of absolute measurements

+number the set number of ratio measurements (as numerator)

+(number) the set number of ratio measurements (as denominator)

A Aerage

S Simultaneous evaluation

SS First simulataneous evaluation for different energy points of same nuclides and then for same energy point of different nuclides

R Recommended

(R) Recommended , but only as reference

N Not recommended

Table5. Comparison between present evaluated data with ENDF/B-6

nuclide	En[1]	present evaluation and recommondation[2]		error	ENDF/B-6	DIFB[3](%)
33-As-85	T	3.449E-01	N	5.5	2.188E-01	36.6
35-Br-88	T	1.636E+00	R	4.9	1.780E+00	-8.8
35-Br-89	T	1.099E+00	R	5.1	1.085E+00	1.2
35-Br-90	T	4.289E-01	R	17.9	5.643E-01	-31.6
35-Br-91	T	3.400E-01	N	26.5	2.242E-01	34.1
38-Sr-92	T	6.000E+00	(R)	2.8	5.938E+00	1.0
42-Mo-97	T	5.967E+00	R	1.5	5.997E+00	-0.5
	F	5.897E+00	R	0.9	6.003E+00	-1.8
48-Cd-115m	T	8.281E-04	R	7.8	1.005E-03	-21.4
	F	1.900E-02	N	21.1	2.801E-03	85.3
	H	7.126E-02	N	7.7	4.561E-01	-540.1
48-Cd-115	T	1.759E-02	R	4.3	1.158E-02	34.2
	F	3.708E-02	R	12.1	3.108E-02	16.2
	H	6.799E-01	R	4.7	6.355E-01	6.5
51-Sb-135	T	1.504E-01	R	5.0	1.458E-01	3.1
53-I-135	T	6.254E+00	R	4.8	6.282E+00	-0.4
	F	6.745E+00	R	2.5	6.296E+00	6.7
	H	4.315E+00	R	5.6	4.218E+00	2.2
53-I-137	T	2.776E+00	R	10.3	3.068E+00	-10.5
	F	3.000E+00	R	20.0	2.566E+00	14.5
55-Cs-136	T	5.497E-03	R	6.7	5.538E-03	-0.7
62-Sm-147	T	2.118E+00	R	1.1	2.247E+00	-6.1
	F	2.165E+00	(R)	1.0	2.139E+00	1.2
62-Sm-152	T	2.532E-01	R	1.7	2.669E-01	-5.4
	F	2.952E-01	R	2.3	2.708E-01	8.3

1) T thermal energy
F fission or fast reactor spectrum
H around 14.5 MeV

2) see table 4

3) $$\text{DIFB} = \frac{\text{present value - ENDF/B-6 value}}{\text{present value}}$$

Reference

[1] Liu Tingjin, "Fission Yield Data Evaluation System FYDES", Attached paper 1. to be published(1998).

[2] Liu Tingjin, "Some U-235 Reference Fission Product Yield Data Evaluation", Commun. of Nuclear Data Progress, No.19, 78 (1998).

[3] Liu Tingjin etc., The RCP (No.9504) Report (1997)

Evaluation of Complete Neutron Nuclear Data for ^{65}Cu

Ma Gonggui Liu Xiaobing

(Institute of Nuclear Science and Technology, Sichuan University, Chengdu, 610064)

Abstract

The following production data were evaluated for ^{65}Cu in the energy range from 10^{-5} eV to 20.0 MeV: total, elastic, nonelastic, total inelastic, inelastic cross sections to 12 discrete levels, inelastic continuum, (n,2n), (n,3n), (n,n'α)+(n,αn'), (n,n'p)+(n,pn'), (n,p), (n,d), (n,t), (n,α) and capture cross sections. The angular distributions of secondary neutron, the double differential cross sections (DDCS), the gamma-ray production data and the resonance parameters are also included. The evaluated data will be adopted into CENDL-3 in ENDF/B-6 format.

Introduction

Copper is a very important structure material in nuclear fusion engineering. A complete neutron nuclear data were evaluated based on both experimental data measured up to 1998 and theoretical calculated data with program UNF[1]. The evaluated data will be adopted into CENDL-3 in ENDF/B-6 format [MAT=3292] and will be utilized in various fields of nuclear engineering.

The level scheme is given in Table 1[2]. The binding energy of emitted final particle are given in Table 2.

Table 1 Inelastic discrete levels (Abundance 30.83%)

E_l/ MeV	J^π	E_l/ MeV	J^π	E_l/ MeV	J^π	E_l/ MeV	J^π
0.0	$3/2^-$	1.6234	$5/2^-$	2.2128	$1/2^-$	2.5257	$9/2^+$
0.7706	$1/2^-$	1.7250	$3/2^-$	2.2785	$7/2^-$		
1.1156	$5/2^-$	2.0943	$7/2^-$	2.3290	$3/2^-$		
1.4818	$7/2^-$	2.1074	$5/2^-$	2.4066	$9/2^-$		

Table 2 Binding energy of emitted final particle (MeV)

Reaction	n, γ	n,n`	n,p	n, α	n, ^{3}He	n,d	n,t
Channels	n,2n	n,n`p	n,n` α	n,pn`	n,2p	n, α n`	n,3n
^{63}Cu	0.0	7.0666	8.4155	7.1496	19.320	12.286	15.6887
	9.90466	7.4447	6.7704	6.0959	12.313	6.6874	7.91609

1 Resonance Parameter

The resolved resonance parameters were taken from ENDF/B-6 in the energy region from 10^{-5} eV to 99.5 keV. Thermal cross sections of (n,tot), (n,n) and (n,γ) reactions are 15.94 b, 13.79 b and 2.15 b, respectively.

2 Neutron Cross Section

The comparison of experimental data with evaluated ones is shown in Fig.1~12. It can be seen that the present evaluation is in agreement with the experimental data.

2.1 Total Cross Section

Above the resolved resonance region, there are still some small structure in energy range 99.5 keV~4.0 MeV. In the energy range from 99.5 keV to 1.12 MeV, the data were mainly taken from Guenther's corresponding experimental data[3]. In the energy range from 1.12 MeV to 4.0 MeV, the data were mainly taken from Perey's corresponding experimental data of ^{Nat}Cu[4]. In the smooth energy range from 4.0 MeV to 20.0 MeV, they were obtained from Larson's experimental data of ^{Nat}Cu[5]. A plot of these data and the evaluated data is shown in Fig. 1.

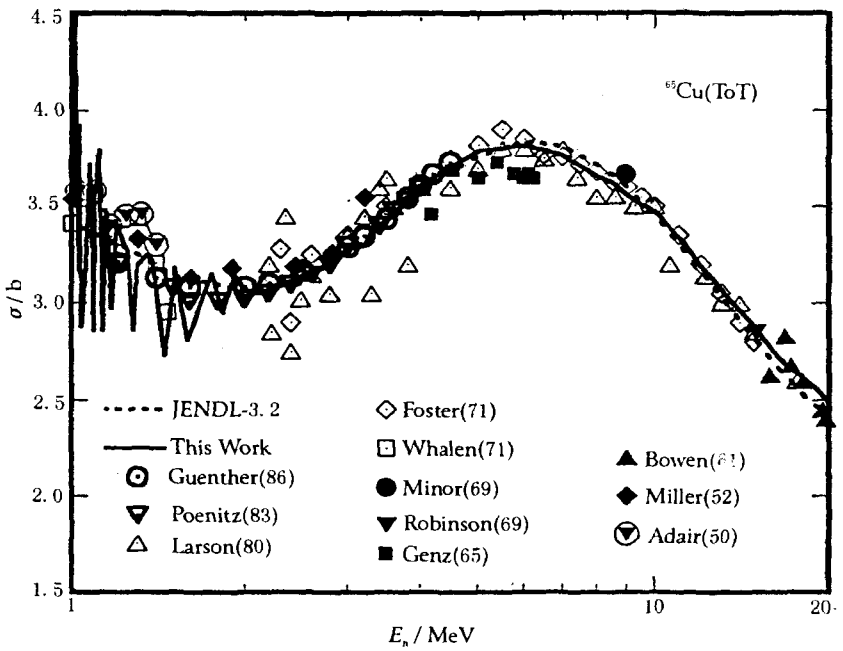

Fig. 1 Total cross section for ^{65}Cu

2.2 Elastic Scattering Cross Section

Above the resolved resonance region, the elastic scattering cross section was obtained by subtracting the summing cross sections of all non-elastic processes from the total cross section. In general, the agreement between the evaluated cross section and the available experimental data of El-Kadi and Kinney[6,7] is good.

2.3 Noelastic Scattering Cross Section

This cross section was obtained by summing cross sections of (n,n'), (n,2n), (n,3n), (n,n'α), (n,n'p), (n, γ), (n,p), (n,d), (n,t) and (n, α) reactions.

2.4 Total Inelastic Cross Section

The experimental data by Shi Xiamin[8] and Joensson[9] around 14.5 MeV were used to normalize the corresponding model calculated results (see Fig. 2).

2.5 Inelastic Cross Section to the Discrete Levels and the Continuum

The inelastic scattering cross section to 12 discrete levels were calculated by using UNF code. For 0.7706 and 1.1156 MeV levels, the data were obtained by fitting experimental data measured by Guenther, Kinney, Almen-Ra. and Holmqvist[10~12]. A plot of these data and the evaluated data is shown in Fig. 3. For 1.4818~2.1074 MeV levels, the calculated results in good agreement with the concerned experimental data. For others, the data were taken from calculated results.

The continuum part was obtained by subtracting the cross section of inelastic scattering to 12 discrete levels from the total inelastic.

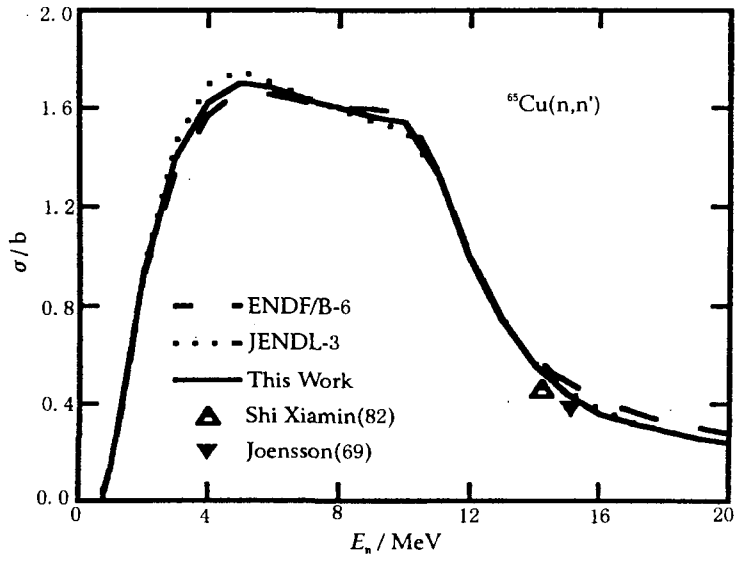

Fig. 2 Inelastic cross section for ^{65}Cu

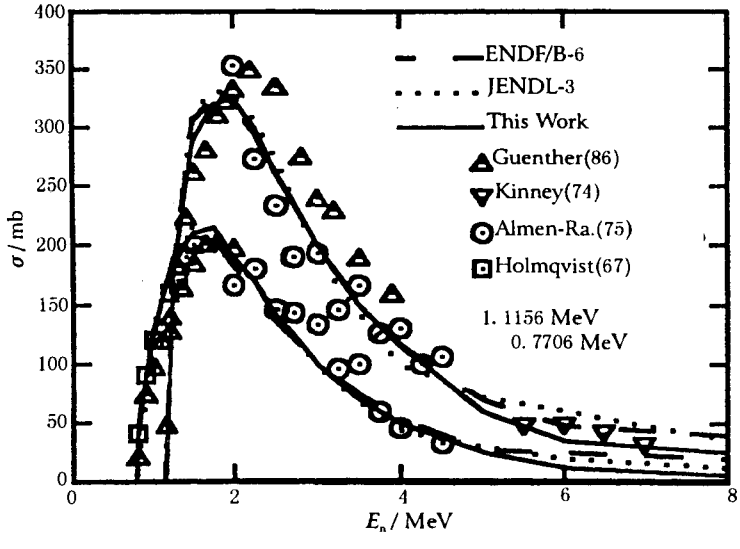

Fig. 3 Inelastic cross section of ^{65}Cu excited states

2.6 (n,2n) and (n,3n) Cross Section

For (n,2n) reaction, the experimental data were measured by Filatenkov, Molla, Ghanbari, Winkler, Csikai, Ryves, Mannhart, Araminowicz, Robertson, Mogharrab, Qaim, Santry, Prestwood[13~25] in the energy range from threhold to 20.0 MeV. The evaluated data were obtained by spline function fitting experimental data (see Fig.4).

The (n,3n) cross section was taken from the model calculation due to lack of the experimental data.

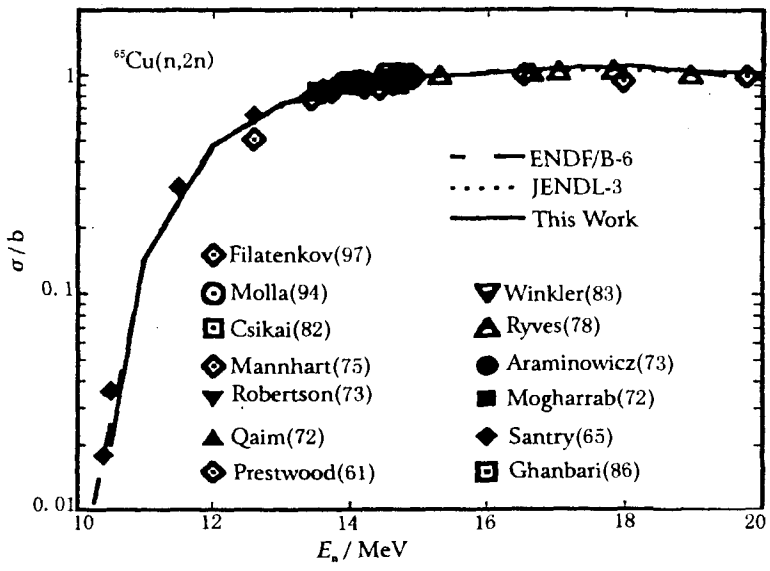

Fig. 4 (n,2n) cross section for ^{65}Cu

2.7 (n,p) and (n,n'p)+(n,pn') Cross Section

For (n,p) reaction, the experimental data were measured by Filatenkov, Molla, Gupta, Meadows. Ryves, Prasad, Vivitskaja, Bonazzoia, Ngoc, Pepelnik, Zhao, Qaim, Mitra, Santry[26~34]. The evaluated data were obtained by spline function fitting experimental data (see Fig. 5).

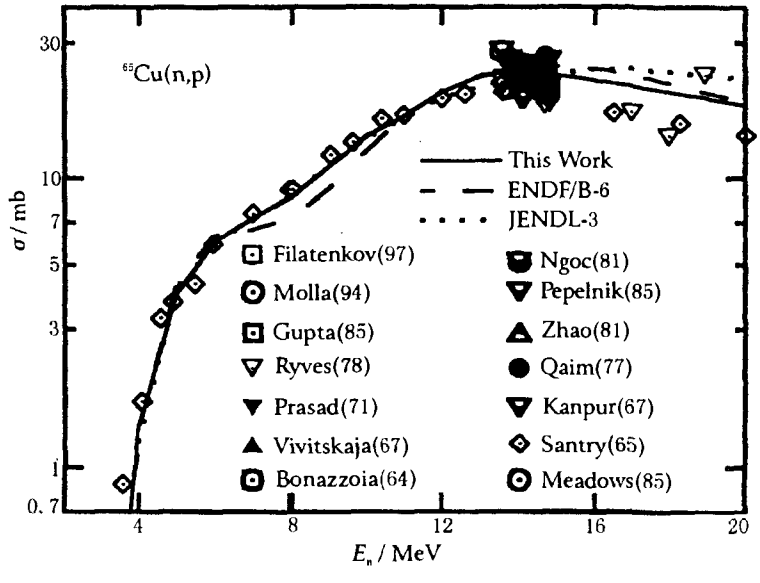

Fig. 5 (n,p) cross section for ^{65}Cu

For (n,n'p)+(n,pn') reaction, the experimental data were measured by Joensson[9] around 15.1 MeV. The evaluated data were obtained by nomalizing the calculated ones to the measured value as 22 mb at 15.1 MeV (see Fig. 6).

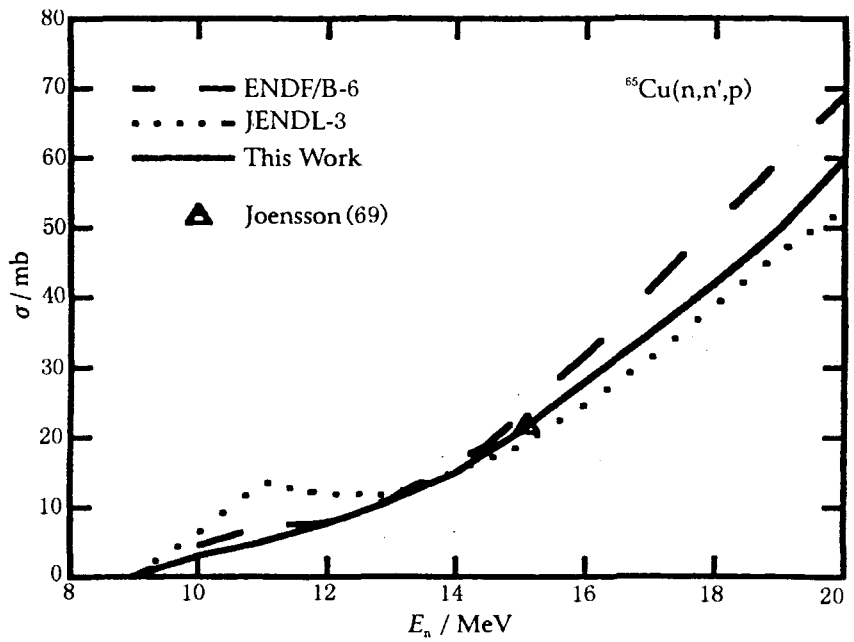

Fig. 6 (n,n'p) cross section for ^{65}Cu

2.8 (n, α), (n,n'α+n, αn') Cross Section

For (n, α) reaction, the experimental data were measured by Majdeddin, Molla, Mclane, Gruzdevich, Cserpak and Clator[35~38]. The evaluated data were obtained by spline function fitting experimental data in the energy range from threhold to 16.0 MeV. Above 16.0 MeV, calculated data were nomalized to fitting value of the experimental data at 16.0 MeV. (see Fig. 7).

For (n,n'α) + (n, αn') reaction, the experimental data were measured by Ryves, Qaim, Santry, Bramlitt[39] and Kantele[40]. The evaluated data were obtained by spline function fitting experimental data in the energy range from threshold to 20.0 MeV. A plot of these data against the evaluated cross section is shown in Fig. 8.

2.9 (n,d) Cross Section

The experimental data were measured by Ahmad[41] and Grimes[42] in the energy range from 9.0 to 14.8 MeV. The experimental datum by Grimes at 14.8 MeV was used to normalize the model calculated results (see Fig. 9).

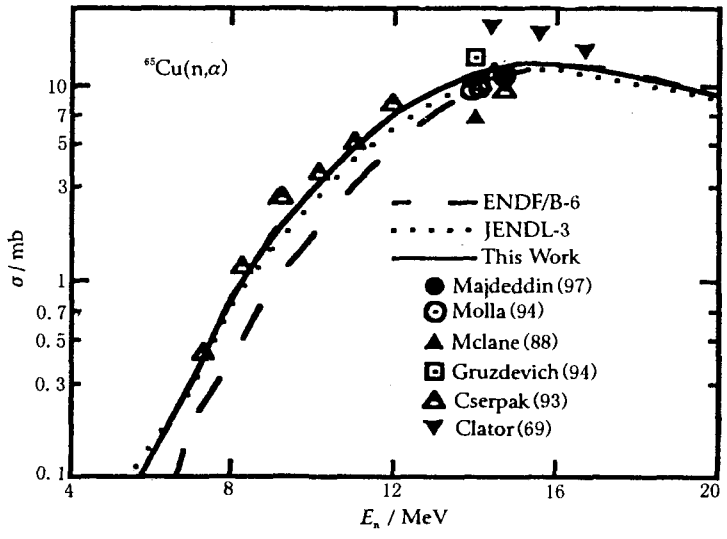

Fig. 7 (n,α) cross section for ^{65}Cu

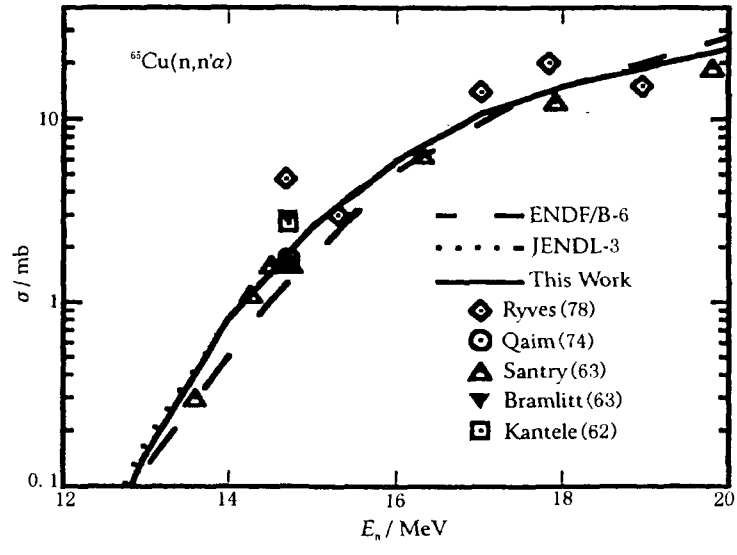

Fig. 8 (n,n'α) cross section for ^{65}Cu

2.10 Capture Cross Section

The cross section was obtained by spline function fitting experimental data, measured by Voignier, Mclane, Ghanbari, Zaikin, Colditz, Peto, Tolstikov, Stavisskij, Lyon and Johnsrud[43~50] in the energy range from 99.5 keV to 14.0 MeV. Above 14.0 MeV, calculated data were nomalized to Mclane's [36] experimental data at 14.0 MeV (see Fig. 10).

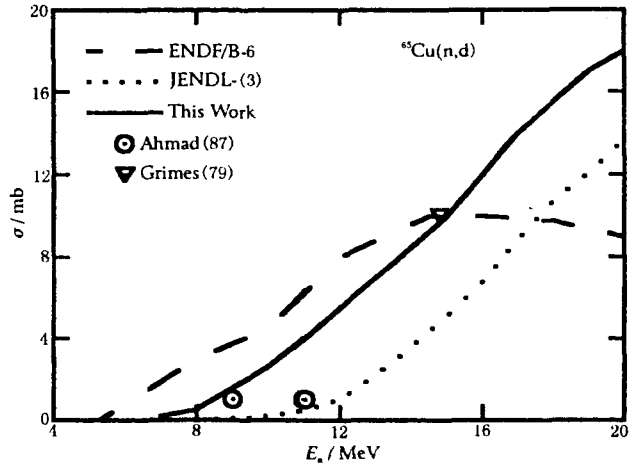

Fig. 9 (n,d) cross section for ^{65}Cu

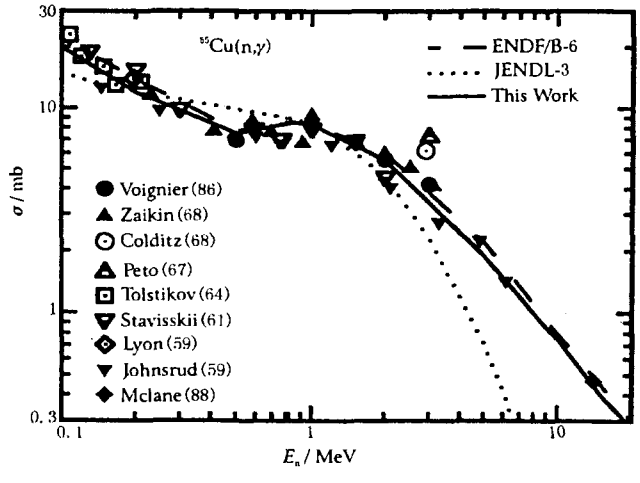

Fig. 10 (n,γ) cross section for ^{65}Cu

3 Secondary Neutron Angular Distributions

For elastic scattering, the experimental data measured by El-Kadi, Kinney and Rodgera[51] were used to adjust the optical model parameters in the calculations. The calculated results in good agreement with the experimental data and used for recommended one (see Fig. 11).

The discrete inelastic angular distributions (MT=51~62) were obtained from theoretical calculation results. the angular distributions for (n,2n), (n,3n), (n,n'α), (n,n'p) and continuum inelastic(MT=16, 17, 22, 28, 91) were assumed to be isotropic.

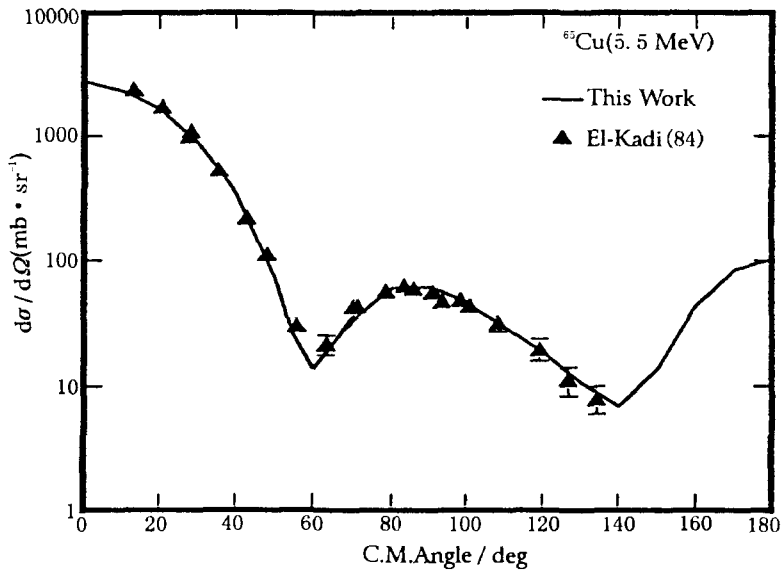

Fig. 11 Elastic scatter angular distribution of ^{65}Cu

4 The Double Differential Cross Section and γ-Ray Production Data

The double differential emission cross section (MF=6, MT=16, 17, 22, 28, 91, 103, 104, 105, 107) and γ-ray production data (MF=12~15) were taken from the calculation results. The contineous neutron spectra are shown in Fig.12. for (n,n') and (n,2n) reactions.

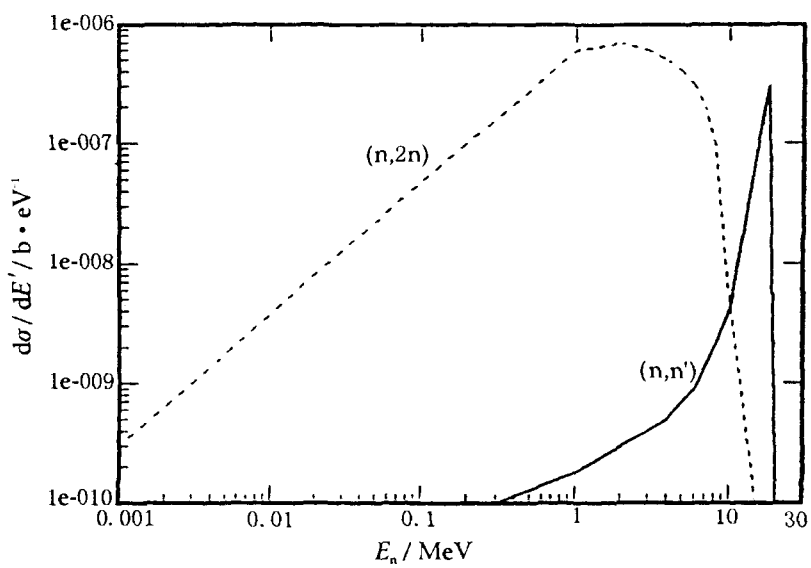

Fig. 12 (n,2n) and (n,n') continuous secondary neutron spectrum for ^{65}Cu at 20.0 MeV

5 Theoretical Calculation

An automatically adjusting optical potential code (APOM)[52] was used for searching a set of optimum neutron spherical optical potential parameters. ECIS95[53] code of coupled channel was used to calculate the direct inelastic scattering for excited levels as the input data of UNF. UNF code, including optical model, Hauser-Feshbach statistical model and exciton model, was used to calculate the data for files 3, 4, 5, 6, 12, 13, 14, 15. The input parameters for UNF are: optical potential, level density, giant dipole resonance[54] and nuclear level scheme. These parameters were adjusted on the basis of experimental data in the neutron energy range from 1 keV to 20 MeV.

5.1 Optical Model, Level Density and Giant Dipole Resonances Parameters

Optical potential parameters are given in Table 3. The level density and pair correction parameters are given in Table 4. The giant dipole resonance parameters are shown in Table 5, the symbols CSG, EE and GG mean the peak cross section, resonance energy and full width at half maximum, respectively.

Table 3 Optical model potential parameters*

	Depth/ MeV		Radius/ fm	Diffuseness/ fm
	V_0=55.563	W_0=16.076	X_r=1.1856	A_r=0.7457
	V_1=-0.4573	W_1=-0.3529	X_s=1.413	A_s=0.2569
Neutron	V_2=-0.00179	W_2=-35.467	X_v=1.413	A_v=0.2569
	V_3=-27.0387	U_0=-0.8459	X_{so}=1.1856	A_{so}=0.7457
	V_4=0.0	U_1=0.2384	X_c=1.0	
	V_{so}=3.41	U_2=0.0		

* Note: $V_r(E)=V_0+V_1E+V_2E(2)+V_3(A-2Z)/A+V_4Z/A(1/3)$;

$W_s(E)=W_0+W_1E+W_2(A-2Z)/A$;

$U_s(E)=U_0+U_1E+U_2E(2)$.

Table 4 Level density parameters and pair correction values of 11 excess nuclei*

	n,γ	n,n'	n,p	n, α	n, ^{3}He	n,d	n,t	n,2n	n,n' α	n,2p	n,3n
L	8.47	8.06	8.36	8.80	9.11	8.23	7.94	7.76	8.20	9.54	7.16
P	-0.1	1.5	1.4	-0.3	1.4	2.7	1.02	-0.2	1.2	-0.2	1.3

* Note: $L=[0.00880(s(z)+s(n))+Q_b]A$; $P=p(n)+P(z)$;

Q_b=0.142 or 0.12(spherical or deformation).

5.2 The Coupled Channel Calculation

The legendre Coefficients (L. C) of direct elastic scattering to ground state and direct inelastic scattering to excited states were calculated with coupled channel code ECIS95 at 19 energies by Han Yinlu in the required input format of UNF.

Table 5 The 11 giant dipole resonance parameters (single peak)

CSG(b)	0.075, 0.075, 0.034, 0.026, 0.026, 0.034, 0.034, 0.075, 0.026, 0.026, 0.075,
EE/ MeV	16.7, 16.7, 16.3, 16.37, 16.37, 16.3, 16.3, 16.7, 16.37, 16.37, 16.7,
GG/ MeV	6.89, 6.89, 2.44, 2.56, 2.56, 2.44, 2.44, 6.89, 2.56, 2.56, 6.89,

6 Concluding Remarks

Due to the new experimental data have been available for recent years, the evaluated data have been considerably improved especially for cross sections of total, (n,2n), (n, γ), (n,p), (n, α), total inelastic reactions and inelastic scattering to some discrete levels.

Acknowledgments

The author wish to thank Prof. Liu Tingjin and Liang Qichang for their helps with this work, also thank Prof. Han Yinlu for his helps in the ECIS code calculation.

References

[1] Zhang Jingshang. Nucl. Sci. Eng., 114, 55-63 (1993).

[2] Nuclear Data Sheets, 61(4),1990; 62(4),1991; 67(2),1992; 69(2),1993; 64(4),1991.

[3] M.S.Pandey et al., Private Communication and Phys. Rev., C15,600(1977).

[4] P.Guenther et al., Nucl.Phys., A448,280 (1986).

[5] D.C.Larson et al.,BNL-NCS-51245(1980); EXFOR-12882.011;80BNL277.

[6] Ei-Kadi et al., Nucl. Phys., A390,509(1982).

[7] W.Kinney et al., ORNL-4908(1974).

[8] Shi Xiamin et al., C.Nucl. Phys., 4(2),120(1982).

[9] B.Joensson et al., Arkiv for Fysik, 39,295(1969).

[10] P.Guenther et al., Nucl. Phys., A448,280(1986).

[11] E.Almen-Ramstrom et al., Atomnaya Energiya, 503(1975).

[12] B.Holmqvist et al., Atomnaya Energiya, 150(1964).

[13] A.A.Filatenkov et al., INDC(CCP)-402(1997).

[14] N.I.Molla et al., Nucl.Data for Sci. and Tech., Gatlinburg, U.S.A.,1994, p.938.

[15] F.Ghanbari et al., Annals of Nucl. Energy, 13, 301(1986).

[16] Winkler et al.,ANE,10(11),801(1983).
[17] Csikai et al., 82ANTWER,414(1982).
[18] T.V.Ryves et al., MET,14(3),127(1978).
[19] Mannhart et al., ZP,A272,279(1975).
[20] Araminowicz et al., INR-1464,14(1973).
[21] Robertson et al., JNE,27,531(1973).
[22] R.Mogharrab et al., AKE,19,107(1972).
[23] S.M.Qaim et al., Nucl. Phys., A185,614(1972); A283,269(1977); EUR-5182E,939(1974).
[24] D.C.Santry et al., CJP,44,1183(1965).
[25] R.J.Prestwood et al., Phys.Rev., 121,1438(1961).
[26] Gupta et al., Pramana, 24,637(1985).
[27] Meadows et al., 85SANTA,1,123(AD01)(1985).
[28] Prasad et al., Nuovo Cimento, A3(3),467(1971).
[29] G.P.Vinitskaja et al., Yademaya Fizika, 5(6),1175(1967).
[30] C.G.Bonazzoia et al., Nucl. Phys., 51,337(1964).
[31] P.N.Ngoc et al., INDC(HUN)-18, 11(1981).
[32] Pepelnik et al., NEANDC(E)-262U(5),32(1985).
[33] Zhao Zhenlan et al., J.Nucl.and Rariochemistry,Beijing, 3(2), 115(1981).
[34] B.Mitra et al., 67KANPUR, 367(1967).
[35] A.D.Majdeddin et al., INDC(HUN)-031(1997).
[36] V.Mclane et al., Neutron Cross Sections,vol.2, Boston(1988).
[37] F.Cserpak et al., Phys. Rev., C49,1525(1994).
[38] Clator et al., Dissertation Abstracts, B30,2850(1969).
[39] Bramlitt et al., Phys. Rev., 131,2649(1963).
[40] Kantele etal., Nucl. Phys., 35,353(1962).
[41] Ahmad et al., GRIMES(1986).
[42] S.M.Grimes et al., Phys. Rev., C19,2127(1979).
[43] J.Voignier et al., Nucl.Sci.Eng., 93,43(1986)
[44] G.G.Zaikin et al., Atomic Energy, 25,526(1968)
[45] Colditz et al., OSA,105,236(1968).
[46] G.Peto et al., Jou. of Nucl. Ener., 21,797(1967).
[47] V.A.Tolstikov et al., Atomic Energy, 17,505(1964).
[48] Yu.Ya.Stavisskij et al., Atomic Energy, 10,508(1961).
[49] Lyon et al., Phys. Rev., 114,1619(1959).
[50] Johnsrud et al., Phys. Rev., 116,927(1959).
[51] Rodgers et al., COO-1573-33,2(1967).
[52] Shen Qingbiao et al., CNDP, No.7, 43(1993).
[53] B.V.Carlson, The optical model ECIS95, Miramare-Trieste, Italy(1996,4,15-5,17).
[54] Zhuang Youxiang et al., Chinese Physics, 8, 721-727(1988).

Prompt γ-Ray Data Evaluation of Thermal-Neutron Capture for A=1~25

Zhou Chunmei
(China Nuclear Data Center, CIAE)

Abstract

The method of prompt γ-ray data evaluation for thermal-neutron capture has been briefly presented. The prompt capture γ-ray data of stable nuclei for A=1~25 are evaluated. The evaluated data have been changed into the ENSDF format and the checks of physics and format have been made.

Introduction

The energies and intensities, and their decay schemes of thermal-neutron capture γ-ray are one of the basic data of nuclear physics research, nuclear technology application and nuclear engineering design. Today, the technique of neutron-induced Prompt γ Activation Analysis (PGAA) is widely applied in material science, chemistry, geology, mining, archaeology, food analysis, environment, medicine, and so on. The availability of high-quality guided (or filtered) thermal and cold neutron beams at high and medium flux research reactors has greatly facilitated the advancement of the PGAA method during the 1990s.

PGAA is a non-destructive radioanalytical method, capable of rapid and simultaneous multielement analysis involving the entire Periodic Table, from hydrogen to uranium. The inaccuracy and incompleteness of the data available for use in PGAA are significant handicap in the qualitative and quantitative analysis of complicated γ spectra. Accurate and complete neutron capture γ-ray energy and intensity data are important for PGAA. The international database for PGAA is developing under the organization of Nuclear Data Section, IAEA.

The method of neutron-induced prompt γ-ray data evaluation is presented , and it is taken as an example to evaluate the prompt γ-ray data and its decay scheme for $^{13}C(n,\gamma)$ in the text.

1 Main Evaluation Program and its Function

Main programs of thermal-neutron capture prompt γ-ray data evaluation and their functions are listed in Table 1. These codes are mainly from International Network of Nuclear Structure and Decay Data Evaluation, the ENSDF data format is adopted in data evaluation.

Table 1 Main codes and their functions of prompt γ-ray data evaluation for thermal-neutron capture

Code name	Main functions
GTOL	level energy calculation by fitting to γ-energies; intensities balance calculation & checking
LWA	limit-weighted and unweighted average of measured data
HSICC	internal conversion coefficients calculation
HSMRG	format conversion from free format to ENSDF format
RADLST	energy balance calculation & checking
FMTCHK	ENSDF data format checking
PANDOR	ENSDF physics checking
ENSDAT	drawing decay schemes & listing data tables

2 Flow Chart of Prompt Neutron Capture γ Data Evaluation

The main flow chart of thermal-neutron capture γ-ray data evaluation is given in Fig.1. The basic characters are as follows:

a. Measured data collection

Evaluator retrieves related references from Nuclear Science References File, NSRF. On the basis of the retrieval, all measured data are collected from journals, reports, and private communications.

b. Measured data evaluation and recommendation of the best measured data

Gathered all related-data are analyzed and compared, treated by mathematical

method (for example, weighted or unweighted average of measured data). And then, the best-measured data and decay scheme can been recommended on the basis of the measured data evaluation.

c. Establishment of temporary data file

After recommendation of the best-measured data, the evaluated data are put into computer by hand, the temporary data file can be set up in ENSDF data format.

d. Theoretical calculation

Format checking must be done for temporary data file, and correction to old one should be done if necessary. Then, physics analysis and theoretical calculation are done and calculation results will be put into the gapes with no measured data so that recommended data become a self-consistent and complete data set.

e. Recommendation of complete data set

A complete data set of thermal-neutron capture prompt γ-ray data and its decay scheme is recommended as evaluated data set.

f. checking

Physics and format checking must be done and correction should be done if necessary. Specifically, checking of intensity balance must be done. The condition of the balance is as follows:

A nucleus captures a neutron and becomes a compound-nucleus. And then, it decays in emitting γ-ray. Assume i levels and j (or k) γ-rays,

i=0, 1 ,···, m

(0 is ground state, m is captured state)

j, k=1, 2 , ···, n are decay-γ-ray

$$\sum_j I_{\gamma ij}(\text{out}) \approx \sum_k I_{\gamma ki}(\text{in}) \qquad i \neq 0, m \qquad (1)$$

$$\sum_j I_{\gamma mj}(\text{out}) \approx \sum_k I_{\gamma ko}(\text{in}) \qquad (2)$$

$$I_{\gamma ij} = I_{ij}(1+\alpha_{ij}) \qquad (3)$$

$$I_{\gamma ki} = I_{ki}(1+\alpha_{ki}) \qquad (4)$$

where, $I_{\gamma ij}$, $I_{\gamma ki}$, I_{ij} ,and I_{ki} are total transition intensities and γ intensities for ij- and ki γ-ray, respectively; α_{ij} and α_{ki} are respectively internal conversion coefficients of ij-

th and *ik*-th γ-rays; "in" is the ray of entrance level, "out" is the ray of out-level. In general, values of in-level and out-level are all the same within their uncertainties.

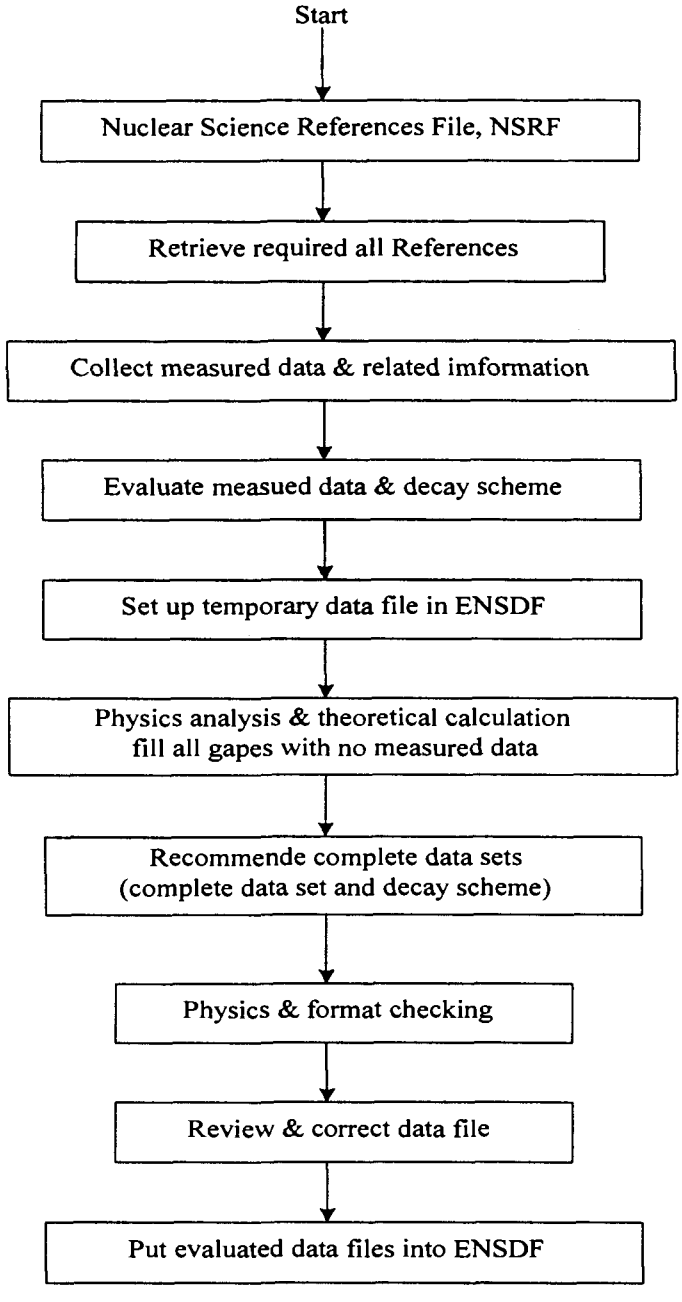

Fig. 1 Flow chart of prompt γ-ray data evaluation for thermal-neutron capture

If a level scheme is complete and internal conversion can be neglected, the

quantities $\sum_j I_j$ (primary ray), $\sum_j E_j I_j$ /S(n), and $\sum_j I_j$ (secondary-ray to ground state) should all be the same within their uncertainties. where, S(n) is neutron binding energy of neutron-captured nucleus.

3 Application

The prompt γ-ray data and their decay schemes of thermal-neutron capture for stable nuclei ^{1}H, ^{2}H, ^{6}Li, ^{7}Li, ^{9}Be, ^{12}C, ^{13}C, ^{14}N, ^{16}O, ^{17}O, ^{19}F, ^{20}Ne, ^{21}Ne, ^{22}Ne, ^{23}Na, ^{24}Mg, and ^{25}Mg have been evaluated by using these programs.

The data evaluation of $^{13}C(n,\gamma)$ reaction at *E*=thermal is taken as an example to show its application. The evaluated data of ENSDF format for $^{13}C(n,\gamma)$ reaction at *E*=thermal are given in Table 2. The evaluated level data and γ-radiation data are listed in Table 3 and 4, respectively. The decay scheme of $^{13}C(n,\gamma)$ reaction at *E*=thermal is given in Fig. 2. The γ-ray intensities balance is given in Table 5. From these tables and scheme it can be seen that the evaluated data are self-consistent in physics and intensity balance.

Table 2 ENSDF format listing of evaluated data for $^{13}C(n,\gamma)$ reaction at *E*=thermal

```
14C      13C(N,G) E=THERMAL                82MU14(Ref.1)
14C  C   TARGET JPI=1/2-.
14C  C   82MU14: MEASURED EG AND IG, DEDUCED SN.
14C  C   EVALUATED SN=8176.44 KEV 1 (95AU04,Ref.2).
14C  CL E          FROM EG USING LEAST-SQUARES FIT TO DATA.
14C  CL J,T        FROM 96FIZY, except as noted.
14C  CG E          FROM 96FIZY, EXCEPT AS NOTED.
14C  CG E(A)       FROM LEVEL ENERGY DIFFERENCES.
14C  CG RI         INTENSITIES PER 100 NEUTRON CAPTURES FROM 82MU14.
14C   N 1
14C  PN
14C   L 0.0          0+                    5730 Y     40
14C 3 L %B-=100$
14C   L     6093.82201-                    7 FS       LT
14C   G 6092.4     2 16.3     8
14C 3 G FL=0.0
14C   L       6589.5 30+                   3.0 FS     4
14C   G 495.4       3 8.0      3
14C 3 G FL=6093.82
14C   L       6902.7 30-                   25 FS      3
14C   G 808.9       2 3.6      3
14C 3 G FL=6093.82
```

(Table 2 Cont.)

```
14C    L   8176.44 1 0-,1-                                S
14C   CL J            FROM S-WAVE NEUTRON CAPTURE
14C    G 1273.81     174.9        10
14C 3 G FL=6902.7$ FLAG=A
14C   CG                EG=1273.9 2 (82MU14)
14C    G 1586.92     188.5        5
14C 3 G FL=6589.5$ FLAG=A
14C   CG                EG=1586.8 2 (82MU14)
14C    G 2082.53     182.5        5
14C 3 G FL=6093.82$ FLAG=A
14C   CG                EG=2082.6 3 (82MU14)
14C    G 8174.0      3 84.0       23
14C 3 G FL=0.0$ FLAG=A
14C   CG                EG=8173.92 (82MU14)
```

Table 3 Level listing of evaluated data for $^{13}C(n,\gamma)$ reaction *E*=thermal

^{14}C Levels

E(level)†	Jπ‡	$T_{1/2}$‡	Comments
0.0	0+	5730 y *40*	%β⁻=100.
6093.82 *20*	1−	<7 fs	
6589.5 *3*	0+	3.0 fs *4*	
6902.7 *3*	0−	25 fs *3*	
(8176.44 *1*)	0−,1−		Jπ: from s-wave neutron capture.

† From Eγ using least-squares fit to data.
‡ From Ref.3, except as noted.

Table 4 γ-ray listing of evaluated data for $^{13}C(n,\gamma)$ reaction *E*=thermal

γ(^{14}C)

Eγ†	E(level)	Iγ§#	Comments
495.4 *3*	6589.5	8.0 *3*	
808.9 *2*	6902.7	3.6 *3*	
1273.81‡ *17*	(8176.44)	4.9 *10*	Eγ=1273.9 *2* (82Mu14).
1586.92‡ *18*	(8176.44)	8.5 *5*	Eγ=1586.8 *2* (82Mu14).
2082.53‡ *18*	(8176.44)	2.5 *5*	Eγ=2082.6 *3* (82Mu14).
6092.4 *2*	6093.82	16.3 *8*	
8174.0‡ *3*	(8176.44)	84.0 *23*	Eγ=8173.92 (82Mu14).

† From Ref.3, except as noted.
‡ From level energy differences.
§ Intensities per 100 neutron captures from Ref.1.
# For intensity per 100 neutron captures, multiply by 1.

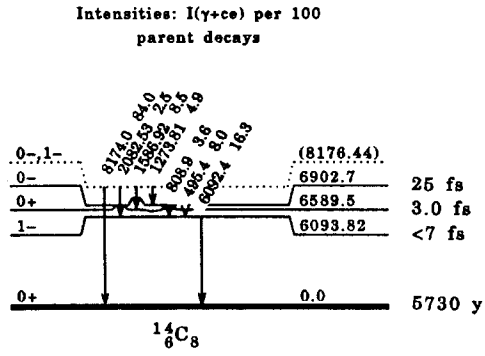

Fig. 2 Decay scheme of evaluated data for $^{13}C(n,\gamma)$ reaction E=thermal

Table 5 Intensities balance listing of evaluated data for $^{13}C(n,^{\gamma})$ reaction E=thermal

LEVEL	RI (OUT)	RI (IN)	RI (NET)	TI (OUT)	TI (IN)	TI (NET)	NET FEEDING (CALC)
0.0	0.000	100.3 25	-100.3 25	0.000	100.3 25	-100.3 25	-0.3 25
6093.82 20	16.3 8	14.1 7	2.2 11	16.3 8	14.1 7	2.2 11	2.2 11
6589.5 3	8.0 3	8.5 5	-0.5 6	8.0 3	8.5 5	-0.5 6	-0.5 6
6902.7 3	3.6 3	4.9 10	-1.3 11	3.6 3	4.9 10	-1.3 11	-1.3 11
8176.44 1	100 3	0.000	100 3	100 3	0.000	100 3	100 3

References

[1] S.F.Mughabghab, et al., Phys. Rev. C26, 2810 (1982)

[2] G.Audi,et al. Nucl. Phys. A 595, 409(1995)

[3] R.B.firestone, et al., Table of Isotopes (8th Edition) Vol.1 (1996)

Evaluation of Complete Neutron Nuclear Data for ^{233}U

Yu Baosheng Shen Qingbiao
(China Nuclear data Center, CIAE)
Cai Chonghai
(Department of Physics, Nankai University, Tianjin)

Abstract

A complete set neutron data, including cross sections, angular distributions and secondary neutron spectra, from 10^{-5} eV to 20 MeV were evaluated based on evaluated experimental data and theoretical calculated results in ENDF/B-6 format.

Introduction

The neutron nuclear data of ^{233}U play an important role for U-Th fuel cycles of all thermal and fast reactor systems. A complete set of neutron nuclear data of ^{233}U was evaluated from 10^{-5} eV to 20 MeV for CENDL-3. The recommended data were performed based on evaluated experimental data and adjusted theoretical calculated results, except the resonance parameters that were taken from JENDL-3. The comparison of our evaluated data with others from ENDF/B-6 and JENDL-3 has been performed.

1 Thermal Cross Sections and Resonance Parameters

The resonance parameters were taken from JENDL-3.2. New analysis with SAMMY code for the resonance parameters were performed by H. Derrin in JAERI/NDC. Resolved resonance parameters for the Reich-more formula were obtained by using SAMMY in the energy region from 1 eV to 150 eV. Unresolved resonance parameters were deduced based on evaluated cross sections in the energy

region from 0.15 keV to 30 keV.

The total neutron number per fission is the sum of prompt and delayed neutron number. The delayed neutron yields evaluated by T.R. England[1] were adopted. The evaluated data for prompt neutron relied heavily on the measurement with respect to ^{235}U and ^{252}Cf using the CSEWG recommended standards.

2 Reaction Cross Section above 30 keV

2.1 Total Cross Section

Before 1974, the measured data for σ_{tot} exist in energy region from 40 keV to 15 MeV. The nonelastic cross section and Elastic Scattering Angular Distribution data were measured by W.P. Poenitz[2,3] from 0.1 MeV to 4.43 MeV in 1978 and from 0.11 MeV to 4.8 MeV in 1981 using time –of –flight technology with enriched 99.97 % of ^{233}U sample at ANL. The data of W.P. Poenitz[2,3] are higher 8% around 1.6 MeV and 4.8% around 14 MeV than previous evaluated data, respectively. The data were also measured by W.P. Poenitz[4] from 1.8 MeV to 20 MeV in 1983, therefore, The measured data cover all energy region from 40 keV to 20 MeV. No experimental data exist from 30 keV to 40 keV, therefore an extrapolation was made to give reasonable agreement with experimental data above 40 keV.

For elastic scattering angular distributions, there are two sets of data at 0.7 MeV and 1.5 MeV, which were measared by G. Haouat[5] in 1982. As the nonrelastic cross section, the data were measured by R.F. Taschch [6] at 1.24 MeV and 1.6 MeV. In order to adjust the parameter of optical potential, below the threshold energy of (n,2n) reaction, the experimental data $\sigma_{n,\gamma}+\sigma_{n,n}+\sigma_{n,f}$ were used as experimental σ_{non}.

2.2 Fission Cross Section

There are lot of the earlier experimental data measured relative to ^{235}U or ^{238}U in the MeV range. However, the difference among different laboratories are 24%~28% around 6 MeV and there are, no experimental data in some energy region. In order to resole the discrepancies and fill the gaps, some new accurate measurements were performed and shown in Table 1.

The measurement technology was improved by J.W. Behrens[7] by using ionization fission chamber in time-of-flight spectrometer at 100 MeV Linac in 1978.

The new procedure is called "threshold cross section method" which use high-purity threshold isotope (TI), fissile isotope ^{235}U (or ^{233}U) to be measured (FI) and mixture of both (HI). The three fission chambers are exposed simultaneously to the same beam.

The R(E) is the ratio of the counting rates of MI to FI. Below the fission threshold of TI, Q represents a constant. η is atom ratio of FI to TI. Mass spectrometer was used to measure the isotopic compositions.

The cross section ratio is shown:

$$\sigma_{TI}(E)/\sigma_{FI}(E)= \eta\,[R(E)/Q-1]$$

Using the "threshold cross section method" , the advantage is not to require knowledge of the relative masses within the high-purity fission chambers and the detector efficiency. Furthermore, the procedure is suitable to the white neutron source.

Table 1 Collected data and relevant information for $^{233}U(n, f)$ reaction[1)]

Year	Author	E_n / MeV	Measured Values at 14.7 or 19.4 MeV	Method	Monitor	Comments
1976	J.W.Behrns	1.0~29.0 MeV		T-O-F	$^{235}U(n,F)$	at LINAC
		14.7 MeV	2.238±0.07			
		19.4 MeV	2.033±0.07			
1978	G.W.Carlson	0.85keV~29 MeV		T-O-F	$^{238}U(n,F)$	at LINAC
		14.7 MeV	2..274±0.06			
		19.4 MeV	2.049±0.07			
1978	W.P.Poenitz	0.137~8.1 MeV		T-O-F	Absolute	
1979	J.W.Meadows	14.74 MeV	2.37±0.02	Chamber	$^{235}U(n,F)$	
1980	E.A.Zhagrov	0.12 MeV				
1981	R.Arlt	14.7 MeV	2.244±0.039	ASSOP[1)]	Absolute	Note 2)
1983	I.D.Alkhazov	14.7 MeV	2.244±0.042	ASSOP	Absolute	Note 3)
1984	K.R.Zasadny	14.62 MeV	2.430±0.080	Activation	$^{56}Fe(n,p)$	Corrected Value
1986	I.D.Alkhazov	19.4 MeV	1.930±0.070	ASSOP	Absolute	Note 3)
1987	V.A.Kalinin	19.4 MeV	1.930±0.070	ASSOP	Absolute	Note 3)

1) Associated Particle Method

2) Enriched Samples 99.99%

3) FISCH (Multilayer Ionization Chambers for Fission Fragments) Metallic Sample

So, the accurate fission cross sections could be obtained in widely energy region using white neutron source. During 1976~1978, the fission cross sections of

^{233}U to ^{235}U were measured by J.W. Behrens [7] in energy region 1.0 MeV~29 MeV and the ratio of ^{238}U to ^{233}U by G.W.Carlson[8] in energy region 0.85 keV~29 MeV. Their data are consistent with each other within errors, and the discrepancies in earlier measurements were either eliminated or significantly reduced.

The data measured by J. Wbehrns[7] and G.W. Carlson[8] were re-normalized to standard cross sections. The standard cross sections for ^{235}U(n, F) and ^{238}U(n, F) reactions were taken from ENDF/B-6.

After 1978 the measurements were made by W. P. Poenitz [9], J. W. Meadiws[10], E.A. Zhagrov [11] R. Arlt [12], I.D. Alkhaziv[13,15], K.R. Zasadny[14] and V.A. Kalinin[16]. Among them the data around 14.7 MeV were measured by J. W. Meadiws[10] and K.R. Zasadny[14] with activation method, and by R. Arlt [12] and I.D. Alkhaziv[13] with enriched sample 99.99% of ^{233}U using associated particle method, the data at 19.4 MeV were measured by I.D. Alkhaziv[15] and V.A.Kalinin[16] by using associated particle method. These measured data are in good agreement with the measured data by J. Wbehrns[7] and G.W. Carlson[8]. So the data of Wbehms and Carlson are reliable.

2.3 Radiation Capture Cross Section

For $^{233}U(n,\gamma)^{234}U$ reaction, there are experimental data available in energy region from 30 keV to 1 MeV, in order to get the (n,γ) cross section, the alpha values measured by J.C.Hopkins[17] were multiplied by the fission cross section. Based on the theoretical calculated and experimental data, the evaluated data were obtained, and could reproduce the experimental data very well.

2.4 Inelastic Scattering Cross Section

In MeV region, the accuracy inelastic scattering cross section of fissile nuclides are quite poor. The total cross sections of ^{233}U measured by W.P. Poenitz[3] are known in the uncertainty $\leqslant$ 1.5%, fission cross sections 2 %~3 %, elastic scattering cross sections be $\leqslant$ 3 %. The radiate-capture cross section is not well known but it is very small. So the inelastic scattering cross section of ^{233}U were obtained by subtraction on the elastic scattering, fission and capture cross sections from the total cross section at 1.27, 1.49, 1.85, 2.55, 3.55 MeV.

3 Theoretical Calculation and Adjusting Data

In order to recommend a complete set of neutron nuclear data of ^{233}U, the theoretical calculation were performed with FUNF code, based on the available total cross section, nonelastic scattering cross sections deduced by us from (n,γ), (n,2n) etc., in energy region 0.001~14 MeV as well as a few experimental data of elastic angular distributions. A set of neutron optical potential parameters were obtained in the energy region 0.001~20 MeV by using automatically searching code APFO96:

$$V = 46.585018-0.21592E-0.011160E^2 - 24(N-Z)/A$$
$$W_s = \max\{0.0, 6.613650- 0.064080E - 12.0(N-Z)/A\}$$
$$W_v = \max\{0.0, -0.0490+ 0.07293E - 0.00822E^2\}$$
$$W_{so} = 6.2$$

r_r=1.30871	r_s=1.30731	r_v=1.19845	r_{so}=1.188
a_r=0.51859	a_s=0.636390	a_v=0.606940	a_{so}=0.8 000

Using this set of neutron optical potential parameters and adjusted level density and giant dipole resonance parameters as well as fission parameters, the reaction cross sections, secondary neutron spectra and angular distribution were calculated by Cai Chonghai[19]. The calculated data can reproduce the measured data very well.

4 Comprehensive Recommendation

The evaluated total cross section and calculated elastic scattering angular distribution with other evaluated data from ENDF/B-6, JENDL-3 are shown in Figs. 1 and 2.

The recommended cross sections for (n, γ) were given based on the measured and theoretically calculated data Fig. 3.

The recommended fission cross sections were obtained based on the evaluated experimental data which with other evaluated data are shown in Fig. 4.

In order to calculate the inelastic scattering cross sections, the direct inelastic scattering data were used as the input data of FUNF. The discrete levels were

taken from China Nuclear Parameter Library, and as following:

No.	Energy/ MeV	Spin-Parity	No.	Energy/ MeV	Spin-Parity
G.S.	0.0	5/2 +	14	0.3985	1/2 +
1	0.0403	7/2 +	15	0.4111	17/2 +
2	0.0922	9/2 +	16	0.4158	3/2 +
3	0.1553	11/2 +	17	0.4320	9/2 +
4	0.1970	3/2 -	18	0.4560	5/2 +
5	0.2294	13/2 +	19	0.4970	11/2 +
6	0.2988	5/2 -	20	0.5038	7/2 -
7	0.3122	3/2 +	21	0.5177	19/2 +
8	0.3147	15/2 +	22	0.5220	15/2 -
9	0.3207	7/2 -	23	0.5466	5/2 +
10	0.3407	15/2 +	24	0.5615	9/2 -
11	0.3538	9/2 -	25	0.5720	1/2 -
12	0.379	7/2 +	26	0.5997	7/2 +
13	0.3976	11/2 -			

Above 0.6 MeV, the states are assumed to be overlapped. The first three levels were calculated with the EXIS-95 code and adjusted the first levels coupled level to reproduce the experimental data by A.B.Smith[18]. The results for first three levels were shown in Figs. 5~7. The calculated results of other levels and total inelastic cross section are shown in Figs. 8~9.

All of the evaluated cross sections are shown in Fig. 10.

Examples of neutron energy spectra calculated for (n,2n) and (n,f) reactions are presented in Fig.s 11 and 12.

5 Summary

The advantage of "threshold cross section method" makes it possible that the accurate fission cross sections could be obtained in widely energy region. The data measured by J. Wbehrns [7] and G.W. Carlson[8] are reliable.

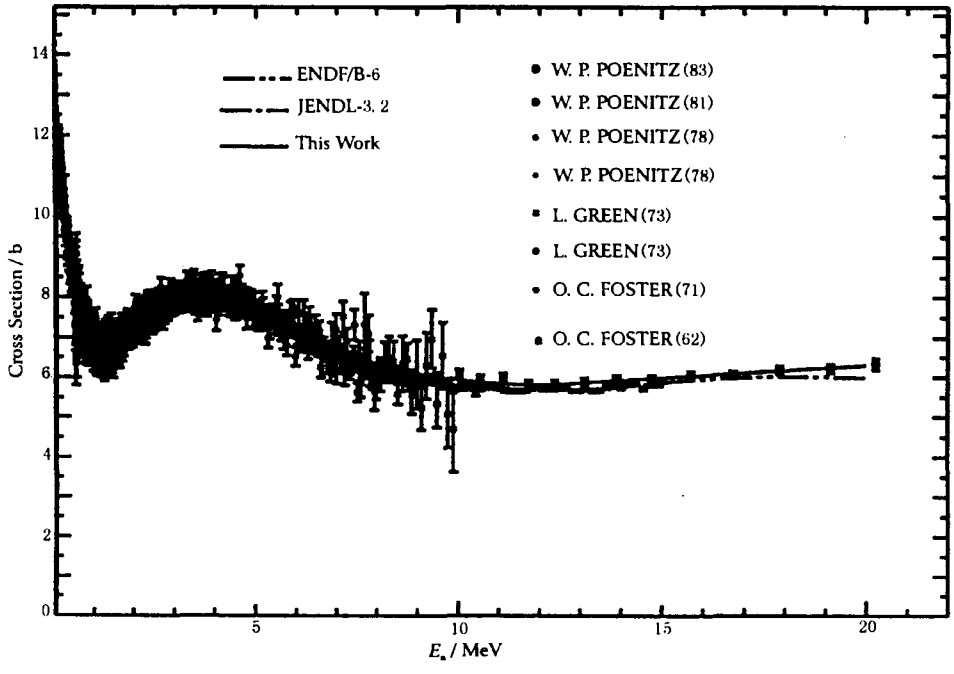

Fig. 1 Evaluated total cross section

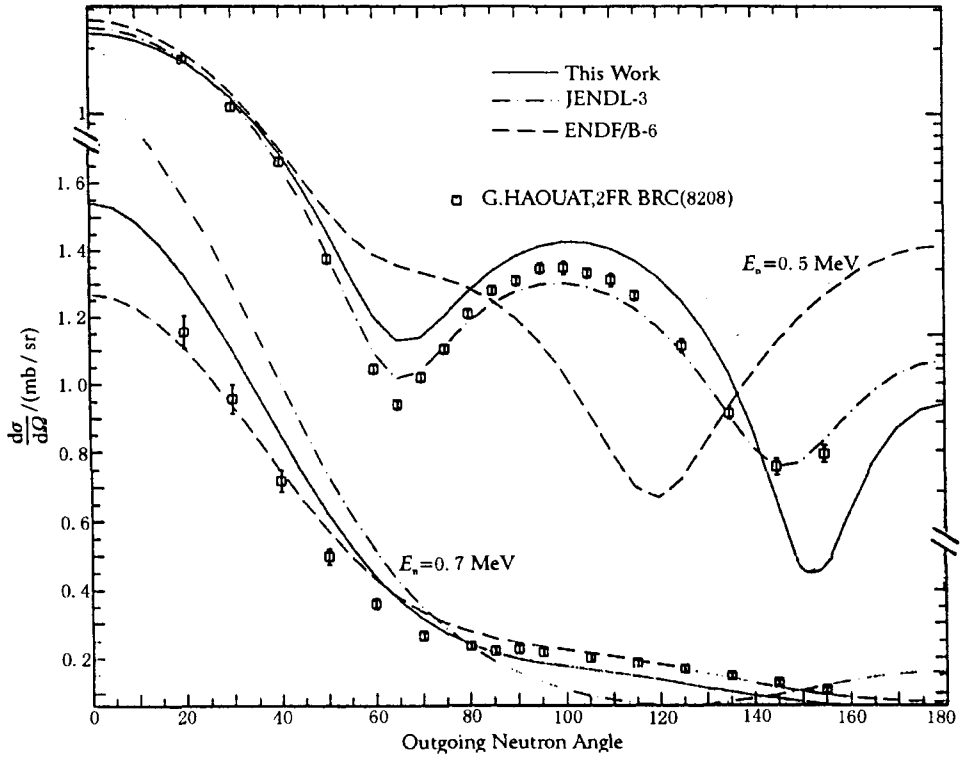

Fig. 2 ^{233}U Elastic scattering differential cross section at 0.7 and 1.5 MeV

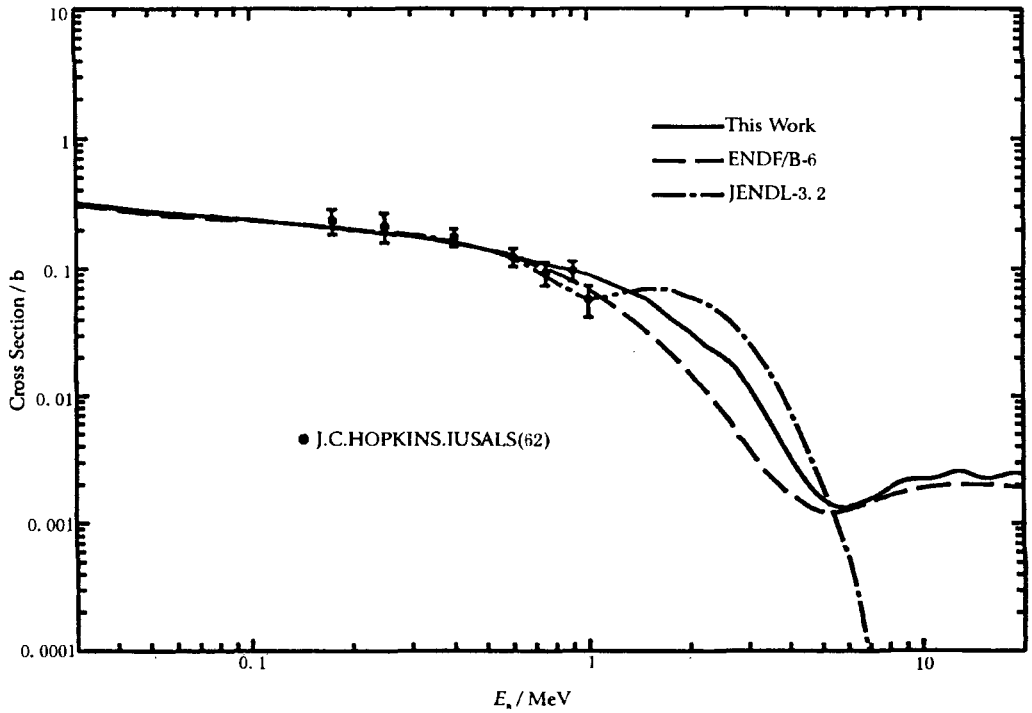

Fig. 3 Evaluated (n,γ) cross section

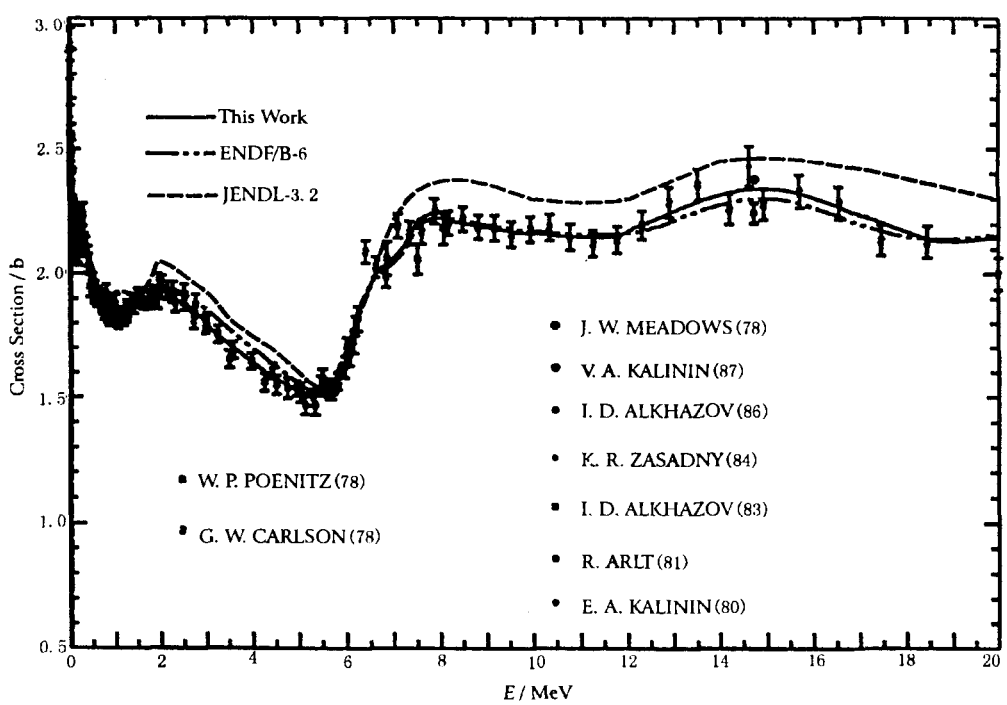

Fig. 4 Evaluated fission cross section

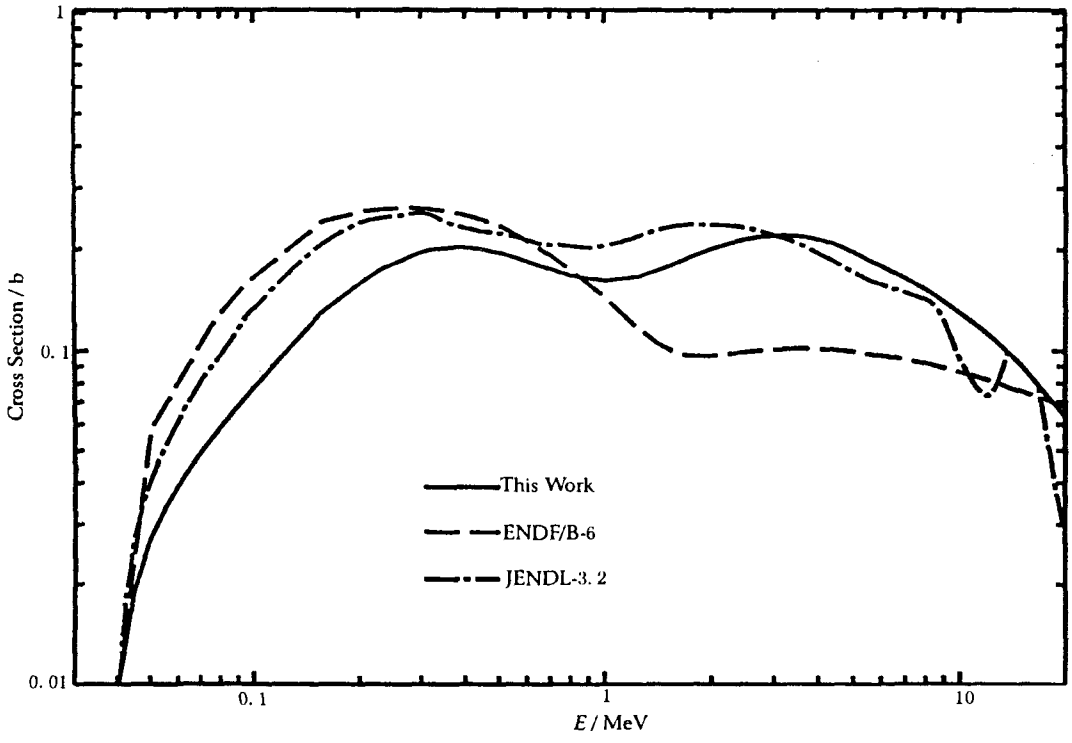

Fig. 5 Cross section of inelastic scattering to the first level

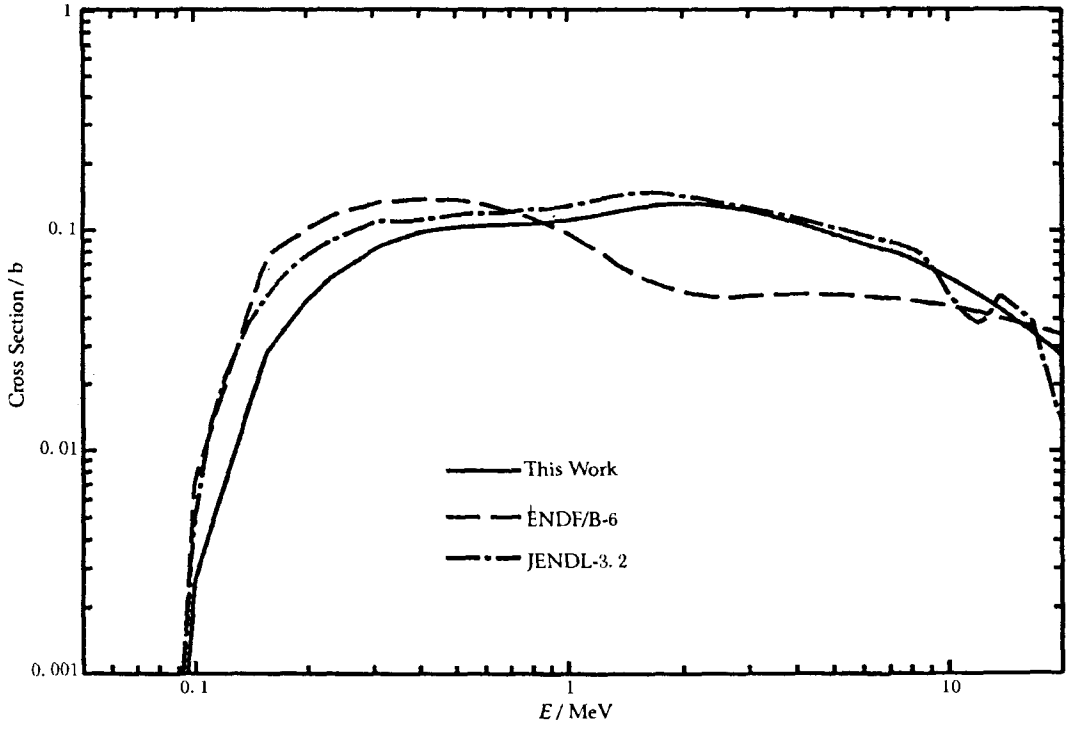

Fig. 6 Cross section of inelastic scattering to the second level

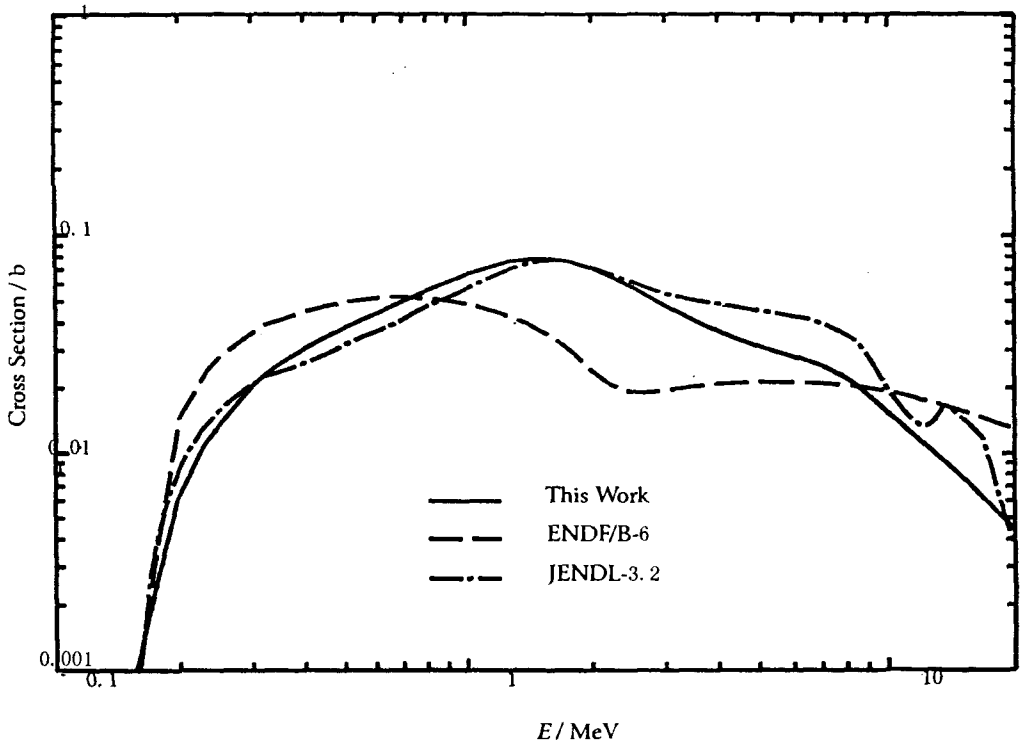

Fig. 7 Cross section of inelastic scattering to the third level

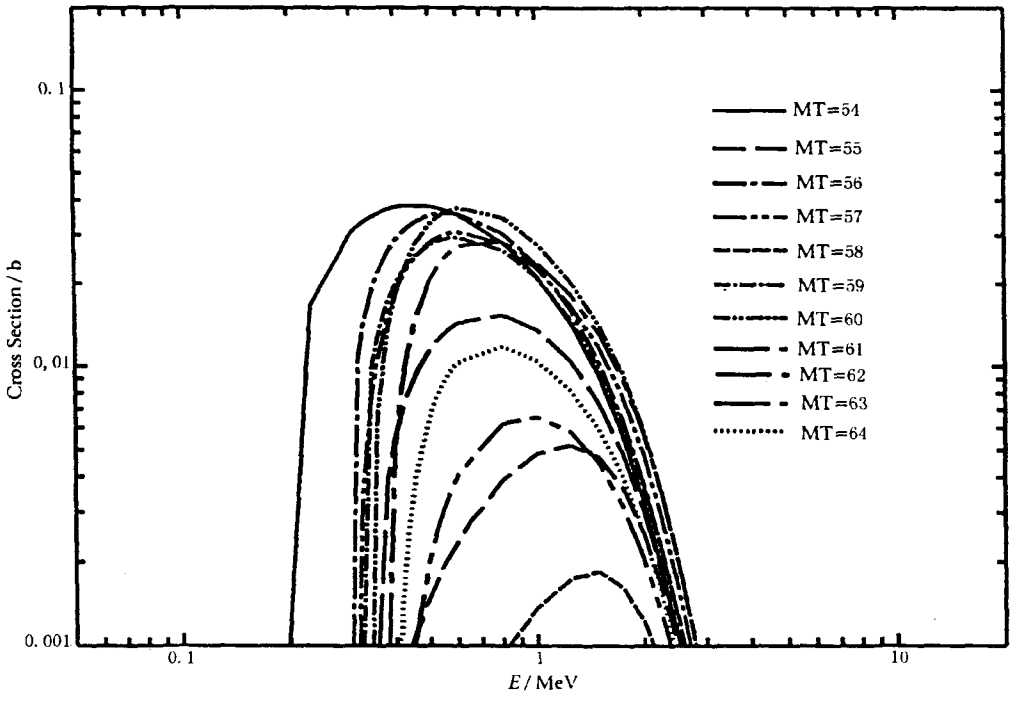

Fig. 8 The cross section of inelastic scattering to the discrete levels

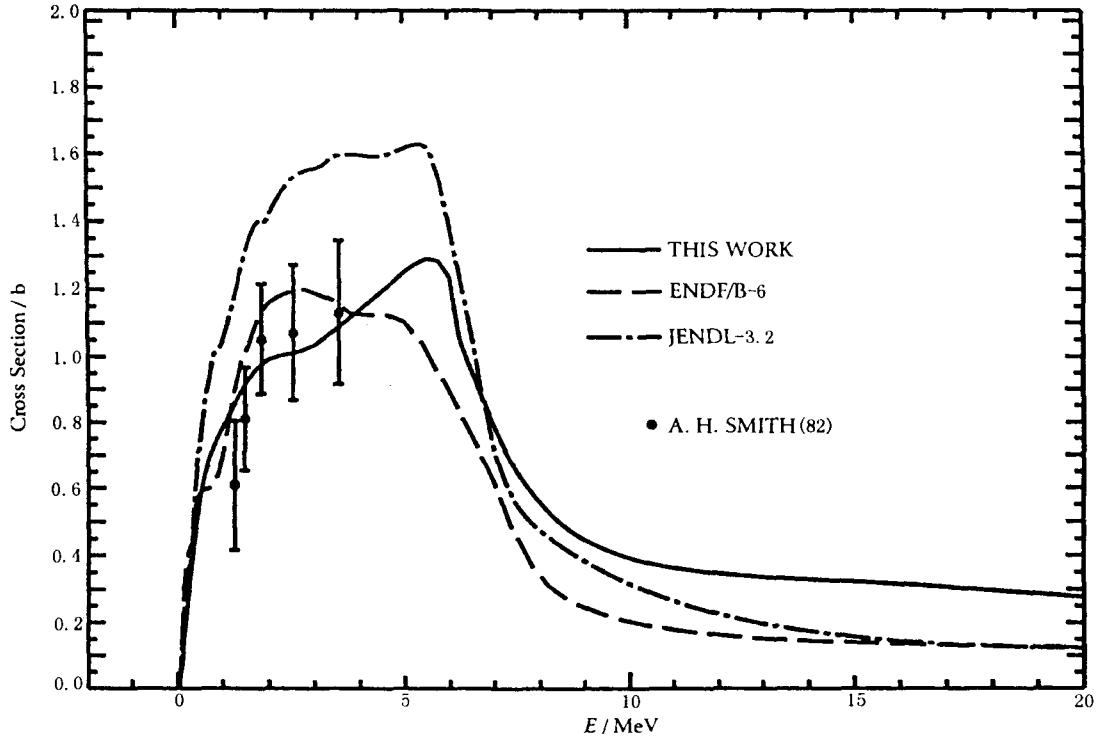

Fig. 9 Evaluated total inelastic scattering cross section

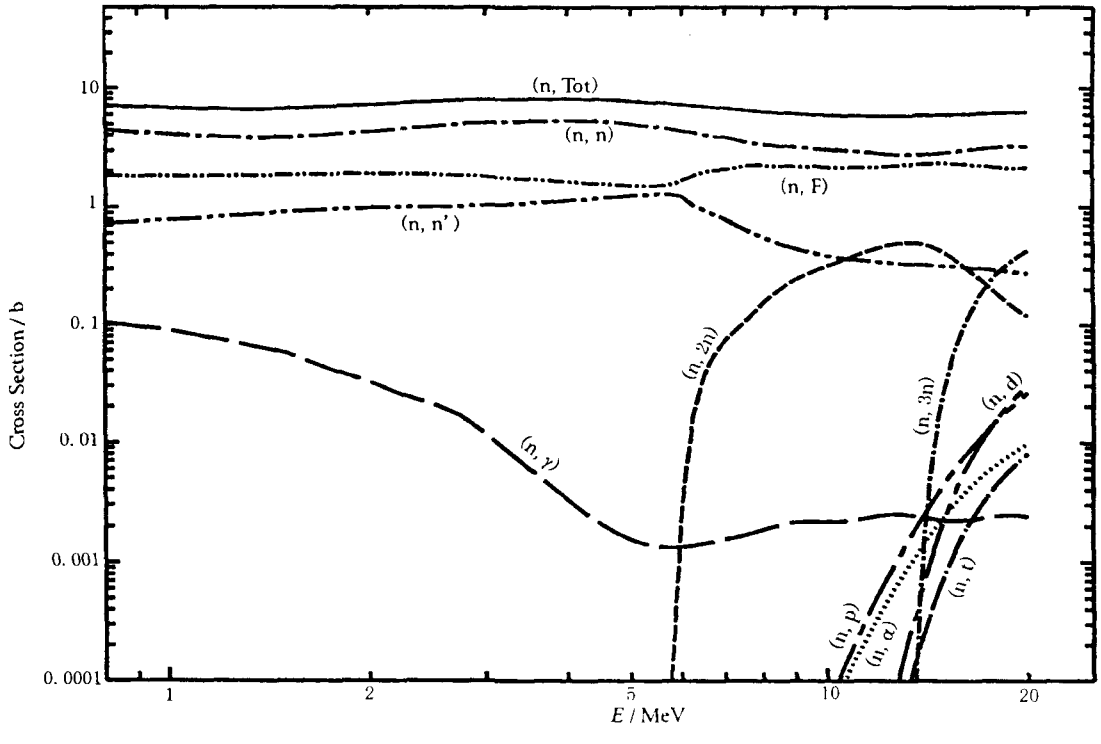

Fig. 10 Evaluated cross sections of ^{233}U

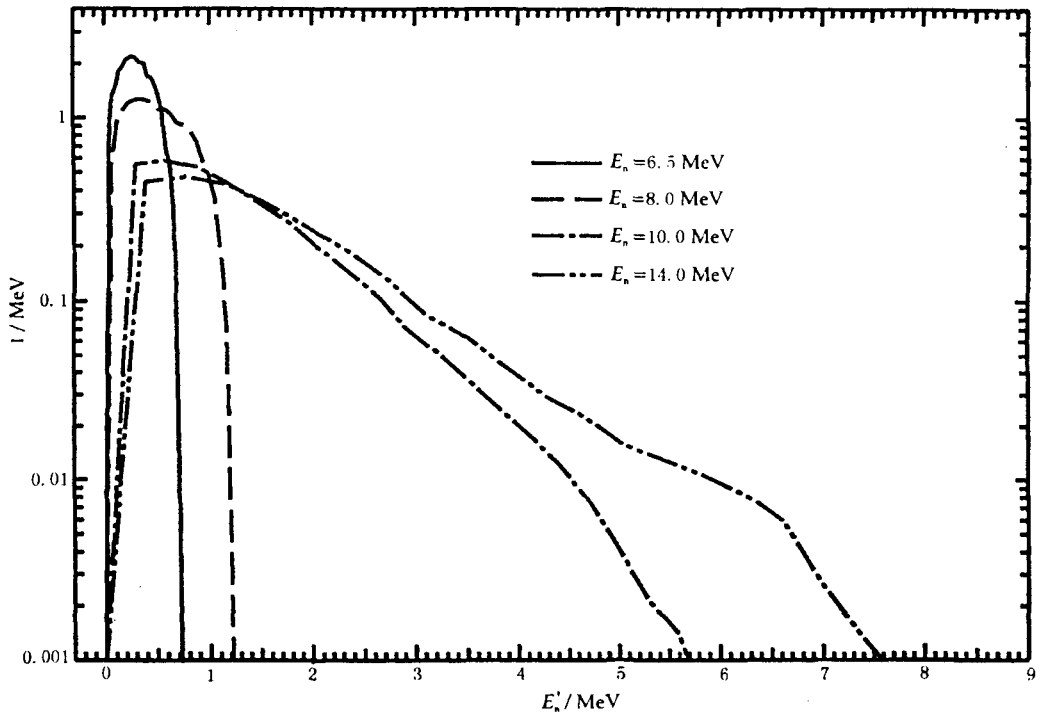

Fig. 11 Normalized secondary neutron spectra for $^{233}U(n,2n)$ reaction

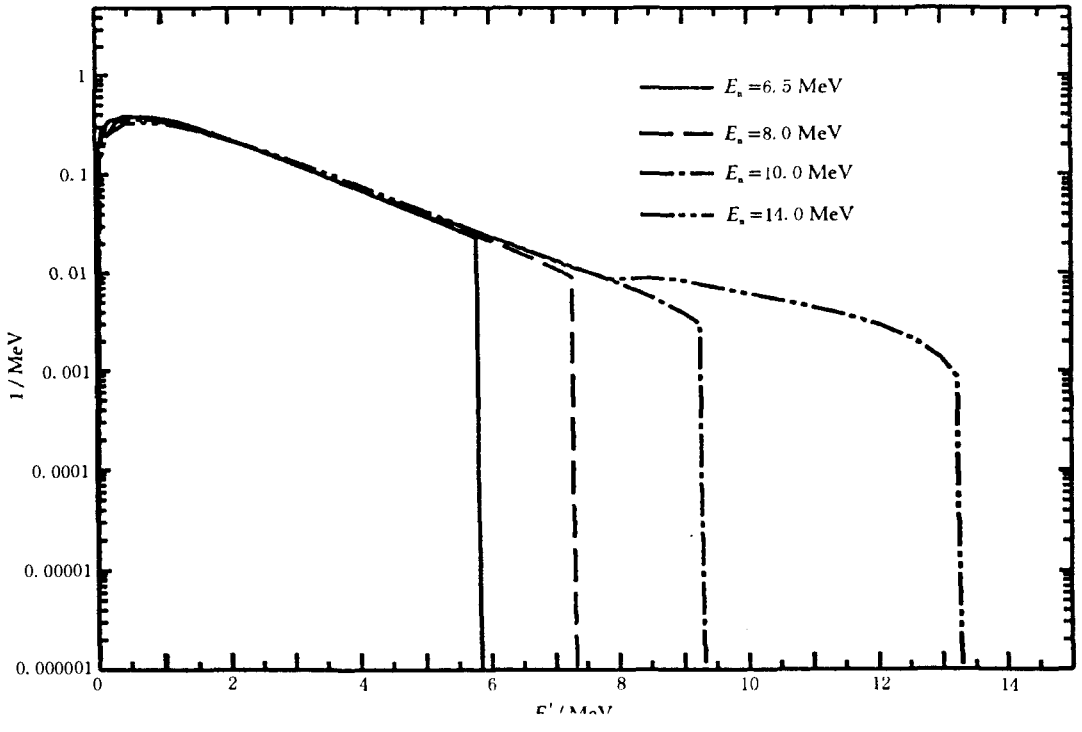

Fig. 12 Normalized secondary neutron spectra for $^{233}U(n,f)$ reaction

The accuracy of inelastic scattering cross sections are quite poor for fissile nuclides. For present work, the calculation was performed based on the measured data by A.B. Smith[18] and the new evaluated discrete levels. The parameters were adjusted carefully to reproduce the experimental data well. The evaluated inelastic scattering cross sections are improved.

Acknowledgments

The authors are indebted to Dr. Li Jingwen for his interesting and benefit discussions.

References

[1] T.R.Englang et al., Nucl. Sci. Eng., 103,129(1989)

[2] W.P.Poenitz et al., Nucl. Sci. Eng., 68,358(1978)

[3] W.P.Poenitz et al., Nucl. Sci. Eng., 78,333(1981)

[4] W.P.Poenitz et al., ANL/NDM-80(1983)

[5] G.Haouat et al., Nucl. Sci. Eng., 81,491(1982)

[6] R.F.Tascheket al., EXFOR Data 12364002(1965)

[7] J.W.Behrns et al., Conf. on Nuclear Cross Sections and Technology, Washington Vol.2,591 (1975)

[8] G.W.Carlson et al., Nucl. Sci . Eng.,66,205(1978)

[9] W.P.Poenitz et al., ANL-NDM-36(1978)

[10] J.W.Meadows et al., Annual of Nuclear Energy,15,421(1988)

[11] E.A.Zhagrov et al., Conf. on Nuclear Physics, Kiev,USSR,15-19 Spe.,P-45(1980)

[12] R.Arlt et al., KE,24,98(1981)

[13] I.D.Alkhaziv et al., Conf. on Nuclear Spectroscopy and Nuclear Structure, Moskva, USSR, 19-21 Apr., Vol2,201(1983)

[14] K.R.Zasadny et al., ANS,47,425(1984)

[15] I.D.Alkhazov et al., YK,4,19(1986)

[16] V.A.Kalinin et al., YK,4,3(1986)

[17] J.C.Hopkins et al., Nucl. Sci. Eng.,12,169(1962)

[18] A.B.Smith et al., Conf. on Nuclear Data for Science and Technology, Antwerp ,P.39(1982)

[19] Yu Baosheng, Cai Chinghai and Shen Qingbiao, private Communication (1999)

The Evaluation of the Experimental Data for $^{90,91,92,94,96,Nat}Zr$ Cross Section

Zhang Wei
(Zhengzhou University, 450052)
Liu Tingjin
(China Nuclear Data Center, CIAE, 102413)
Liu Jianfeng
(Zhengzhou University, 450052)

Abstract

On the basis of the experimental measurements, some new evaluations of neutron cross section for $^{90,91,92,94,96,Nat}Zr$ are performed by using the nuclear data evaluation methods CNDC. The evaluated energy region is from 10^{-5} eV or the threshold energy to 20 MeV.

Introduction

The nuclear data evaluation methods and system have been developed in CNDC[1], including the EXFOR experimental data retrieval, correction, evaluated experimental data processing, and spline fitting.

1 General Procedures of the Evaluation

1.1 EXFOR data retrieval and format standardization

The retrieval can be done from the EXFOR (experimental neutron data) master library by using EXFOR library manager system and the retrieval program RETRIVE for each reaction channel data or measured years or access number (mostly using reaction quantities).

It is well known that the EXFOR format is very flexible and complicated. So the format, especially the data table, needs to be changed and standardized for using and processing the data conveniently later. This can be completed with codes FORM[1], which includes column exchange, column adding, data normalization, unit conversion, error correction, etc. The difficulty of this step is that some nuclear data (for example, the energy) must be found and obtained under some key words, such as TITLE, COMMON or DATA manually.

The following reaction type data have been retrieved:(n, tot), (n,el), (n,inl), (n,2n), (n,3n), (n,n'p), (n,n'α), (n, γ), (n,p), (n,d), (n,t), (n,^{3}He) , (n,α), (n,xp), (n,xα)for each isotopes and natural element. As a result, the following available data were got. Cross section: ^{90}Zr(n, p),^{90}Zr(n, inl) to first, second and third energy level, ^{90}Zr(n,2n), ^{90}Zr(n,tot), ^{90}Zr(n,3n), ^{90}Zr(n,d), ^{90}Zr(n,γ), ^{90}Zr(n,el),^{90}Zr(n,t), ^{90}Zr(n,x)p, ^{90}Zr(n,x) α; ^{91}Zr(n,p), ^{91}Zr(n,inl) to second and third energy level, ^{91}Zr(n,tot), ^{91}Zr(n,γ); ^{92}Zr(n,p), ^{92}Zr(n,inl), ^{92}Zr(n,tot), ^{92}Zr(n,α); ^{94}Zr(n,p), ^{94}Zr(n,inl), ^{94}Zr(n,tot), ^{94}Zr(n,α), ^{94}Zr(n,γ); ^{96}Zr(n,p), ^{96}Zr(n,2n); ^{Nat}Zr(n,p), ^{Nat}Zr(n,inl), ^{Nat}Zr(n,tot), ^{Nat}Zr(n,γ); angle distribution: ^{Nat}Zr(n,el), ^{90}Zr(n,el), ^{91}Zr(n,el), ^{92}Zr(n,el), ^{94}Zr(n,el), ^{Nat}Zr(n,inl), ^{90}Zr(n,inl), ^{91}Zr(n,inl)da, ^{92}Zr(n,inl), ^{94}Zr(n,inl).

The measured experimental data relative to a monitor must be corrected using the new standard data. The ratio of the new monitor data to the old one is the correction factor, which is usually in 0.80~1.2. It is clear that any energy point in any entry (reference) must be processed by finding out monitor reference, calculating the correction factor and multiplying the experimental data. This is necessary and important because the process makes us find out the physical law more clearly.

The following new standards are used in the order is follows: (1) International recommended ones: ENDF/B-6, INDC(SEC)-10' (1992); (2) newly evaluated ones at home[2]; (3) ENDF/B-6 (not as standards).

1.2 Data correction and evaluation

The experimental data must be analyzed and evaluated carefully for the followings, which can be done by code SIG[1].

1) Experimental methods. Time of flight, activation and large liquid scintillator are very different. The reliability of every method is not the same. For example, the relative activation measurement dependends on the monitor threshold. For certain

reaction, the energy threshold is very different. The measurement with monitor threshold which is near the reaction threshold to be measured can gave better result than others. The experiment of $^{94}Zr(n,p)$ showed that applying $^{27}Al(n,\alpha)$ as monitor gave more reliable data than that of $^{56}Fe(n,p)$ as monitor. For details see Section 2, Subsection 5.

2) Identify the measured quantity. For example, whether measured quantity is total inelastic cross section or inelastic cross section to first energy level.

3)Whether the standard cross section used is the newest, internationally recommended one. Otherwise, the renormalization needs to be done with the new standard.

4)Analyze the data error. For some old data the error was not provided, but the error should be given. So an experimental data error table (see Table 1) for different were be applied. The error were given by considering the measured method and the year when experiment was carried out.

Table 1 The error range of different measured methods

Cross Section	Error Range	Methods
σ_{tot}	2%~5%	Transmission, Time of Flight, $\Delta t/L$= 0.05~0.5ns/m (LINAC)
$\sigma_{n,n}(E)$	5%~10%	Time of Flight, $\Delta t/L$= 0.2~0.7ns/m (VAG,Tandem,CCW)
$\sigma_{n,n}(\theta)$	5%~15%	
$\sigma_{n,n'}(E)$	5%~20%	
$\sigma_{n,n'i}(E)$	8%~20%	
$\sigma(E,E',\theta)$	8%~30%	
$\sigma_{n,2n}$		Activation method 1) NaI (before 1975) 2) Ge Li
$\sigma_{n,p}$	1) 5%~15%	
$\sigma_{n,\alpha}$	2) 2%~10%	
$\sigma_{n,\gamma}$		
$\sigma_{n,n'}$		

In some cases, there is not enough description for some experiment, and there are other experimental data in this energy region. In this case, the data without description were usually abandoned.

1.3 Data Processing

Data processing is a very important step in the evaluation. In the system[1], it includes the data processing at certain energy point, curve fitting.

The data at certain energy point are very significant for determining the absolute value of the recommended curve in the evaluation.

The curve fitting is essential treatment in the experimental data evaluation. Through it, the smooth optimum values in mathematics can be got as the recommended data. The program SPF have been developed by Liu Tingjin[1] for this purpose. The program includes the following features: 1) Knot optimization; 2) Any spline order; 3) Strict error calculation.

Before spline fitting, The initial knots were selected. Just because the knots can be optimized by the program SPF, the knots can be selected more freely. The only requirement is that the knots must be given at the peaks and volleys, or the certain structure. We apply a program DRAW for displaying the multi-sets of the on screen and can see the structure to give the initial knots for SPF.

2 The Evaluation of Some Typical Reactions.

It is difficult to give the evaluation of all reactions of so many isotopes. The following are only some typical reactions.

2.1 ^{90}Zr(n, 2n) reaction.

The data were evaluated by Zhao Wenrong[2] in 1989. Based on this, we collected all experimental data measured since 1989. There are 14 entries from EXFOR library associated with this reaction. The experimental data error of J.Csikai[3] and K.T. Osman[4] are so small, and it is not in correspondence with the statistic, so the data error was changed to 7%. The data of I. Kimura[5], K. Kobayashi[6], Shafiqul[7] were abandoned because they are only for ground state or isometric state. The data of N.L. Maidana[8] and E.I. Grigor'EV[9] were also abandoned because they were average ones over a spectrum. The data error at 16.6 MeV is 82 mb in the evaluated data of 1989[2], but in Entry 30686 (performed by Zhao himself)[10], it is 45mb. Considering the errors at other energy point, 45 mb is more reliable, so 45mb is reserved. As a result of elimination, 5 sets [3,4,10,11,12] of data were adopted. The data were corrected to the new standards. The data were fitted with spline function. The results are compared with ENDF/B-6 and JENDL-3 and are shown in Fig. 1.

2.2 ^{90}Zr(n, total)

There are 10 sets[13~22] of experimental data for this reaction. The data of M.B. Fedorov[22] were abandoned because the energy resolution is 1.2 ns/m, as L. Green[14] is 0.5 ns/m; the data of Z.M. Bartolome[13] were abandoned because they were relative ones, and the trend is not correct. The evaluated data were obtained by spline fitting from 0.5 MeV to 20 MeV. For details see Fig. 2.

2.3 ^{Nat}Zr(n, total).

There are so many measured data sets for this reaction (more than 30 entries)[23~59]. We eliminated entries measured before 1960 and in the energy lower than 50 keV. After this, there remains 18 sets of data. Among them 3 sets of data were given by L. Green[23]. We took the data measured with thinner sample. But it was found that the trend is not in correspondence with others. So eliminated all. The datum at first energy point of R.W. Stooksberry[25], deviated from others, so this energy point were eliminated. The data of K.K. Seth[41], S. Rapeanu[56], V.V. Filippov[57] and G. Deconninck[59] were also abandoned because they are discrepant with others. As a result, the data of were taken and fitted with SPF code (see Fig. 3).

2.4 ^{92}Zr(n,p)

The data are in agreement in the error bar region. But F. Strohal[60] applied old method, the half-life of R. Prasad[61] experiment is not correct. The data of V.N.Levkovskij[62] has no monitor information, so these data were eliminated. The evaluation data were obtained by spline fitting from 6 MeV to 14.2 MeV. The comparison is shown in Fig 4.

2.5 ^{94}Zr(n,p)

There are two trends before evaluation. We found that the data measured with ^{27}Al(n,α) as monitor in high group, others with ^{56}Fe(n,p) or ^{63}Cu(n,2n) in low group. As we knew, the threshold energy of ^{27}Al(n,α) is near the threshold energy of ^{94}Zr(n,p), so we adopt the data with ^{27}Al(n,α). After this ,we also found the data of S.M. Qaim[63] is more reliable because the data just in high or low data's error region, so when spline fitting we let the curve go through it by setting the highest weight to these data. The evaluation data were obtained by spline fitting from 11.5 MeV to 16.52 Mev. The comparison of experimental data with evaluated ones is shown in Fig. 5.

2.6 ^{94}Zr(n,)

The data with ^{27}Al(n,α), ^{56}Fe(n,p) as monitor were abandoned because of the threshold energy analysis. After this, there remains 5 sets of data[64~68]. The energy of B.P. Bayhurst[64], C.H. Reed[65], V.N. Levkovskij[67] is near 14 MeV, so we average them and, let the curve go through it by setting high weight to this datum. The evaluated data were obtained by spline fitting from 12 MeV to 20 MeV. The comparison of experimental data with evaluated ones is shown in Fig 6.

2.7 natural Zr(n,EL) DA

There are some experimental data in energy region 0.314MeV. (0.3 MeV, 0.5 MeV, 3.6 MeV, 1 MeV, 5 MeV, 7 MeV, 14 MeV). Here are the reasons for choosing: Entries 10332, 11854, 11637 of EXFOR data are in energy region 0.9~1 MeV, we eliminated entry 11854 because of deviation. Entry 11130, 11617, 11867, 12801 of EXFOR data are in agreement near 3.6 MeV, We recommended the data at 0.3 MeV, 0.9 MeV, 3.5 MeV, 5 MeV, 7 MeV, 8.5 MeV, 10 MeV and 14.2 MeV.

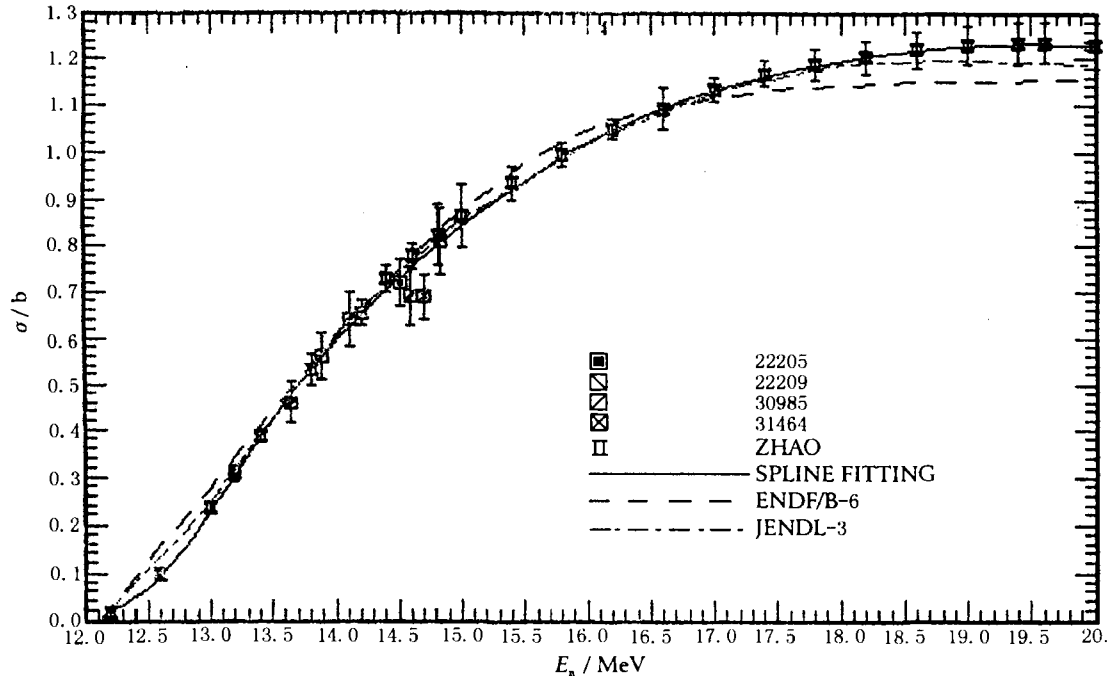

Fig. 1 ^{90}Zr (n,2n) reaction

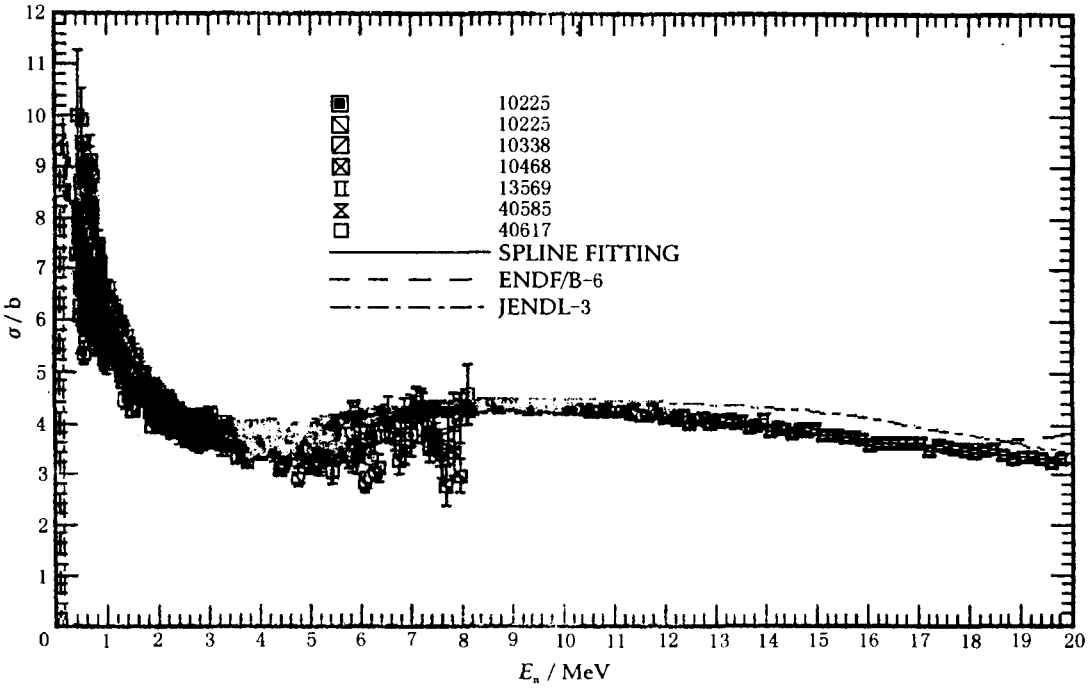

Fig. 2 ^{90}Zr (n,total) reaction

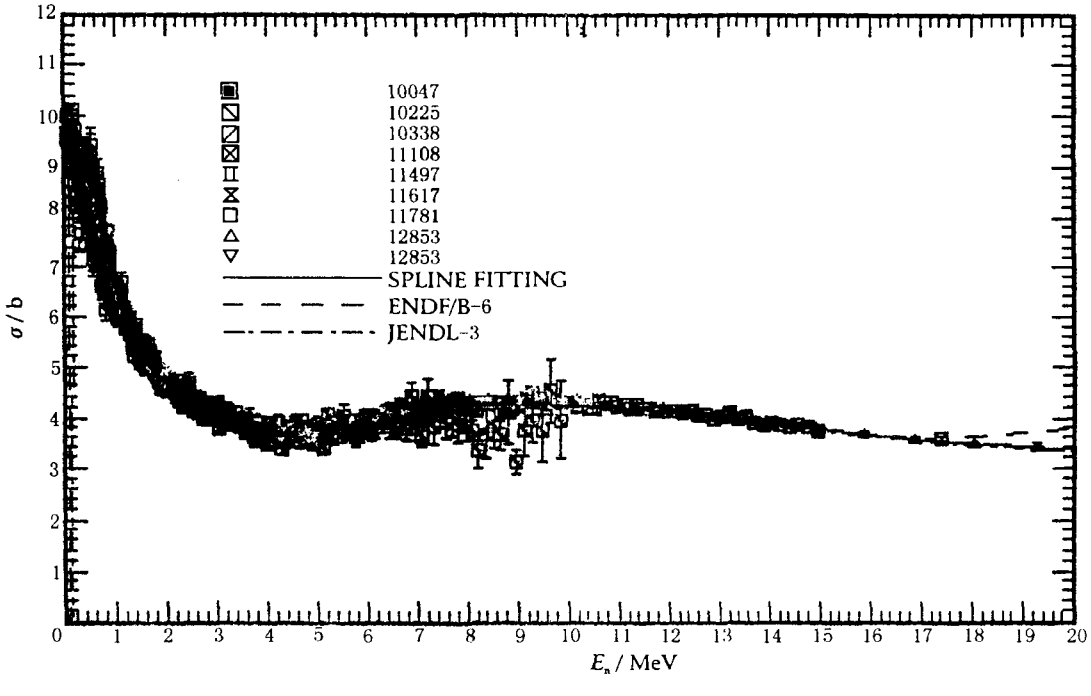

Fig. 3 Natural Zr (n,2n) reaction

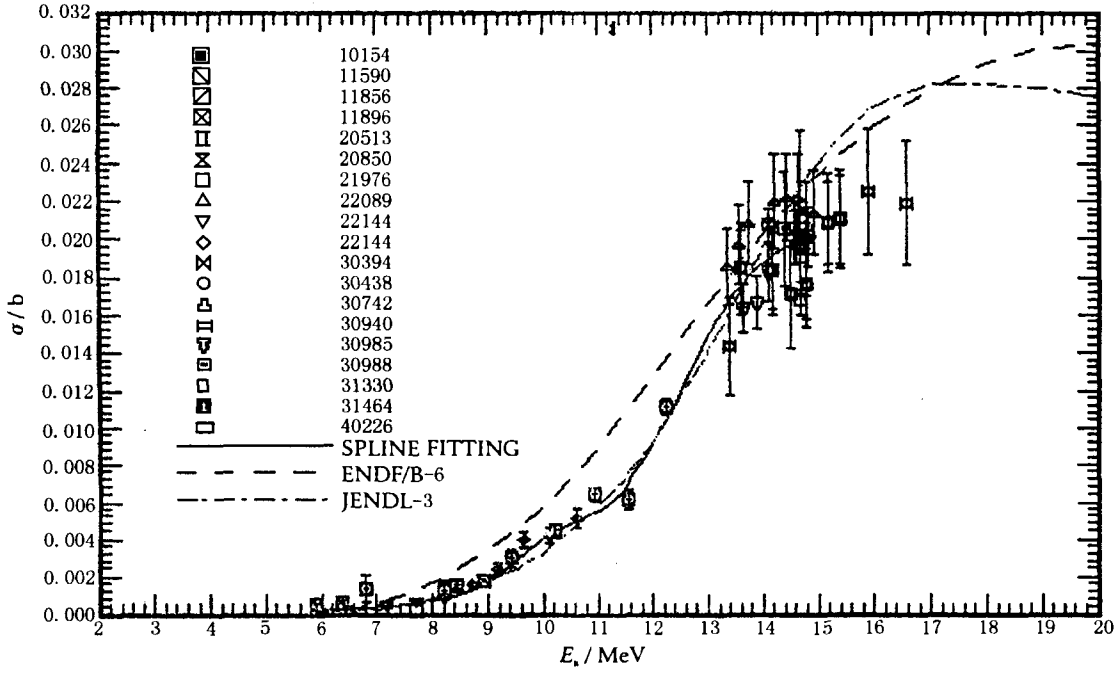

Fig. 4 ^{90}Zr (n,p) reaction

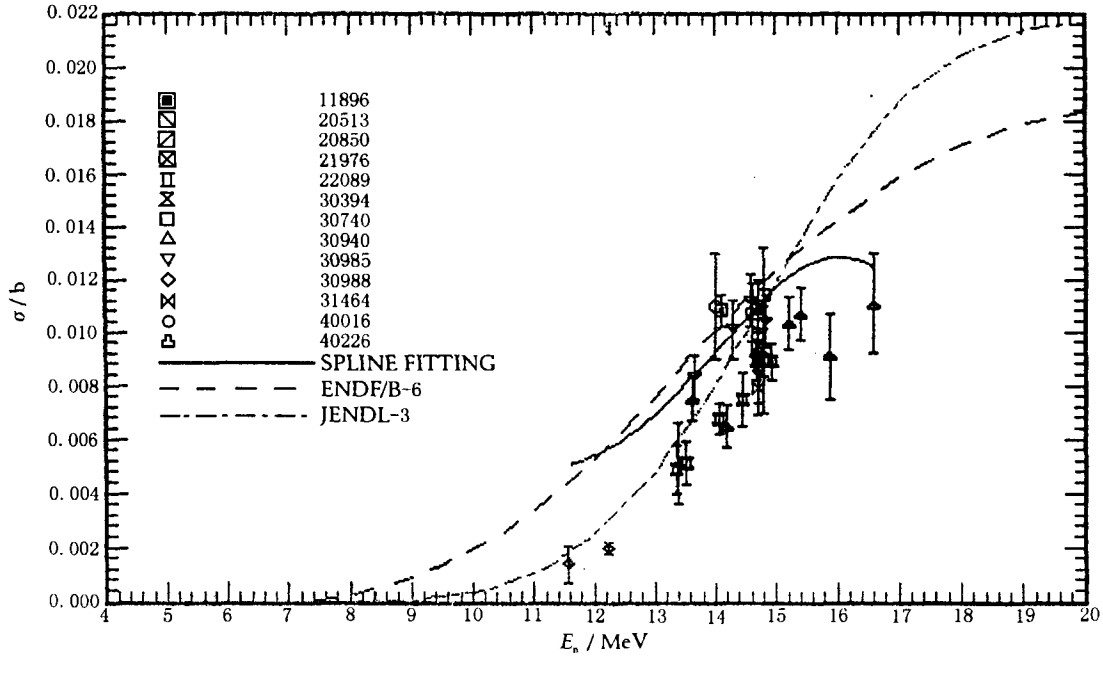

Fig. 5 ^{94}Zr (n,p) reaction

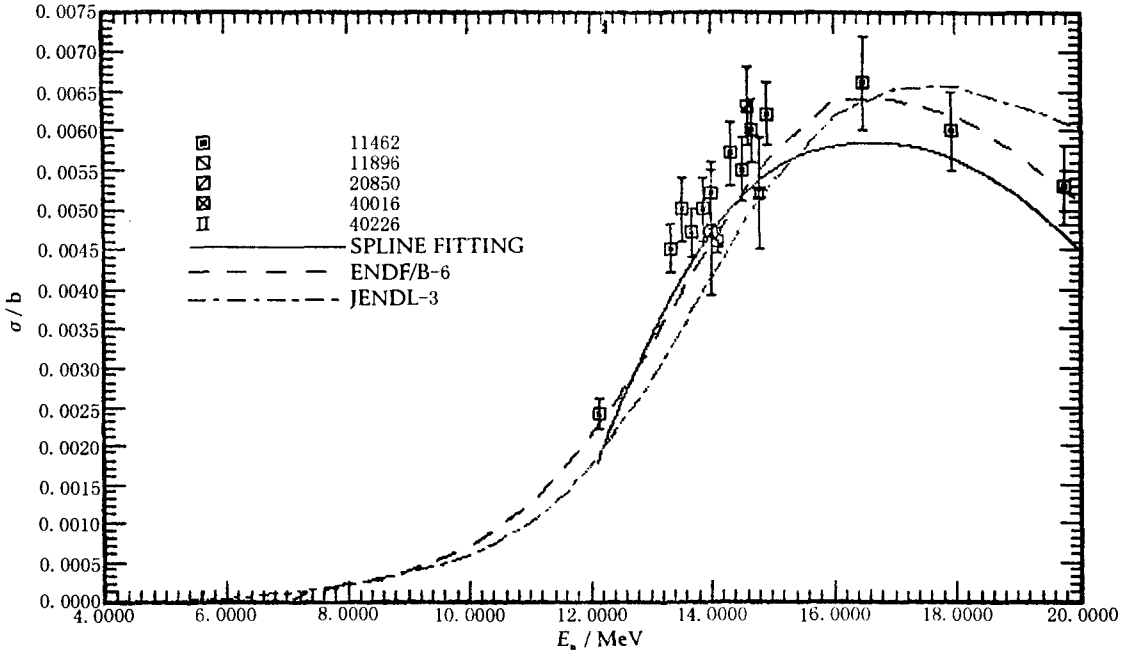

Fig. 6 ^{94}Zr (n,α) reaction

3 Remarks

The data of ^{90,91,92,94,96,Nat}Zr were evaluated up to 20 MeV. The evaluated data were compared with ENDF/B-6 and JENDL-3. It was shown that present data reproduce the experimental data well. The data were updated and improved. The data will be as a part and as a base of the completed evaluated data of these isotopes for CENDL-3.

Acknowledgement

The authors would like to thank Professor Zhang Xizhi for his support and benefit discussion.

References

[1] Liu Tingjin,CNDC-0016,INDC(CPR)-034/L,1995

[2] Zhao Wen-rong, R, INDC(CPR)-16,1989

[3] J. Csikai,et al.,ANE,18,(1),1,91

[4] K.T. Osman, et al.,R, INDC(SUD)-001,9610

[5] I. Kimura, et al.,NSE,106,332,90

[6] K. Kobayashi, et al., NEANDC(J)-155,52,9008

[7] SHAFIQUL, BHUIYAN,890912

[8] N.L. Maidana, et al.,RCA,64,(1),7,94

[9] E.I. Grigor'EV, et al.,YK,,(3),117,8912

[10] Zhao Wen-rong, et al., R,INDC(CPR)-16,8908

[11] Y. Ikeda, et al., JAERI-M-91-032,281,9103

[12] N.I. Molla, et al., 91JUELIC,,355,9105

[13] Z.M. Bartolome, et al., NSE,37,137,6907

[14] L. Green, et al., WAPD-TM-1073,7304

[15] R. W.Stooksberry, et al., NSE,51,235,7306

[16] P. Guenther, et al., PR/C,12,1797,7512

[17] H.W. Newson, et al., AP,8,211,59

[18] W.M. Good, et al., PR,165,1329,68

[19] R.W. Finlay, et al., PR/C,47,237,9301

[20] A.N. Djumin,A.I.Egorov, V. M.Lebedev,,(C,77KIEV,2,74,7704)

[21] M.V. Pasechnik, et al., 80KIEV,1,304,8009

[22] M.B. Fedorov, et al., YK,,(1),69,85

[23] D.G. Foster JR, et al., PR/C,3,576,7102

[24] L. Green, et al., WAPD-TM-1073,7304

[25] R.W. Stooksberry, et al., NSE,51,235,7306

[26] S.S. Malik, et al., NIM,86,83,70

[27] A.H. Lasday PR,81,139,51

[28] J.H. Coon, et al., PR,88,562,5211

[29] L.S. Goodman PR,88,686,5211

[30] N. Nereson, et al., PR,89,775,5302

[31] R.B. Day, et al., PR,92,358,5310

[32] J.M. Peterson, et al., PR,120,521,6010

[33] Bratenahl, et al., PR,110,927,5805

[34] M. Walt, et al., PR,98,677,5505

[35] J.R. Beyster, et al., PR,104,1319,56

[36] C.T. Hibdon, et al., PR,98,223(B3),5504

[37] A.D. Carlson, et al., PR,158,1142,67

[38] D.W. Kent, et al., PR,125,331,62

[39] E.G. Joki, et al., NSE,11,298,61

[40] D.W. Miller, et al., PR,88,83,5210

[41] K.K. Seth, et al., PL,16,306,65

[42] H. Palevsky, et al., PR,99,611(B11),55

[43] K.K. Seth, et al., PR,110,692,58

[44] H.W. Newson, et al., PR,102,1580,56

[45] R.S. Carter CARTER,5504

[46] C.K. Bockelman, et al., PR,76,277,4907

[47] J.B. Guernsey, et al., PR,101,294,5601

[48] J.R. Dunning, et al., PR,48,256,3508

[49] W.P. Poenitz, et al., ANL-NDM-80,8305

[50] CORGE CORGE,6211

[51] P.A. Egelstaff EGELSTAFF,,52

[52] L. Koester, et al., ZP/A,301,215,8104

[53] M. Mazari, et al., 58GENEVA,15,28,5809

[54] E. Islam, et al., NP/A,209,189,7307

[55] E. Islam, et al., AKE,22,(2),87,7310

[56] S. Rapeanu, et al., INDC(SEC)-35,180,7308

[57] V.V. Filippov, et al., 68DUBNA,ASS-68/17,68

[58] V.V. Filippov 83KIEV,3,107,8310

[59] G. Deconninck ASS,74,64,60

[60] F. Strohal, et al., NP,30,49,6202

[61] R. Prasad, et al., NC/A,3,(3),467,7106

[62] V.N. Levkovskij ZET,45,(2),305,63

[63] S.M. Qaim, et al., EUR-5182E,939,7409

[64] B.P. Bayhurst, et al., JIN,23,173,61

[65] C.H. Reed TID-11929,60=T,REED,6002

[66] Y. Fujino, et al., NEANDC(J)-51,60,7709

[67] V.N. Levkovskij ZET,45,(2),305,63

[68] V.N. Levkovskij, et al., YF,10,(1),44,6907)

Evaluation of Complete Neutron Nuclear Data for ^{69,71}Ga

Zhang Songbai Yu Baosheng
(China Nuclear Data Center, CIAE)

Introduction

Gallium is an important nuclide in nuclear science and engineering. The natural gallium consists of two stable isotopes. The neutron nuclear data were evaluated for ^{69,71}Ga in energy range from 10^{-5} eV to 20 MeV. The data includes total, elastic, non-elastic, total inelastic, inelastic to discrete levels, inelastic to continuum, (n,2n), (n,3n), (n,nα)+(n, αn), (n,np)+(n,pn), (n,p), (n,d), (n,t), (n, α), (n,2p) and (n,γ). The angular distributions, energy distributions of secondary neutrons, the resonance parameters are also included. The evaluation is based on both experimental data measured up to 1999 and calculated data[1] with SUNF[2] and DWUCK[3] code. The evaluated data were given in ENDF/B-6 format.

1 Resonance Parameter

The resolved resonance parameters were given below 5.9 keV for ^{69}Ga and 5.6 keV for ^{71}Ga, they were taken from JENDL-3.2.

2 Neutron Cross Section

2.1 Total Cross Section

There is only one experimental datum at one energy point for ^{69}Ga measured by L. KOESTER[4], while no data for ^{71}Ga. So the experimental data of natural Ga were used in the evaluation for ^{69,71}Ga.

2.2 Elastic Scattering Cross Section

Elastic scattering cross sections for both nuclides were obtained by subtracting

the sum of all non-elastic processes from the total cross sections.

2.3 Non-Elastic Scattering Cross Section

The non-elastic scattering cross sections for both nuclides were the sum of all cross sections of nonelastic channels.

2.4 Total Inelastic Cross Section

The total inelastic cross sections for both nuclides were the sum of all cross sections of the discrete levels and continuum.

2.5 Inelastic Cross Section to the Discrete Levels and the Continuum

The inelastic scattering cross sections to 7 discrete levels for ^{69}Ga and 10 discrete levels for ^{71}Ga were calculated with SUNF code. For ^{69}Ga, the direct reaction to first four levels were calculated by DWUCK code; for ^{71}Ga this affection was considered for the first four discrete levels.

The discrete level parameters were given in Table 1, they were from China Evaluated Nuclear Parameter Library.

Table 1 Discrete levels of Ga isotopes (Abundance %)

^{69}Ga (60.018)		^{71}Ga (39.892)	
E_1	J^π	E_1	J^π
0.0	3/2-	0.0	3/2-
0.3187	1/2-	0.3900	1/2-
0.5742	5/2-	0.4837	5/2-
0.8721	3/2-	0.5115	3/2-
1.0286	1/2-	0.9101	3/2-
1.1070	5/2-	0.9647	5/2-
1.3367	7/2-	1.1074	7/2-
1.4881	7/2-	1.1093	1/2-
		1.3950	7/2-
		1.4759	5/2-
		1.4937	9/2+

The discrete level cross sections are shown in Fig.1 and Fig.2 for both nuclides.

2.6 (n,2n) Cross Section

The experimental data of ^{69}Ga (n,2n) ^{68}Ga were listed in Table 2.

The data of 71Ga were measured by E.B. Paul[5] (53), J. Csikai[6] (67), D.V. Viktorov[7] (72) and J.L. Casanova(76) [8] from 14 to 15MeV, respectively.

The evaluated data for both nuclides were obtained by fitting experimental data

from threshold to 20 MeV, respectively. The results were shown in Fig. 3 for ^{69}Ga, and Fig. 4 for ^{71}Ga.

Table 2 the experimental data of $^{69}Ga(n,2n)^{68}Ga$

Year	Author	E_n/MeV	Menitor	σ±Δσ/mb	R_1	R_2	R_3	Crooected σ/mb
1953	E.B.Paul	14.5	LBROC*	552±166	1.0325		0.9916	565±169
1961	L.A.Rayburn	14.4	$^{63}Cu(n,2n)^{62}Cu$	923±69	1.0551	1.0060	0.9840	964±72
1961	C.S.Khurana	14.8	$^{56}Fe(n,p)^{56}Mn$	1070±107	0.9845	0.8421		887±88
1962	M.Cevolani	14.13	$^{27}Al(n,\alpha)$	735±44	1.1217		1.0160	837±50
1965	M.Bormann	14.8	ABSOLUTE	1057±86	0.9845	1.0000	1.0000	1040±84
1967	B.Mitra	14.4	$^{63}Cu(n,2n)^{62}Cu$	983±150	1.0551			1075±162
1967	A.Chatterjee	4.5,14.8	$^{63}Cu(n,2n)^{62}Cu$	950 ±95	0.9845			935±44
1967	J.Csikai	14.7	$^{27}Al(n,\alpha)$	1088±100	1.0000	1.5370		1672±154
1969	A.Chatterjee	14.8	ABSOLUTE	930±60	0.9845			915±59
1971	I.Wagner	14.7	$^{27}Al(n,\alpha)$	830±41	1.0000	1.0018	1.0000	831±42
1972	D.V.Viktorov	14.1	ASSOP*	989±40	1.1296			1117±45
1973	J.Araminowicz	14.6	$^{63}Cu(n,2n)^{62}Cu$	908±88	1.0160	0.9951	1.0000	918±89
1976	R.A.Sigg	14.6	$^{27}Al(n,\alpha)$	1000±70	1.0160	0.9921	0.9971	1005±70
1976	M.Valkonen	14.7	$^{103}Rh(n,\gamma)^{104}Rh$	820±80	1.0000			820±80
1976	J.L.Casanova	14.1	$^{63}Cu(n,2n)^{62}Cu$	1090±90	1.1296	0.9680		1197±98
1983	N.T.Motra	14.8	$^{27}Al(n,\alpha)$	803±153	0.9845	0.9174	1.0606	769±147
1999	G.Zhang	14.9		891±34	0.9695	1.0000	1.0000	863.8±33

ASSOP :Associated α Particles

LBROC: A Long Boron Counter

*R*1 : adjusted factor for Evaluated Cross section at 14.7 MeV due to neutron energy changing

*R*2 : adjusted factor for relevant cross section

*R*3: adjusted factor for half-life and gamma branching.

2.7 (n,γ) Cross Section

For both nuclides, the evaluated data were obtained by fitting the experimental data; The results are shown in the Fig. 5 and Fig. 6, respectively.

2.8 (n,α) Cross Section

There are nine energy points data from 13 to 15 MeV for ^{69}Ga, and two data at one energy point for ^{71}Ga. The calculated data are in good agreement with the experimental data. The calculated data were recommended.

2.9 (n, nα)+(n, αn) Cross Section

Due to no experimental data for these reactions, the cross sections were taken from calculated results.

2.10 (n, p), (n, np)+(n, pn) Cross Section

There are only one energy point datum for $^{71}Ga(n,p)\ ^{71}Zn$, no data for other. So the cross sections were taken from calculated results.

2.11 (n, 3n), (n, d), (n, t), (n, ^{3}He) and (n,2p) cross section

Due to no experimental data for these cross sections, the recommended data for these cross sections were taken from calculated results.

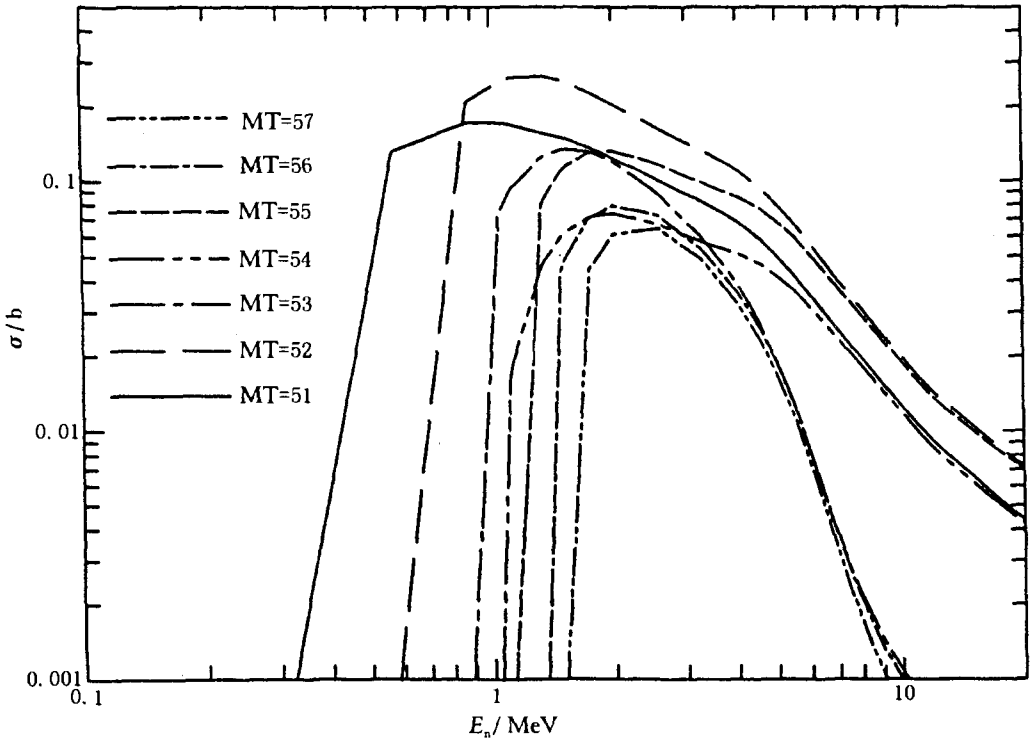

Fig.1 ^{69}Ga(n, n') of MT=51~57

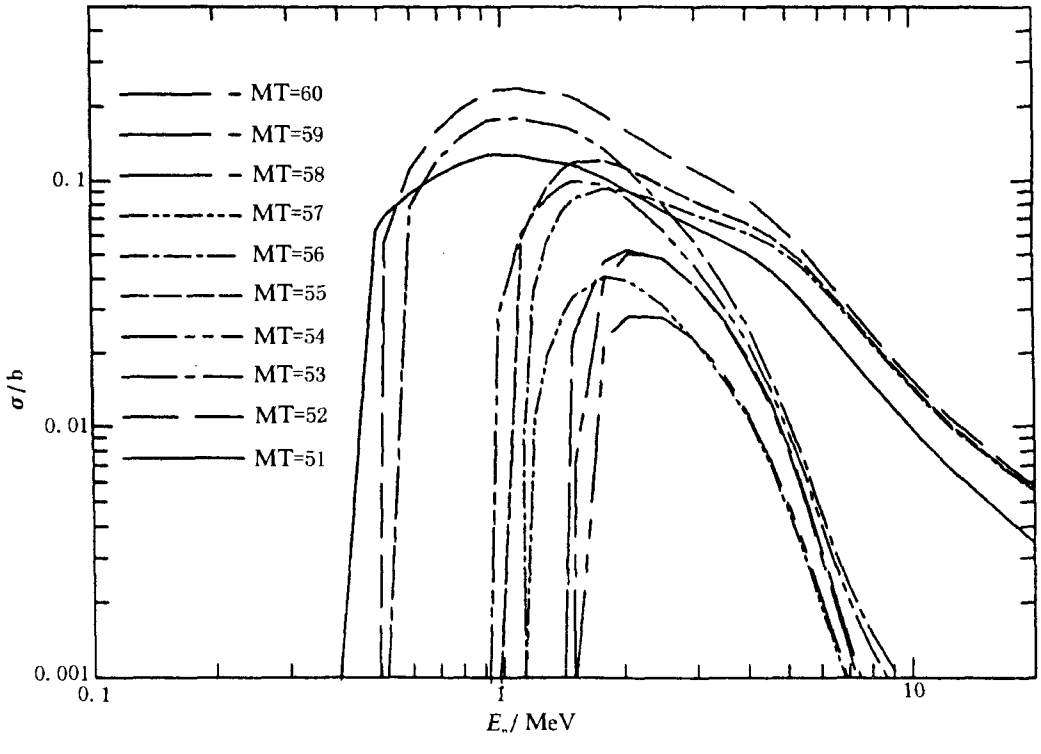

Fig.2 ^{71}Ga(n, n') of MT=51~60

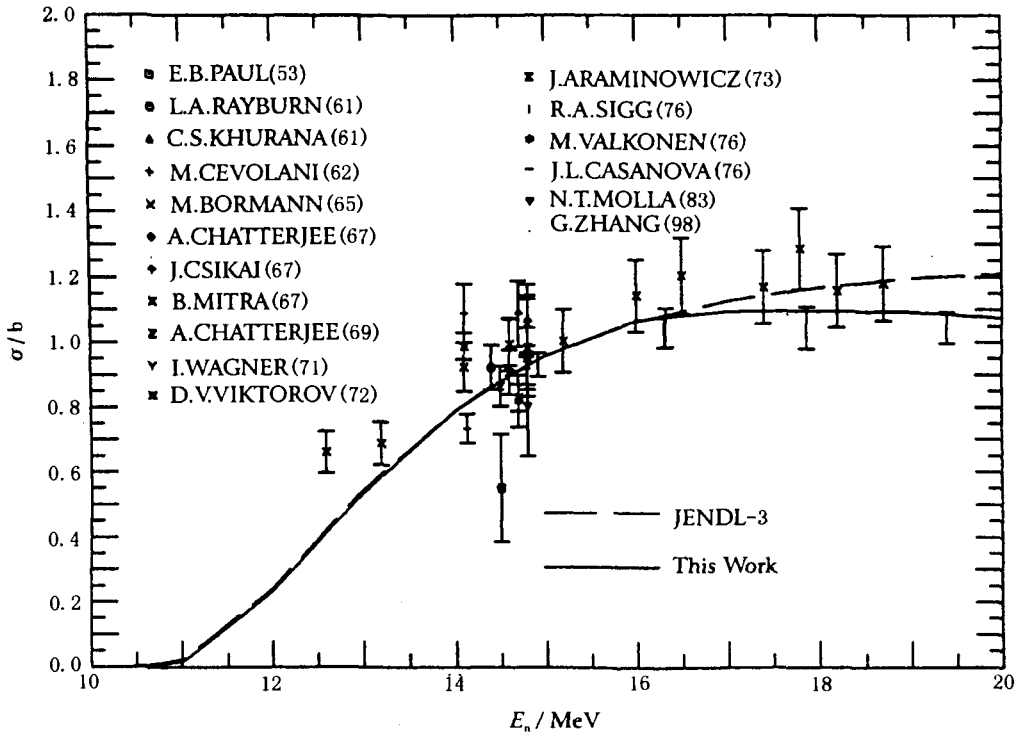

Fig.3 ^{69}Ga(n,2n) cross section

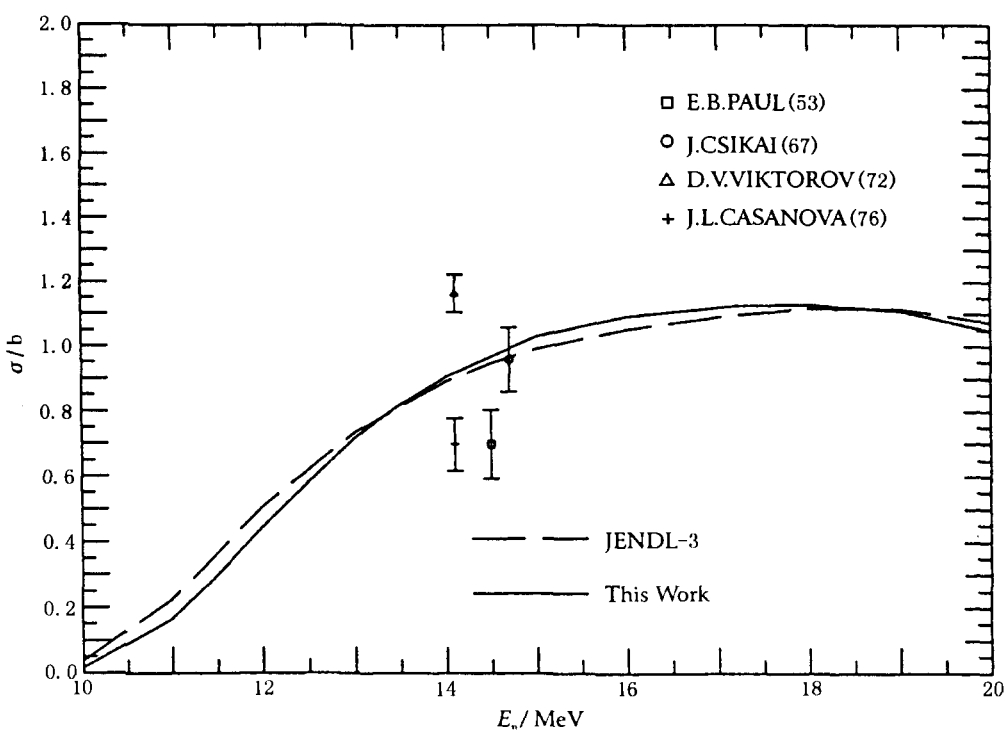

Fig.4 ^{71}Ga(n,2n) cross section

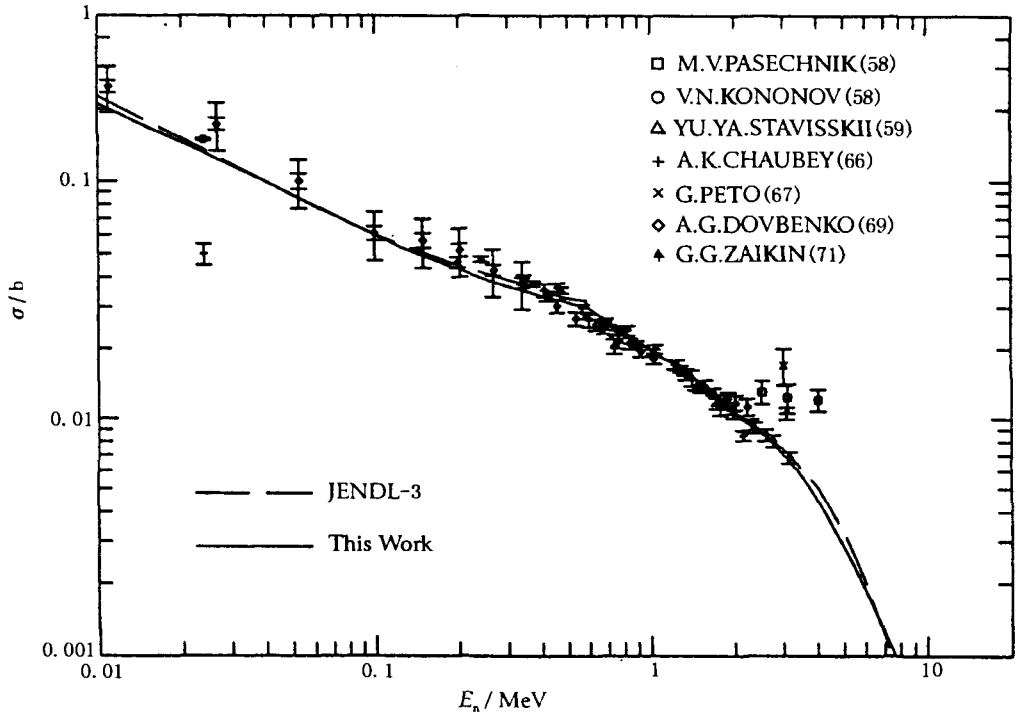

Fig.5 ^{69}Ga(n,γ) cross section

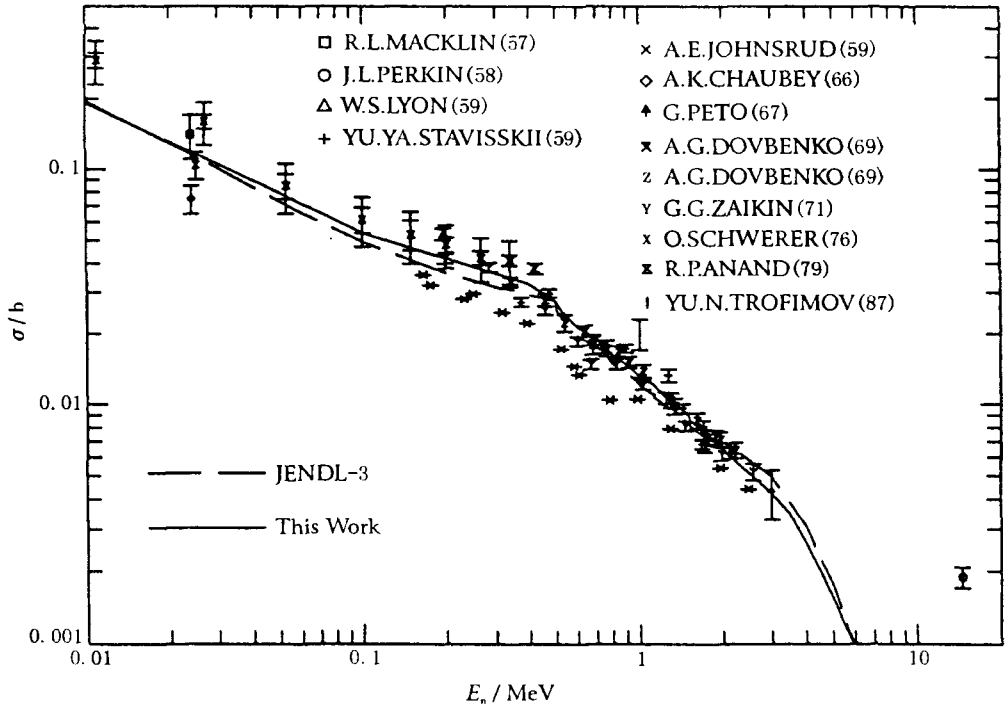

Fig.6 ^{71}Ga(n,γ) cross section

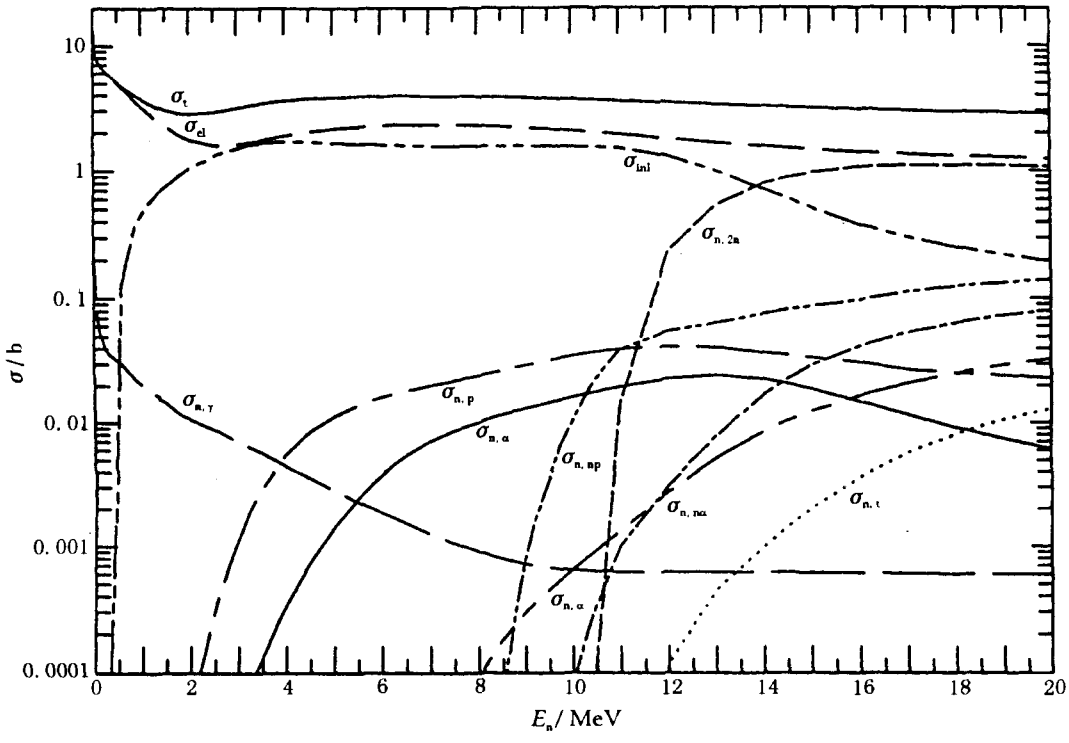

Fig.7 All evaluated cross sections of ^{69}Ga

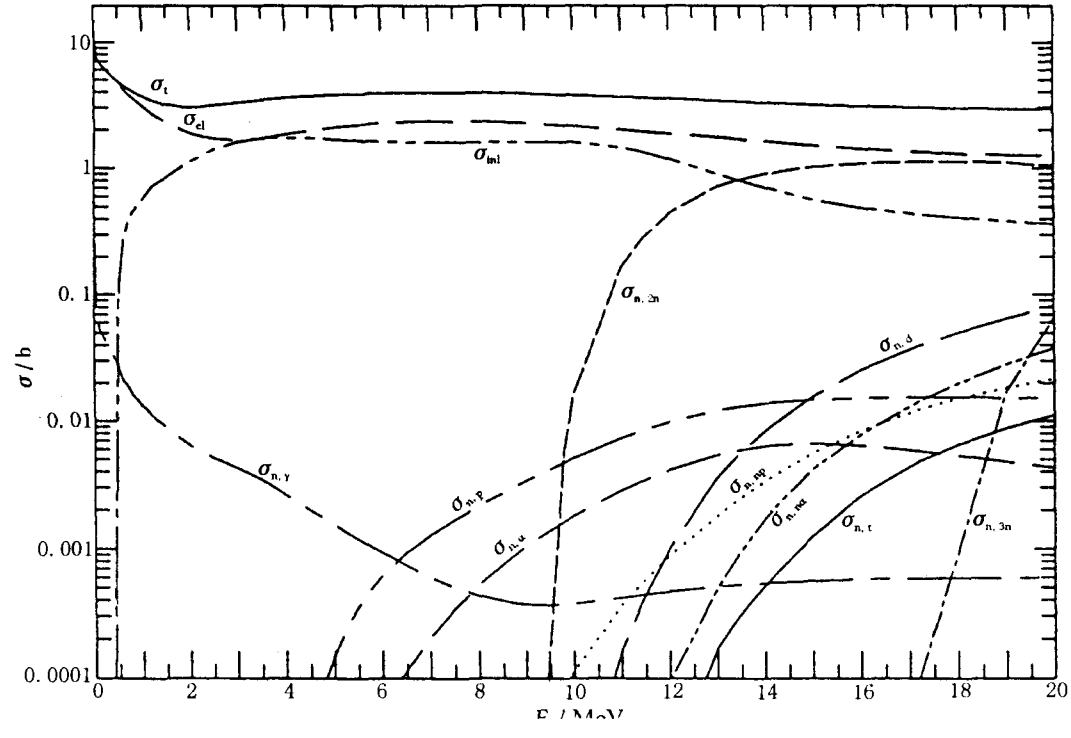

Fig.8 All evaluated cross sections of ^{71}Ga

3 Summary

All evaluated cross section data are shown in Fig. 7 for ^{69}Ga and Fig. 8 for ^{71}Ga. The recommended data could reproduce experimental data very well.

Acknowledgments

The authors would like to extend our thanks to Shen Qingbiao, Zhang Jingshang, Zhang Guohui, Zhang Zhenjun, Rong Jian and all the other members of CNDC for their kind help and suggestions.

References

[1] Zhang Songbai et.al., INDC(CPR)-048/L 52,21(1999)
[2] Zhang Jingshang, Commu of Nucl. Data Prog., 7,14(1992)
[3] P.D.Kunz, 'Distorted Wave Code DWUCK4', University of Colorado
[4] L.Koester et.al.,J.ZP/A,318,(3),347(1984)
[5] E.B.Paul et.al., J,CJP,31,267(1953)
[6] J.Csikai et.al.,J,AHP,23,87(1967)
[7] D.V.Viktorov et.al., J.YF,15,(6)1099(1972)
[8] J.L.Casanova et.al., J.ARS,72,(3),186(1976)

Chinese Evaluated Photonuclear Data File

Yu Baosheng Zhang Jingshang Han Yinlu
(CNDC, China Institute of Atomic Energy)

The photonuclear data up to 30 MeV are very important for radiation damage, radiation safety, reactor dosimetry, accelerator shielding and radiation therapy etc. Meanwhile, the study of the properties of photonuclear reactions is a subject of widespread interest. The Chinese Evaluated Photonuclear Data File (CEPDF) has been established in ENDF/B-6 format based on the experimental data evaluation and theoretical calculations.

There is a Coordinated Research Program of IAEA, the main goals are to develop an IAEA Photonuclear Data Library and producing an IAEA Technical Document (TECDOC) on Photonuclear Data for Application. China group joined the CRP and has engaged in the study on the method for producing evaluated libraries in terms of the experimental data evaluation and theoretical calculations.

1 Status of Chinese Evaluated Photonuclear Data File

The evaluated work of China group has been performed according to IAEA contract No. 8833 for last 3 years.

According to the contract, the evaluation of photonuclear reaction data up to 30 MeV for ^{54,56,57,58}Fe, ^{63,65}Cu and ^{209}Bi nuclides were performed[1] and the code GUNF was developed, which were reported on the first CRP meeting in 1996.

In the second period, the improvement of the code GUNF and methods for calculating the data were improved [1]; the recommended data for ^{180,182,183,184,186}W , ^{90,91,92,94,96}Zr and ^{51}V in ENDF/B-6 format were evaluated. The comparisons of these data with other evaluated data were given on the second CRP meeting in 1998.

The evaluations of ^{9}Be, ^{27}Al and ^{50,52,53,54}Cr and the code GLUNF for γ+ ^{9}Be data calculation were performed in 1999[2]. Based on the comparison in the second CRP Meeting, the data for ^{54,56,57,58}Fe, ^{63,65}Cu and ^{209}Bi have been revised and the new recommended data were issued.

So far, the evaluated photonuclear data for 24 nuclides in CNDC for last 3 years. They are ^{9}Be, ^{27}Al, ^{51}V, ^{50,52,53,54}Cr, ^{54,56,57,58}Fe, ^{63,65}Cu, ^{90,91,92,94,96}Zr, ^{180,182,183,184,186}W and ^{209}Bi.

The evaluated data include (γ,1n), (γ,1p), (γ,1α), (γ,1 ^{3}He), (γ,1d), (γ, 1t), (γ, 2n), (γ, np), (γ, nα), (γ, 2p),(γ, 3n) and the outgoing particle spectra. The concerned reports and calculation codes were given in the references [3~13].

2 An outline on Producing Chinese photonuclear Data File

The diagram for producing Chinese Photonuclear Data File is shown Fig.1.

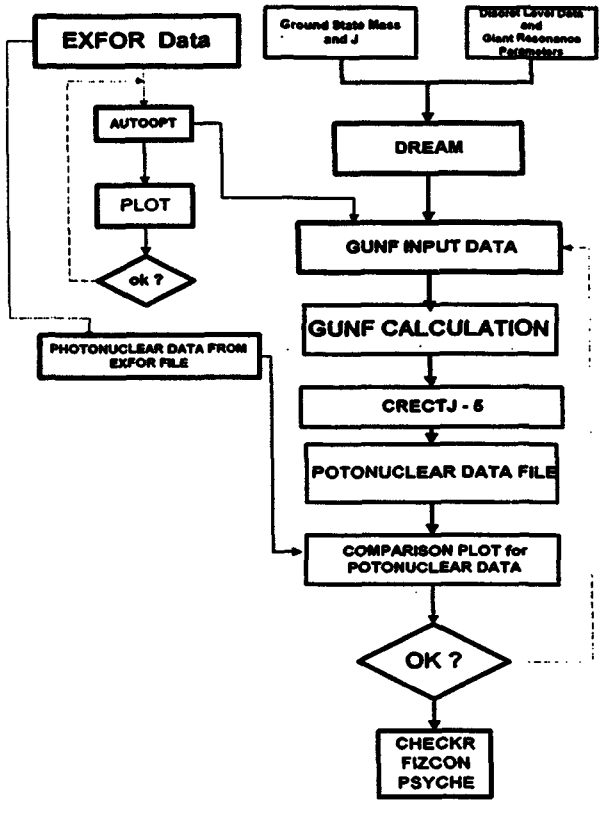

Fig.1. Schematic flow of evaluation for photonuclear data

The experimental data stored in CNDC were obtained from EXFOR master file of IAEA, which was revised every half year. The various available measured data of photonuclear reaction from threshold to 30 MeV were retrieved and collected.

The available experimental data were analyzed and evaluated and used for the model calculation. The parameters of the model calculation were adjusted based on evaluated experimental data.

The giant dipole resonance parameters were obtained by fitting the experimental data of the photoabsorption cross section with code GUNF, meanwhile, the neutron optical potential parameters were obtained by fitting (γ,1n) cross section. If lack of experimental photonuclear data, the best neutron optical potential parameters were searched automatically using the code ATOOPT from neutron induced reaction accordingly. Based on the fitting experimental total, nonelastic scattering cross sections and elastic scattering angular distributions of n + target nucleus reactions, a set of optimum neutron optical potential parameters were

obtained. The optical potential parameters for particle p, α, ^{3}He, d and t were taken from concerned references.

Using the code DREAM, a set of discrete level, pair correction parameter and level density parameters and concerned ground state mass and J^{π} of the levels used for the calculation were formed from Chinese Evaluated Nuclear Parameter Library (CENPL). Then the photonuclear reaction data were calculated by the code GUNF.

The total photonuclear reaction cross section is given by the summation over all reaction channels. Since the calculated results for many channels are in pretty agreement with available experimental data, so reliably to some extentl, the cross sections without experimental data were predicted.

The CRECTJ-5 code was used to make the evaluated photonuclear data to a required data file so as to compare with experimental data and adjust the giant dipole resonance parameters to consist with experimental data. Meanwhile, it is also used to make the evaluated photonuclear data file in ENDF/B-6 format.

The recommended data were checked with ENDF-UTILITY programs, including format, the consistence between the total and partial cross sections, the physics characterization and the energy balance.

3 Recommended Photonuclear Data in ENDF/B- 6 Format

The photonuclear data were recommended in ENDF/B-6 format. The file descriptions for recommended data are as following:

MF = 1 General information

MT = 451 The general description of recommended data including the contents of MF and MT.

MF = 3 Photonuclear reaction cross section

MT = 3 Photoabsorption cross section

MT = 4 Photoneutron (γ, 1n) cross section

MT = 50, 51 ..66... and 91 Photoneutron cross section to discrete excitation state and continuum state.

MT = 16, 17 (γ, 2n) and (γ, 3n) reaction cross sections

MT = 102, 103, 104, 105, 106, 107, 111 (γ, 1γ), (γ, 1p), (γ, 1d), (γ, 1t), (γ, 1^{3}He), (γ,1α) and (γ, 2p) reaction cross sections.

MF = 6 The double differential cross sections

MT = 16, 17, 22, 28, 91 (γ, 2n),(γ, 3n), (γ, nα), (γ, np) and (γ, $n_{continum}$) Reactions

Taking $\gamma+^{9}Be$ as an example, the recommended photonuclear data are as following:

At low energy (<30 MeV), the giant-dipole resonance is the dominant excitation mechanism, in this energy region a simple isotropic approximation was used for the angular distribution of outgoing particles.

MF=3, MT=3 for (γ, abs) reaction and the cross section is given.

MT=16 for (γ,2n) cross section.

MT=4 and MT=28 for (γ,1n) and (γ,np) reaction (Fig.2).

MF=6 is also given by the GLUNF code,

MT=16 for (γ,2n) reaction, the spectra of neutron and ^{7}Be are given.

MT=28 for (γ,np) reaction, the spectra of neutron, proton, ^{7}Li and gamma as well as the gamma-Multiplicity are given;

MT=29 for (γ,1n2α) reaction, the spectra of neutron and alpha particles are given.

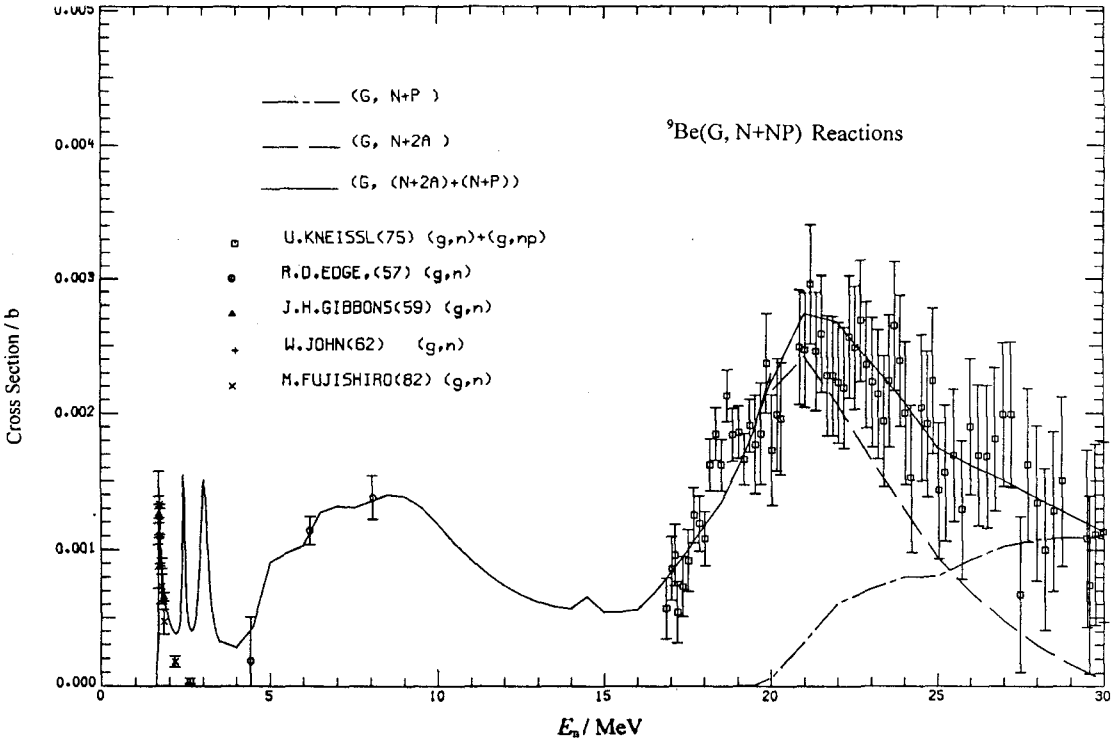

Fig.2. Comparison of evaluated and measured data on ^{9}Be

4 Conclusion

Under Research Contract No. 8833, the research programs for last 3 years were finished on time. The calculation method and code GUNF were developed, and the photonuclear reaction data for 14 nuclides were evaluated. In particular a new model has been developed for light nuclei, which has been employed in the calculation of neutron and gamma induced reactions.

Acknowlegements

The authors are indebted to IAEA (International Atomic Energy Agency) and CIAE for their supports, and thank to Drs. Oblozinsky, T.Benson and O.Schwerer for their kind helps and suggestions.

References

[1] P. Oblozinsky, INDC(NDS)-364, P-9(1997)

[2] P. Oblozinsky, INDC(NDS)-384, P-16(1998)

[3] Zhang Jingshang, INDC(CPR)-044/L,CNDP N0.*19,* p33 (1998).

[4] Yu Baosheng et al., INDC(CPR)-044/L,CNDP N0. *19,* p143 (1998).

[5] Han Yinlu et al., INDC(CPR)-047/L, CNDP N0. *20,* p87 (1998).

[6] Yu Baosheng et al., INDC(CPR)-047/L, CNDP N0.*20,* p95 (1998).

[7] Zhang Jingshang INDC(CPR)-047/L, CNDP N0.*20,* p5 (1998).

[8] Zhang Jingshang INDC(CPR)-047/L, CNDP N0.*20,* p17 (1998).

[9] Yu Baosheng et al., INDC(CPR)-048/L, CNDP N0.*21,* p108 (1999).

[10] Zhang Jingshang et al., *Nucl. Sci. Eng., 133,* p1 (1999).

[11] Zhang Jingshang et al., xCNDP N0.*22* (1999) (to be published).

[12] Zhang Jingshang CNDP N0.*22* (1999) (to be published).

[13] Yu Baosheng et al., CNDP N0.*22* (1999) (to be published).

Evaluation and Calculation of Photonuclear Reaction Data for Five Isotopes of Cr and Al below 30 MeV

Yu Baosheng Han Yinlu Zhang Jingshang
(China Nuclear Data Center, CIAE)

Abstract

Based on available experimental data of neutron and photonuclear reaction, both neutron optical potential parameters and giant resonance parameters of Gamma for Cr and Al were obtained, respectively. The photonuclear reaction data for five isotopes of Cr and Al were calculated and compared with experimental data and Al were recommended below 30 MeV.

Introduction

Chromium and aluminum are very important structure material in nuclear reactor engineering. The photonuclear data of five isotopes of Chromium and Aluminum up to 30 MeV play on very important role concerned radiation induced material damage, radiation safety, reactor dosimetry etc. Meanwhile, the study of the properties of photonuclear reactions on Cr and Al is a subject of widespread interest.

In this work, the experimental data of photonuclear reaction for five isotopes of Cr and Al were evaluated, and theoretical calculation were used to supplement some energies where measured photonuclear data are scarce. The recommended data were obtained on the basis of the evaluated and calculated data, and compared with existing measured data.

1 Evaluation and Analysis of Experimental Data

The available experimental data for photonuclear reaction cross sections of ^{50,52,53,54}Cr and ^{27}Al up to 1998 are collected and analyzed. Many data were retrieved

from EXFOR master files of International Atomic Energy Agency from threshold to 40 MeV.

1.1 Al

Abundance of isotope ^{27}Al is 100.0 %. At present work, the photonuclear reactions, for which the cross sections were evaluated, are as follows: $^{27}Al(\gamma, ABS)$, $^{27}Al(\gamma,n)+(\gamma,n+p)$, $^{27}Al(\gamma,2n)+(\gamma,2n+p)$, $^{27}Al(\gamma, n+p)$, $(\gamma, n+\alpha)$, (γ, p), (γ, d), (γ, t), $(\gamma, {}^{3}He)$, (γ, α) ···, and the double differential cross sections of $(\gamma,2n)$, $(\gamma, n+p)$, $(\gamma, n+\alpha)$ and $(\gamma, n'_{continue})$.

The available experimental data[1~6] for are shown in Table 1. There are 13 sets of measured data from 6 laboratories [1~6] from threshold to 40 MeV. Among them 2 sets[6] are for $^{27}Al(\gamma, x)\,^{24}Na$, 3 sets for $^{27}Al(\gamma, abs)$ reaction, 3 sets for $^{27}Al(\gamma, n)+(\gamma, n+p)$ or (γ, n), 2 sets for $^{27}Al(\gamma, 2n)+(\gamma, 2n+p)$ and one set for $^{27}Al(\gamma, n)+(\gamma, n+p)+(\gamma,2n)+(\gamma, 2n+p)$ reactions, as well as 2 sets for $^{27}Al(\gamma,n)+(\gamma, n+p)+2(\gamma, 2n)+2(\gamma, 2n+p)$ reactions.

Table 1 Collected Data of Photonuclear Reactions for ^{27}Al

Year	Author	En / MeV	Sample	Detector	Reactions	Comment
1961	J.E.E.Baglin	13.0 to 18.0	^{27}Al	PROPC	(γ, n)	
1966	S.C.Fultz	13.0 to 37.0	^{27}Al	PROPC	$(\gamma, n)+(\gamma, n+p)$	
		23.0 to 37.0	^{27}Al	PROPC	$(\gamma, 2n)+(\gamma, 2n+p)$	
		12.9 to 36.64	^{27}Al	PROPC	$(\gamma, n)+(\gamma, n+p)+(\gamma, 2n)+(\gamma, 2n+p)$	
		12.9 to 36.64	^{27}Al	PROPC	$(\gamma, n)+(\gamma, n+p)+2(\gamma, 2n)+2(\gamma, 2n+p)$	
1974	A.Veyssiere	13.0 to 30.0	^{27}Al	STANK	$(\gamma, n)+(\gamma, n+p)$	
		27.0 to 30.0	^{27}Al	STANK	$(\gamma, 2n)+(\gamma, 2n+p)$	
		13.3 to 30.28	^{27}Al	STANK	$(\gamma, n)+(\gamma, n+p)+2(\gamma, 2n)+2(\gamma, 2n+p)$	
1975	J.Ahrens	10.2 to 30.8	^{27}Al	MAGSP	$^{27}Al(\gamma, abs)$	
1975	J.Ahrens	13.2 to 15.5	^{27}Al	MAGSP	$^{27}Al(\gamma, abs)$	
1980	N.K.Sherman	3.87 to 12.6	^{27}Al	SCIN	$^{27}Al(\gamma, abs)$	
1976	A.S.Danagulyan	2000to4500	^{27}Al	Ge(Li)	$^{27}Al(\gamma, X)^{24}Na$	Activatin Method
		3.5	^{27}Al	Ge(Li)	$^{27}Al(\gamma, X)^{24}Na$	

PROPC : Paraffin moderator with BF_3 counters

STANK : Gd - loaded liquid scintillator tank; SCIN: Liquid scintillator

MAGSP: Magnetic compton spectrometers in the photon beam

The early data for $^{27}Al(\gamma, n)$ reaction were measured by J.E. Ebaglin[1] only in energy region from 13.0 to 18 MeV in 1961, and are higher than other ones. The data for $^{27}Al(\gamma, n)+(\gamma, n+p)$, $(\gamma, 2n)+(\gamma, 2n+p)$, $^{27}Al(\gamma, n)+(\gamma, n+p)+(\gamma, 2n)+(\gamma, 3n)$, $(\gamma,$

n)+(γ, n+p) +(γ, 2n)+(γ, 2n+p) and (γ, n)+(γ, n+p) +2(γ, 2n)+2(γ, 2n+p) reactions were first measured by S.C. Fultz[2] in gamma energy region from 13.0 to 37.8, 23.0 to 37.0, 12.9 to 27.8 MeV and 12.9 to 27.8 MeV , respectively in 1966. In the measurement of S.C.Fultz[2], the neutron emitted by the sample were detected in a 4π paraffin moderator neutron detector which consists of 48 BF_3 proportional counters. In order to accurately monitor the photon flux, a xenon-filled transmission ionization chamber was located between the photon collimator and sample and calibrated by using a NaI(Tl) gamma-ray spectrometer. The photon beam energy collimated were determined by using NaI γ-ray spectrometer which was located after neutron detector system. The aluminum sample was used and the attenuation of photon flux in the sample was taken into account and the necessary corrections were made. The peaks structure of photonuclear cross section corresponding to ^{27}Al(γ, n)+ (γ,n+p), (γ, 2n)+ (γ, 2n+p) reactions can be observed in measured data..

The sequential measurement was performed by A. Veyssiere[3] using the improved Ga-loaded liquid scintillation tank with aluminum metal sample in gamma energy region of 13.2 to 30.0 MeV in 1974. In order to overcome the disadvantage of insufficient signal to noise ratio the STANK method was used. In the improved apparatus, two NaI crystal were used in coincidence for detecting annihilation radiation, together with some considerations on the optimal signal to noise ratio, the neutron background were reduced. The data measured were corrected for pile up in the detector, the neutron detector efficiency, the photon beam attenuation in the sample etc.. The experimental results were also refined.

The results measured by A. Veyssiere[3] for the (γ, n)+ (γ, n+p) reactions were compared with ones of S.C. Fultz[2]. There are not large different, only the high energy part of giant resonance peak measured by A. Veyssiere[3] is slightly higher than the data of S.C. Fultz[2] between 25 to 30 MeV. A. Veyssiere[3] gives only the statistical errors. When the systematically errors were added, the data measured by A. Veyssiere[3] will be very good in agreement with the data of S.C. Fultz[2] within errors. The comparison of cross sections for ^{27}Al(γ, n)+ (γ, n+p) reactions is shown in Fig. 1. For ^{27}Al(γ, 2n)+ (γ, 2n+p) reactions, the data measured by A.Veyssiere[3] were lower than S.C.Fultz' [2]. The comparison of both[2,3] is shown in Fig. 2. It was noted that the contribution of the ^{27}Al(γ, 2n) cross section is very small with large errors.

For ^{27}Al, the photonuclear cross section is the sum of (γ, n)+(γ, n+p)+(γ, 2n)+(γ, 2n+p)+(γ, 3n). Because the threshold energy for (γ, 3n) is 31.9 MeV, and the (γ, 2n+p) reaction is much less than the (γ, 2n), the contributions of photonuclear cross section up to 30 MeV are mainly from (γ, n)+(γ, n+p)+(γ,2n). Therefore, the data measured by S.C.Fultz[2] were taker as main reference below 30 MeV. The data corresponding to sum of (γ, n)+(γ, n+p)+2(γ, 2n)+ 2(γ, 2n+p) cross sections measured by S.C. Fultz[2] and A. Veyssiere[3] are in agreement with each other within errors, and can be used to guide model parameters adjustment. These experimental data are shown in Fig. 3.

The photoabsorption cross section (γ, ABS) was measured by J. Ahrens[4], twice in 1975. The cross section can be as reference below 30 MeV and shown in Fig. 4. The photonuclear cross section for ^{27}Al(γ,X)^{24}Na reaction was measured by A.S.Danagulyan[6].

1.2 Cr

The natural chromium consist of four isotopes, i.e. ^{50}Cr (4.345 %) which is a radionuclide with half-life of 1.8×10^{17} year, ^{52}Cr (87.789 %),.^{53}Cr (9.501 %) and ^{54}Cr (2.365%). For present work, evaluated photonuclear reaction cross sections are as follows: ^{50,52,53,54}Cr(γ, ABS), ^{50,52,53,54}Cr (γ,n)+(γ,n+p), ^{50,52,53,54}Cr (γ,2n)+(γ,2n+p),, (γ, n+p), (γ,n+α), (γ,2n), (γ, p), (γ,d), (γ,t), (γ,^{3}He), (γ,α) ··· And also the double differential cross sections of (γ,2n), (γ, n+p), (γ, n+α) and (γ, $n'_{continue}$) are given.

For ^{52}Cr, there is the only one measurement for photonuclear cross section of ^{52}Cr(γ,n)+(γ,2n) reaction in energy region from 11.5 to 30.75 MeV performed by B.I.Goryachev[7] in 1969.

For ^{50}Cr, there only exist the photonuclear cross section data of ^{50}Cr(γ,n) reaction at one energy point 20.5 MeV by W.E. Del.Bianco[8] in 1962.

Other data were not found for ^{50,52,53,54}Cr(γ,abs),(γ,x),···, etc.. The available experimental data were analyzed and evaluated so as to guide the theory calculation.

2 Theoretical Calculation and Recommendation

2.1 ^{27}Al

Using the code APOM[9], the best neutron optical potential parameters can be searched automatically by fitting experimental total, nonelastic scattering cross

sections and elastic scattering angular distributions of n+^{27}Al reactions, a set of optimum neutron optical potential parameters were obtained:

$$V=50.9823+0.0609E-0.0055E^2-24(N-Z)/A$$
$$W_s=\max\{0.0,\ 13.6519-0.3252E-12(N-Z)/A\}$$
$$W_v=\max\{0.0,\ -1.4878+0.1988E-0.0015E^2\}$$
$$U_{so}=6.2$$
$$r_r=1.1379,\ r_s=1.1663,\ r_v=1.3618,\ r_{so}=1.1370\ \ r_c=1.2500$$
$$a_r=0.6851,\ a_s=0.5338,\ a_v=0.9100,\ a_{so}=0.6851$$

The optical potential parameters for particle p, α, ^{3}He, d and t were taken from concerned references[10].

The photonuclear reaction data for ^{27}Al can be calculated by the code GUNF[11] and the giant resonance parameter of gamma were adjusted to make the calculated results in agreement with existing experimental data.

The optical model potential parameters are as following:

The total photoneutron cross section (γ, n) is the sum of the photoneutron excitation states, from ground state to the highest state and continuum state. The continuum state is assumed above 4.3493 MeV. The level scheme used for theoretical calculation are as fellows:

No.	Energy/ MeV	Span-Parity	No.	Energy/ MeV	Span-Parity
1	0.0000	5.00 +	16	3.1599	2.00 +
2	0.2283	0.00 +	17	3.4026	5.00 +
3	0.4169	3.00 +	18	3.5076	6.00 +
4	1.0577	1.00 +	19	3.5963	3.00 +
5	1.7590	2.00 +	20	3.6749	4.00 +
6	1.8506	1.00 +	21	3.6807	3.00 +
7	2.0689	4.00 +	22	3.7238	1.00 +
8	2.0695	2.00 +	23	3.7509	2.00 +
9	2.0716	1.00 +	24	3.7536	0.00 +
10	2.3651	3.00 +	25	3.9220	7.00 +
11	2.5454	3.00 +	26	3.9628	3.00 +
12	2.6609	2.00 +	27	3.9779	0.00 −
13	2.7400	1.00 +	28	4.1919	3.00 +
14	2.9134	2.00 +	29	4.2059	4.00 +
15	3.0736	3.00 +	30	4.3493	3.00 +

Based on evaluated experimental data, the calculated results of photoabsorption cross sections were compared with experimental data taken from Ref. [4].

The theoretically calculated values pass through the experimental data, and are shown Figs. 1~4. Because the calculated data for many photonuclear reaction channels are in pretty agreement with existing experimental data, the predicted cross sections are reasonable. The recommended cross sections for $\gamma+{}^{27}Al$ reaction from threshold to 30 MeV are given in Fig. 5.

2.2 Cr

The optical model parameters were also adjusted to the neutron nuclear reaction data for ${}^{Nat,50,52}Cr$. The optical model potential parameters are as following:

$$V=530826+0.0011E-0.0252E^2-24(N-Z)/A$$
$$W_s=\max\{0.0, 6.0329-0.0436E-12(N-Z)/A\}$$
$$W_v=\max\{0.0, -2.3810+0.2114E+0.00030E^2\}$$
$$U_{so}=6.2$$
$$r_r=1.1884,\ r_s=1.2053,\ r_v=1.3976,\ r_{so}=1.1884,\ r_c=1.2500$$
$$a_r=0.6405,\ a_s=0.6721,\ a_v=0.4974,\ a_{so}=0.6405$$

The total photoneutron cross section is the sum of the photoneutron excitation states from ground state to the highest state. The continuum states are above 1.9822, 2.8912, 4.7021 and 3.0841 MeV for ${}^{50}Cr$, ${}^{52}Cr$, ${}^{53}Cr$ and ${}^{54}Cr$ respectively.

The level scheme of ${}^{50}Cr$ for theoretical calculation is as follows:

No.	Energy/ MeV	Span-Parity
1	0.0000	2.50 −
2	0.2719	3.50 −
3	1.0825	4.50 −
4	1.5613	5.50 −
5	1.7034	0.50 −
6	1.7414	1.50 −
7	1.9822	1.50 +

The discrete level, the pair correction parameter and level density parameters for ${}^{50}Cr$ ${}^{52}Cr$,${}^{53}Cr$ and ${}^{54}Cr$ were taken from Chinese Evaluated Nuclear Parameter Library (CENPL).

The calculations have already been performed by using GUNF Code[11]. In present work, the recommended cross sections for four isotopes of Cr from threshold to 30 MeV are given. The photonuclear cross section for $^{52}Cr(\gamma, n)+(\gamma,2n)$ and $^{50}Cr(\gamma, n)$ are in agreement with experimental data and shown in Figs. 6,7. The recommended cross sections are given in Figs. (8~11).

For the photonuclear double differential cross sections of Al and Cr isotopes, the experimental data are very scarce. Therefore, the recommended data were taken from the theoretical calculations.

Summary

The cross sections of photonuclear reactions Al and Cr isotopes were evaluated. The recommended data could reproduce experimental data very well. Since the calculated results for many channels are in pretty agreement with existing experimental data, the predicted photonuclear reaction data for those are deficient in experimental ones are reasonable.

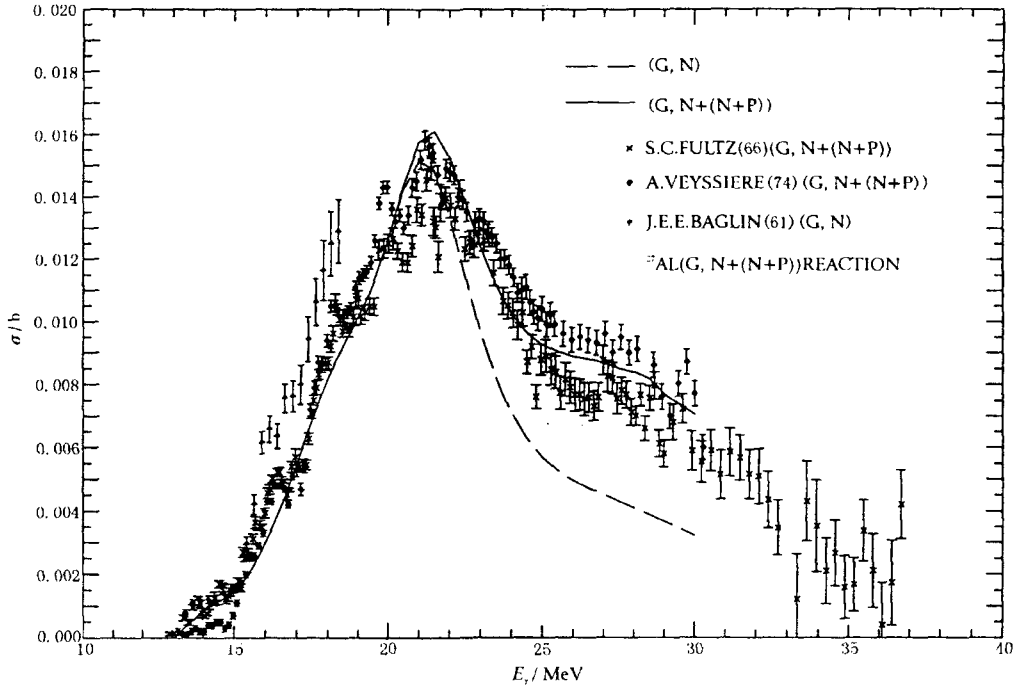

Fig. 1 Comparison of evaluated & measured data for $^{27}Al(\gamma, n+(n+p))$ reactions

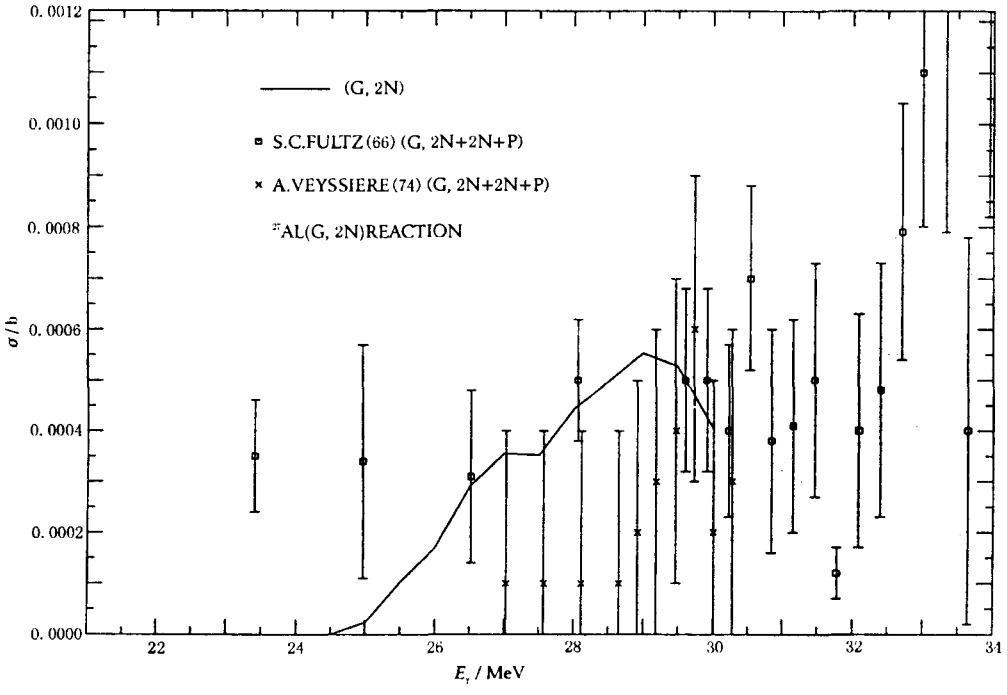

Fig. 2 Comparison of evaluated & measured data for $^{27}Al(\gamma, 2n+(2n+p))$ reactions

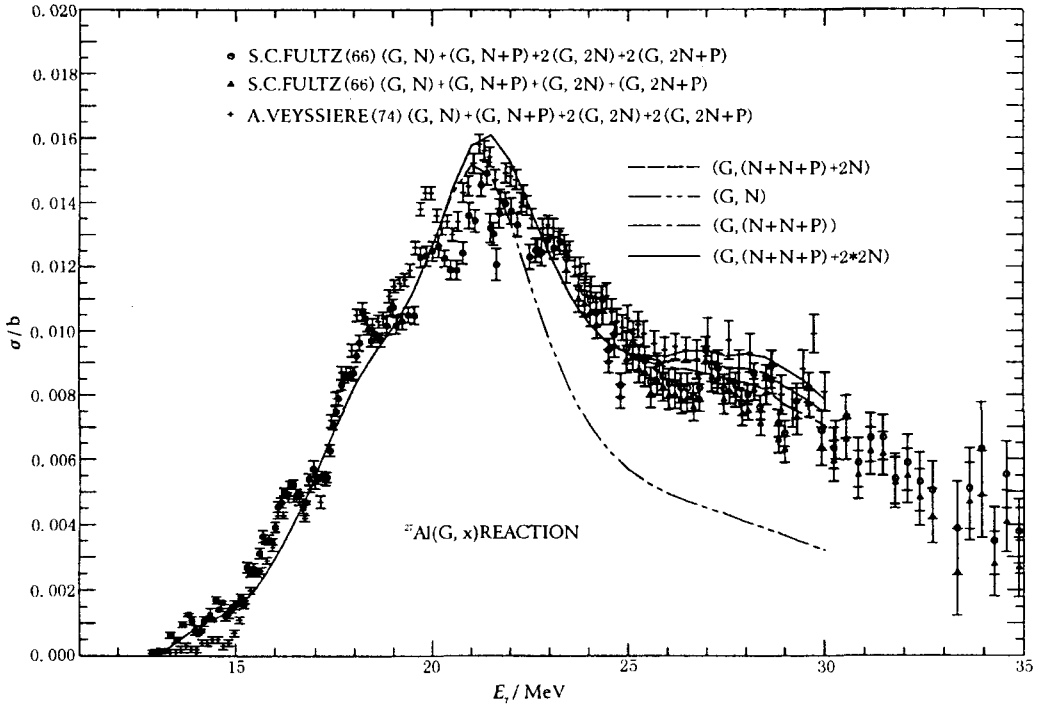

Fig. 3 Comparison of evaluated & measured data for $^{27}Al(\gamma, n+(n+p)+2n+(2n+p))$ and $^{27}Al(\gamma, n+(n+p)+2(2n)+2(2n+p))$ reactions

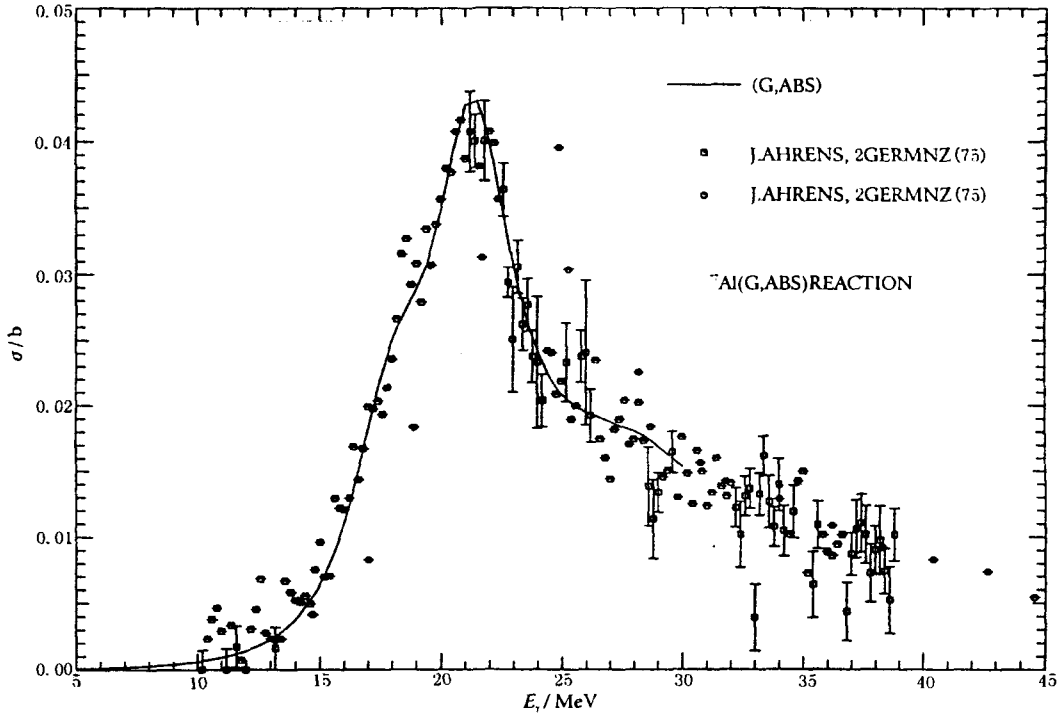

Fig. 4 Comparison of evaluated & measured data for $^{27}Al(\gamma, abs)$reactions

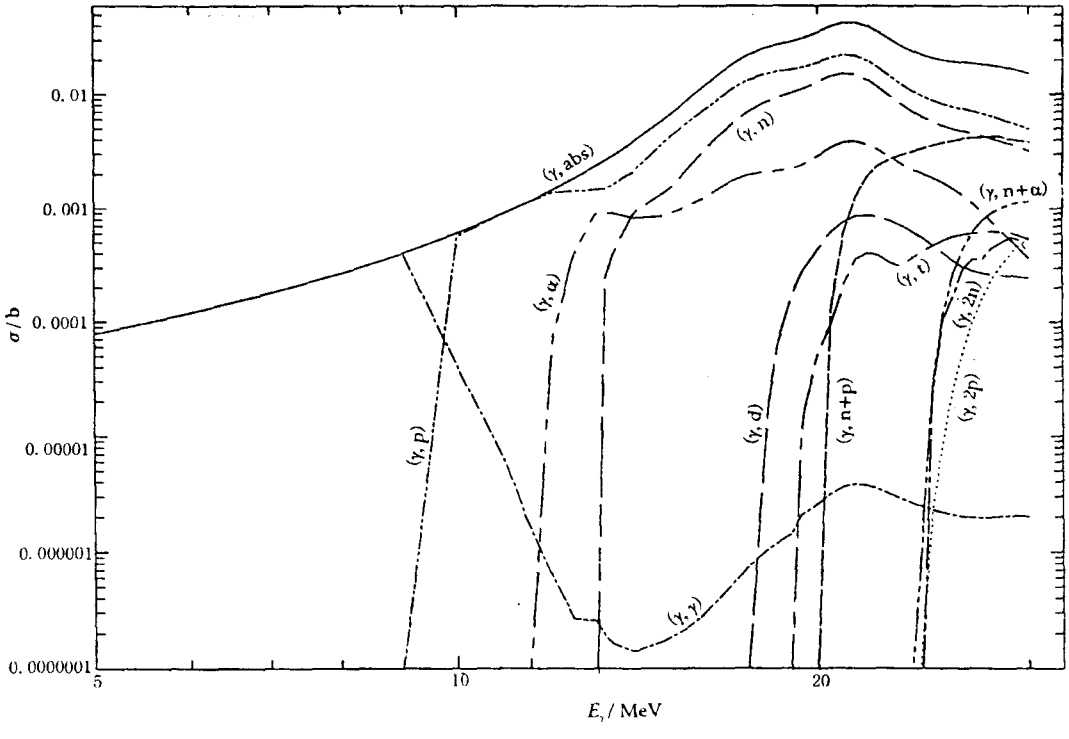

Fig. 5 Evaluation of photonuclear reaction cross sections for ^{27}Al

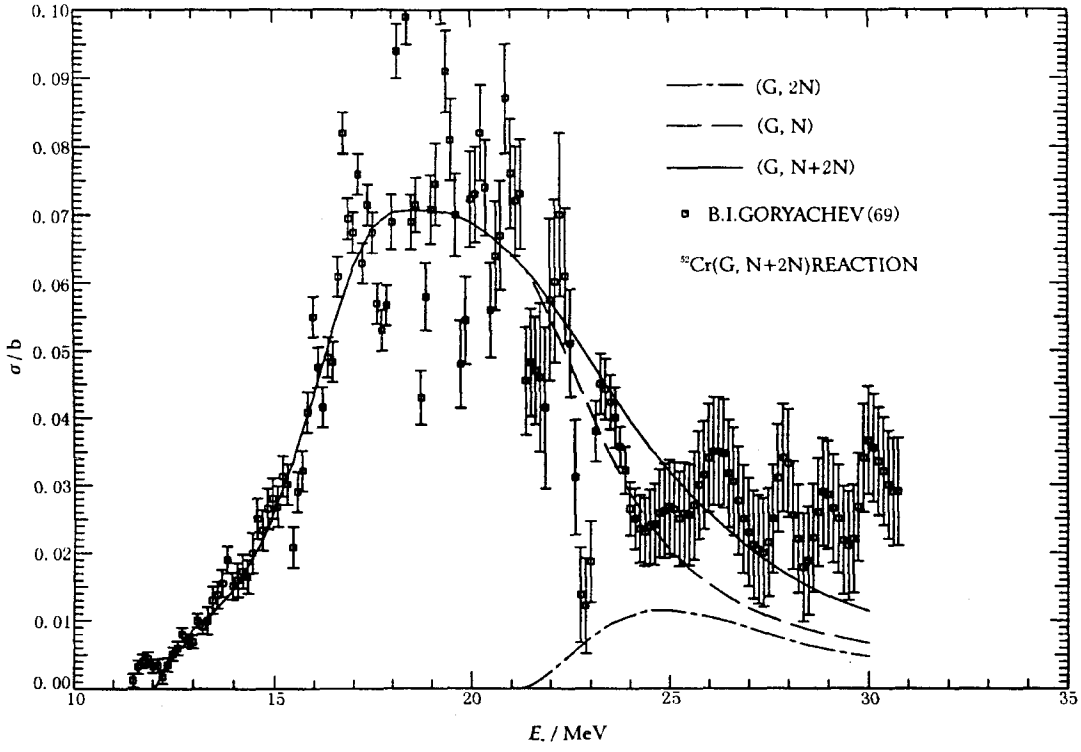

Fig.6 Comparison of evaluated & measured data for $^{52}Cr(\gamma, n+2n)$ reactions

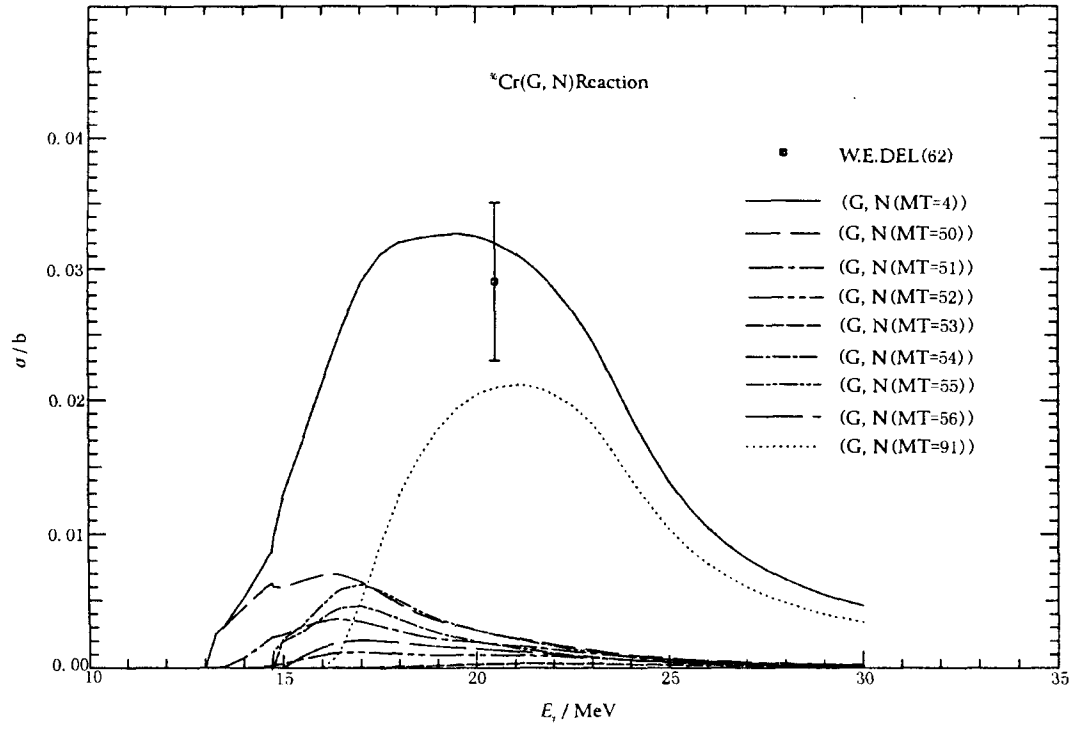

Fig.7 Comparison of evaluated & measured data for $^{50}Cr(\gamma, n)$ reaction

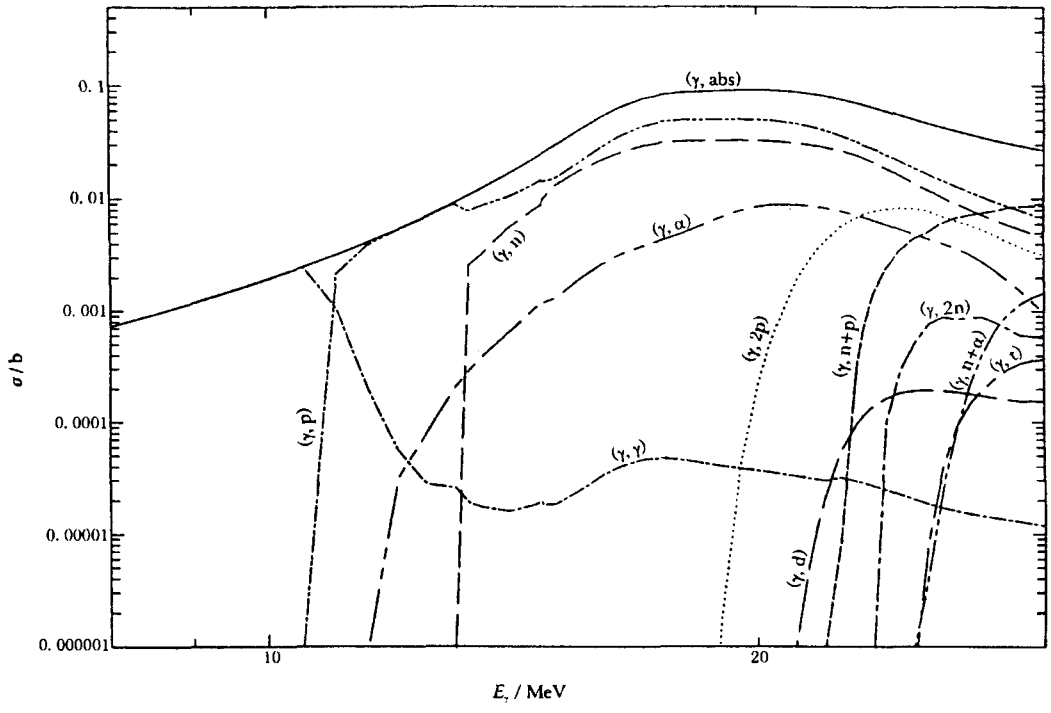

Fig. 8 Evaluation of photonuclear reaction cross sections for ^{50}Cr

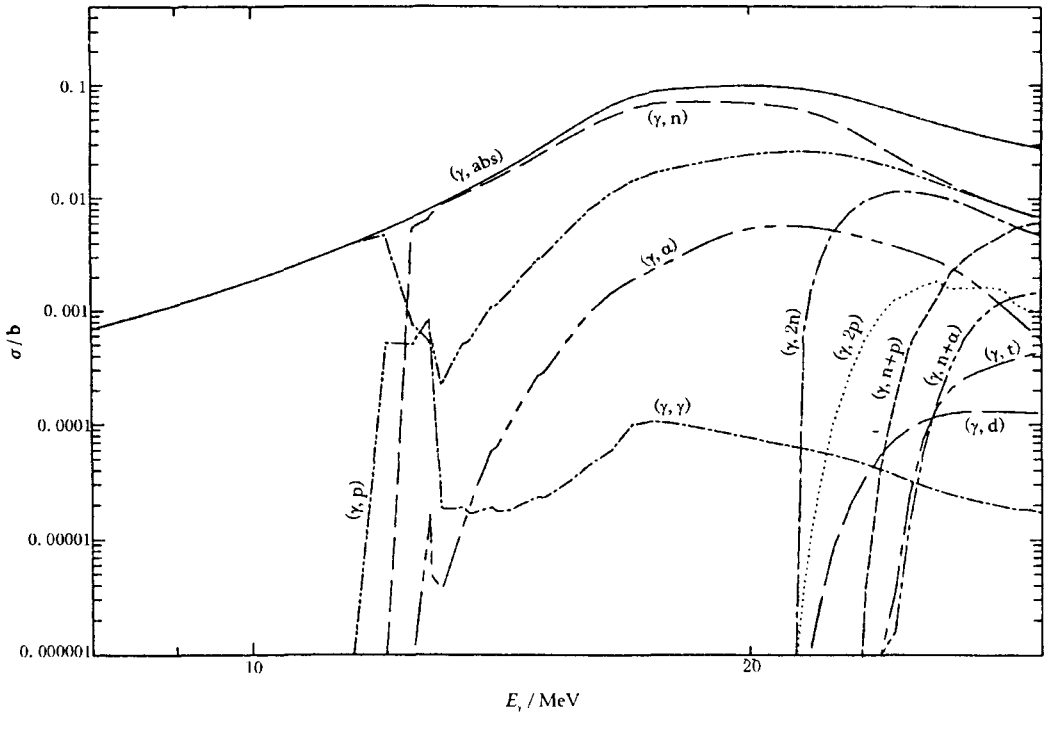

Fig. 9 Evaluation of photonuclear reaction cross sections for ^{52}Cr

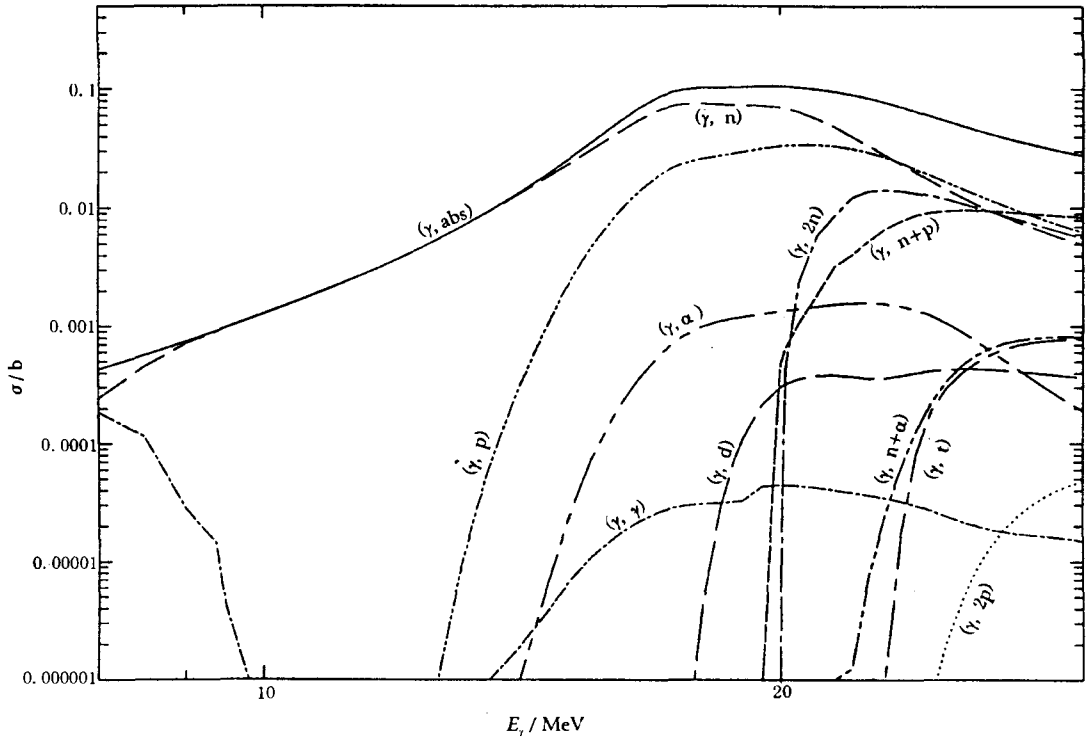

Fig. 10 Evaluation of photonuclear reaction cross sections for ^{53}Cr

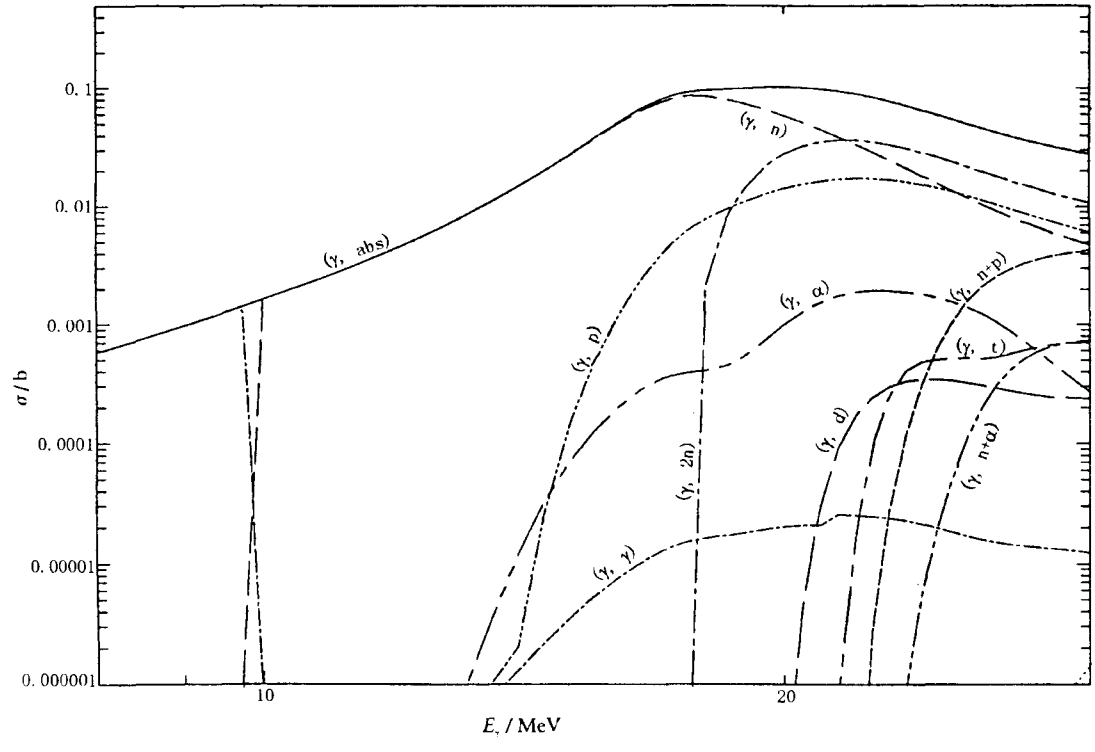

Fig. 11 Evaluation of photonuclear reaction cross sections for ^{54}Cr

Acknowledgments

The authors are indebted to IAEA and CIAE for their supports, and thank to Drs. Oblozinsky, T. Benson and O. Schwerer for their kind helps and suggestions.

References

[1] J.E.E.Baglin et al., Nucl. Phy.,22,207(1975)

[2] S.C.Fultz et al., Phy.Rew.,143,790(1966)

[3] A.Veyssiere et al., Nucl. Phy./A,227,513(1974)

[4] J.Ahrens et al., Nucl. Phy./A,251,479(1975)

[5] N.K.Sherman et al., Phy.Rew./C,21,2328(1980)

[6] A.S.Danagulyan et al., J.YF,24,681(1976)

[7] B.I. Goryachev et al., J.IZV,33,1736(1969)

[8] W.E.Del Bianco et al., Phy. Rew,126,709(1962)

[9] Shen Qingbiao ET AL,, CNDP,7,43(1992)

[10] C.M.Perey et al., Atomic Data and Nuclear Data Table,17,1(1976)

[11] Zhang Jingshang et al., Illustration of Photonuclear Data Calculation with GUNF code, INDC(CPR)-044/L.No.19,33(1998)

Evaluation of Activation Cross Sections for $^{89,88}Y(n,2n)^{88,87}Y$

Zhang Songbai Yu Baosheng

(China Nuclear Data Center, CIAE)

Abstract

Based on the experimental data and the theoretical calculated results, the activation cross sections of (n, 2n) nuclear reaction for $^{88,89}Y$ are recommended from threshold to 20 MeV.

1 Evaluation of $^{89}Y(n, 2n)^{88}Y$ Cross Section

1.1 Experimental Data Analysis

Most experimental data come from the EXFOR and other resources, and they can be divided into three sets as follows.

1.1.1 Around 14 MeV

Around 14 MeV[1~12], the data were measured with activation method in eight laboratories, while in one laboratory with large liquid STANK method. The other measurements were done by L.R. Greenwood[10] from 14 to 15 MeV (1987), M. Wagner[11] (1989) and Huang Jianzhou[12] from 13 to 18 MeV at CIAE (1989), respectively. All the data are listed in Table 1.

Around 14MeV, the cross section changes quickly with neutron energy. Because for the early measured data, the standard cross section and the decay data were not used, the data measured in 1960's have large errors. The measurement completed by Huang Jianzhou[12] are very important for the recommendation, because this measurement were made in the large energy region from 13 to 18 MeV and the evaluated standard cross section and the new decay data were used.

The decay data of ^{88}Y, taken from Isotope Table (8th Version), are as follows.

Half-life: 106.65 d; E_γ: 898.04 keV; p_γ: 0.93689; E_γ: 1836.063 keV; p_γ: 0.9924.

Table 1 The experimental data of $^{89}Y(n,2n)^{88}Y$

Year	Author	Method	En/MeV	$\sigma\pm\Delta\sigma$ /mb	Monitor
1959	H.Vonach	Activation	14.1	0.540±0.08	$^{27}Al(n, \alpha)$
1961	O.M.Huandson	Activation	16.0	1.125±0.293	
1962	F.Strohal	Activation	14.6	0.542±0.06	$^{27}Al(n, \alpha)$
1963	B.Granger	Activation	14.0	1.350±0.34	
1966	D.G.Vallis	Activation	14.7	1.052±0.05	$^{27}Al(n, \alpha)$
1969	D.S.Mather	STANK	14.06	1.142±0.23	$^{238}U(n,f)$
1973	J.Araminowicz	Activation	14.6	0.572±0.065	$^{63}Cu(n,2n)$
1974	S.M.Qian	Activation	14.7	0.907±0.068	$^{27}Al(n, \alpha)$
1984	M.Berrada	Activation	14.6	0.877±0.029	$^{27}Al(n, \alpha)$
1987	L.R.Greenwood	Activation	14.5	0.929±0.014	$^{27}Al(n, \alpha)$
			14.9	0.991±0.015	$^{27}Al(n, \alpha)$
1989	M.Wangner	Activation	14.789	1.016±0.015	$^{93}Nb(n,2n)^{92m}Nb$
1989	Huang Jianzhou	Activation	14.61	1.018±0.034	$^{27}Al(n, \alpha)$

1.1.2 From threshold to 15MeV

In this energy region, there are experimental data from 6 laboratories. The data

are in agreement within errors with each other, except the data measured by H.A. Tewes[13] (1960) and M. Bormann[14] (1976) which are lower than others. The data (from 12.6 to 17.8 MeV) measured by S.K. Ghorai[15] are in good agreement with Huang's data[12]. From 13.58 to 14.78 MeV, the measurements of M. Wanger[11] in HUNKOS and AUSIRK used the new standard cross section and decay data, the early experimental data measured by P. Racis[16] were updated by M. Wanger[11]. So the data of Huang Jianzhou[12], S.K. Ghorai[15] and M. wanger[11] were taken as the foundation of the evaluation in this energy region.

1.1.3 From 14 to 26MeV

In this region, B.P. Bayhurst[17] (1975) measured the data from 14.1 to 26.07 MeV with the activation method, while L.R. Veeser[18] measured the data from 14.7 to 19.0 MeV, from 13.3 to 14.7 MeV and from 14.7 to 24 MeV by using the large liquid stank method in 1977. The data obtained from the two different methods are in good agreement with the data measured by Huang Jianzhou[12] near 18 MeV. So the trend of the data measured by B.P. Bayhurst[17] and L.R. Veeser[18] are used as the reference of recommended data in this energy region.

1.2 The recommended data of $^{89}Y(n, 2n)^{88}Y$

The data of Huang[12], Wagner[11], Veeser[18], and Bayhurst[1] were fitted by using the orthogonal polynomial, the recommended data obtained. The results were compared with the data from ENDF/B-6 and JENDL-3 and shown in Fig. 1 and Fig. 2.

2 $^{88}Y(n, 2n)^{87}Y$ Cross Section

^{88}Y is a radionuclide (half-life:106.64 d), at the energy points 14.2 MeV and 14.8 MeV. Only two data were measured by R.J. Prestwood[19].

At Peking University, Huang Feizeng[20] used the replace method to do the experiment. The replacement reaction was $^{87}Sr(d, 2n)^{87}Y$, the cross section can be of ^{88}Y (n,2n) obtained from the theoretical calculation on the supposition that the decay of compound nucleus is not relative to its form

Based on these evaluated experimental data and calculated results, the recommended data were obtained. The result is shown in Fig. 3.

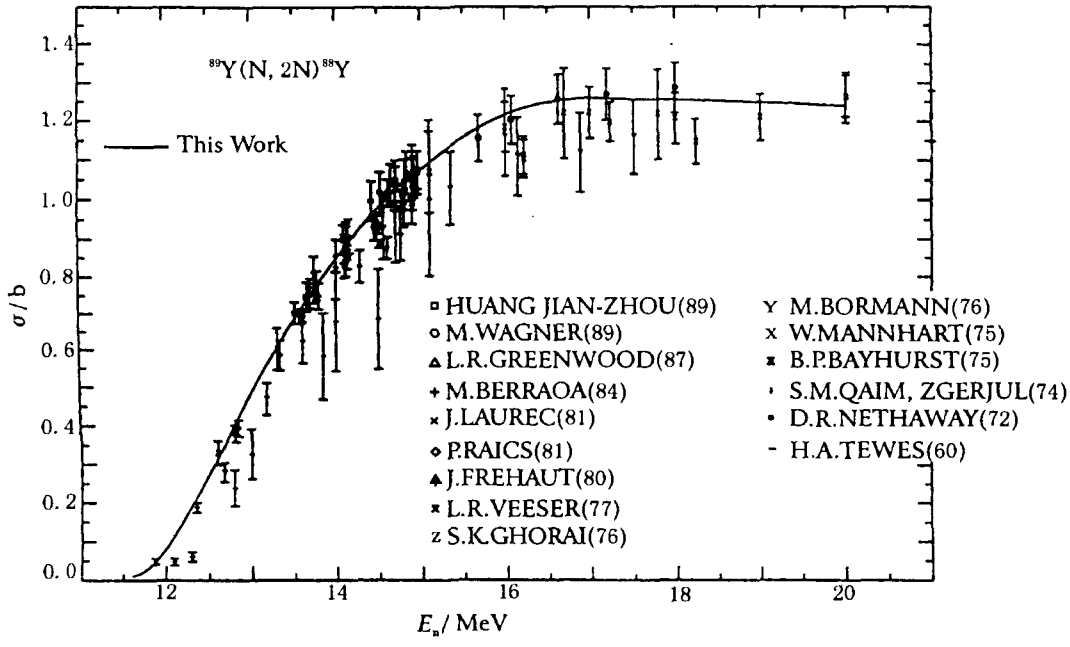

Fig.1 ^{89}Y(n,2n)^{88}Y cross section

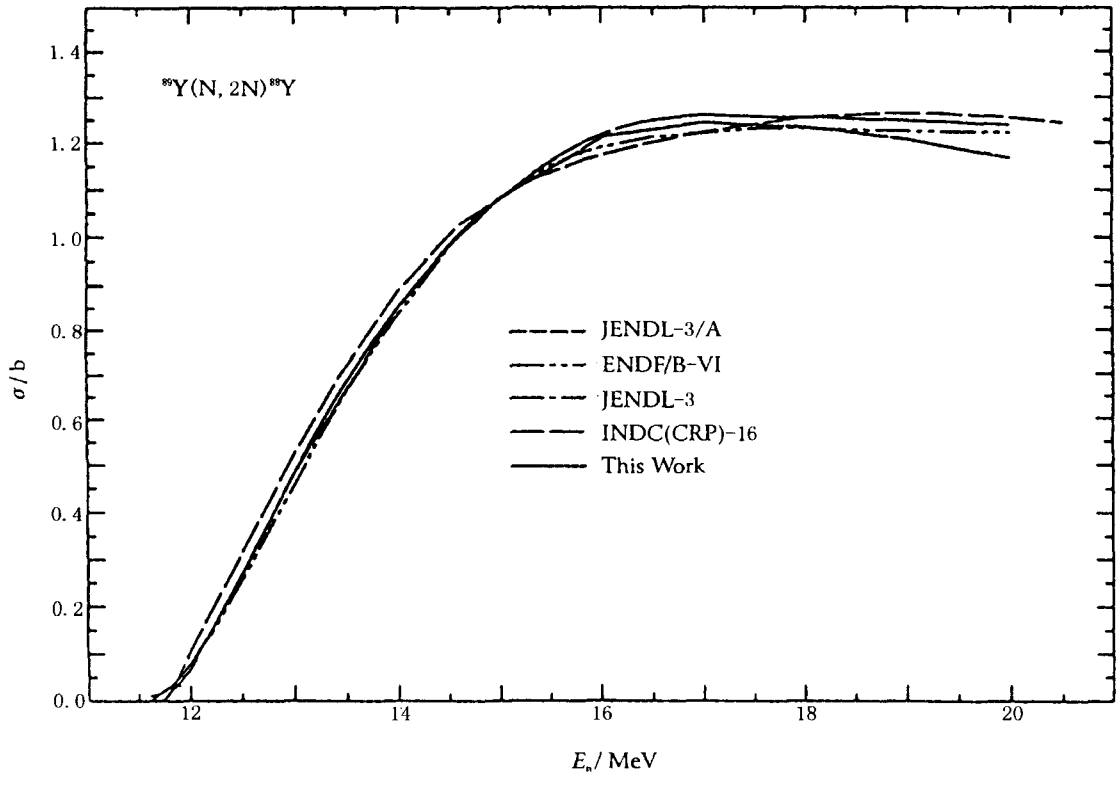

Fig.2 The comparison of the evaluation for ^{89}Y(n,2n)^{88}Y reaction

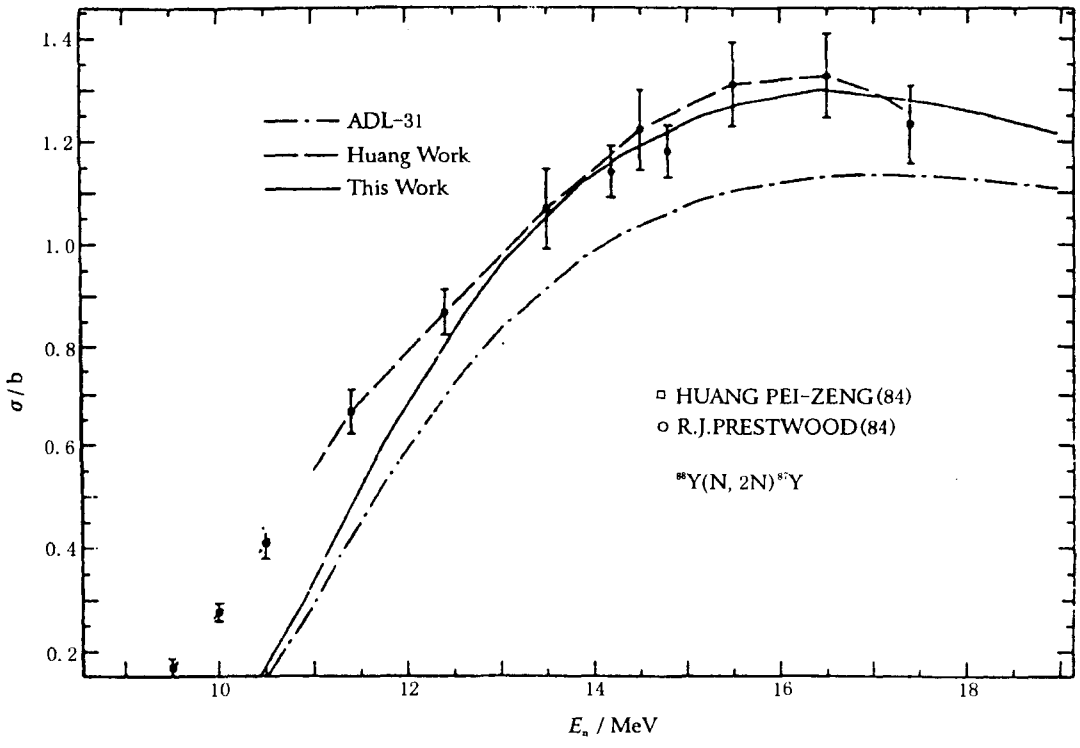

Fig.3 $^{88}Y(n,2n)^{87}Y$ cross section

3 Summary

The evaluated cross section of $^{89,88}Y(n,2n)^{88,87}Y$ were given. The evaluation were based on the available experimental data measured by using the direct measurement and the replace methods. The data were improved.

Reference

[1] H.V.Onach et al., J.OSA, 96,120(1959)

[2] O.M.Hudson et al., J.BAP,6,506(1961)

[3] F.Strohal et al., Nucl.Phys.,30,49(1962)

[4] B.Granger et al.,EANDC(E)-49L,83(1963)

[5] D.G.Vallis et.al., AWRE-O-76(1966)

[6] D.S.Mather et al., AWRE-O-47(1969)

[7] J.Araminowicz et al., INR-1464,14(1973)

[8] S.M.Qaim et al., EUR-5182E,939(1974)

[9] M.Berrada et al., EXFOR Data 30805003(1984)

[10] L.R.Greenwood et al., ASTM-STP-956,743(1987)

[11] M.Wanger et al., J.ANE, 16,623(1989)

[12] Huang Jianzhou et al., INDC(CPR)-16(1989)

[13] H.A.Tews et al.,UCRL-6028-T(1960)

[14] M.Broraman et al., ZP/A,277,203(1976)

[15] S.K.Ghorai et al., Nucl.Phys./A,266,53,(1976)

[16] P.Paics et al.,AK,23,45(1981)

[17] B.P.Bayhurst et al., Phys.Rev./C,12,451(1975)

[18] L.R.Veeser et al., Phys.Rev./C,16,1792(1977)

[19] R.J.prestwood et al., Phys.Rev./C,29,805(1984)

[20] Huang Feizeng et al., Private communication(1995)

III ATOMIC AND MOLECULAR DATA

Wavelength Calculation of Highly Stripped Ions $S^{10+} \rightarrow S^{13+}$, Br^{23+}, Br^{24+}, Ge^{20+}, Ge^{21+}

Chen Huazhong
(China Institute of Atomic Energy, Beijing 102413)

Abstract

Wavelengths of highly stripped ions $S^{10+} \rightarrow S^{13+}$, Br^{23+}, Br^{24+}, Ge^{20+}, Ge^{21+} are calculated by means of GRASP code. The calculations are performed based on multiconfiguration Dirac-Fock technique. Corrections to the energy levels due to the retarded Coulomb interaction (Breit interaction) and the polarization of the vacuum by the nuclear distribution and electron self-energy are included in a perturbation approximation. Comparisons with the experimental data are presented.

Introduction

Recently, interest in spectroscopy has increased particularly. Spectra are fundamental characteristics of atoms and ions, the main source of information on their structure and properties. Important applied problems have arisen: diagnostics of thermonuclear plasmas, laser physics, solid physics, biomedicine, beam-foil spectroscopy and so on. Laser in the "water window" wave band (2.33~4.37nm) can be used in biological specimen photography. A extremely interesting and original world of multiply charged ions was discovered, of which radiation are in the X-ray wavelengths region.

Identification of the spectra of all these above mentioned systems is practically impossible without corresponding theoretical analysis. Laser research needs parameters of atomic structure of highly ionized atoms, whose shell structure and

spectra differ considerably from those of neutral or just a few times ionized atom.

We obtained parameters of atomic structure by means of GRASP[1] (General-purpose Relativistic Atomic Structure Program). This program extends the previously published program[2] which solved the atomic multiconfigurational Dirac-Fock (MCDF) equations and supplied atomic orbital wavefunctions and energy levels. The extension involves the inclusion of the transverse Breit, self-energy corrections[3] and vacuum polarization corrections to the energy levels.

1 Theory and program[1,2]

There are 176 subroutines in GRASP. Nature of physical problem in GRASP is the theoretical calculation of atomic energy levels, orbits, and radiative transition data within the relativistic formalism. Making use of GRASP one can be in a position to perform calculations of the energy spectra, transition probabilities of all atoms of the Periodical Table and ions of any ionization degree. Such calculations could be done prior to the corresponding experimental observations or after them to help to explain the interesting phenomena found in experimental analyzing.

Relativistic atomic structure theory is ultimately based on quantum electro-dynamics.

From the theoretical point of view the atom is considered a many-body system. Instead of considering the wave function of the whole atom, we find it for each electron moving in the central nuclear charge field and in the screening field of the remaining electrons. The wave function of this electron is represented as a product of radial and spin-angular parts.

We can write the central-field Dirac orbital $|n\kappa m\rangle$ as:

$$\left\langle \vec{r} \middle| n\kappa m \right\rangle = \frac{1}{r}\begin{bmatrix} P_{n\kappa}(r)\chi_{\kappa m}\left(\frac{\vec{r}}{r}\right) \\ \mathrm{i}Q_{n\kappa}(r)\chi_{-\kappa m}\left(\frac{\vec{r}}{r}\right) \end{bmatrix} \tag{1}$$

where $P_{n\kappa}(r)$ and $Q_{n\kappa}(r)$ are , respectively, the large and small component radial wavefunctions, and the function $\chi_{\kappa m}\left(\frac{\vec{r}}{r}\right)$ are the spinor spherical harmonics, n is the principal quantum number, K is the relativistic angular quantum number.

Configuration state functions (CSF) of an N-electron system are formed by taking linear combinations of Slater determinants of order N constructed from the orbits (1).

Atomic state function (ASF) is linear combinations of CSFs.

Applying the variation principle gives the following pair of Dirac equations for a subshell λ:

$$\begin{cases} \left(\frac{\mathrm{d}}{\mathrm{d}r}+\frac{\kappa_\lambda}{r}\right)P_{n_\lambda\kappa_\lambda}(r)-\left(2c-\frac{\varepsilon_\lambda}{c}+\frac{Y_\lambda(r)}{cr}\right)Q_{n_\lambda\kappa_\lambda}(r)=-\frac{\chi_\lambda^{(P)}(r)}{r}, \\ \left(\frac{\mathrm{d}}{\mathrm{d}r}-\frac{\kappa_\lambda}{r}\right)Q_{n_\lambda\kappa_\lambda}(r)+\left(-\frac{\varepsilon_\lambda}{c}+\frac{Y_\lambda(r)}{cr}\right)P_{n_\lambda\kappa_\lambda}(r)=\frac{\chi_\lambda^{(Q)}(r)}{r}, \end{cases} \tag{2}$$

Such equations are solved by a self-consistent-field (SCF) procedure.

The potential energy function $Y_\lambda(r)$ used in this work is Thomas-Fermi potential function taken from [1].

We considered Breit interaction $B(r_{ij})$ (the lowest order correction to the Conlomb interaction between two electrons.) due to the exchange of a single transverse polarized photon as follows:

$$B(r_{ij})=-\alpha_i\cdot\alpha_j\frac{\cos(\omega r_{ij})}{r_{ij}}-(\alpha_i\cdot\nabla_i)(\alpha_j\cdot\nabla_j)\frac{\cos(\omega r_{ij})-1}{\omega^2 r_{ij}}, \tag{3}$$

Where $\vec{\alpha}$ are forth order Dirac matrices, ω is the wavenumber of the transferring photon. Breit correction and low order QED correction are necessary for multiply charged ions.

In calculation we choose the GRASP code's extended optimized (EAL) level option[2]. The radiative corrections can show large fluctuations due to admixtures of wavefunctions. In order to minimize the fluctuations indicated in the radiative

corrections, the radiative corrections should be calculated by using EAL option of the code[12].

2 Results

Table 1 gives out the comparison of wavelengths between theoretical calculations performed by this work and experimental data for neutral atom Iron, Cobalt, Nickel, Copper, Zinc, Germanium, and Bromine. From Table 1 we can see that the wavelengths calculated by means of GRASP are in close agreement with experimental data for neutral elements. GRASP calculation can reproduce the measured data quite accurately. It shows that GRASP is an available program for researching the atomic structure.

Table 1 Wavelength comparison between evaluated and measured data for neutral atoms

Elements	Configuration	Terms	J—J	Wavelength(in Å)*	
				Exp.	This work
Iron	$4s^2$—$4s4p$	^5D—^5D	4—3	1855.58[5]	1855.51
Cobalt	$4s^2$—$4s4p$	^4F—^4D	3/2—1/2	1981.97[6]	1981.92
Nickel	3d4s—4s4p	^3D—^3F	3—4	1976.87[7]	1976.83
Copper	$4s^2$—$4s5p$	^2D—^2F	3/2—5/2	1621.296[8]	1621.27
Zinc	$4s^2$—$4s9p$	^1S—^3P	0—1	1362.526[9]	1362.51
Germanium	$4p^2$—4p8d	^3P—^3F	1—2	1592.846[10]	1592.83
Bromine	$4p^5$—4p45d	^2P—^2D	3/2—3/2	1098.881[11]	1098.86

*, 1Å=10^{-10}m.

Wavelengths for highly ionized atoms $S^{10+}\rightarrow S^{13+}$, Br^{23+}, Br^{24+}, Ge^{20+}, Ge^{21+} calculated in this work are given in Table 2~9. We offer the transition wavelengths for highly charged atoms to serve as rough approximations for experimentalists. The experimental data carried out in HI–13 Tandem Accelerator (CIAE) are taken from [4]. From these comparisons we can see that there are differences of wavelengths between theory and experiment for most highly ionized atoms. In this work, the main differences come from correlation effects not being considered completely. We will improve the GRASP code to include more correlation effects completely in the future.

Table 2 Wavelength comparison between calculated and measured data for Sulphur X(S^{10+})

Configuration	Terms	J—J	Wavelength(in Å)	
			Exp.(CIAE)	This work
$2s^22p^2$—$2s2p^3$	^1D—^1P	2—1	189.54	188.23
$2s^22p^2$—$2s2p^3$	^3P—^3P	2—1	247.18	246.41
$2s^22p^2$—$2s2p^3$	^3P—^3D	0—1	281.85	279.76
$2s^22p^2$—$2s2p^3$	^3P—^3D	1—1	285.58	283.91
$2s^22p^2$—$2s2p^3$	^3P—^3D	2—3	291.58	290.11

Table 3 Wavelength comparison between calculated and measured data for Sulphur XI(S^{11+})

Configuration	Terms	J—J	Wavelength(in Å)	
			Exp.(CIAE)	This work
$2s^22p$—$2s2p^2$	^2P—^2P	3/2—3/2	212.45	211.96
$2s^22p$—$2s2p^2$	^2P—^2S	1/2—1/2	227.59	224.85
$2s^22p$—$2s2p^2$	^2P—^2S	3/2—1/2	234.33	231.68
$2s^2p2$—$2p^3$	^2P—^2S	1/2—3/2	240.08	238.12
$2s^2p2$—$2p^3$	^2P—^2S	3/2—3/2	243.08	240.86
$2s^2p2$—$2p^3$	^2P—^2S	5/2—3/2	247.18	244.81

Table 4 Wavelength comparison between calculated and measured data for Sulphur XII(S^{12+})

Configuration	Terms	J—J	Wavelength(in Å)	
			Exp.(CIAE)	This work
$2s2p$—$2p^2$	^3P—^3P	1—2	298.99	298.18
$2s2p$—$2p^2$	^3P—^3P	0—1	303.64	301.64
$2s2p$—$2p^2$	^3P—^3P	1—1	307.22	305.60
$2s2p$—$2p^2$	^3P—^3P	2—2	309.00	307.03
$2s2p$—$2p^2$	^3P—^3P	1—0	312.92	310.80
$2s^2$—$2s2p$	^1S—^3P	0—1	492.49	489.00

Table 5 Wavelength comparison between calculated and measured data for Sulphur XIII (S^{13+})

Configuration	Terms	J—J	Wavelength(in Å)	
			Exp.(CIAE)	This work
$1s^22s$—$2s^22p$	^3S—^2P	1/2—1/2	445.74	443.36

Table 6 Wavelength comparison between calculated and measured data for Bromine XXIII (Br^{23+})

Configuration	Terms	J—J	Wavelength(in Å)	
			Exp.(CIAE)	This work
$3s3p—3p^2$	$^3P—^3P$	0—1	172.58*	171.28
$3s3p—3p^2$	$^3P—^3P$	1—1	179.03*	177.84
$3s3p—3p^2$	$^1P—^1S$	1—0	184.45*	183.87
$3s3p—3p^2$	$^3P—^3P$	1—0	200.76*	198.00
$3s3p—3p^2$	$^3P—^3P$	2—1	203.69*	201.77
3s3p—3s3d	$^3P—^3D$	0—1	133.40*	133.22
3s3p—3s3d	$^3P—^3D$	1—1	137.20*	137.16
3s3p—3s3d	$^3P—^3D$	2—3	147.68	147.44
3s3p—3s3d	$^3P—^3D$	2—2	149.87*	149.74
3s3p—3s3d	$^3P—^3D$	2—1	151.14*	150.97
$3p^2—3p3d$	$^3P—^3P$	1—0	137.20*	137.79
$3p^2—3p3d$	$^3P—^3D$	0—1	138.42*	139.03
$3p^2—3p3d$	$^3P—^3D$	1—2	144.11*	144.75
$3p^2—3p3d$	$^3P—^3D$	1—1	151.14*	151.82
$3p^2—3p3d$	$^3P—^1D$	1—2	157.58*	158.80
3s3d—3p3d	$^3D—^3P$	2—2	179.03*	178.64
3s3d—3p3d	$^3D—^3P$	2—1	180.69*	180.20
3s3d—3p3d	$^3D—^3D$	2—3	182.85*	181.06
3s3d—3p3d	$^3D—^3P$	3—3	185.72*	184.55
3p3d—3d2	$^3F—^3D$	3—2	151.14*	150.17
3p3d—3d2	$^3F—^3F$	4—4	149.87*	149.20
3p3d—3d2	$^3D—^3F$	1—2	152.07*	151.91

* measured data are published first.

Table 7 Wavelength comparison between calculated and measured data for Bromine XXIV (Br^{24+})

Configuration	Terms	J—J	Wavelength(in Å)	
			Exp.(CIAE)	This work
2p63s—2p63p	$^2S—^2P$	1/2—3/2	189.57	189.10
2p63s—2p63p	$^2S—^2P$	1/2—1/2	229.18	228.34

Table 8 Wavelength comparison between calculated and measured data for Germanium XX (Ge^{20+})

Configuration	Terms	J—J	Wavelength(in Å)	
			Exp.(CIAE)	This work
$3s^2—3s3p$	$^1S—^1P$	0—1	196.56	194.34
$3s3p—3p^2$	$^3P—^3P$	0—1	205.32	203.51
$3s3p—3p^2$	$^3P—^3P$	1—1	211.73	209.96
$3s3p—3p^2$	$^1P—^1S$	1—0	220.14*	219.23

(Table 8 Cont.)

Configuration	Terms	J—J	Wavelength(in Å)	
			Exp.(CIAE)	This work
$3s3p—3p^2$	$^3P—^3P$	2—1	232.54	230.21
3s3p—3s3d	$^3P—^3D$	1—1	160.15*	159.77
3s3p—3s3d	$^3P—^3P$	2—3	168.76	168.50
3s3p—3s3d	$^3P—^3D$	2—2	170.57	170.24
$3p^2—3p3d$	$^3D—^3P$	2—2	158.87	158.36
$3p^2—3p3d$	$^3P—^3P$	1—2	160.15	160.75
$3p^2—3p3d$	$^3P—^3D$	2—3	176.39	175.59
$3p^2—3p3d$	$^1D—^1D$	2—2	180.76	179.80
$3p^2—3p3d$	$^3P—^3D$	2—2	184.36	183.69
$3p3d—3d^2$	$^3F—^3P$	3—2	149.38*	149.75
$3p3d—3d^2$	$^3F—^3F$	2—2	157.33*	156.45
$3p3d—3d^2$	$^1F—^1G$	3—4	203.88	205.69
3s3d—3p3d	$^3D—^3F$	3—4	246.60	247.32
3s3d—3p3d	$^3D—^3F$	2—3	266.68	267.15
3s3d—3p3d	$^3D—^3F$	3—3	271.20*	271.56
3s3d—3p3d	$^3D—^3F$	1—2	285.56	286.42
3s3d—3p3d	$^3D—^3F$	2—2	288.70*	289.25

*, measured data are published first.

Table 9 Wavelength comparison between calculated and measured data for Germanium XXI (Ge^{21+})

Configuration	Terms	J—J	Wavelength(in Å)	
			Exp.(CIAE)	This work
$2p^63s—2p^63p$	$^2S—^2P$	1/2—1/2	261.50	260.53
$2p^63s—2p^63p$	$^2S—^2P$	1/2—3/2	226.51	225.93
$2p^63p—2p^63d$	$^2P—^2D$	1/2—3/2	174.40	174.23
$2p^63p—2p^63d$	$^2P—^2D$	3/2—5/2	190.59	190.43

Reference

[1] K.G.Dvall et al., Comput. Phys. Commun. 55(1989)425 ;

[2] I.P.Grant et al., Comput. Phys. Commun. 21(1980)207 ;

[3] P.J.Mohr, Am. Phys. 88(1974)52 ;

[4] Zeng Xiantang , "Measurement of energy level and spectra for highly stripped ions" , to be published ;

[5] Russell, H.N. and C.E.Moore, Trans. Amer. Phil. Soc. 34, II ,113-79(1944) ;

[6] Russell, H.N., R.B.King, and C.E.Moore, Phys. Rev. 58, 407-36(1940) ;

[7] Russell, H.N., Phys. Rev. 34, 821-57(1929) ;

[8] Longmire, M.S., C.M.Brown, and M.L.Ginter, J. Opt. Soc. Am. 70, 423-29(1980) ;

[9] Brown, C.M. and S.G.Tilford, J. Opt. Soc. Am. 65, 1404-9(1975) ;

[10] Brown, C.M. and S.G.Tilford, and M.L.Ginter, J. Opt. Soc. Am. 67, 584- 606(1977) ;

[11] Tech, J.L., J. Res. Nat. Bur. Stand. 67A, 505-54(1963) ;

[12] G.X.Chen, Q.Y.Fang, W.Cai, Chinese Journal of Atomic & Molecular Physics 12(1995)91 .

Ⅳ BENCHMARK TESTING

Benchmark Testing of CENDL-2.1 for Heavy Water Reactor

Liu Ping
(China Nuclear Data Center, CIAE)

Introduction

The new version evaluated nuclear data library of ENDF-B6.5 has been released recently. In order to compare the quality of evaluated nuclear data CENDL-2.1 with ENDF/B-6.5, it is necessary to do benchmark testing for them.

In this work, CENDL-2.1 and ENDF/B-6.5 were used to generate the WIMS-69 group library respectively, and the benchmarks testing was done for the heavy water reactor, using WIMS5A code, WIMSD[1] which is a good lattice physics code and has been widely used in the world.

1 Generating of group constants library

The generation of the new group constant libraries based on CENDL-2.1 and ENDF/B-6.5 was done with NJOY94.35[2] code system, in which the modules MODER、RECONR、BROADR、UNRESR、THERMR and GROUPR were used to produce 69-group data file GENDF from ENDF/B format evaluated nuclear data according to the temperatures, weighting function and so on. The module WIMSR converts the GENDF file to the WIMSD format. The resonance reconstruction tolerance was 0.1%, and the tolerance for thinning of 0.2% was used.

In the old WIMS library, only one fission spectrum was given. In this work, the fission spectrum was composed of 7.5% ^{238}U and 92.5% ^{235}U fission spectrums. In the group averaging cross section calculations, input weight function(IWT=1)[3] was used for weighting.

In the WIMS 69-groups library, only absorption and neutron yield per fission integrals were tabulated, and all other cross sections were entered corresponding to a σ_0, which was chosen from input values. Clearly, the results of benchmark calculations are sensitive to the selection of σ_0. In this work, σ_0 was derived from the calculation according to normal reactor cells. Table 1 shows the selected reference values for each isotope.

The Goldstein-Cohen λ values should be consistent with the resonance integral tabulation. In this work, the selection of λ is similar to the old WIMS library. Table 2 shows the selected reference values for some isotopes.

Table 1 List of applied reference σ_0 values

Material	Reference σ_0 values.
^{1}H	1.E10
$^{16}O_8$	40.
D	1.E10
$^{27}Al_{13}$	1.E10
$^{235}U_{92}$	1.E3
$^{238}U_{92}$	28

Table 2 List of applied reference λ values

Materials	λ values
H	1.0
D	1.0
O	1.0
Al	1.0
^{235}U	0.2
^{238}U	0.2

2 Description of Benchmark Experiments

In order to test the data files, three benchmarks lattices containing ^{235}U and ^{238}U , which include ZEEP-1,2,3, were chosen.

The natural uranium fuel, and heavy water (D_2O)-moderated, are wed in ZEEP-1,2,3. Details of these lattices are given in Table 3.

For these lattices, experimental buckling values are available. It is easy to do leakage calculations using the input buckling values.

Table 3 Brief Characteristics of ZEEP-1,2,3

Region	Outer radius (mm)	Isotope	Concentration (10^{24} atoms / cm^3)
Fuel	16.285	^{235}U	3.454E-4
		^{238}U	4.760E-2
Air Gap	16.470		5.0E-5
Cladding	17.490		6.025E-2
		^{1}H	1.529E-4
Moderator		^{2}H	6.633E-2
		O	3.324E-2

3 Method of cell calculation

The cell calculations were used with WIMS/D4 code. At first, according to real cell composition, intermediate approximation was used to calculate resonance self-shielding. The main transport equation was solved using Sn method, and the cylindrical cell approximation was used to simplify the geometry of the cell. Leakage calculations had been done with input buckling values and B1 method. The reaction rates of ^{235}U and ^{238}U were given in output files in two groups.

4 Results and Discussions

For ZEEP-1,2,3, the results of CENDL-2.1 , old WIMS library and ENDF/B-6.5 are given in Table 4. The $C^*_{Maxwellian}$ given in Ref.[4] is 0.654.

All the integrals parameters are defined as follows:

ρ^{28} — epithermal / thermal captures for ^{238}U

δ^{25} — epithermal / thermal fission for ^{235}U

δ^{28} — ^{238}U / ^{235}U fission

C^* — ^{238}U capture / ^{235}U fission

RCR — $C^*_{lattice} / C^*_{Maxwellian}$

Although there are no quite enough experiment data with heavy water moderated lattices, the available data have shown that the calculated results based on CENDL-2.1 are within or close to the experimental uncertainty limits. All the

lattices parameters calculated with CENDl-2.1 are in good agreement with those values of experiments.

Table 4 Integral parameter comparison for heavy water reactor benchmarks

Lattices	Integral parameter	Experiment	WIMS/D4	CENDL-2.1	ENDF/B-6.5
ZEEP-1	k_{eff}	1.0000	0.99398	1.0032	0.99790
	ρ^{28}	-----	0.26026	0.28687	0.28488
	δ^{25}	-----	0.0258	0.0256	0.02557
	δ^{28}	0.0675	0.06804	0.06785	0.06892
	RCH	1.16	1.279	1.274	1.29226
ZEEP-2	k_{eff}	1.0000	0.9993	0.99993	0.99465
	ρ^{28}	-----	0.4688	0.52713	0.52368
	δ^{25}	-----	0.04891	0.048715	0.04849
	δ^{28}	-----	0.07261	0.07192	0.07332
	RCR	-----	1.464	1.489	1.50807
ZEEP-3	k_{eff}	1.0000	1.00384	0.99752	0.99237
	ρ^{28}	----	0.62021	0.70397	0.69603
	δ^{25}	----	0.06539	0.06538	0.06504
	δ^{28}	----	0.07672	0.07583	0.07748
	RCR	----	1.5968	1.6424	1.66292

5 Conclusions

It is obvious that different evaluation nuclear data library is the cause of the difference of the results between old and new WIMS 69-group library. Through the comparison of ^{238}U scattering cross sections between old and new library, a big difference was found. In the resonance energy region, the values of old library is much bigger than that of the new ones. The difference arises from the evaluation data and resonance self-shielding treatment for scattering cross sections as well. The bigger scattering cross section of old library caused relative lower possibility of absorption, higher slowdown power and therefore softer neutron spectrum.

Owning to the ^{238}U inelastic cross sections of ENDF/B-6.5 make neutron spectrum of assembly hardened and underestimated neutron moderating power, the neutron production rate in the high energy region is remarkably overestimated and the neutrons number in the low energy region is remarkably overestimated. Consequently, k_{eff} for thermal reactor calculations is underestimated. It seems that the data of ^{238}U in the ENDF/B-6.5 is not the best.

It is obvious that data files of CENDL-2.1 is better than that of old WIMS library for the heavy water reactors calculations, and is in good agreement with those of ENDF/B-6.5.

References

[1] "WIMSD, A Neutron Code for Standard Lattice Physics Analysis", ANSWERS Software Service, AEA Technology, Winfrith, UK, March 1996. See also "Code Package for WIMSD5A", NEA1507/01, OECD Nuclear Energy Agency, Pairs, France.

[2] R. E. MacFarlane and D. W. Muir, " The NJOY Nuclear Data Processing System Version 91", Los Alamos National Laboratory Report LA-12740-M (October 1994). For a summary of updates leading to NJOY94.105, see http://t2.lanl.gov/codes /njoy94/Readme105, prepared by R. E. MacFarlane

[3] S.Gan esan. "Update of the WIMS-D4 Nuclear Data Library Status Report of the IAEA WIMS Library Update Project", Report INDC(NDS)-290 (December, 1993).

[4] T.Zidi, Nuclear Data Processing and Applications, P,214.

CINDA INDEX

Nuclide	Quantity	Energy/ eV		Lab	Type	Documentation					Author, Comments
		Min	Max			Ref	Vol	Page	Date		
^{9}Be	γ-reaction	Thrsh	3.0+7	AEP	Theo	Jour CNDP	22	35	Dec	99	Zhang Jingshang+, Code GUNF
^{27}Al	γ-reaction	Thrsh	3.0+7	AEP	Theo	Jour CNDP	22	120	Dec	99	Yu Baosheng +, Code GUNF,SIG,DA,DE
	γ-reaction	Thrsh	3.0+7	ZHN	Eval	Jour CNDP	22	120	Dec	99	Yu Baosheng +, SIG,DA,DE
^{50}Cr	γ-reaction	Thrsh	3.0+7	ZHN	Theo	Jour CNDP	22	120	Dec	99	Yu Baosheng +, Code GUNF,SIG,DA,DE
	γ-reaction	Thrsh	3.0+7	ZHN	Eval	Jour CNDP	22	120	Dec	99	Yu Baosheng +, SIG,DA,DE
^{52}Cr	γ-reaction	Thrsh	3.0+7	ZHN	Theo	Jour CNDP	22	120	Dec	99	Yu Baosheng +, Code GUNF,SIG,DA,DE
	γ-reaction	Thrsh	3.0+7	ZHN	Eval	Jour CNDP	22	120	Dec	99	Yu Baosheng +, SIG,DA,DE
^{53}Cr	γ-reaction	Thrsh	3.0+7	ZHN	Theo	Jour CNDP	22	120	Dec	99	Yu Baosheng +, Code GUNF,SIG,DA,DE
	γ-reaction	Thrsh	3.0+7	ZHN	Eval	Jour CNDP	22	120	Dec	99	Yu Baosheng +, SIG,DA,DE
^{54}Cr	γ-reaction	Thrsh	3.0+7	ZHN	Theo	Jour CNDP	22	120	Dec	99	Yu Baosheng +, Code GUNF,SIG,DA,DE
	γ-reaction	Thrsh	3.0+7	ZHN	Eval	Jour CNDP	22	120	Dec	99	Yu Baosheng +, SIG,DA,DE
^{69}Ga	Evaluation	1.0-5	2.0+7	AEP	Eval	Jour CNDP	22	107	Dec	99	Zhang Songbai+, SIG,DA,DE
^{71}Ga	Evaluation	1.0-5	2.0+7	AEP	Eval	Jour CNDP	22	107	Dec	99	Zhang Songbai+, SIG,DA,DE
^{65}Cu	Evaluation	1.0-5	2.0+7	AEP	Eval	Jour CNDP	22	64	Dec	99	Ma Gonggui+, SIG,DA,DA/DE
^{88}Y	(n,2n)	Thrsh	2.0+7	AEP	Eval	Jour CNDP	22	132	Dec	99	Zhang Songbai+, SIG
^{89}Y	(n,2n)	Thrsh	2.0+7	AEP	Eval	Jour CNDP	22	132	Dec	99	Zhang Songbai+, SIG
^{90}Zr	Evaluation	1.0-5	2.0+7	ZHN	Eval	Jour CNDP	22	96	Dec	99	Zhang Wei+, Liu Jianfeng, SIG,DA,DA/DE
^{91}Zr	Evaluation	1.0-5	2.0+7	ZHN	Eval	Jour CNDP	22	96	Dec	99	Zhang Wei+, Liu Jianfeng, SIG,DA,DA/DE
^{92}Zr	Evaluation	1.0-5	2.0+7	ZHN	Eval	Jour CNDP	22	96	Dec	99	Zhang Wei+, Liu Jianfeng, SIG,DA,DA/DE
^{94}Zr	Evaluation	1.0-5	2.0+7	ZHN	Eval	Jour CNDP	22	96	Dec	99	Zhang Wei+, Liu Jianfeng, SIG,DA,DA/DE
^{96}Zr	Evaluation	1.0-5	2.0+7	ZHN	Expt	Jour CNDP	22	96	Dec	99	Zhang Wei+, Liu Jianfeng, SIG,DA,DA/DE
^{Nat}Zr	Evaluation	1.0-5	2.0+7	ZHN	Eval	Jour CNDP	22	96	Dec	99	Zhang Wei+, Liu Jianfeng, SIG,DA,DA/DE
^{233}U	Evaluation	1.0-5	2.0+7	AEP	Eval	Jour CNDP	22	83	Dec	99	Yu Baosheng+, SIG,DA,DA/DE
^{235}U	Fission Yield	2.5-2	1.5+7	AEP	Eval	Jour CNDP	22	54	Dec	99	Liu Tingjin+,Reference Fission Product Yield
^{239}Pu	Evaluation	1.0-5	2.0+7	AEP	Eval	Jour CNDP	22	42	Dec	99	Yu Baosheng+, SIG,DA,DA/DE

图书在版编目（CIP）数据

中国核科技报告. CNIC-01430. CNDC-0025：核数据进展通讯. NO.22：英文 / 刘挺进等著. —北京：原子能出版社，1999. 12

ISBN 7-5022-2120-4

Ⅰ. 中… Ⅱ. 刘… Ⅲ. 核技术-研究报告-中国-英文 Ⅳ. TL-2

中国版本图书馆 CIP 数据核字（1999）第 54016 号

原子能出版社出版发行

责任编辑：李曼莉

社址：北京市海淀区阜成路 43 号 邮政编码：100037

中国核科技报告编辑部排版

核科学技术情报研究所印刷

开本 787×1092 1/16・印张 9.7・字数 152 千字

1999 年 12 月北京第一版・1999 年 12 月北京第一次印刷

印数：1—600

定价：10.00 元